ABSTRACT

Title of Document:	IMPROVEMENT OF DYNAMIC PROPERTIES AND SEISMIC RESPONSE OF CLAY USING FIBER REINFORCEMENT
	Behzad Amir Faryar, Doctor of Philosophy, 2012
Directed By:	Professor M. Sherif Aggour, Department of Civil and Environmental Engineering

In recent years, earthquakes have caused heavy damage to buildings and infrastructure. One of the causes of heavy damage due to earthquake motions is the role of soft clay in amplifying bedrock ground motions. Improving the soil conditions at a site in order to mitigate earthquake damage can be one of the methods of modifying site conditions and thus reduce its effects on the seismic site response. The inclusion of randomly distributed short virgin polypropylene fibers (C_3H_6) in clay has proven to significantly improve the static geotechnical properties of clay such as shear, compression, tensile strengths, and so on. These improvements have triggered great interest in the possibility of mixing fibers with clay to improve the clay's dynamic properties. Because the percentage of fibers is currently arbitrarily chosen by users, a procedure was set up in this study to determine the optimum fiber content for a fiber-clay composite.

Experimental testing was performed using the Resonant Column Method to obtain both the shear modulus and the material damping for a clay and the fiber-clay composite to determine the effect of fiber inclusion on the dynamic properties of clayey soil. The research showed that the inclusion of fiber at optimum fiber content as a ground improvement technique can improve the dynamic properties of soft clayey soils at low shear strain. Test results indicated that both the shear modulus and damping increased. Hence, the inclusion of fiber in clay can provide a double benefit for the dynamic response of a site by increasing the stiffness of the site and reducing its amplitude of vibration. General formulas for shear modulus and damping were developed as functions of the shear strain amplitude for the clay and for fiber reinforced clay.

The effect of fiber inclusion on the seismic site response using two different earthquake motions was also studied. One-dimensional wave propagation analysis was performed to investigate the effect of the modification of the clay dynamic properties using fibrillated fiber reinforcements on the site response. The results indicated that by modifying the clayey soil using fiber, the seismic site response can be improved.

IMPROVEMENT OF DYNAMIC PROPERTIES AND SEISMIC RESPONSE OF
CLAY USING FIBER REINFORCEMENT

By
Behzad Amir Faryar

Dissertation submitted to the Faculty of the Graduate School of the
University of Maryland in partial fulfillment
of the requirements for the degree of
Doctor of Philosophy
2012

Advisory Committee:

Professor M. Sherif Aggour, Chair
Professor Amde M. Amde
Associate Professor Peter C. Chang
Associate Professor Dimitrios G. Goulias
Professor Sung Lee

Dedication

To my:
> Mother, Mrs. Mahsa Hariri
> Father, Mr. M. Reza Amir-Faryar
> Brother, Mr. Farzad Amir Faryar, P.E.
> Late Grandfather, Mr. Jafar Hariri
> Late Grandfather, Mr. Reza Amirfaryar
> Late Grandmother, Mrs. Sedigheh Zendehrokh
> Late Grandmother, Mrs. Ashraf Tassouji

Acknowledgements

It looked so far-fetched one day!

The author wishes to express his thanks to the following people who helped him achieve his research's mammoth tasks and get to this very page of his dissertation and his life:

- The chairman of his doctoral committee, Professor M. Sherif Aggour, for his continued guidance, generosity, and constant support, and for the time he generously shared with the author. His objective and invaluable criticism of the manuscript was of great assistance in the preparation of this dissertation. It has been an extreme pleasure learning from and working with him.

- Member of his doctoral committee, Professors Amde M. Amde, Peter C. Chang, Dimitrios G. Goulias, and Sung Lee, for accepting to be part of his dissertation committee.

- The Civil and Environmental Engineering Department of the University of Maryland for allowing me to use the facilities in the Geotechnical Laboratory.

- The technical personnel at the Civil and Environmental Engineering Laboratory, University of Maryland, especially Mr. Alfred Bituin, for assisting in connecting water and air pipes to the test apparatus and providing assistance during the experimental stage of the work.

- Colleague, Mr. Robert S. Woodke, professor at Northern Virginia Community College (NVCC), who helped machine laboratory pieces required for testing.

And above all his thanks goes to the Lord of the Universe without whose help this work could not have been accomplished.

Behzad Amir Faryar, P.E. - Fall 2012
A. James Clark School of Engineering,
University of Maryland, College Park

TABLE OF CONTENTS

vii

LIST OF FIGURES

xiii

LIST OF TABLES

CHAPTER 1

RESEARCH BACKGROUND & LITERATURE REVIEW

1.1   Introduction

In recent years, earthquakes have caused heavy damages to buildings and infrastructure. One of the causes of heavy damages due to earthquake motions are the role of soft clay in amplifying bedrock ground motions. Modifying the soil conditions of sites in order to mitigate earthquake damages can be one of the methods of enhancing site conditions and its effects on seismic site response.

Every once in a while a revolutionary idea or method comes along that changes everything. The idea of using reinforcement steel in concrete is one of those ideas. It changed the entire construction industry. Nowadays, barely any concrete structure is constructed without using reinforced steel in the concrete. The idea of using fiber as reinforcement for clayey soil follows a similar idea to reinforced steel-concrete. The inclusion of randomly distributed short virgin polypropylene fibers (C_3H_6) in clay has proven to significantly improve geotechnical properties of clay such as shear, compressive, tensile strength, and so on. These improvements have triggered great attention on the possibility of mixing fibers with clay to from a desirable composite.

In Chapter one, a brief overview of dynamic field and laboratory test equipment, clayey soils and different modification techniques, descriptions and properties of geofibers, dynamic properties of cohesive soils, and shear modulus and damping ratio equations are presented.

A general overview of the dynamic test equipment used in this study along with calibration of the test equipment and resonant column data reduction calculations are described in Chapter Two. The preliminary work and testing involved in determining the right mix design for fiber-clay composite is discussed in Chapter Three. In that chapter, a new compaction procedure was developed for finding the optimum fiber content (OFC) and its compaction test data. The recommended mix design was used to prepare soil and composite specimens in Chapter Four's dynamic test program.

Dynamic experimental testing was performed using the Resonant Column Method to obtain the shear modulus and material damping ratio for clay and fiber-clay composites to investigate the dynamic effect of fiber inclusion in clayey soil. The results of the dynamic experimental testing are shown in the Chapter Four. The research presented in Chapter Four has been performed for four main purposes: (1) investigate the effect of fiber inclusion on the dynamic properties of clay; (2) study the effect of fiber content on the dynamic properties of the composite; (3) further investigate the effect of type of fibers on the dynamic properties of clay; (4) determine an analytical relationship between shear modulus and shear strain and also between material damping and shear strain of the composite; and (5) develop a general formula correlating material damping to shear strain of soil. The developed formula in Chapter Four can be applied to all soil types and fiber-reinforced soil composites.

The effect of fiber inclusion on the seismic site response using two different earthquake motions was also presented in Chapter Five. One dimensional wave propagation analysis was performed using DEEPSOIL software (Hashash, et al., 2011) to investigate the effect of modification of clay using fibrillated fiber reinforcements on the

site response. Two different material types, clay and fibrillated fiber reinforced clay, were used for different soil columns. The research presented in Chapter Five was performed to study the following: (1) investigate the effect of modification of clay using fibrillated fiber reinforcements on the site response; (2) study the effect of depth to bedrock on the site response of the fiber reinforced site; (3) investigate the effect of the thickness of the soil reinforced layer; and (4) study the effect of different earthquake motions on the site response.

A summary of the study and conclusions along with recommendations for further research was summarized in Chapter Six.

1.2   Methods Used in the Determination of Shear Modulus and Damping

With recent advances in the analytical and testing methods, the behavior of soils subjected to various types of dynamic loading; such as, earthquakes, ocean waves, machine vibrations, and blasts, are being better understood. The measurement of dynamic soil properties is a vital task in the solution of geotechnical earthquake engineering problems. Any analysis of dynamic engineering problems requires the determination of the shear modulus and damping ratio. These two parameters are usually determined using laboratory or field methods. The selection of testing methods for measurement of dynamic soil properties requires thorough consideration and understanding of the specific problem at hand.

The shear modulus (G) and damping ratio (D) are the two variable properties in the dynamic response analysis of soils. They are the reason that soils are not considered a linear-elastic material. The shear modulus, and damping of soils are strain dependent.

3

The vibratory motion of shear waves can cause shear strains on a soil element. The stress-strain curve forms a closed loop, called hysteresis loop, as shown below.
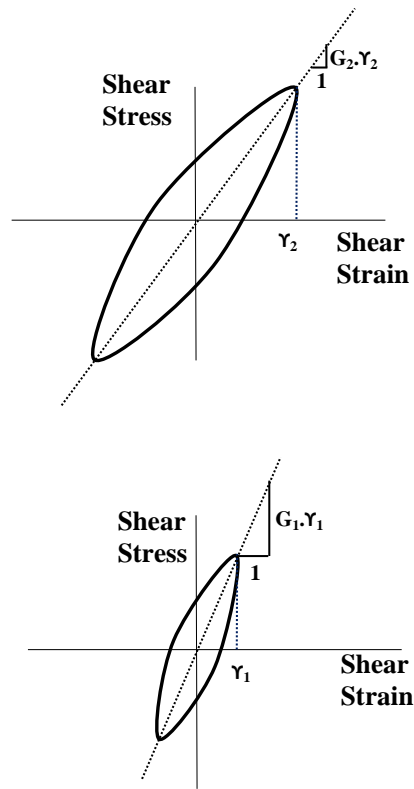
Figure 1-1: Stress–strain relationship in cyclic loading (Shannon & Wilson, 1972)

Shear modulus and damping can be directly obtained from Figure 1-1. The damping ratio increases with increasing strains while the shear modulus decreases. The shear modulus and damping can be obtained both in the laboratory and field. Each technique has an associated strain range in which the test is conducted. A summary of the laboratory and field tests for soil dynamics, along with the advantages and disadvantages of the testing methods are tabulated in Table 1-1 (Tawfiq, 1986).

Table 1-1: Advantages and disadvantages of laboratory and field testing methods (Tawfiq, 1986)

Laboratory Techniques	Field Techniques
1 – Cyclic Triaxial	1 – In-Hole Methods
2 – Cyclic Simple Shear	- Cross Hole
3 – Cyclic Torsional Shear	- Down Hole
4 – Resonant Column	- Up Hole
5 – Ultrasonic	2 – Surface Wave Methods
6 – Shaking Table	

Advantages	Advantages
1 – Better control of boundary conditions	1 – Measure large masses
2 – Evaluate different parameters of soil behavior	2 – Less soil disturbance
3 – Provide wide ranges of strain amplitudes	3 – Measurements under actual field conditions
4 – Evaluate damping characteristics	

Disadvantages	Disadvantages
1 – Sample disturbance	1 – Low strain amplitude
2 – In general, the advantages and disadvantages of laboratory testing methods depend on the minimum criteria for obtaining adequate values of soil behavior	2 – Damping characteristics cannot be measured

A comprehensive review of laboratory and field techniques and procedures to obtain dynamic soil properties are given by Woods, 1978; Hoadley, 1985; Kramer ,1996; Towhata, 2008.

1.3   Laboratory Methods

Laboratory tests are typically performed on relatively small soil specimens that are assumed to be representative of a larger body of soil. The ability of laboratory tests to provide accurate rather than precise measurements of soil properties depends on their ability to simulate the initial conditions and loading conditions of the problem of interest

on a smaller scale. The proficiency of the laboratory technician also factors into the results.

Laboratory tests provide an opportunity to determine the dynamic properties of soils under dynamic loading for a wide range of strain levels. Figure 1-2 shows the strain levels induced in soils under different loading conditions and the strain amplitude capacities of each laboratory testing procedure.

Shearing strain amplitude (%)

10^{-4} 10^{-3} 10^{-2} 10^{-1} 1

Resonant Column (Solid samples)

Resonant Column (Hollow samples)

Torsional Shear (Hollow samples)

Pulse Methods

Cyclic Triaxial

Cyclic Simple Shear

Shake Table

Typical Motion Characteristics

Properly designed machine foundation

Strong ground shaking from earthquake

Close-in nuclear explosion

10^{-4} 10^{-3} 10^{-2} 10^{-1} 1
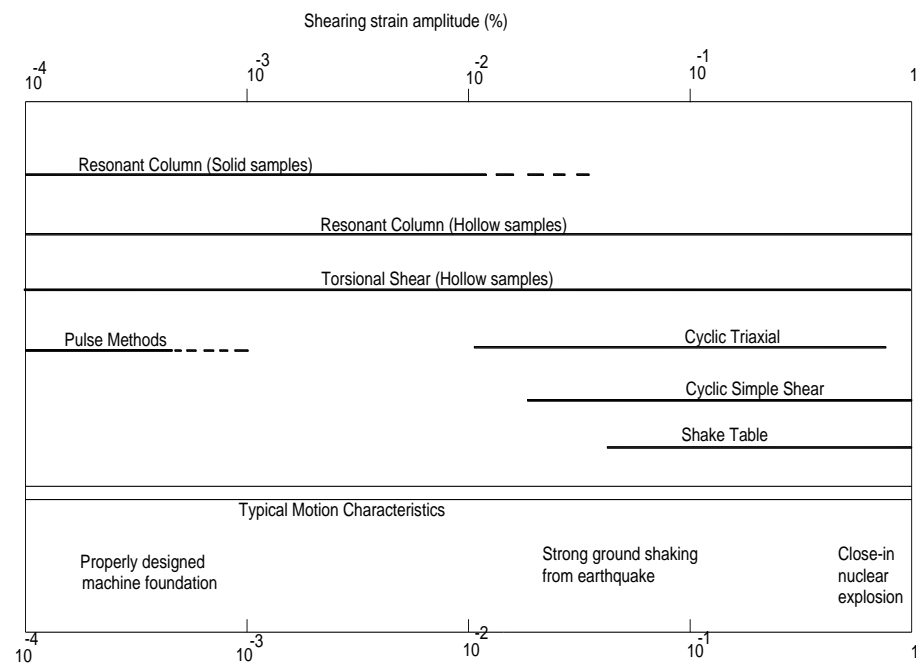
Figure 1-2: shear strain amplitude capacities of laboratory apparatus (Woods, 1978)

1.3.1 Cyclic Triaxial Test

The cyclic triaxial test has been the most regularly used experiment for the measurement of dynamic properties of soil at high strain levels. In a triaxial test, a cylindrical soil sample is situated between top and bottom loading platens and surrounded by a relatively thin rubber membrane. The soil specimen is subjected to a radial stress and

an axial stress, which are pneumatically applied. The difference between the radial and axial stresses is called the deviator stress. The deviator stress, in cyclic triaxial testing, is applied cyclically (Kramer, 1996). Since soil characteristics are governed by effective stresses, all methods of testing soils at high strain levels must be capable of controlling the porewater pressure of the specimen and also the porewater drainage from the soil sample to determine volume change and porewater pressures in the soil sample.

There has been extensive research conducted on dynamic properties of clay using cyclic triaxial testing. Moreover, the use of lime as a stabilizer in clayey soils has been studied and dynamic properties of lime stabilized clay are determined (Fahoum, 1994).

To determine the shear modulus and damping ratio in this method, the sample is first consolidated under a confining and all-around pressure, σ_3, and subsequently a vertical predetermined cyclic stress (stress controlled) or strain (strain controlled) is applied. A typical axial stress-strain curve (hysteresis loop) from a triaxial test is obtained from a special data acquisition device. From such a loop the elastic modulus, E, is calculated by having the slope of the straight line connecting the two extreme points of the hysteresis loop.

$$E = \frac{\Delta \partial_a}{\varepsilon_a} \qquad (1.1)$$

where: $\Delta \sigma_a = \sigma_{dp;}$ $\varepsilon_{a:}$ maximum axial strain.

The shear modulus can also be calculated using:

$$G = \frac{E}{2(1 + \mu)} \qquad (1.2)$$

where: G: shear modulus; μ: Poisson's ratio.

The damping ratio can be determined from the hysteresis stress-strain graph using:

$$D = \frac{1}{4} \times \frac{Area\ of\ loop}{Area\ of\ triangle} \tag{1.3}$$

where: D: damping ratio.

This equation shows how much energy is dissipated in each cycle of loading. Shear strain can also be measured by:

$$\gamma_s = \varepsilon_a \times (1 + \mu) \tag{1.4}$$

where: γ_s: shear strain.

To determine shear stress, τ, the following equation can be used:

$$\tau = \frac{\Delta \partial a}{2} \tag{1.5}$$

1.3.2   Cyclic Direct Simple Shear Test

The cyclic direct simple shear test is more accurate in terms of reproducing earthquake stress conditions compared to the cyclic triaxial test. In this test, a short, prismatic soil sample is kept under restriction against lateral expansion by a rigid boundary platen. The test soil sample is deformed when cyclic horizontal shear stresses are applied to the top or bottom of the soil sample (Kramer, 1996).

The drawback of the cyclic direct simple shear test is that shear stresses are only applied on the top and bottom surfaces of the specimen. It creates nonuniformity of stresses on the vertical side. The effects of nonuniformity of stresses are intensified by

8

decreasing the diameter/height ratio of the soil sample (Kramer, 1996). These effects are small at diameter/height ratios greater than about 8:1 (Kovacs & Leo, 1981).

The shear modulus is calculated directly from a shear stress vs. shear strain diagram. The equation used to calculate the shear modulus is given by:

$$G = \frac{\tau_{max}}{\gamma_{max}} \tag{1.6}$$

where: G: shear modulus (the slope of the line connecting the two extreme end points of the hysteresis loop); τ_{max}: maximum shear stress; γ_{max}: maximum shear strain.

The damping ratio is also directly calculated from the stress-strain diagram using the same equation in the cyclic triaxial test. It also can be determined using the free vibration method. In this method, the soil sample is subjected to a predetermined strain in the horizontal direction then released to vibrate freely. The displacement decay is then measured with time by a linear variable differential transformer (LVDT) to determine the damping using:

$$\lambda_f = \frac{1}{2\pi} \times ln\frac{X_n}{X_{n+1}} \tag{1.7}$$

where: λ_f: percent of critical damping in free vibration; X_n: the ordinate of the *n*th cycle

X_{n+1}: the ordinate of the *n*th+1 cycle.

The shear modulus is determined using the theory of transverse vibration of shear beams by:

$$G = \frac{24 \gamma H^2}{g T^2} \tag{1.8}$$

where: H: height of soil block; g: gravity acceleration; T: period of free vibration;

γ: unit weight of soil.

1.3.3 Cyclic Torsional Shear Test

By loading cylindrical soil samples in torsion, many problems associated with the cyclic triaxial and cyclic direct simple shear tests can be resolved. Both isotropic and anisotropic initial stress conditions are allowed using the cyclic torsional shear test. This test is mostly used to determine stiffness and damping characteristics over a wide range of strain levels. This test has two methods of forced and free vibration (Kramer, 1996).

Solid or hollow samples can be used in the forced vibration method. Solid samples have the drawback of nonuniform shear strains (being zero at the center and maximum at the edges). Therefore, hollow cylinders are introduced to resolve this problem (Kramer, 1996).

In the free vibrating method, a solid cylindrical soil sample is initially twisted at one free end and then released to vibrate freely. A relatively heavy weight is placed on the free end of the soil sample making a one degree of freedom system, with the stiffness given by the soil and the inertia offered by the weight (Kramer, 1996). The resulting frequency and shear modulus of the soil sample is then determined using the following equation for a single degree of freedom system (Shannon & Wilson, 1972).

$$G = \frac{W_{nc}^2 \, K}{1 - \frac{W_{nc}^2}{W_{ni}}} \tag{1.9}$$

$$W_{nc} = \frac{W_{dc}}{1 - D_c^2} \tag{1.10}$$

$$W_{ni} = \frac{W_{di}}{1 - D_i^2} \tag{1.11}$$

where: K: constant characteristic dependent upon the geometry of the system; W_n: the natural frequency of either the apparatus (i) or the entire system (n); D: the critical damping ratio of either the apparatus (i) or the entire system (n).

The damping ratio of soil is measured the same way it was measured in the large scale free vibration simple shear test. The cyclic torsional shear test has almost the same limitations as the cyclic triaxial test due to their similar configurations.

1.3.4   Piezoelectric Bender Element Test

This type of test allows measurement of shear wave velocity on laboratory specimens using piezoelectric bender elements (Shirley & Anderson, 1975); (Dyvik & Madshus, 1985); and (De Alba & Pyke, 1987). Bender elements are made by bonding two piezoelectric materials together in such a way that a voltage applied to their faces causes one to expand while the other contracts forcing the entire element to bend as shown in Figure 1-3 (Kramer, 1996). In the same way, a lateral disturbance of the bender element will generate a voltage, so the bender elements can be used as both s-wave transmitters and receivers (Kramer, 1996).
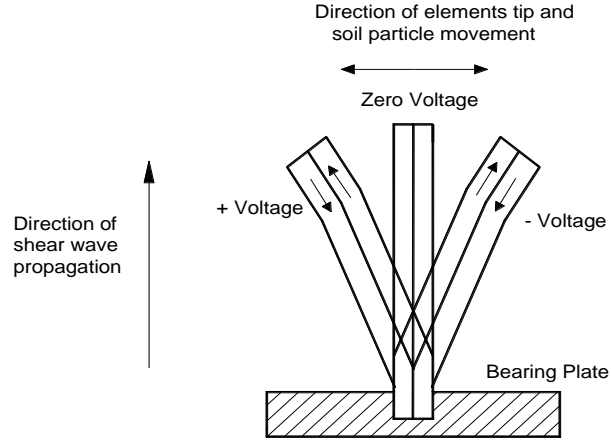
Figure 1-3: Piezoelectric bender elements.
Positive and negative voltage charges cause the element to bend (Kramer, 1996)

In most setups, the bender elements are installed in opposite ends of a soil specimen. A voltage pulse is applied to the transmitter element, which causes it to generate an S-wave (Kramer, 1996). The transmitter element shakes at high frequencies in the horizontal direction and generates s-wave propagation from one end towards the other end of a soil sample where it is picked up by the receiver element (Towhata, 2008). When the S-wave arrives at the other end of the specimen, distortion of the receiver element generates another voltage pulse. The time difference between the two voltage pulses is measured with an oscilloscope and divided into the distance between the tips of the bender elements (tip to tip/end to end distance) to give the s-wave velocity of the specimen (Kramer, 1996).

$$V_s = \frac{Travel\ distance}{Travel\ time} \tag{1.12}$$

The piezoelectric bender elements test can be performed in conjunction with running other tests on a specimen at the same time. It has been run with conventional and cubical triaxial devices, direct simple shear devices, oedometers, model tests (Arulnathan,

12

et al., 2000), and resonant column tests. The benefit of using it with a high voltage type of testing is that it can provide a value for maximum shear modulus (G_{max}) of soil specimens. It is also used with a low voltage type of testing, i.e., resonant column testing (RC) to increase the accuracy of test results. The operator can compare the G_{max} obtained from RC with the one obtained from bender elements.

Shear wave velocity is measured in triaxial specimens using piezoceramic bender elements (Bates, 1989); (Brignoli, et al., 1996); (Blewett, et al., 2000); (Pennington, et al., 2001); (Greening & Nash, 2004); (Leong, at al., 2005). Small strain stiffness, G_{max}, of soil specimens is determined in resonant column (Dyvik & Madshus, 1985), oedometer (Dyvik & Madshus, 1985); (Kawaguchi, et al., 2001), and direct simple shear (Dyvik & Madshus, 1985) apparatuses using piezoelectric bender elements. Finally, a bender element device is used in a triaxial cell material to calculate the damping ratio (Karl, et al., 2008).

To date, the bender element test has yet to be standardized. This is due to the fact that differences arise with respect to method of interpretation (Viana da Fonseca, et al., 2008) and some uncertainties; such as, not being clear whether the travel distance is the distance between two ends of the specimen, the distance between tips of bender elements, etc. Furthermore, the time traveled is supposed to be the time difference between transmitted wave and arrived wave. The arrived wave cannot be clearly defined to be the arrival of initial shaking or the arrival of the wave peak (Towhata, 2008). This uncertainty is due to the fact that the wave field is not one-dimensional but is subjected to a more complex near-field effect (Brignoli, et al., 1996).

1.3.5 Resonant Column Test

The resonant column test is the most frequently used laboratory soil test for measuring low strain properties 10^{-6} to 10^{-4} (10^{-4} % to 10^{-2} %). The method of resonant column testing was first developed by K. Iida in 1939s. It has become well accepted worldwide since the 1950s. In the beginning, Ishimoto and Iida (1936, 1937) established both a theory and a device for resonant column tests, in which the loading frequency was used to determine the elastic properties of soils. During that time period, they were not able to apply confining pressure to consolidate the specimen; thus, soil samples with fines and moisture that could maintain shape without pressure application, were put into testing. Afterward, Iida (1938) performed tests on dry sand, which was supported by cellophane sheets (Towhata, 2008). The test is used to indirectly measure the shear modulus or elastic modulus and damping of soils based on the theory of wave propagation in prismatic rods by Richart el al. 1970 (Woods, 1978). It can be run on both solid and hollow specimens.

Resonant column testing has been gaining popularity in soil dynamics laboratory studies since it was first used by Japanese engineers. It is modified based on the needs of different research purposes. There are two methods, a Fixed-Free and a Free-Free method to determine dynamic properties of soil.

Vincent P. Drnevich patented the most commonly used fixed free resonant column apparatus on December 9, 1975[1]. As shown in Figure 1-4, the apparatus is used

---

[1] United States Patent, Patent#: 3,924,451, Inventor: Vincent P. Drnevich, Resonant Column Testing Apparatus

for testing the behavior of a column of soil placed between a pair of platens within a

pressurized chamber in which torsional or longitudinal vibrations can be applied.
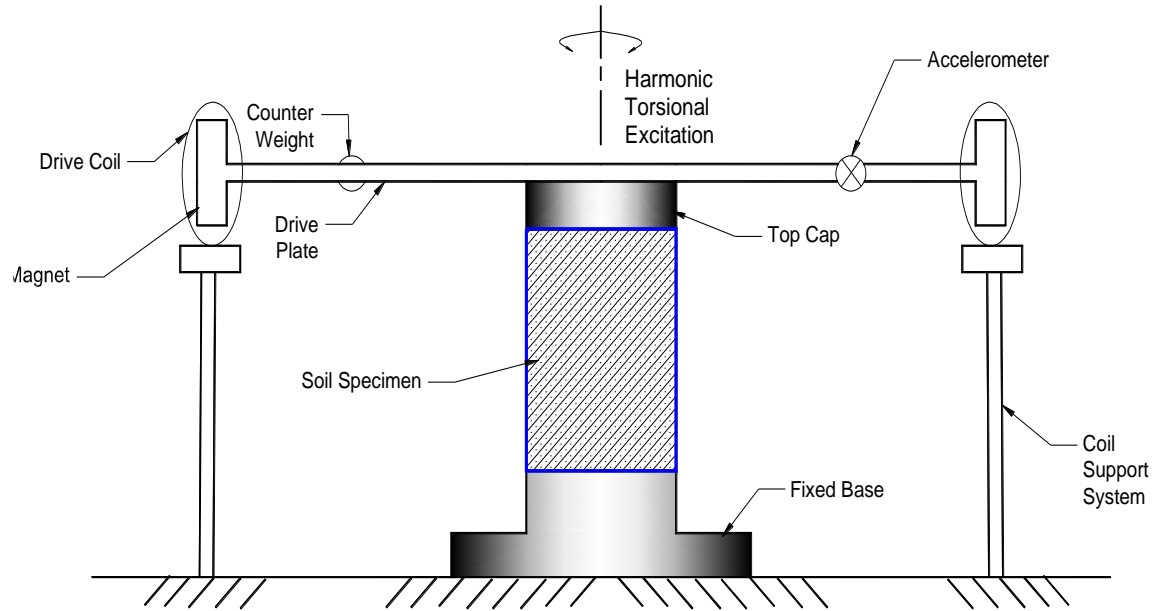
Figure 1-4: Specimen in the resonant column apparatus without the
confining chamber (Kim & Stokoe, 1992)

Harmonic loads are usually the most common loading system for which the frequency

and amplitude are controlled. However, random loading (Al-Sanad, et al., 1983); (Al-

Sanad & Aggour, 1984); (Amini, et al., 1988); (Aggour, et al., 1989) and impulse loading

(Tawfiq, 1986); (Tawfiq, et al., 1988) have also been used as a loading system in

resonant column devices. The effect of coupled loading on the dynamic properties of

clayey (Tawfiq, 1986) and sandy (Aggour & Zhang, 2006) soils has also been examined.

A relatively new Non-Resonance method (NR) has been introduced to determine

dynamic properties of soils at low strains over a broad range of frequencies (Rix & Meng,

2005). The NR method can be implemented using conventional resonant column or

torsional shear apparatus. The advantage of the NR method is that continuous

measurements can be taken over a broader input frequency range. Frequency dependent

behavior of the soil dynamic properties was studied using the method (Meng, 2007).

In the conventional method, the elastic or shear modulus, depending on the

vibration directions, can be indirectly calculated in terms of the resonant frequency.

Shear modulus can be calculated in terms of specimen dimensions and testing apparatus

condition using the following equation:

$$G = 4\pi^2 \rho \left(\frac{f_r L}{F}\right) \tag{1.13}$$

where: G: shear modulus; ρ: mass density of soil specimen; L: height of specimen

F: dimensionless frequency[2]; f_r: resonant frequency of the system.

Damping is determined by switching off the driving power at resonance and recording

the decaying vibration from which the logarithmic decrement is calculated using the

following equation:

$$\delta_s = \frac{1}{n} Ln \frac{A_1}{A_{n+1}} \tag{1.14}$$

where: δ_s: logarithmic decrement (damping); A_1: initial value of amplitude; A_{n+1}:

amplitude after n oscillations.

Damping ratio is also calculated using following equation:

$$D = \frac{1}{2\pi} [\delta_s \ 1 + S \ - \delta_A] \tag{1.15}$$

where: δ_A: logarithmic decrement of the apparatus without specimen; S: system energy

ratio; D: damping ratio; δ_s: logarithmic decrement (damping).

---

[2] It is dependent on the apparatus used in the experiment.

Another type of testing for measurements of G_{max} and D_{min} is called the free-free resonant column method, which was developed by Stokoe et al. in 1994. Using the free-free configuration, the soil specimen is oriented horizontally inside a latex membrane with end caps as shown in Figure 1-5.
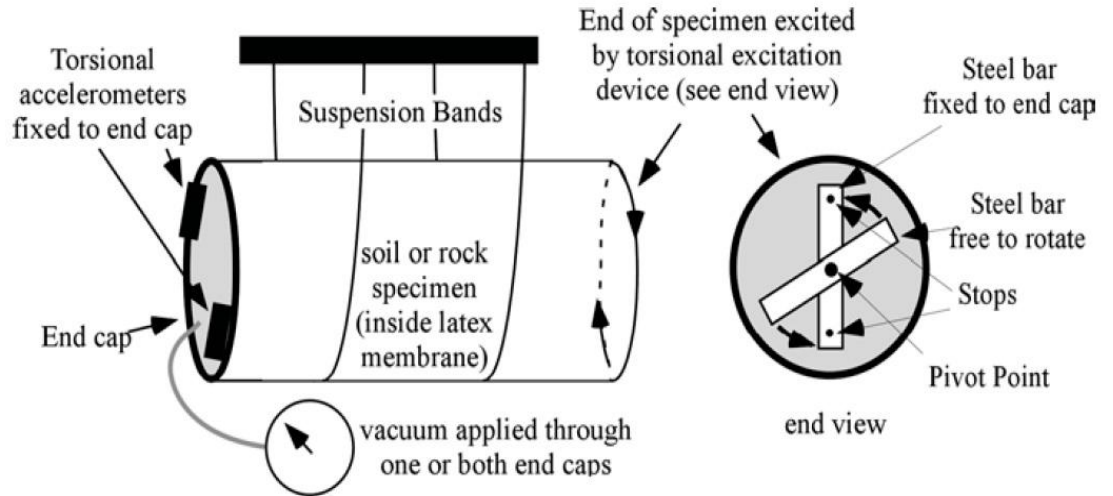
Figure 1-5: Schematic illustration of the free-free resonant column device
(Stokoe, et al., 1994)

The traditional free-free device was limited to a maximum attainable vacuum pressure of around 80 kPa. This was due to the fact that the test had not been configured in a pressurized cell. Therefore, a new free-free device was developed to allow measurements in a pressurized cell with confining pressures greater than 80 kPa that are more representative of in situ conditions. Figure 1-6 shows the schematic configuration for a new free-free device (Kalinski & Thummaluru, 2005).
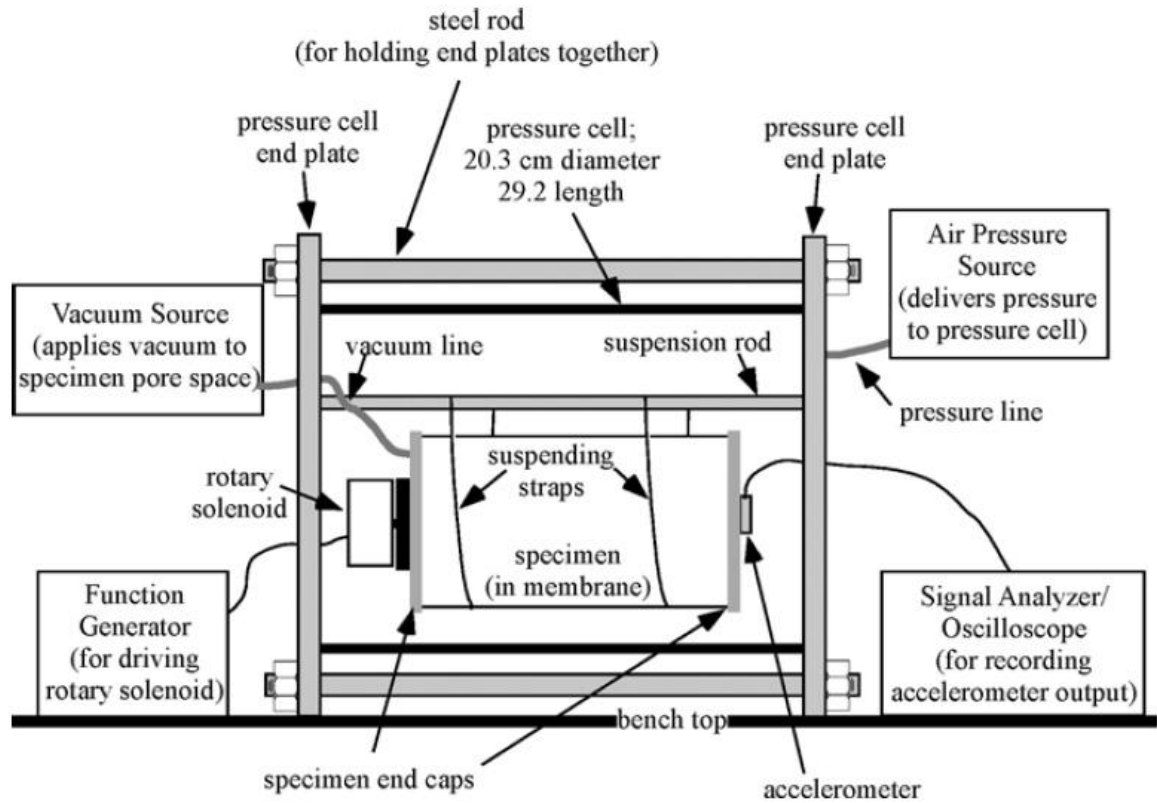
Figure 1-6: Schematic configuration for the new free-free resonant column device (Kalinski & Thummaluru, 2005)

There have been researches conducted on natural clayey soils (Hardcastle & Sharma, 1998); (Hoyos, et al., 2008); (Kallioglou, et al., 2008) and synthetic clay (Tawfiq, et al., 1988); (Chepkoit, 1999); (Amir-Faryar & Aggour, 2012b) using the fixed-free resonant column apparatus. In addition, Bentonite[3] has been blended with the soils to create samples with higher plasticity index (PI) for experimental investigation (Inci, et al., 2003).

---

[3] Bentonite is an absorbent aluminum phyllosilicate, generally impure clay made up of mostly Montmorillonite.

1.3.6 Shake Table Test

This technique uses large size material samples benefiting the free vibration method. 1-G Shaking table research has provided helpful insight into liquefaction, post-earthquake settlement, foundation response, and lateral earth pressure problems (Kramer, 1996). The current version of shaking tables uses multiple degrees of freedom compared to old single-degree-of-freedom[4] devices.
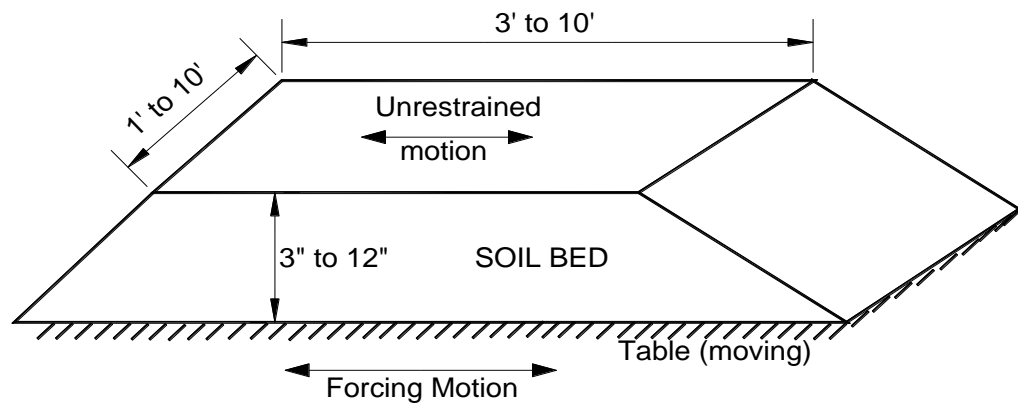
Figure 1-7: Shake table test set up (Wilson & Associates, 1972)

Figure 1-7 shows a typical shake table set up.

The benefit of 1-G shaking table testing comparing to a centrifugal model is that preparation of a model is easier due to its practically larger size. It also has a lower maintenance cost (Towhata, 2008). For a bigger size device like a shaking table, soils can be simply placed, compacted, and instrumented. In addition shaking table models can be viewed without difficulty from different perspectives during tests (Kramer, 1996).

---

[4] Horizontal translation

On the contrary, high gravitational stresses cannot be generated in a 1-G shaking table test. (Kramer, 1996). It also cannot replicate the field stress level and accordingly the stress-strain behavior of tested soil under low-effective stress (Towhata, 2008). Thus, correction procedures have been developed to modify shaking table test results (Hettler & Gudehus, 1985); (Iai, 1989).

Different materials including clayey (Kovacs, et al., 1971) and sandy (Seed, et al., 1977) soils have been tested using this method. The procedure in which shear modulus and damping ratio of soils are determined involved firstly exciting the base of the soil specimen and then measuring the vibration response when the excitation is stopped. Afterwards, the frequency of the first mode is measured and the shear modulus is obtained using the following formula:

$$G = \frac{16 \, \gamma \, H^2 f^2}{g} \qquad (1.16)$$

where: γ: shear strain (%); H: thickness of soil sample; f: frequency of oscillation (1st mode); g: gravity acceleration.

γ is calculated as the soil being vibrated in the steady state condition prior to stopping the excitation. By measuring the frequency of oscillation (f) and acceleration (a) of the steady state vibration, γ can be obtained using the following equation:

$$\gamma = \frac{81.7 \, a}{f^2 g \, H} \qquad (1.17)$$

The damping ratio is computed using a similar approach to that using free vibration excitation.

1.3.7 Ultrasonic Wave Propagation Test

In the laboratory, wave propagation velocities can be measured by means of an ultrasonic pulse test (Lawrence, 1963); (Naccy & Taylor, 1967). An ultrasonic pulse of either compression or shear waves can be produced and received by a piezoelectric[5] material (Hoadley, 1985). By measuring the travel time of the waves over a known distance, the wave velocity and shear modulus can be calculated. This technique has also been used to determine Young's modulus and shear modulus of silty clay (Stephenson, 1978). It has also been used for the ultrasonic assessment of highly plastic clay stabilized with lime, cement, and lime-fly ash class F mixtures (Yesiller, et al., 2001).

A relationship between the wave amplitude of the compression and shear waves and the speed of propagation can be measured as:

$$E = V_c{}^2 \times \rho \times \frac{1 + \mu\ (1 - 2\mu)}{(1 - \mu)} \tag{1.18}$$

$$G = V_s{}^2 \times \rho \tag{1.19}$$

$$\mu = \frac{1 - \frac{1}{2}\ \frac{V_c}{V_s}{}^2}{1 - \frac{V_c}{V_s}{}^2} \tag{1.20}$$

$$\delta = \frac{2.302}{n} \times \log_{10} \frac{A_0}{A_n} \tag{1.21}$$

where: V_c: compression wave velocity; V_s: shear wave velocity; μ: Poisson's ratio; E: Young's modulus; δ: logarithmic decrement (damping); G: shear modulus; P: mass density; A_0: initial value of amplitude; A_n: amplitude after n oscillations.

---

[5] some materials, notably crystals and certain ceramics, that can generate an electric field (Holler & Skoog, 2006)

Not being able to identify and interpret the exact wave arrival time is one of the major weaknesses of this technique (Woods, 1978). This method is only suitable for low amplitude vibrations such as vehicular traffic vibrations because of its low range of strain amplitudes over which the test is conducted. The damping ratio is difficult to determine from this test because of difficulties in obtaining the arrival times of reflecting waves.

1.4   Field Methods

Field techniques are used in the determination of dynamic soil properties and depend mainly on either the measurements of wave velocities (shear or compression), or on the response of soil structure systems (Woods, 1978). There are two types of waves that can propagate through soils, body and surface waves. Body waves are made up of compression waves (P waves) and shear waves (S waves), while the surface waves consist of Raleigh waves (R waves) and Love waves (L waves) (Hoadley, 1985).

Damping measurements are not very reliable if performed in the field. This is due to the fact that the field techniques involve small strain amplitudes. Therefore, the damping values are more reliable if they are obtained from lab experiments. Damping values can be theoretically obtained in the field by observing the decay of the wave motion amplitude with distance from an energy source using the following equation (Shannon & Wilson, 1972):

$$D = \frac{1}{2\pi} \, Log \, \frac{A_1}{A_2} \tag{1.22}$$

where A_1 and A_2 are the vibration amplitudes at successive peaks of the decay curve.

Figure 1-8 shows a typical displacement-frequency curve.
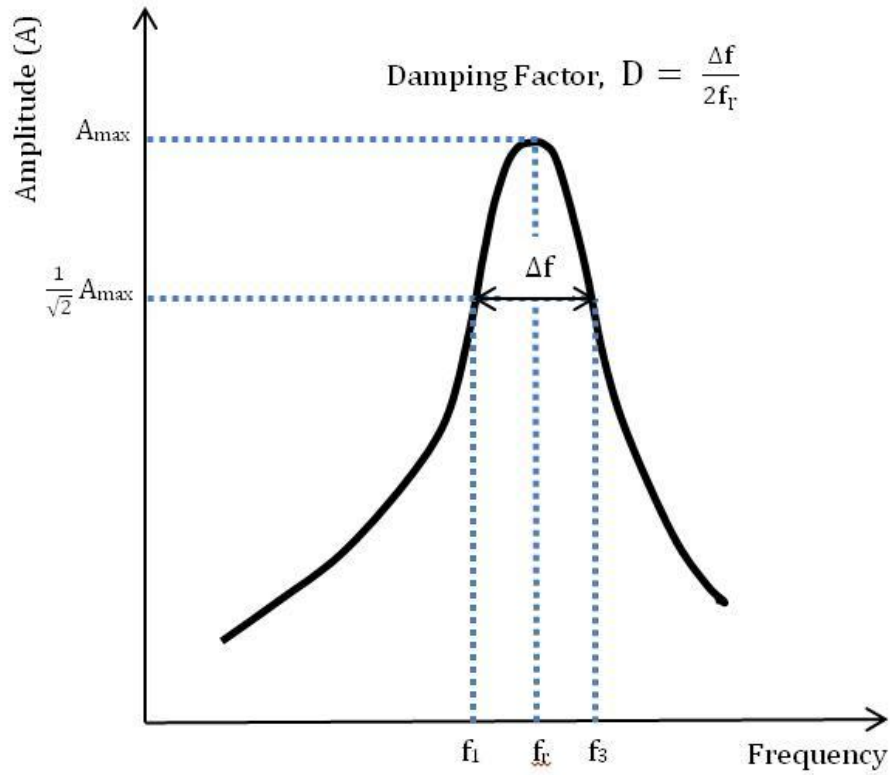
Figure 1-8: Response curve under forced vibration (Hoadley, 1985)

By using such a curve, it is possible to calculate damping by the following equation:

$$D = \frac{\Delta f}{2f_r} \tag{1.23}$$

where: Δf: width of response curve at an amplitude equal to $\frac{A_{max}}{2}$; A_{max}: maximum

amplitude; f_r: resonant frequency.

Equation 1.23 is valid when a constant force oscillator is used. Therefore, the values

obtained from this method cannot be directly applied to soil problems induced by a strong

earthquake motion. This is due to the much larger shear strain associated with

earthquakes (Hoadley, 1985). A brief summary of the popular field methods used to

determine dynamic soil properties is described in the following sections.

23

1.4.1 Geophysical Tests

In-hole geophysical testing is a widely used technique among the various field methods. It depends on the measurements of the arrival of shear waves generated by a small explosion or a hammer and collected by one or more geophones[6]. As shown in Figure 1-9, three configurations of the test procedure can be set up based on the placement of energy source and geophones (Hoadley, 1985).
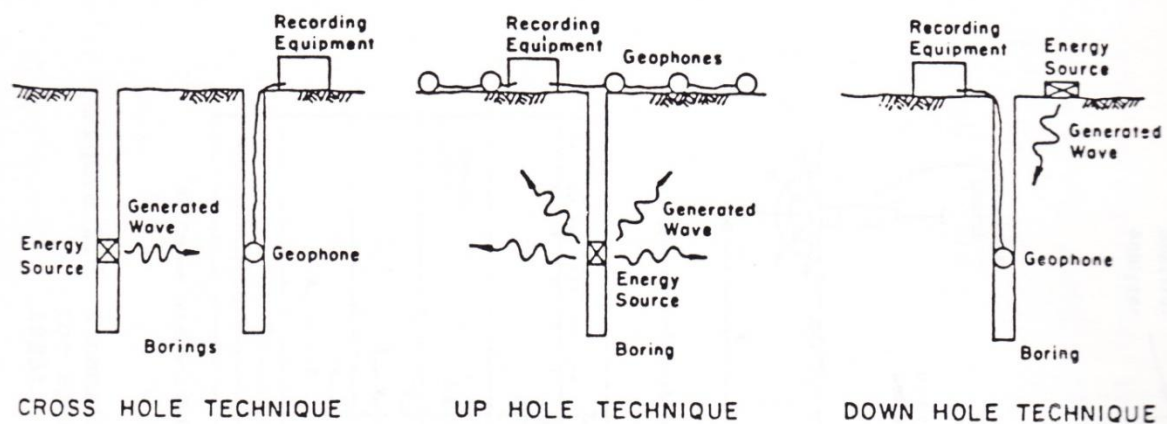
Figure 1-9: Geophysical test setup (Shannon & Wilson, 1972)

Seismic cross-hole tests use two or more boreholes to determine wave propagation velocities at an equivalent depth. The simplest cross-hole test consists of two boreholes, one of which contains an energy source and the other a receiver (Kramer, 1996). To measure the average shear velocity in the up-hole technique, the energy source is placed in the hole while the geophone is placed at the ground surface, contrary to the down-hole technique, where the energy source is placed at the ground surface and the geophone is placed in the hole (Hoadley, 1985).

---

[6] A Geophone is a device that converts ground movement (displacement) into voltage, which may be recorded at a recording station.

In all the geophysical tests, the shear wave velocity is measured in the field, from which the shear modulus is calculated using the following equation:

$$G = \rho V_s{}^2 \qquad (1.24)$$

where: G: shear modulus; ρ: mass density; V_s: shear wave velocity.

It is also possible to measure the compression wave velocity of soil using these geophysical methods. The elastic modulus is obtained in terms of compression wave velocity by using the following equation:

$$E = \rho V c^2 \frac{1 + \mu \ (1 - 2\mu)}{(1 - \mu)} \qquad (1.25)$$

where: E: elastic modulus; V_c: compression wave velocity; μ: Poisson's ratio.

One major difficulty of the geophysical technique is filtering the slower shear waves from the compression waves. This problem can be resolved by reversing the polarity of the energy source in the down-hole technique (Shannon & Wilson, 1972). Another difficulty arises when water table is present. Presence of water table affects the speed of the compression wave, unlike shear waves. Therefore, it is preferable to utilize the shear wave velocity measurements to determine the corresponding shear modulus values.

Another drawback is the low strain amplitude ranges through which these techniques are utilized. Some different techniques can be utilized to increase the strain amplitude range, such as loading the soil cyclically with an in-hole (up-hole technique) anchor connected by a heavy pipe to a large surface vibrator. Difficulties in equipment design and other factors made the technique unfeasible (Wilson, et al., 1978).

A cylindrical in situ test (CIST) is another technique used to measure field soil dynamic properties. The CIST involves deploying accelerometers in the field spaced out at various depths and distances from a central borehole in which explosives are placed. The explosive charge generates a very high pressure causing failure in close proximity to the central borehole and large shear strains at a greater distance from the central borehole. Particle velocity-time records are gained from the accelerometers. Following data retrieval, an iterative one or two dimensional finite difference analysis, which requires initial material properties assumptions, is performed. Adjustments to the initial model are made to regenerate the particle-time velocity histories over a range of dynamic strain levels for each layer of soil (Hoadley, 1985).

One more technique that involves using many boreholes is known as the in situ impulse test. This test is very similar to the cross-hole test except in the generation of controlled shear waves and the spacing of the boreholes. Smaller shear strains are obtained by increasing the distance between the energy source and the boreholes. One of the drawbacks of this procedure is the extra cost involved in drilling more boreholes and placing sophisticated in-hole recording equipment (Hoadley, 1985).

1.4.2   Surface Vibrator Test

In this method, a mechanical or electromagnetic oscillator is used to generate steady-state Raleigh waves. The Raleigh wave velocity can be computed using the following equation:

$$V_R = \lambda_R\, f \tag{1.26}$$

where: V_R: Raleigh wave velocity; λ_R: Raleigh wavelength; f: frequency.

It is assumed that, at low strains, Raleigh wave velocity is approximately equal to the shear wave velocity (Richart, 1960). Therefore, the shear modulus can be directly measured from the Raleigh wave velocity. About one half of the wavelength is an estimate for the effective depth of a Raleigh wave. This introduces a major limitation that deep exploration would require large power generating equipment operating at a low frequency (Hoadley, 1985).

1.4.3 Plate Bearing Tests

The modulus of soil can be either directly measured from the stress-strain curve generated by applying a slow repeated load (Static load test) or by measuring the resonant frequency of a small vibrator placed on the soil in situ (Dynamic load test). Major drawbacks are associated with these two techniques such as the lack of confinement, the modulus being dependent on the size of the plate, and the fact that measurements are limited to the near surface soil (Hoadley, 1985).

1.5   Cohesive Soils

1.5.1   Introduction

Clay is known to be a material whose properties puzzled engineers for centuries. There is hardly any type of soil that is likely to cause more exasperating problems in connection with engineering projects than clay (Terzaghi, 1928). Engineers are frequently required to build a structure on, through, or with clay materials. Therefore, the nature of clay particles and engineering properties of this type of soil needs to be investigated.

Clay is a rock term, and like most rocks it consists of a number of different minerals in varying portions. In soil mechanics, Clay also carries the implication of very

small particle size. Usually the term clay is used in accordance with what is called fine-grained material in soil mechanics. Clay shows plastic behavior when mixed with a small amount of water (Klein & Hurlbut Jr., 1985).

1.5.2 Clay Mineralogy

Clays have been shown to be made up of mainly a group of crystalline constituents known as the clay minerals. They are all fundamentally hydrous aluminum silicates. In some clay minerals, magnesium (Mg) or iron (Fe) substitute in part for aluminum (Al) and alkalis[7] may exist as essential constituents. Although clay may consist of a single clay mineral, there are typically several clay minerals mixed with other minerals such as feldspar, quartz, carbonates, and micas (Klein & Hurlbut Jr., 1985). Montmorillonite, illite, and kaolinite are the most frequently encountered soils in the field (Eades & Grim, 1960).

Kaolinite ($Al_2Si_2O_5 (OH)_4$) is a two layered mineral that is a combination of a silicate sheet with a gibbsite[8] sheet. This two layer arrangement can be repeated many times and the repeated layers are held together by hydrogen bonding[9] and a secondary valence force[10] (Das, 1983). Kaolinite is a common mineral, the main constituent of kaolin or clay. It is always a secondary mineral formed by hydrothermal alteration or weathering of aluminum silicates, specifically feldspar. In rocks that are undergoing alteration, it can be found mixed with feldspar. Kaolinite is one of the common and

---

[7] Alkaline earths

[8] $Al(OH)_3$, is one mineral form of aluminum hydroxide.

[9] Hydrogen bond is an attractive interaction of a hydrogen atom with an electronegative atom, such as: nitrogen, oxygen or fluorine. The hydrogen must be covalently bonded with another electronegative atom to create the bond (Jeffrey, 1997).

[10] Valence force fields are used to describe intra-molecular interactions.

extensive products of the decomposition of rocks found in soils. It has been transported by water and accumulated in lakes in the form of beds of clay deposits. The kaolinite mineral can be found mixed with quartz and other materials (Klein & Hurlbut Jr., 1985).

Illite is a broad term for the mica-like clay minerals (Klein & Hurlbut Jr., 1985). It is a three layer sheet mineral that is made up of an octahedral sheet in the middle and silica sheet on the top and the bottom. The sheets are connected together by potassium ions (Das, 1983). The illites differ from the micas in having less substitution of Al for silicon (Si), and in having potassium (K) partly replaced by calcium (Ca) and Mg (having less potassium than well-crystallized micas (Gaudette, et al., 1964)). Illite is the main constituent in many types of shale (Klein & Hurlbut Jr., 1985).
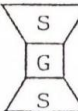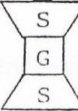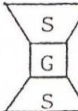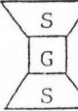
Montmorillonite is the main constituent of clay mineral in bentonite. It can be formed from altered volcanic ash. Bentonite has the rare property of expanding several times its original volume when wetted (Klein & Hurlbut Jr., 1985). Montmorillonite is the clay mineral that is known for most expansive soil problems. Structurally, it is the same as the illite mineral except that the bonding between the sheets is provided by water layers (Das, 1983).

Talc ($Mg_3Si_4O_{10}(OH)_2$) is a secondary mineral shaped by the alteration of magnesium silicates, such as pyroxenes, olivine, and amphiboles, and may be found as pseudomorphs[11] after these minerals. It can be seen in massive form, soapstone, or as a prominent constituent in schistose rocks (Klein & Hurlbut Jr., 1985).

---

[11] A mineral or mineral compound that appears in an atypical crystal form, resulting from a substitution process in which the appearance and dimensions remain constant, but the original mineral is replaced by another. The name literally means "false form".

The specific surface of the clay mineral is expressed as being the surface area of clay particles per unit mass. Table 1-2 shows the symbolic structures of the mentioned clay minerals together with their properties.

Table 1-2: Diagram and properties of clay minerals (Gromoko, 1974)

Property (1)	Mineral		
	Kaolinite (2)	Illite (3)	Montmo-rillonite (4)
Schematic structure [a]			
Particle thickness	$0.5\mu-2\mu$	$0.003\mu-0.1\mu$	9.5 Å
Particle diameter, in microns	$0.5\mu-4\mu$	$0.5\mu-10\mu$	$0.5\mu-10\mu$
Specific surface	5–30	65–100	600–800
Cation exchange capacity	3–15	10–40	80–150
Maximum swelling % for surcharge ton per square foot			
0.1	Negligible	350	1,500
0.2	Negligible	150	350

[a]G = Gibbsite sheet; S = Silica sheet; k = Potassium ion.

From Table 1-2, it can be seen that Montmorillonite minerals have the largest specific surface values (600 – 800 m^2/gram) and the largest percentage of swelling.

1.6   Expansive Soils

Clayey soils generally experience a volumetric change associated with the change in their water content. An increase or decrease in the water content respectively can cause heave or shrinkage in clayey soils. The magnitude of such volumetric change depends mainly on the clay mineral present in the soils. Three primary clay minerals are identified

to exist in most clayey soils. These minerals are illite, montmorillonite, and kaolinite (Das, 1983).

In engineering practice, soils are considered expansive if they meet all four of the following provisions. The tests to show compliance with items 1, 2, and 3 are not required if the test prescribed in item 4 is conducted (IBC, 2006).

1- Plasticity index (PI) of 15 or greater, determined in accordance with ASTM D 4318.

2- More than 10 percent of the soil particles pass a No. 200 sieve (75µm), determined in accordance with ASTM D 422.

3- More than 10 percent of the soil particles are less than 5 micrometers in size, determined in accordance with ASTM D 422.

4- Expansion index greater than 20, determined in accordance with ASTM D 4829.

Expansive soils occur in different parts of the world. The countries in which expansive soils have been reported are as follows: Argentina, Australia, Burma, Canada, Cuba, Ethiopia, Ghana, India, Iran, Mexico, Morocco, Rhodesia, South Africa, Spain, Turkey, USA, and Venezuela (Chen, 1988). Expansive soils can cause more damage to structures, especially light buildings and pavements, than any other natural hazard, including earthquakes and floods. In the United States, expansive soils instigate more damage than earthquakes, tornadoes, hurricanes, and floods combined (Jones & Holtz, 1973). The annual costs of these damages are approximated to be about $ 7 billion (Wray & Meyer, 2004); excluding Hurricane Katrina that hit in year 2005 and cost $ 25 billion alone.

31

Expansive soils originate from two parent material sources. These two groups are soils derived from basic igneous rocks and also soils derived from sedimentary rocks. They are derived from the sedimentary rock parent material that contains montmorillonite as a constituent. These soils are found in North America (Donaldson, 1969).

Clay particles carry a negative charge at their face. In order to balance this negative charge in their porewater, they attract positively charged ions from salt (Das, 1983). Some minerals are attracted more than others and cation exchange takes place from left to right as follows:

$$Al^{3+}>Ca^{2+}>Mg^{2+}>NH4^{+}>K^{+}>H^{+}>NA^{+}>Li^{+}$$

Two types of water concerning clay minerals exist. The first is the double water layer which is electrically attracted and encloses the clay particle. The second one is the adsorbed water which is very close and robustly connected to the clay particle. The double layer of water brings about the plasticity of clay. The thickness of this double layer is different from mineral to mineral, thus, the plasticity of each minerals is different. Plasticity is also dependent on the nature and the amount of clay minerals (Bowles, 1979).

The activity of clay is a proposed term used to differentiate clay minerals in terms of their swelling potential. Activity is associated with the plasticity index and clay percentage that exists in certain soils as in the following equation:

$$A = \frac{PI}{C} \tag{1.27}$$

where: A: activity; PI: plasticity index; C: percent of clay size fraction ($< 2mm$).

Typical values of A, for the three clay minerals mentioned above, are given Table 1-3 (Bowles, 1979):

Table 1-3: Typical activity values for three clay minerals (Bowles, 1979)

Kaolinite	0.4 – 0.5
Illite	0.5 – 1.0
Montmorillonite	1.0 – 7.0

Swelling of expansive soils is found to be related to the existence of active clay minerals, such as montmorillonite, and the increase in the natural water content (Das, 1983). Swell potential is defined as the percentage of swell of a laterally confined soil specimen, which has been soaked under 1 psi surcharge after being compacted according to the AASHTO compaction test (Warner & Brown, 1974). After conducting many tests on compacted clay, the following general formula is suggested for predicting swell potential (Seed, at al., 1962):

$$S = \ 3.6 \times 10^{-5} \ \ A^{2.44} \ (C^{3.44}) \tag{1.28}$$

where: S: swell potential; A: activity; C: clay percentage by weight.

Based on this equation, the following classification is presented for the degree of expansion of clayey soils:

Table 1-4: Degree of expansion classification of clayey soils based on swell potential
(Seed, Woodward, & Lundgren, 1962)

Degree of expansion	Swell Potential (S)
Low	0.0 – 1.5
Medium	1.5 – 5.0
High	5.0 – 25.0
Very high	> 25.0

The previous equation is further simplified to incorporate plasticity index:

Table 1-5: Equations for predicting swell potential of clayey soils using plasticity index
(Seed, et al., 1962)

$19 < C < 70$ $\quad\quad S = 3.6 \times 10^{-3} (PI)^{2.44}$ $\quad$ Error within 20 % S

$40 < C < 80$ $\quad\quad S = 2.16 \times 10^{-3} (PI)^{2.44}$ $\quad$ Error within 30 % S

There are many other similar equations in the literature to determine the swell potential of

clay. Swell potential can also be obtained in the laboratory by the following tests

(Gromoko, 1974):

1- Free swell index: In this test, the volume change of soils is obtained after they are

submerged underwater.

2- Atterberg limits: Liquid limit, plastic limit, plasticity index, and shrinkage limit

are all determined. Then, swell potentials are calculated using correlations such as

the one mentioned above.

3- Colloid content: In this test, percentages of soils having fractions of less than 1-2

µ in diameter are measured. These percentages are deemed to contribute the most

to soils expansion.

4- Consolidation: This procedure depends on the comparison between two samples under swell and pressure. One is allowed to swell under a load while the other is consolidated under pressure. The void ratio against the logarithm of pressure plot is then determined for both samples.

The Transportation Research Board (TRB) gave a full study of the evaluation and control of expansive soils in 1985.

1.7 Lime Stabilization

Lime is an additive used for soil stabilization and improving soil physical and mechanical properties such as minimizing swelling, reducing soil plasticity, and increasing workability. Lime stabilization has been used since the beginning of clearly recorded history and is still being used (McDowell, 1959). The Appian Way[12] is believed to be the first Roman road to feature the use of lime (Winterkorn & Pamukcu, 1991). Lime was extensively utilized during the 2nd world war for roadway and runway construction (Bell, 1996). Examples of projects where lime has been used are the Dallas/Fort Worth Regional Airport in Dallas, TX constructed in 1973, and the Railroad Embankment in Chicago, IL built in 1976 (Boynton & Blacklock, 1986).

Various types of lime are available for the purpose of soil stabilization. The most common used types are hydrated high calcium lime (Ca $(OH)_2$), monohydrated dolomitic lime $Ca(OH)_2.MgO$, and calcitic quicklime $CaO.MgO$. Since most soils are made up of silica and aluminosilicates, the simple addition of lime and water provides the desired environment for the chemical composition and ultimately stabilization (Chepkoit, 1999).

---

[12] Appian Way was one of the earliest and most important Roman roads. It connected Rome to Brindisi, and Apulia in Southwest of today's Italy.

1.7.1 Mechanism of Lime-Soil Chemical Reactions

The chemical reactions between soil constituents and lime can be categorized into short term or immediate reactions and also long term reactions.

1.7.1.1 Short Term/Immediate Reactions

When lime is combined in a clay-water system, the calcium cations with a valence of two (divalent) replace the cations of single valence (e.g., Na^+, K^+), which are typically adsorbed at the clay surface. The cations exchange because the addition of lime causes stabilization of the diffused water layer and a reduction in its size. The clay particles move more closely toward each other. Ultimately, attraction of broken bonds at the edge of the clay particles to the oppositely charged surfaces of neighboring clay particles takes place (Little, 1987). This immediate phase of reaction is termed "lime modification" of soil (Hsay-Yang, 1990). The above reaction (cation exchange and flocculation[13]/agglomeration) takes place within 96 hours of commencement of reaction (Little, 1987). These two reactions tend to decrease the liquid limit and the plasticity index, increase the plastic limit, the shrinkage limit, and workability, and also improve the strength (Das, 1984).

The effects of short term reactions on the particles are as follows (Little, 1987):

1- Substantial decline and stabilization of the adsorbed water layer.

2- Increased internal friction among the flocculates and greater aggregate shear strength provided by edge to face contact of the clay particles.

---

[13] As defined by IUPAC (International Union of Pure & Applied Chemistry), flocculation is "a process of contact and adhesion whereby the particles of dispersion form larger-size cluster". Flocculation is synonymous with agglomeration and coagulation.

3- Textural change from plastic clay to friable, sand-like material that helps improve workability

Figure 1-10 and 1-11 respectively show parallel arrangements of natural clay particles and edge to face contacts of lime-treated clay particles.
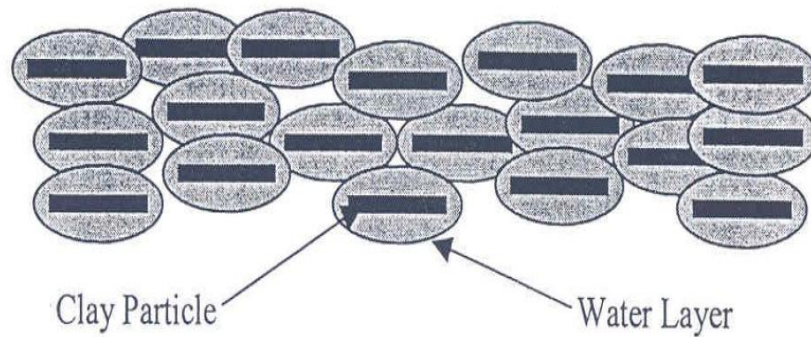
Figure 1-10: Parallel arrangements of natural clay particles (Carmeuse Technical Training, 2002)
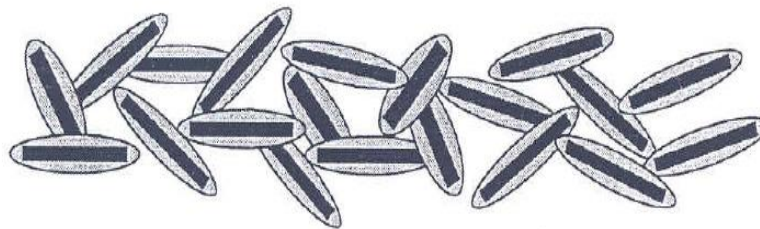
Figure 1-11: Edge to face contacts of lime-treated clay particles (Carmeuse Technical Training, 2002)

The degree of effect and the amount of lime required to cause cation exchange is based on the chemical and mineralogical state of the soil and the water environment (Little, 1987).

1.7.1.2 Long Term Reactions

The long term effect is broken down into two phases of Pozzolanic action (long term strength gain) and Carbonation.

Pozzolanic action is more complex reaction that increases the strength with time. It is greatly influenced by soil conditions and mineralogical properties. Clays mostly contain finely divided siliceous or aluminous materials, which in the presence of water and calcium will shape calcium-silicate-hydrates or calcium-aluminate-hydrates. The reactions are shown by the following chemical equations (Carmeuse Technical Training, 2002):

$Ca^{++} + OH + $ Soluble clay silica $\rightarrow$ Calcium Silicate Hydrate (CSH)

$Ca^{++} + OH + $ Soluble clay alumina $\rightarrow$ Calcium Aluminate Hydrate (CAH)
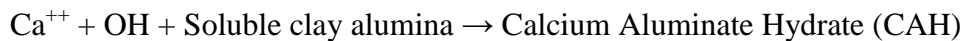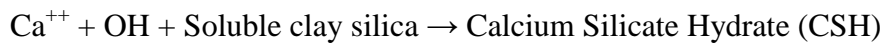
It is proposed that these two hydrates are the cemented products that contribute to the development of a cemented matrix among the soil particles (Little, 1987). Pozzolanic reaction is effective at a high PH condition, hence the soil-lime-water system should have a pH high enough (about 12.45) to facilitate this reaction. Lime is then used in two ways in this phase of the reaction (Carmeuse Technical Training, 2002):

1- To induce high pH condition, which makes soluble or increases the solubility of the silica and alumina.

2- To supply the residual free calcium, which combines with the silica and alumina provided by the clay.

In general, cementation is a time dependent reaction. Also, it depends on the soil type and amount of lime.

Carbonation is an undesirable reaction that takes place when the lime added to the soil does not react with the soil, but pulls out carbon-dioxide (CO_2) from the air or soil to form insoluble calcium carbonate ($CaCO_3$) (Thompson, 1969). Calcium carbonate is a plastic material that increases the plasticity of the soil and lime blends and prevents the pozzolanic reaction. This undesired situation is obtained when the soil does not contain an adequate amount of siliceous and aluminous material, and also when excess lime is used (Carmeuse Technical Training, 2002).

1.7.2 Soil-Lime Mixture Design

The major objective of the mixture design is to assign the quantity of lime required to produce an optimum quality mixture to attain the stabilization objectives and anticipated field conditions. The type of lime is an important factor in soil-lime mixture design. The US government authorities, despite finding a good result using quicklime, has discouraged utilizing it due to possible environmental problems associated with quicklime (Chepkoit, 1999).

Many researchers have used the lime addition of 2% to 8% by weight (Winterkorn & Pamukcu, 1991); (Fahoum, 1994); (Chepkoit, 1999); (He, et al., 2006), and also 1% to 7% by weight (Sakr, at al., 2009). It substantially reduces the plasticity index of clayey soil and also reduces its expansion potential (Fahoum, 1994).

Many procedures are followed to evaluate the soil-lime mixture. They normally include Atterberg Limits tests, California Bearing Ratio test (CBR), R value test[14], swell tests, unconfined compression, and triaxial testing. In the Atterberg Limits tests, the mixture of appropriate amounts of dry soils, lime, and water is generally left for about an hour before conducting the test (TRB, 1987). In the various strength tests, soil samples are typically compacted at optimum water content and prepared according to ASTM D-698 or ASTM D-1557. Afterwards, samples with the required size are extruded and wrapped to prevent any possible moisture loss and carbonation reaction. The soil samples are then cured. The period and temperature of curing varies considerably from one procedure to another. An elevated temperature of 48ºC for 48 hours is usually considered to be equivalent to the occasionally used 30 day room temperature curing (Thompson, 1969). Most of empirical tests to this date follow the same curing pattern of 48ºC for 48 hours (Fahoum, 1994); (He, et al., 2006) unless the effect of different curing temperatures is studied (Rao & Shivananda, 2005); (Sakr, et al., 2009).

The addition of lime causes the following effects on soils properties:

1- Compaction: The addition of lime decreases the maximum dry density and increases the optimum water content (Neubauer & Thompson, 1972).

2- Plasticity and Workability: An immediate change in the Atterberg limits is related to the addition of lime and water. It is proven when the amount of colloidal clay and the chemo-physical activity of the soils are higher and is more likely to see a decrease in liquid limit of the soil (Brandl, 1981). This statement implies that

---

[14] This test is used by Caltran (California Department of Transportation) for pavement design, replacing the California Bearing Ratio test.

montmorillonite clay, which is very active, would be affected the most and the changes in the Atterberg limits would be substantial.

3- Volumetric Change: One of the measuring indices of swelling potential of cohesive soils is the plasticity index. Since this parameter considerably decreases with the addition of lime, it is safe to conclude that the swelling potential will also decrease (Fahoum, 1994).

Many tests are conducted on various types of cohesive soils treated with lime and cured to 48 hours at 48ºC. Consequently, the swelling is reduced to 0% - 0.1% as compared to the swelling values, before treatment, of 2.6% - 0.1% for the soils tested (Thompson, 1969).

4- Strength: The strength of compacted samples is generally measured by different methods. The most widely used method is the unconfined compression test. Other methods include the undrained triaxial test, CBR, and R value. At first, an immediate increase in strength is noticed followed by much higher strength with time as a result of the pozzolanic reaction (Fahoum, 1994).

Lime stabilization in the field can be accomplished in three ways (Fahoum, 1994):

1- Mixing in with original or borrowed materials in the field and then compacting with the addition of water.

2- Soil-lime mixture is attained at the plant and then compacted at the site.

3- Pressure injecting lime slurry to a depth 2 – 3.5 m at a spacing of 2 - 2.5 m.

A general study of lime-soil mixture with regard to reaction, strength, sample preparation, and methods of construction is given by the Transportation Research Board, State of the Art Reports, 1987.

1.8   Fiber Reinforcement

Use of fiber reinforcement in construction materials can be traced back to prehistoric times, when civilizations in Mesopotamia[15] added straw to mud bricks (sun-dried soil bricks). The goal was to provide strength to a weak matrix by taking control of the growth of cracks and improve soil properties. Europeans utilized horse hair for reinforcing plastic materials, and civilizations in Australia and New Zealand used vegetable fibers as reinforcement for plaster-boards at a much later date. The mentioned applications were limited to a fairly small scale. Composite material technology continued to remain fairly undeveloped until the early part of the 20th century, when it took a giant leap with the development and production of reinforced concrete (Majundar, 1975).

Early applications of soil fiber composites were in the area of reinforced earth. In the late 1960s, some research investigations were conducted on utilization of galvanized steel for reinforcing earth retaining structure backfill (Vidal, 1978).

In 1966, the evaluation of random fiber reinforced concrete took a new turn since the formation of the America Concrete Institute Committee 544 (American Concrete Institute Committee, 1973). Determination of design strength and various moduli have been determined by taking fiber concentrations, orientation, and geometry into account,

---

[15] Mesopotamia is a toponym for the area of the Tigris and Euphrates rivers system. It largely corresponds to modern Iraq, as well as parts of Northeastern Syria, parts of Southeastern Turkey, and parts of Khuzestan province in Southwestern Iran (Bottero, 1992).

as well as the usual water-cement ratio, air content, density, and other related factors. It was concluded that the occurrence and development of bonds between the matrix and fiber is of vital importance (Hoff, 1979). In addition, empirical verification of fiber reinforced concrete has led to the application of classical composite theory (Hoover, 1982).

In the mid-1970s, the idea of using Sulfur treated Bamboo to reinforce earthen slopes, dams, and backfill material was introduced and some studies were performed on the possibility of using Bamboo for earth retaining structures. The studies indicated that Bamboo reinforcement improved the shear strength of soil and could be economical when used to reinforce engineered structures. For existing dams and also embankments, it was recommended that the Bamboo be vertically placed, with its length extending further than the depth of a theoretical failure plane. For new embankments or dams, it was recommended that the Bamboo should be horizontally placed, either in the form of strips or the form of a mat. It is also noteworthy to mention that Bamboo reinforced earth retaining structures have shown better resistance to seismic excitations than non-reinforced earth retaining structures (Fang & Meleta, 1979).

Some research on utilization of fabrics in roadway soils were first conducted in the mid-1970s (International Conference on the Use of Fabrics in Geotechnics, 1977). It was also shown that non-woven fabrics could increase the stability of aggregate roads as well as soil roads (Hoover, et al., 1981).

The utilization of both natural and synthetic fibers as reinforcements for cohesionless soils was investigated at prearranged fiber orientations in the mid-1980s.

The study showed that shear strength is a function of fiber type, fiber length (FL), fiber orientation, and fiber volume fraction (Gray & Ohashi, 1983).

The use of randomly reinforced fibers with cohesive soils was examined in 1986. It was shown that the inclusion of fiber could result in greater strength as well as toughness in compacted fine-grained soil (Freitag, 1986).

1.8.1 Discrete Geofibers

Geofibers are defined as any type of fiber material that is mixed with soil for improving geotechnical properties of soil. Geofibers are blended into soils to enhance geotechnical properties of soil and to create an improved reinforcement-soil system. Geofibers, by mixing or meshing with the soil already on site, can help to create a soil reinforcement system that work together to improve soil engineering properties. In addition, reinforcement of expansive soils with discrete geofibers (flexible polymeric fibers) can be an alternative method to chemical stabilization techniques and other methods for enhancing geotechnical properties of clayey soil.

A broad classification of Geofibers in terms of material is as follows:

1- Synthetic fibers are man-made flexible polymeric fibers, such as: Olefin fibers (Polypropylene (PP) fibers, Polyethylene (PE) fibers).

2- Natural fibers are made from natural (animal, plant) materials, such as: cellulose fibers (e.g. Coir fibers), asbestos fibers.

Various chemical processes are sources for manufacturing synthetic fibers. Synthetic fibers are classified into high modulus, high strength fibers, and low modulus, high elongation fibers. The former includes fibers composed of materials such as steel,

fiberglass, carbon, etc., while the latter comprises fibers such as polypropylene and polyethylene (Mangat, 1976).

Cellulose fibers are reinforcing fibers that can be found in their crystalline form. They can be classified according to the part of the plant from which they are obtained (Parrat, 1972). Cellulose fibers typically have lower values of elastic modulus and tensile strength than most synthetic fibers but are plentifully available in bulk (Krenchel, 1973). It is known that natural fibers may be affected by varying environments (Parrat, 1972). Furthermore, because natural fibers are not homogeneous, a constant parameter cannot be obtained for their geometry; hence, it can complicate any design procedure. Also, another drawback in using natural fibers is that they are biodegrade when placed in alkaline environments and may also be susceptible to microbiological attack and rotting (Parrat, 1972); (Krenchel, 1973).

Asbestos fibers are known to have high chemical resistance and provide good mechanical properties, such as high tensile strength and elastic modulus. They can also undergo severe pretreatment conditions during mixing and are available at low cost and in bulk quantities. These fibers had been extensively used as reinforcement for cement mortars, but due to the fact that they are a hazardous material and can cause human cancer, the usage of these fibers has been limited (Krenchel, 1973).

Synthetic fibers have two well-recognized advantages over natural fibers. First, these fibers can be manufactured according to users' desired specifications; for example, the geometry of fibers can be controlled, and the shape of fibers and surface conditions can be modified in order to improve the frictional properties of the fibers. Second,

synthetic fibers do not biodegrade when subjected to extreme environments in engineering scales such as variability of moisture, cold, heat, or sunlight (Krenchel, 1973).

Olefin fiber is a man-made fiber in which the fiber-forming substance is a long-chain synthetic polymer made up of at least 85% by weight of ethylene, propylene, or other olefin units. Olefin fiber is a broad description that covers thermoplastic fibers obtained from olefins, predominately aliphatic[16] hydrocarbons[17]. Olefins can be produced from polymerization of propylene and ethylene gases. Polypropylene (PP) and Polyethylene (PE) are the two most frequently used members of the Olefin family. Polypropylene is extremely versatile as a fiber-forming material, whereas polyethylene is not when formed as fiber (Kadolph & Langford, 2002).

Table 1-6: Properties of fibers commonly used in civil engineering materials (Hannant, 1978)

Fiber Type	Subcategory	Diameter (μm)	Length (mm)	Density (kg/m$^3\times10^3$)	Young's Modulus (MN/M^2)	Poisson's Ratio	Tensile Strength (MN/M^2)	Elongation at Break (%)	Typical Volume in Composite (%)
Asbestos[18]	Chysotile	0.02-30	40	2.55	164	0.3	200-1800	2-3	10
Asbestos	Crocidolite	0.1-20	-	3.37	196	-	3500	2-3	-
Cellulose		-	-	1.2	10	-	300-500	-	10-20
E-Fiberglass		8-10	-	2.54	72	0.25	3500	4.8	-
Polypropylene	Monofilament	100-200	5-50	0.9	5	0.29-0.46	400	18	0.1-6
Polypropylene	Fibrillated	500-4000	20-75	0.9	8	0.29-0.46	400	8	0.1-6

Fiber content is typically expressed in terms of volume fraction or weight fraction, either term characterizing the amount of fiber in a composite as a percentage of

---

[16] In organic chemistry, compounds composed of carbon and hydrogen are classified into two classes: aromatic compounds, which contain benzene (C_6H_6) rings or similar rings of atoms, and aliphatic compounds, which do not comprise aromatic rings (Gold, 1995).

[17] A hydrocarbon is an organic compound consisting of hydrogen and carbon in its entirety (McMurry, 2000).

[18] Nowadays, the use of Asbestos in the construction industry is limited due to its hazardous nature.

total volume or total weight of the composite, respectively (Agrawal, et al., 1980). One of the advantages of polypropylene over other types of olefin is its ability to be used in a wide range of fibrous forms.

1.8.2   Description of Geofibers

Geofibers can be produced in three forms: continuous filaments, staple fibers, and slit films. A filament has infinite length and is produced by extruding melted polymer through dies[19] or spinnerets[20]. The filament is usually stretched to longitudinally orient its molecules after extrusion, resulting in greater strength. Monofilament yarns consist of a single filament. Two or more filaments may be arranged in line to form a multifilament yarn. Staple fibers are manufactured by cutting filaments in lengths of 1 to 4 inches. A spun yarn is produced by inter-connecting and twisting staple fibers together. Slit film (plain tape) is produced by cutting a cast film into narrow tapes that are oriented and drawn in the machine direction (uniaxially). A fibrillated yarn is a slit film fiber which has been partially slit to make a series of connected fibers, and then twisted (Maier & Calafut, 1998).

1.8.3   Geotechnical and Dynamic Properties of Clayey Soils Stabilized with Polypropylene Fibers

In recent years, short virgin monofilament fibers have been added and mixed into clayey soils to improve the compressive strength behavior (Freitag, 1986); (Maher & Ho, 1994); (Tang, at al., 2007); (Harianto, et al., 2008), shear strength (Tang, et al., 2007), and also increase their ductility (Maher & Ho, 1994); (Tang, et al., 2007); (Harianto, et

---

[19] A die is a specialized tool used in textile manufacturing industries to cut or shape material using a press.

[20] Spinneret refers to a multi-pored textile machine through which a plastic polymer melt is extruded to form fibers.

al., 2008); (Ple & Le, 2012), tensile strength (Maher & Ho, 1994); (Harianto, et al., 2008), and flexural toughness (Maher & Ho, 1994).

The utilization of recycled short monofilament fibers in clayey soil has also resulted in increasing the compressive and shear strength characteristics of clay (Akbulut, et al., 2007).

Short fibrillated fiber reinforcements have been observed to increase the unconfined compressive strength (Nataraj & McManis, 1997); (Puppala & Musenda, 2000) and shear strength (Nataraj & McManis, 1997); (Zhang, et al., 2000), and also reduce the swelling potential (Puppala & Musenda, 2000) of clayey soils. Tension cracking and volume change due to swelling/shrinking in compacted clays are also reduced when reinforced with PP fibers (Al Wahab & El-Kedrah, 1995); (Nataraj & McManis, 1997).The inclusion of fibrillated fibers can increase the tensile strength of the clay and provide a ductile behavior that was not otherwise present (Ziegler, et al., 1998).

The utilization of recycled short fibrillated fibers in clayey soil has also resulted in increasing the unconfined compressive strength characteristics of clay. It is shown that fiber reinforcement decreased the vertical shrinkage strains; however, it increased the free swell value of raw expansive soils by 2% (Puppala, et al., 2001).

A summary of advantages of using short virgin fiber reinforcement is shown in Table 1-7.

Table 1-7: Advantages of using commercially available short virgin PP fiber reinforcements in clayey soils

Fiber Type	Shear Strength	Tensile Strength	Unconfined Compressive Strength	Swelling Potential	Tension Cracking
Monofilament	Increased	Increased	Increased	-	-
Fibrillated	Increased	Increased	Increased	Decreased	Decreased

Some researchers found that lime treatment is a contributing factor to the soil brittleness that results in relatively rapid and great loss in strength when failure occurs (Sabry, et al., 1996). PP fibers have recently been used in conjunction with lime as a novel stabilization method to reduce the brittle behavior of soil stabilized by lime (Cai, et al., 2006) and shrinkage-induced soil cracking (Puppala, et al., 2001). The effects of moisture content and confining pressure have also been investigated on the dynamic properties of PP reinforced lime modified clayey soil using the resonant column test (Hoyos, et al., 2004).

Furthermore, it has been shown that the inclusion of short PP fiber reinforcement in cemented clayey soil, changes cemented soils' brittleness to a more ductile one. It also increases the unconfined compressive strength, shear strength, and axial strain at failure of cemented clay and decreases the loss of post-peak strength, and the stiffness (Tang, et al., 2007).

1.8.4 Mechanism of Fiber Reinforced Clayey Soil (Geofiber Composite)

The mechanism by which discrete fibers limits swelling of expansive soil is different from using a chemical additive like lime. When swelling occurs in soils, the flexible polymeric fibers used as reinforcement in the soil are stretched out and this is

when the tensile resistance of the fibers against tension comes into assistance and resists further swelling. It is also shown that this resistance to swelling offered by the fibers depends upon the contact area between soil and fiber (Viswanadham, et al., 2008).

The amount of swelling can be reduced in the case of fiber-reinforced swelling clays through the following (Viswanadham, et al., 2008):

1- Tensile resistance offered by the fiber to swelling that depends upon the contact area between clay and fiber.

2- Non-swelling fiber are replaced with swelling clay.

Some laboratory experiments, such as: swell consolidation tests, volumetric shrinkage, and swell pressure tests, have been conducted to assess the feasibility of using fibrillated and slit film fibers in an expansive soil to reduce swell potential. The results indicate that the fiber reinforcement reduces volumetric shrinkage strains, swell pressure, and swell potential of the fiber-soil composite (Puppala & Musenda, 2000); (Viswanadham, et al., 2008).

Swell potential (S%) is reported as the ratio of the increase in the thickness of the sample upon inundation (ΔH) to its initial thickness (H) and swelling pressure (P_s). It is determined by inundating the soil and measuring the pressure required to prevent its expansion (Sowers, 1979).

1.8.5 Fiber Geometry

Length is a main criterion used for fiber classification. Composites produced with fibers shorter than 3 inches are generally called "short fiber composites". Composites consisting of longer fibers are classified as "continuous fiber composites". This is due to

the fact that in most cases the fibers extend throughout the mass of the matrix (Agrawal, et al., 1980).

The mechanics of stress transfer in both classifications are not similar. In the short fiber composite case, applied stresses are first transferred to the matrix material then to the fibers through the fiber ends and also the surfaces of fibers near the fiber ends. On the contrary, in the continuous fiber composite case, applied stresses to the composite are transferred to the fibers and matrix at the same time (Agrawal, et al., 1980).

For short fiber composites, the length parameters, load transfer length (L_t) and critical fiber length (L_{cr}), can be defined. Load transfer length indicates the minimum fiber length in which maximum fiber stress can be attained. It is noted that the maximum fiber stress is a function of the stress applied to the composite. For a stress applied to the composite, the value of maximum fiber stress can be limited by the stress that would be accepted by a fiber of infinite or continuous length. Critical fiber length is defined as the minimum fiber length in which the fiber ultimate strength is achieved. The fiber ultimate strength is not a function of the stress applied to the composite, and hence the critical fiber length is also not a function of applied stress, denoting the maximum value of load transfer length (Agrawal, et al., 1980).

A widely used parameter related to fiber length is aspect ratio defined by length divided by diameter (L/d). The aspect ratio plays an important role in determining the magnitude of interfacial accumulated shear during loading. The larger the aspect ratio, the smaller the amount of interfacial shear developed during loading and hence the stronger the fiber matrix interfacial bond must be (Agrawal, et al., 1980). In the case of a

clayey matrix using slit film fibers; it is shown that at shorter lengths or lower aspect ratios of the fiber, the contact between clay and fiber would be more pronounced resulting in higher resistance to swelling. At longer lengths or higher aspect ratios, the fiber would be more susceptible to bending and folding. It can reduce the contact area between clay and fiber, leading to lesser resistance to swelling.

Furthermore, at higher aspect ratios, compaction efficiency could decrease; consequently, heave reduction is proven to be less at higher aspect ratios. It has been proven when long fibers are randomly mixed, they tend to twist or fold. This reflects in the form of loss of effective soil-fiber contact area for limiting swelling (Viswanadham, et al., 2008).

1.8.6   Fiber Orientation

In fiber-matrix composite fabrication, fibers may be arranged in one, two, or three dimensional orientations. In one dimensional orientation, fibers are aligned parallel to one another and in the direction of the possible applied stress. For two and three dimensional arrangements, fibers maybe either randomly oriented during construction, or ordered to be arranged when fabricated. The difference between two and three dimensional orientations is that in the two dimensional orientation, fibers are positioned almost in a plane; while in the three dimensional, fibers lie in all directions (Allen, 1971).

The principles of reinforcement are similar in all three cases, except that for two and three dimensional orientations some strength reduction factors occur. This is due to the fact that, in fiber-matrix composites, only the fibers normally positioned to the applied stress can carry the applied stress. Hence, for two and three dimensional

52

orientations, some fibers do not bear any stress at all and this is accounted for by applying strength reduction factors. The strength reduction factors are more commonly known as efficiency factors (Hoover, 1982).

When the application of loading direction and magnitude is known, long fiber composites perform well. On the contrary, when the load and its direction can vary or is not known, long fiber reinforced composites do not perform as well. In such cases, short, randomly oriented fiber reinforced composites are desired (Agrawal, et al., 1980).

The main advantages in using randomly distributed fiber reinforcement over typical geosynthetics used in construction are as follows: First, the inclusion of randomly distributed fibers limits any potential planes of weakness that otherwise can develop when oriented reinforcement is used. Secondly, the simplicity of using randomly oriented fibers in the field using self-propelled rotary mixers or other applicable methods. It is used to great extent the same way as other chemical additives such as lime, cement, etc. The discrete fibers are simply mixed randomly with soil to make a uniform distribution. The above mentioned advantages have made randomly oriented distribution of fibers very desirable in recent years (Tang, et al., 2007).

1.8.7 Fiber Material Properties

In order to select Synthetic fibers, a degree of familiarity with terminology used within the textile and fiber industry is required. A brief summary of the most applicable terms follows:

1- Fiber: A general term used for all filaments, yarns, bristles, staples and non-woven entities.

53

2- Filament: An untwisted, individual fiber. Filaments typically have a high aspect ratio and are classified as crimped or uncrimped. Crimping is used to prevent filament separation when bundles are formed in a fiber production plant.

3- Yarn: Refers to a bundle or series of filaments twisted together to produce a single fiber in which the individual filaments cannot be detached.

4- Tow: A long continuous roll of a single filament, groups of filaments, or yarns.

5- Staple: A cut length of fiber measured and expressed in inches; as an example in case, a 0.75-inch staple refers to a cut length of 0.75 inch.

6- Denier: A term used widely in the textile industry and is defined as the weight in grams of 9000 meters (9842.49 yards) of a fiber. As an example in case, if 9000 meters of nylon filament weigh 100 grams, it is classified as a 100 denier filament. Denier can also be an indirect measure for fiber diameter since it is scaled and measured in a constant length of fiber.

7- Aspect ratio: In order to present fiber dimensions in a more conventional manner, an aspect ratio consisting of length divided by diameter is used. This terminology is more applicable to civil engineering and construction than to the textile industry.

8- Tenacity: A measure of tensile strength that can be expressed in terms of grams/denier. As an example, a 100 denier filament that breaks under a 250 gram load is rated at 2.5 grams/denier.

9- Elongation at break: Refers to the strain characteristic of the fiber; i.e., a gauge to measure the amount of longitudinal deformation that occurs prior to failure. Elongation at break is expressed as a percentage.

10- Regain: Tendency of the fiber material to absorb moisture.

Different materials can have a variety of physical and chemical properties. Physical properties of typical fiber materials, along with approximate cost associated with each fiber type are listed in Table 1-8.

Table 1-8: Typical fiber material properties, after (Hoover, 1982)

Fiber Type	Specific Gravity	Tensile Strength (ksi)	Average Tensile Modulus (psi)	Elongation at Break (%)	Elastic Recovery	Survivability	Approximate Cost ($/lb)
Nylon (monofilament 0.9 mm diameter)	1.14	131.3	6×10^5	10-15	High	Moderate	2-4
Polypropylene	0.91	64.1	1.1×10^6	70	High	High	0.75-1.5
Polyester	1.39	103.2	1.6×10^6	30	Low	Moderate	2-7
Polyester	1.39	92.5	1.6×10^6	45	Low	Moderate	2-7
Polyester	1.39	71.2	1.6×10^6	60	Low	Moderate	2-7
Polyester	1.39	58.7	1.6×10^6	43	Low	Moderate	2-7
Type E Fiberglass	2.54	300	10×10^6	2-3.5	Low	High	<1.0

Another factor to take into account is the availability of these materials in desired staple (cut length). All of the synthetic fibers could be commercially made available in different staples and denier within the possible range; however, manufacturers require a minimal order (eg. 1500-2000 lbs) of fiber in order to justify resetting of their cutters to produce specially requested lengths and customized fiber (Hoover, 1982).

Another consideration in the fiber material selection process is paying attention to the range of mechanical properties of the fiber materials. While this consideration in fiber selection might normally be of significance, it is not a critical determinant when dealing with a soil-fiber composite. By a qualitative analysis, it is determined that the degree of

excellent quality of the soil-fiber interfacial bond would be greatly below that normally found in fiber reinforced concrete, or reinforced plastics. Hence, it is not very critical to match fiber properties to those of the soil as a means of controlling the mode of failure that might occur. In other words, the degree of criticality is reduced in soils. Any fiber materials, that are ultimately considered, would be able to provide tensile strengths and moduli far in excess of any desired properties anticipated in soil systems (Hoover, 1982).

Table 1-8 shows that the utilization of PP fiber is economically justified because of its low purchasing cost compared to other fiber materials. It also has a high rate of survivability of the fiber within the soil (Hoover, 1982) and has demonstrated an acceptable resistance to biochemical degradation (Halpin & Tsai, 1969). To determine the rate of survivability, the varying nature of the soil-water system in regards to alkalinity, chemical composition, temperature, and environmental variations are taken into consideration (Hoover, 1982).

1.9 Dynamic Properties of Soil

Small-strain shear modulus (G_{max}) and shear wave velocity (V_s) values of soil are indirect measurements of soil stiffness against dynamic shear force. They are directly related to each other by $G_{max} = \rho \times V_s^2$, where, ρ = mass density of soil (total unit weight of the soil divided by the acceleration of gravity). The values of shear modulus and shear wave velocity of soil can be an indicator of resistance of soil to dynamic shear forces. For instance, the larger values of shear modulus and shear wave velocity of soil can indicate that the soil has a large stiffness to tolerate dynamic shear forces.

Secant value of the shear modulus is called the secant shear modulus (G). It is

used to represent the average soil stiffness at larger strains. The relationship between G,

G_{max} and shear strain (γ) and shear stress (τ) is shown in Figure 1-12.
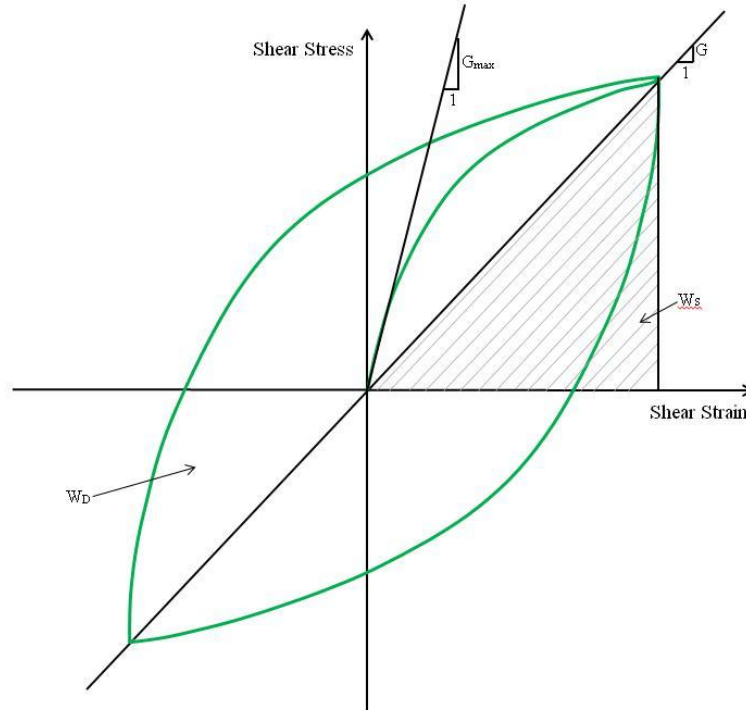
Figure 1-12: Shear stress versus shear strain cyclic graph

The soil damping ratio (D) indicates the dissipated energy in soil. The damping is caused

by friction taking place between particles, strain rate effect, and nonlinear soil behavior.

The hysteretic damping ratio can be obtained by the following formula:

$$D = \frac{W_D}{4 \times \pi \times W_S} \qquad (1.29)$$

where, $W_D =$ energy dissipated in one cycle of loading and W_s = maximum strain stored

during the cycle.

The area of the hysteresis loop is W_D and the area of the triangle is W_s. Ideally, there should be no loss of energy in the linear elastic range for the hysteretic damping model expressed by equation 1.29. However, even at very low strain levels, there is always some energy dissipation observed by laboratory testing. The damping ratio at very low strain levels is considered to be a constant value and is called the small-strain damping ratio (D_{min}). At larger strains, the nonlinearity in the stress–strain relationship causes an increase in material damping ratio with increasing strain amplitude.

1.9.1 Dynamic Properties of Cohesive Soils

Several researchers have studied about dynamic soil properties of cohesive soils and factors affecting them (Hardin & Drnevich, 1972a); (Hardin & Drnevich, 1972b), (Kokusho, et al., 1982); (Aggour, et al., 1987); (Sun, et al., 1988); (Vucetic & Dorby, 1991); (Kagawa, 1992); (Ishibashi & Zhang, 1993); (Lanzo, et al., 1997); (Vucetic, et al., 1998); (Darendeli, 2001); (Stokoe, et al., 2004); (Zhang, et al., 2005); (Nie, 2008); (Kallioglou, et al., 2008); (Biglari, 2012). In comparison with non-cohesive soils, dynamic materials properties of cohesive soils such as the modulus, the damping ratio and their strain dependency are more variable due to the physical and other conditions affecting the soils. The most significant factors affecting the shear modulus and damping of cohesive soils are discussed below. These factors include shear strain amplitude, plasticity index, confining stress, frequency of loading, previous stress history (over-consolidation ratio), void ratio, degree of saturation, and geologic age.

The shear modulus of soils in general and cohesive soils in particular reduces sharply with increasing strain amplitude, γ. On the contrary, the damping ratio increases as shear strain increases. The modulus versus strain amplitude curves are generally

expressed by a normalized reduction curve in which modulus values at any strain are normalized by the small strain shear modulus, G_{max} or G_0. The value of G_{max} is approximately constant for strains below $\gamma = 1 \times 10^{-5}$ or 1×10^{-3} % where the deformations are fully recoverable (linear elastic). In other words the strain-dependent change of shear modulus of clay is very small for the strain less than 1×10^{-5}; therefore, it is almost negligible. In higher strains, the soil behaves as nonlinear elasto-plastic and consequently results in irrecoverable permanent deformations.

As discussed before, PI is an indirect measure of clay mineralogy. It has been shown that the PI of clayey soil has a noticeable influence on the form and location of the normalized modulus reduction curves. Hence, it can be noted that PI is one of the main factors controlling the variation of shear modulus reduction and damping ratio versus shear strain curves. Higher plasticity clays show a slower rate of modulus reduction as well as a gradual shift of the curve location to the right (Kokusho, et al., 1982); (Sun, et al., 1988); (Vucetic & Dorby, 1991). It has also been determined that at the same shear strain value, a clay soil with larger PI has a smaller damping ratio, as shown in the damping ratio versus cyclic shear strain curve shown in Figure 1-13.
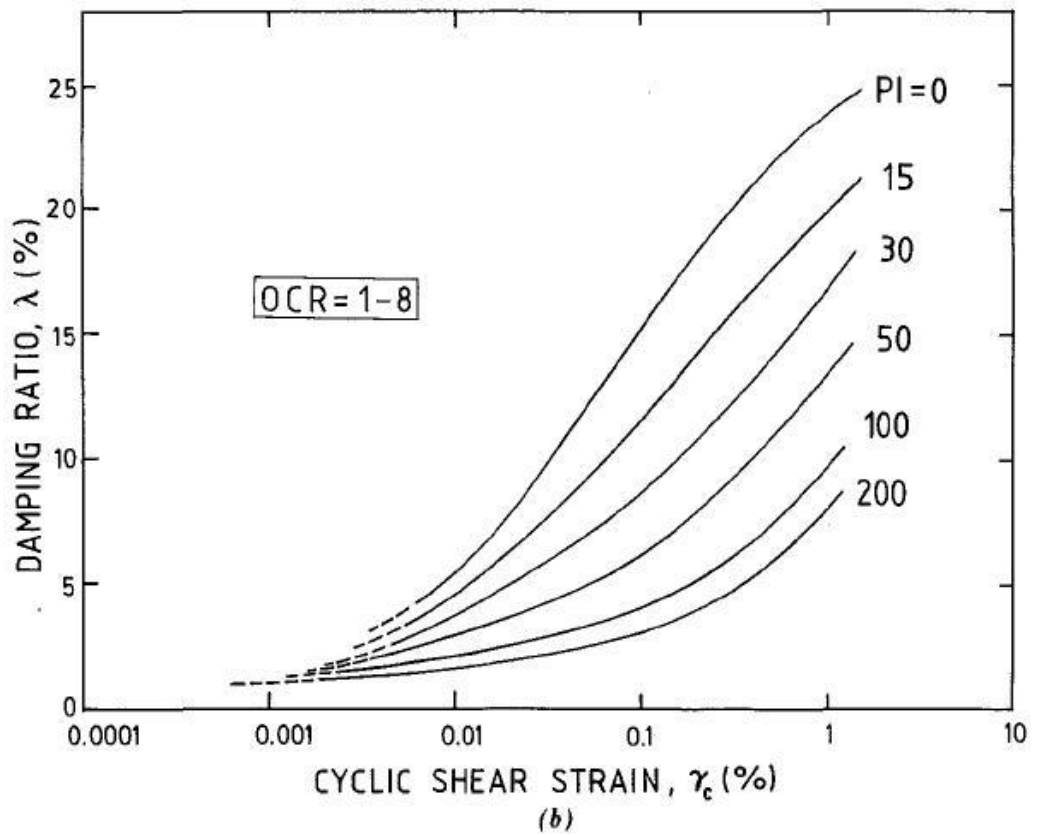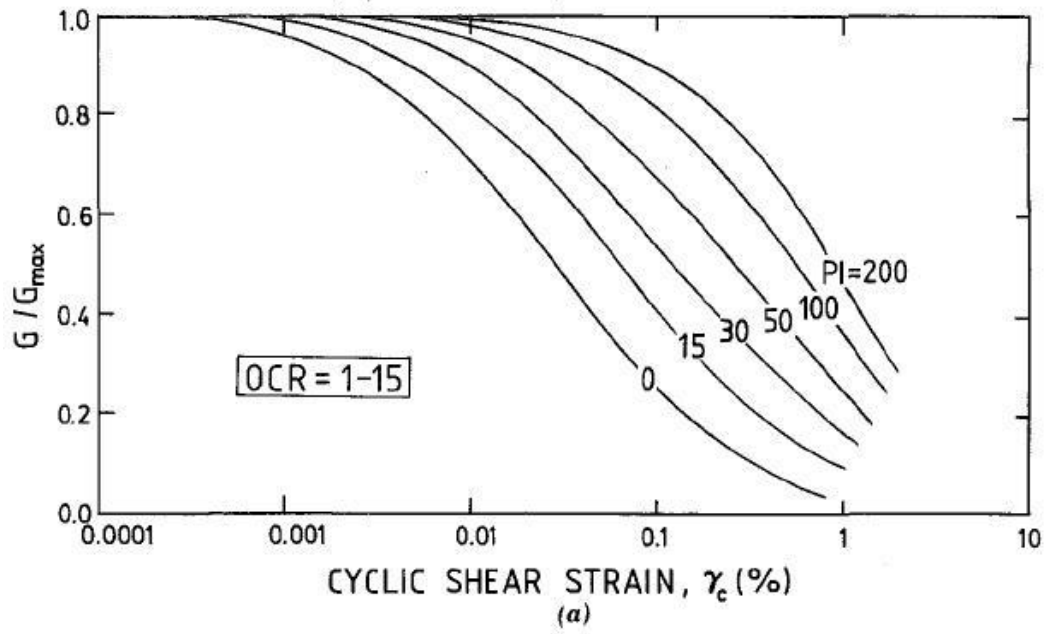
Figure 1-13: Effect of PI on normalized shear modulus (a) and damping (b) versus cyclic shear strain curves of clay (Vucetic & Dorby, 1991)

It is not possible to independently vary both the void ratio and confining pressure for normally consolidated samples. It can be seen that recent research performed varied confining pressures rather than void ratio. This can be due to the fact that void ratio depends on soil structure (fabric and bonding) and composition as well as consolidation stress and over consolidation ratio (OCR) (Hwang, 1997). It has been extensively determined by researchers that shear modulus of soil can increase when confining stress is increased. In addition, the damping ratio of soil decreases as the confining stress is increased.

Stress history also plays an important role in determination of the dynamic properties of cohesive soils. The effect of over-consolidation on the small strain shear modulus of virgin cohesive soils is to increase the modulus as compared to the normally consolidated condition. As the OCR and confining pressure increase, the normalized shear modulus - shear strain curves shift upward. However, as the PI of clays increases, the effects of OCR and confining pressure become less pronounced and may eventually disappear when dealing with high plasticity cohesive soils (Lanzo, et al., 1997). Furthermore, damping generally decreases with the OCR and confining pressure. However, if the PI and confining pressure increase, these effects become less pronounced and may eventually disappear (Vucetic, et al., 1998).

It was determined that the effect of confining stress is more significant and the effect of the PI is less significant than previously thought for virgin clayey soils of different geological ages. The research suggests taking into consideration the effect of geology and confining pressure (Zhang, et al., 2005).

It has been experimented that by varying frequency contents the normalized shear modulus curve can be affected. Aggour et al. applied random vibrations with varying cut-off frequencies to investigate the effect of loading frequency on the normalized shear modulus curves for cohesive soils. In the case of random loading, the soil shear modulus were found to increase with higher frequency content and were lower than the shear modulus obtained from sinusoidal testing as shown in Figure 1-14 (Aggour, et al., 1987).
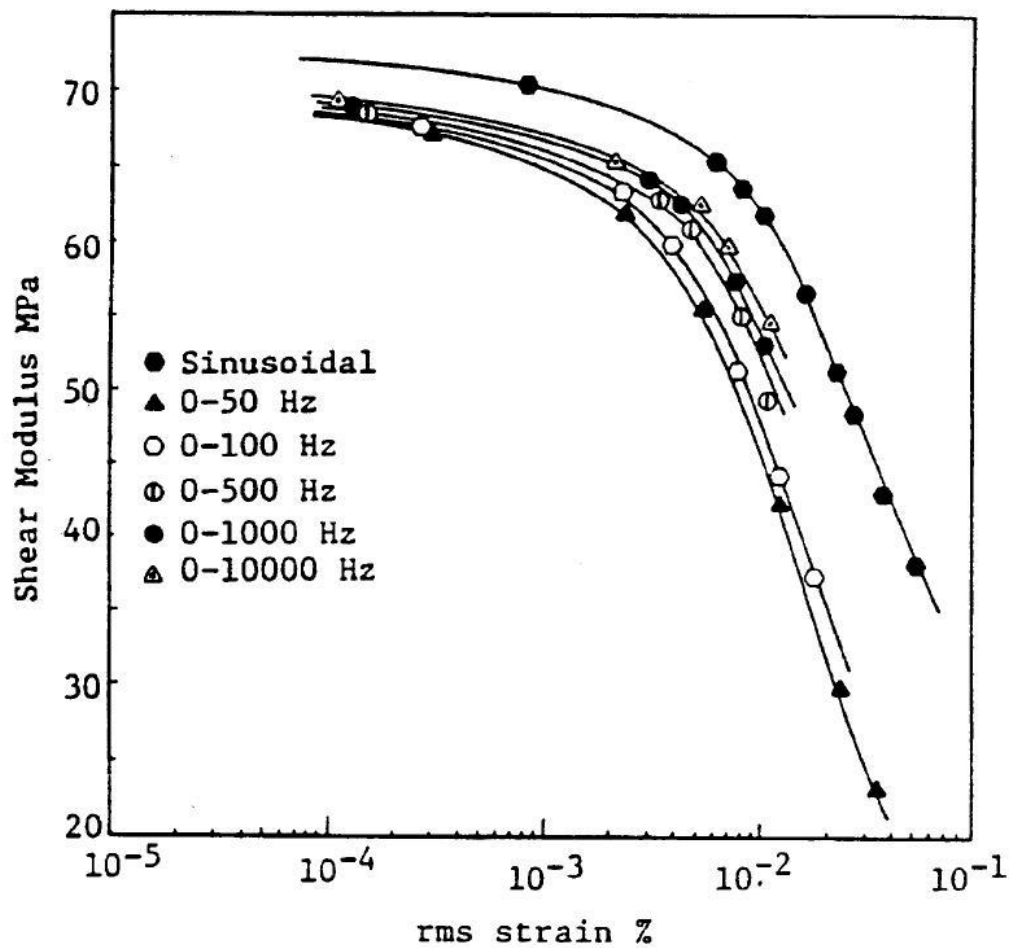
Figure 1-14: Effect of varying frequency content on the shear modulus of Clay (Aggour, et al., 1987)

The effect of varying cut-off frequencies on the damping ratio of clayey soil was also investigated using a series of random vibration tests. It was indicated that higher frequencies are attributed to lower values of damping, as shown in Figure 1-15.
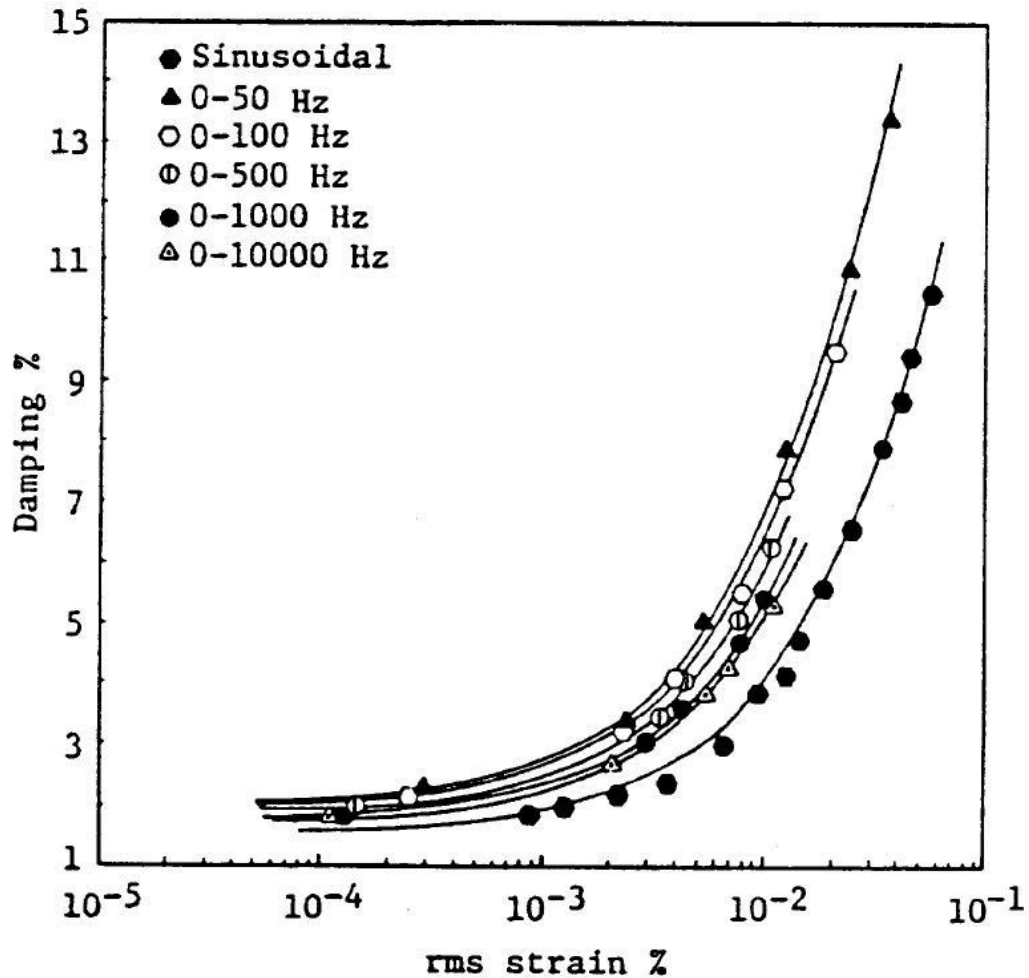
Figure 1-15: Effect of varying frequency content on damping ratio of clay (Aggour, et al., 1987)

It was also shown that the damping curve for conventional sinusoidal loading is located below the curve with highest frequency of random vibration as shown in Figure 1-15. It indicates that the damping ratio of the soil is greater in a condition of the random vibration than sinusoidal vibration.

Because of a wide range of factors affecting dynamic properties of cohesive soils

engineers are recommended to perform in situ and lab testing of cohesive soil properties

to evaluate appropriate design values and to avoid significant errors.

1.9.2   Shear Modulus and Damping Equations

Empirical curves that represent G/G_{max}-Log γ and D- Log γ are broadly used in

geotechnical earthquake engineering practice. Several researchers have proposed various

analytical models to predict the nonlinear clay behavior (Hardin & Drnevich, 1972a);

(Hardin & Drnevich, 1972b); (Anderson, 1974); (Borden, et al., 1996); (Darendeli,

1997); (Darendeli, 2001). The most widely used models in engineering practice are

explained in this section.

1.9.2.1 Hardin and Drnevich Design Equations

The first design equations with parameters that control soils' nonlinear behavior

were introduced by Hardin and Drnevich (Hardin & Drnevich, 1972a), (Hardin &

Drnevich, 1972b). They proposed a hyperbolic relationship that can relate shear stress

and shear strain in an empirical equation as below:

$$\tau = \frac{\gamma}{\frac{1}{Gmax} + \frac{\gamma}{\tau max}} \tag{1.30}$$

where: τ is shear stress; γ is shear strain; G_{max} is small-strain shear modulus; and τ_{max} is

shear strength.

Equation 1.30 can be rephrased by dividing both sides of the equation by γ to obtain the

secant shear modulus (G) as below:

$$\tau = \cfrac{1}{\cfrac{1}{Gmax} + \cfrac{\gamma}{\tau max}}$$ (1.31)

A new term was defined as reference strain using following equation:

$$\gamma_r = \frac{\tau max}{Gmax}$$ (1.32)

The normalized modulus reduction curve can be evaluated using equation 1.30 and rearranging it based on equation 1.31 as follow:

$$\frac{G}{Gmax} = \cfrac{1}{1 + \cfrac{\gamma}{\gamma_r}}$$ (1.33)

Hardin and Drnevich also proposed an approximate model for the material damping:

$$\frac{D}{Dmax} = \cfrac{\cfrac{\gamma}{\gamma_r}}{1 + \cfrac{\gamma}{\gamma_r}}$$ (1.34)

where D_{max} is the maximum damping ratio of the soil that depends on soil type, confining pressure, number of cycles, and loading frequency.

They also observed that soil type can have an impact on the stress-strain relationship. As a result, they proposed to approximately model the observed soil behavior by changing the strain scale to logarithmic scale. This change in scale makes the measured stress-strain curve have a hyperbolic shape. Hence, they defined a new parameter called hyperbolic strain (γ_h), which replaced the γ/γ_r term in equations 1.32 and 1.33. Hyperbolic strain was defined as:

65

$$\gamma_h = \frac{\gamma}{\gamma_r}(1 + a \times e^{-b \times \frac{\gamma}{\gamma_r}})$$ (1.35)

where "a" and "b" are coefficients that control the shape of the stress-strain curve for soil type, number of cycles, and loading frequency. The other benefit of using the logarithmic scale is that a stress-strain curve can be plotted in one graph covering a very large strain range.

1.9.2.2 Modified Hyperbolic Model

Many other researchers have been influenced by Harding and Drnevich's work and have made efforts to refine their equations. A modified hyperbolic model was introduced by Darendeli as follows (Darendeli, 1997):

$$\frac{G}{Gmax} = \frac{1}{1 + \frac{\gamma}{\gamma_r}^a}$$ (1.36)

where: γ_r = reference strain; a = curvilinear coefficient.

Darendeli utilized a relatively simple approach to fit measured stress-strain curves. He introduced a reference strain different from Hardin and Drnevich's reference strain. Darendeli's reference strain (γ_r) corresponds to the strain amplitude when the shear modulus is reduced to one half of the maximum shear modulus, G_{max}. The advantage of the modified hyperbolic model is its simplicity.

Darendeli (1997) also modeled the relationship between material damping ratio and strain using the modified hyperbolic model:

$$\frac{D_s}{D_s, min} = 1 + \frac{\gamma}{\gamma_{rD}}$$ (1.37)

where, γ_{rD} is the reference strain with respect to normalized material damping ratio. The value of D_s equals to $2D_{S,min}$ at $\gamma = \gamma_{rD}$. It is noteworthy to mention that the value of γ_{rD} is different from the value of γ_r of most models.

1.9.2.3 Ramberg-Osgood Model

The other applicable model is a Ramberg-Osgood model. Anderson used the Ramberg-Osgood stress-strain relationship to predict the variation of shear modulus with shearing strain (Anderson, 1974). The general form of the Ramberg-Osgood model is defined as:

$$\frac{G}{Gmax} = \frac{1}{1 + \propto (\frac{\tau}{\tau_y})^{R-1}} \tag{1.38}$$

where: α = shape factor; τ = shear stress at yield; and R = correlation number for Ramberg-Osgood curve.

It was suggested that values of 1.0 and 3.0 are used for α and R for various clays, respectively as below:

For various clays: $$\frac{G}{Gmax} = \frac{1}{1 + (\frac{\tau}{\tau_y})^2} \tag{1.39}$$

1.9.2.4 Borden Equation

Borden presented a curve fitting model function for soils. The function correlates the decay rate of G/G_{max} with an increase in shear strain amplitude (γ). The suggested function is (Borden, et al., 1996):

$$\frac{G}{Gmax} = \frac{1}{1 + a\ \gamma^{\ b\ c}}$$ (1.40)

where, constants a, b, and c represent the decay rate of G/Gmax with an increase in shear

strain amplitude (γ). The advantage of the Borden equation is its simplicity and the

capability of being adapted for both cohesive and cohesionless soils. An equation similar

to the Borden equation has been modified and used for modeling the relationship between

the normalized shear modulus and shear strain of soils in this study. The relationship

between normalized shear modulus and shear strain of clayey soil and fiber-reinforced

clayey soil is discussed in Chapter 4.

The normalized shear modulus and damping ratio were also correlated by Borden using

the following general equation:

$$D\ \% \ = a\ \left(\frac{G}{Gmax} - 1\right)^2 + b$$ (1.41)

1.9.2.5 Modified Masing Behavior for Damping Ratio

Material damping increases with increasing strain amplitude. The increasing

damping in the nonlinear range (large strain range) is a result of increasing nonlinearity at

particle contacts. This suggests that if the relationship between G/G_{max} and $\log \gamma$ are

determined, then the $D - \log \gamma$ curve can be simply defined with the $D - G/G_{max}$

relationship. Several models have been used to define the relationship between the

material damping ratio and the normalized shear modulus in the nonlinear range

(Ishihara, 1996); (Hwang, 1997); (Darendeli, 2001). Because of its simplicity, the

"Masing behavior" is one of the most commonly used models. The cyclic stress-strain

68

behavior proposed by Masing (1926) and the modification of the "Masing behavior" proposed by Darendeli (2001) are discussed below.

Masing (1926) proposed that the stress-strain path during cyclic loading could be related to the backbone curve or monotonic loading stress-strain path. As illustrated in Figure 1-12, Masing suggested that the reloading stress-strain curve follows the same scaled backbone curve to the initial point of the unloading curve. These sets of unloading and reloading curves are said to follow "Masing behavior" (Masing, 1926).

The unloading curve is the backbone curve scaled by two, in terms of absolute value. The initial shear modulus of the unloading curve is assumed to be G_{max} according to the hysteresis loop. This assumption is similar to the behavior of metals rather than soils. In a soil specimen, particles deform and move as the specimen is placed under loading. At the initial point of the unloading curve, soil particles have deformed from the initial condition at loading. Hence, at the initial unloading, the shear modulus is expected to be lower than G_{max}. Since the initial shear modulus is overestimated in Masing behavior, the area of the hysteresis loop obtained from Masing behavior is larger than those in actual soil behavior. As a result, material damping calculated from Masing behavior is larger than those of determined in the laboratory, especially at larger strain levels ($> 10^{-4}$). Also, it is noteworthy to mention that damping calculated from Masing behavior lacks small-strain damping.

To overcome the shortcoming of the Masing behavior approximation at larger strains, Darendeli (2001) adjusted the material damping ratio determined by assuming Masing behavior with a correction function as:

69

$$D_{Adjusted} = b. \ \frac{G}{Gmax}^{0.1} \times D_{Masing} + Dmin \qquad (1.42)$$

where: $D_{Adjusted}$ = scaled and capped material damping,

b = scaling coefficient (= 0.6329 - 0.0057 × ln (N)); N = number of cycle; G/G_{max} =

normalized shear modulus; and D_{Masing} = material damping ratio determined from the

Masing behavior.

Figure 1-16 shows the comparison between D_{Masing} and $D_{Nonlinear}$.
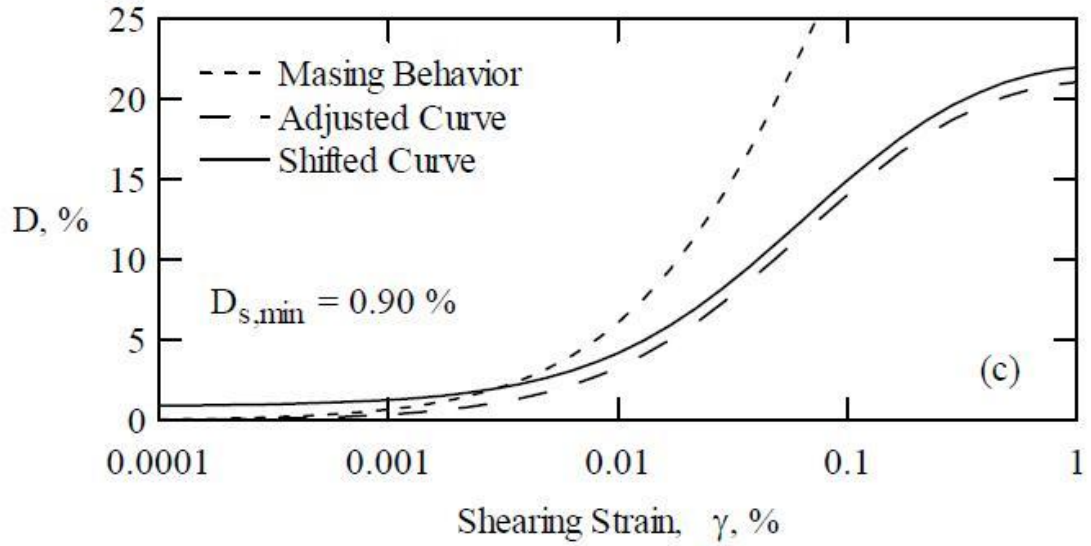
Figure 1-16: Darendeli's shifted damping curve (Darendeli, 2001)

As depicted in Figure 1-16, the amount of adjustment of the material damping

ratio increases with increasing shear strain, and the actual material damping ratio at a

shear strain is the summation of scaled Masing damping and D_{min}, as noted in Figure 1-

16.

The Masing damping, D_{Masing}, presented in Figure 1-16, is determined from a modified hyperbolic $G/G_{max} - \log \gamma$ curve with $\gamma_r = 0.03\%$ and a = 0.90. The theoretical value of D_{Masing} can be determined, only when a = 1 as:

$$D_{Masing} \; \% \; = \; \frac{100}{\pi} \times [\, 4 \frac{\gamma - \gamma_r \ln(\frac{\gamma + \gamma_r}{\gamma_r})}{\frac{\gamma^2}{\gamma + \gamma_r}} - 2] \qquad (1.43)$$

where: $\pi = 3.1416$. For values of D_{Masing} with a curvature coefficient "a" other than 1 ($D_{Masing}{}'$), Darendeli (2001) suggested calculating the values numerically as:

$$D_{Masing'} \; = \; C_1 D_{Masing} + C_2 D_{Masing}^2 + C_3 D_{Masing}^3 \qquad (1.44)$$

where: $C_1 = -1.1143a^2 + 1.8618a + 0.2523$; $C_2 = 0.0805a^2 - 0.0710a - 0.0095$; and

$C_3 = -0.0005a^2 + 0.0002a + 0.0003$.

CHAPTER 2

TEST EQUIPMENT

2.1   Introduction

Soil dynamics is the study of the dynamic properties of soils including moduli and damping ratios under dynamic loadings or deformation. Unlike many structural materials the samples of soils, which may be cohesive or cohesionless, do not have a readily measurable elasticity and yet the dynamic behavior of the soil specimen needs to be tested in accordance with concepts of elasticity. The main objective of this research is to study the effect of fiber reinforcement on the dynamic properties of clayey soils using the resonant column test. The resonant column testing technique has gained popularity among researchers due to its accuracy. It was accepted by ASTM as a standard testing method in 1978. This chapter describes in detail the test equipment used in this research.

2.2   The Drnevich Resonant Column Apparatus and Attached Equipment

The Drnevich resonant column apparatus, a relatively nondestructive testing equipment, was used in this research. The resonant column testing apparatus employs a chamber having a lower and a top platen (active platen) confining a column of soil in between and with the means to provide water and compressed air into the chamber for subjecting the column of soil to conditions representative of in-situ soil. Figure 2.1 shows a sketch of the Drnevich resonant column apparatus.
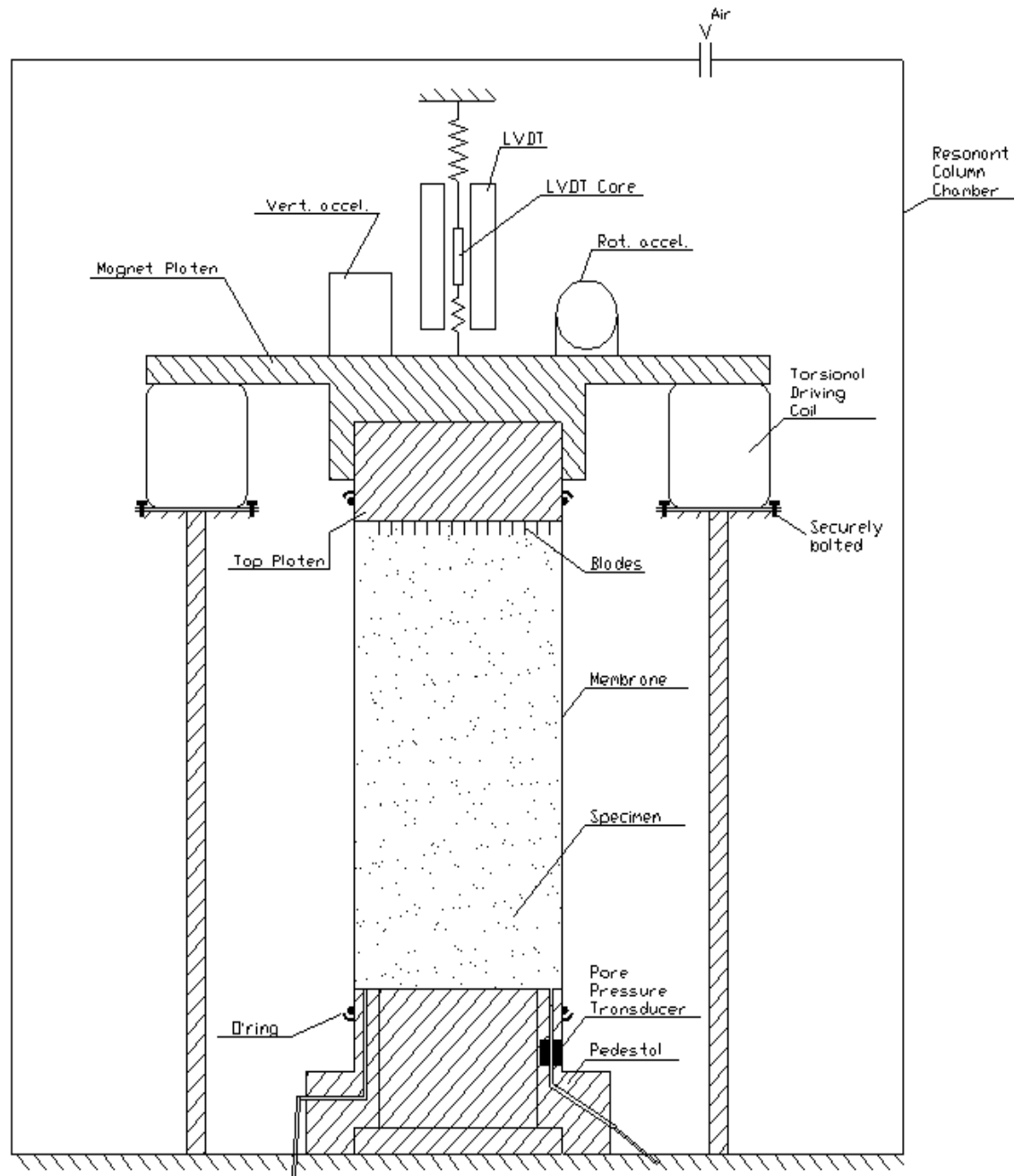
Figure 2-1: Drnevich Resonant Column Apparatus

A magnet plate supporting torsional and longitudinal accelerometers, in association

with fixed coils connected with an electrical circuit, provides for torsional vibration of the

soil column. A centrally placed coil on the torsional magnet plate in cooperation with a

vertically adjustable magnet provides for longitudinal vibration of the soil column and a

length measuring transducer[21] attaching to the upper platen serves to give constant readings of the length changes of the soil column resulting from the compaction of that column (Drnevich, 1975). According to the specification of the LVDT, the excitation signals should be 6 volts peak to peak (4.25 rms) with a frequency equal to 2.5 kHz. There are three ways to obtain the length measurements from an LVDT:

1- Using a conditioning module (e.g., Schaevitz LDM-1000) to excite the LVDT and reading the length measurements from a digital multimeter. A calibration chart needs to be developed to convert the rms readings of the voltmeter to length units.

2- Using an audio generator as an excitation source and a power amplifier to amplify the signals in accordance with the LVDT specifications.

3- Using a digital panel meter as a combined readout and conditioning unit.

All of the above mentioned methods provide the same measurements; hence, it is the researchers' decision to choose the method of measurement depending on the availability of devices at the laboratory. For this research, a combined LVDT readout and condition unit (Digital Panel Meters Model PML-1000) was used as a conditioning module to excite the LVDT and reading the response received from the LVDT.

The excitation system of the resonant column device is an electromagnetic system comprising of a permanent magnet and coil that can move in the gap between the North and South Poles of the permanent magnet. For longitudinal excitation, the assembly comprises one set of a coil and magnet. The magnet is connected to a heavy steel base and held up by a bracket, while the coil is housed in the top active platen and penetrates

---

[21] The length change of the soil column is measured with a Measurement Specialties (Schaevitz), type 300HR displacement transducer (LVDT) that has a linear range of ±0.300 inch and linearity error less than 0.25%.

concentrically into the magnet at least 15 mm (0.5 inch). For the torsional mode, the assembly comprises four rectangular coils and horseshoe-shaped magnets. The coils are connected to the brackets and the magnets to the top active platen. Equal gaps should be maintained between the magnets and the coils to minimize the development of any bending forces. The important consideration is that the magnets can move freely within each coil without touching it.

The torsional coils allow movements (0.5 inch) in the vertical direction to accommodate the change in length during the consolidation process of clay. Torsional coils are shown in the Figure 2-2.
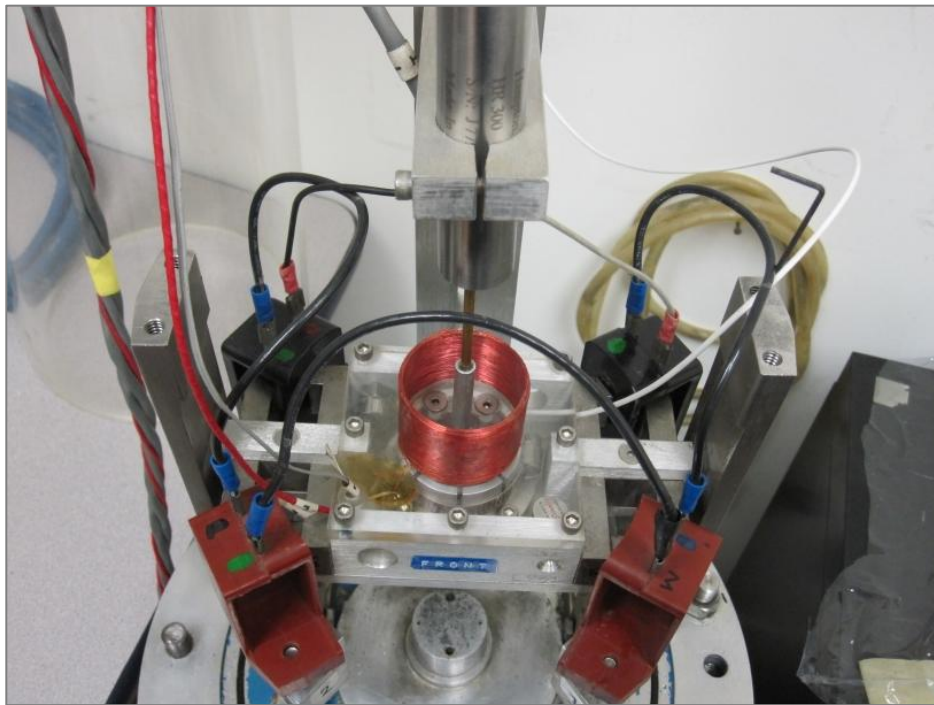
Figure 2-2: Torsional Coils set up

By generating an AC current of controlled frequency through the coils, a magnetic field would be generated, which in turn develops longitudinal or torsional forces on the top of the soil column.

The polarity of the torsional wiring system should be checked; meaning that the polarity of the system should create a moment in the same direction, e.g., clockwise. In order to check the polarity, test leads or other convenient temporary connections can be used to short out coils 2, 3, and 4. The coils should be slightly loosened (not tightly fixed) but still in place. A 6 volt DC current should be connected to the main lead for the torsional coils from the Control Box in lieu of the AC voltage provided by the power amplifier. This should place a current of less than one amp through coil number 1. That current should be sufficient to cause the magnet and top platen system to rotate in either clockwise or counter clockwise. The operator should make note of the rotation direction. Then, the short from coil 2 should be removed and coils 1, 3, and 4 should be shorted out. The same 6 volt DC current should be connected and the system should experience a motion in the same direction as noted above. If it is not, the leads to coil 2 should be reversed. The procedure should be continued for coils 3 and 4 making sure that connections to each coil produce the same rotation motion of the magnet-top platen system for the same voltage applied. Figure 2-3 shows the voltage test set up. All the shorted connections should be removed and a convenient scheme to code the connections to the coils should be sketched and used for the testing program.
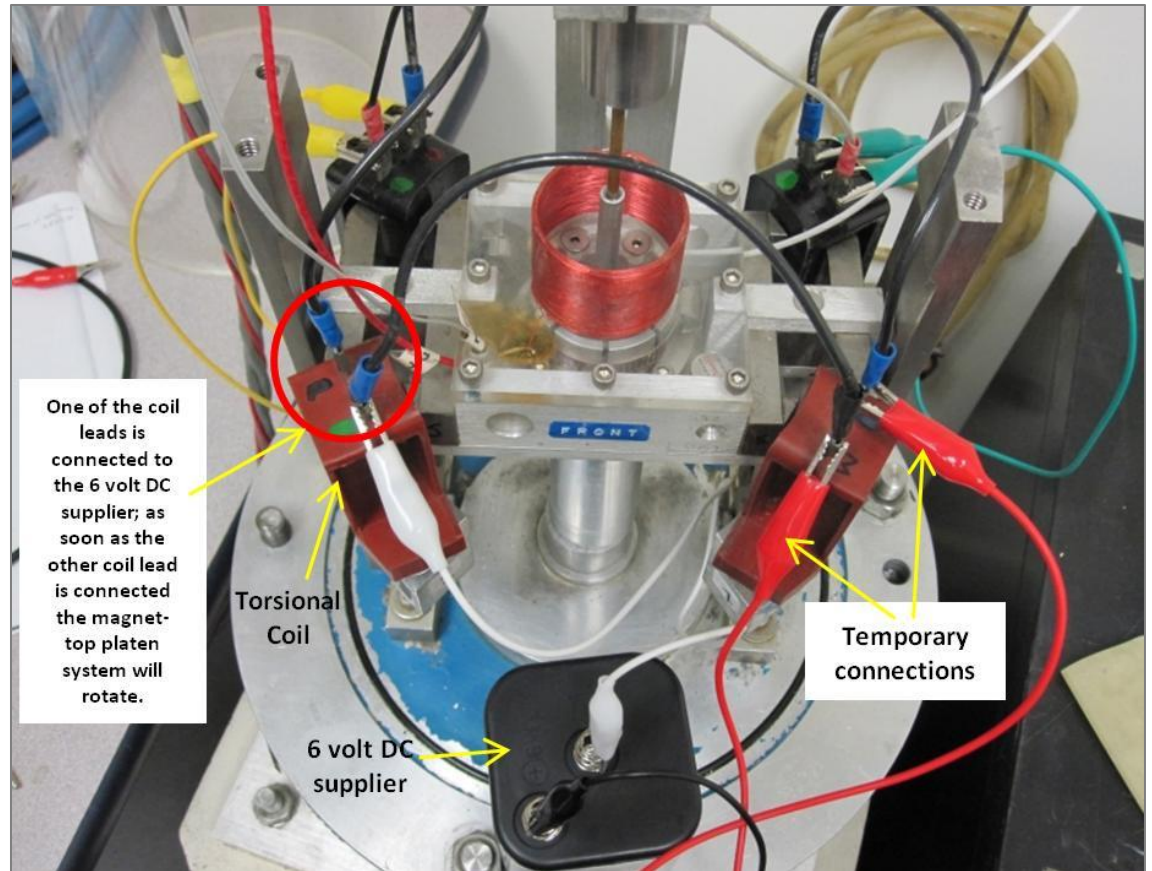
Figure 2-3: Voltage test set up

The accompanying devices, required for the excitation system, are a wide range

oscilloscope (Tektronix model T912), a sine wave generator (GW Instek), and an

amplifier (Bogen Model MT125B). Adjoining equipment is a frequency counter (VC

2000) used to accurately give the value of the circular frequency and a digital multimeter

(BK Precision 2831E) utilized to measure the current passing through the drive coils. The

digital multimeter, operating in true root mean square (rms), also measures the voltage

drop across an accurate 5 ohm power resistor placed in the control box of the resonant

column. Table 2-1 is a summary of the specifications for the electronics.

Table 2-1: Electronic equipment used with the resonant column apparatus

Equipment	Manufacturer	Model	Function
Sine Wave Generator	GW Instek	GAG-809/810	Providing sinusoidal input voltage for driving coils (either directly or thru power amplifier)
Frequency Counter	TUV	VC2000	Measuring frequency of input signal
Power Amplifier	Bogen	MT125 B	Amplifying input signal from signal generator to coils
Oscilloscope	Tektronix	912	Displayed and stored output signal from accelerometer
Charge Amplifier	Columbia Research Lab	4102	Exciting transducer and conditioning output voltage from accelerometer
Digital Multimeter & Frequency Counter	BK Precision	2831E	Measuring the input and output voltage to/from transducer thru charge amplifier. Also, measuring frequency of input signal
LVDT Readout	Measurement Specialties	PML-1000	Exciting and conditioning LVDT and measuring the output from LVDT

Figure 2-4 shows a setup of the resonant column attached devices.

Figure 2-4: Set up of the resonant column attached devices

During each testing routine, the wave oscillator signals are amplified with the power

amplifier and then input to the drive coils after passing through the power resistor in the

control box. Figure 2-5 shows the wiring diagram for control box.
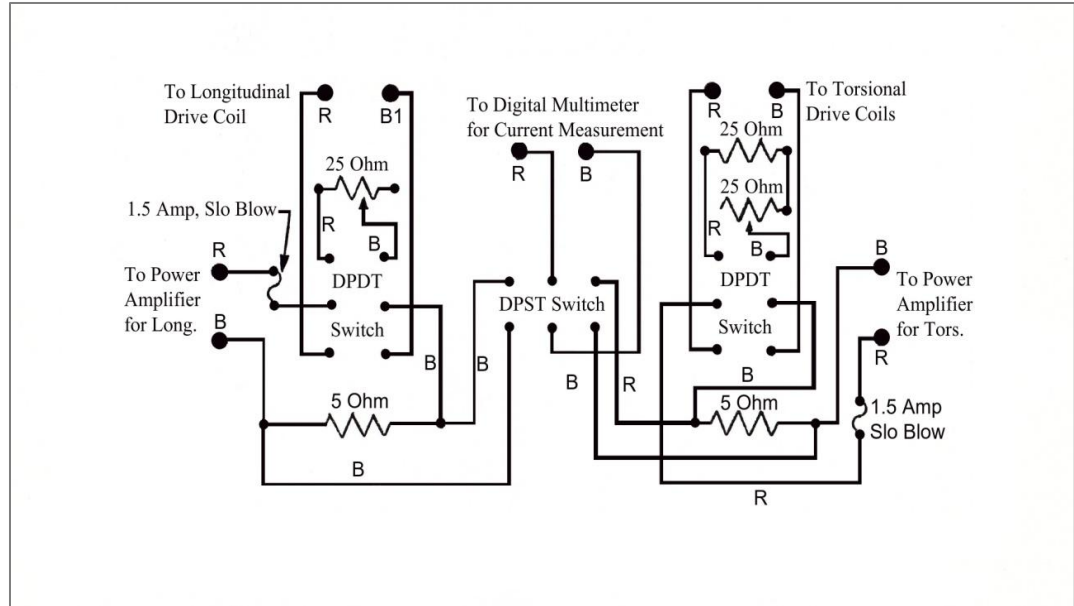
Figure 2-5: Wiring diagram for control box

The pick-up system comprises of a piezoelectric meter (Columbia Model 200-1-H) placed in the active-end platen. The transducer is mounted at a distance of 0.0316 meter from the axes of rotation. The transducer has a charge sensitivity of 36.3 pk-pcmb/pk-g. A charge amplifier (Columbia Model 4102) is used to operate the accelerometer by converting the charge into emf[22]. The output would be 2.5 pk-volts/pk-g, 0.25 pk-volts/pk-g, or 0.025 pk-volts/pk-g, depending on whether the left, center, or right button is depressed on the panel of the charge amplifier. The digital multimeter and oscilloscope are used to record the responses. The digital multimeter gives readings of sample acceleration in terms of rms, which in turn can be converted to define the shear strain. The oscilloscope monitors the frequency response of the sample. The electrical connections are outlined in Figure 2-6.

---

[22] Electromotive force is the energy per unit charge that is converted reversibly from mechanical, chemical, or other forms of energy into electrical energy.
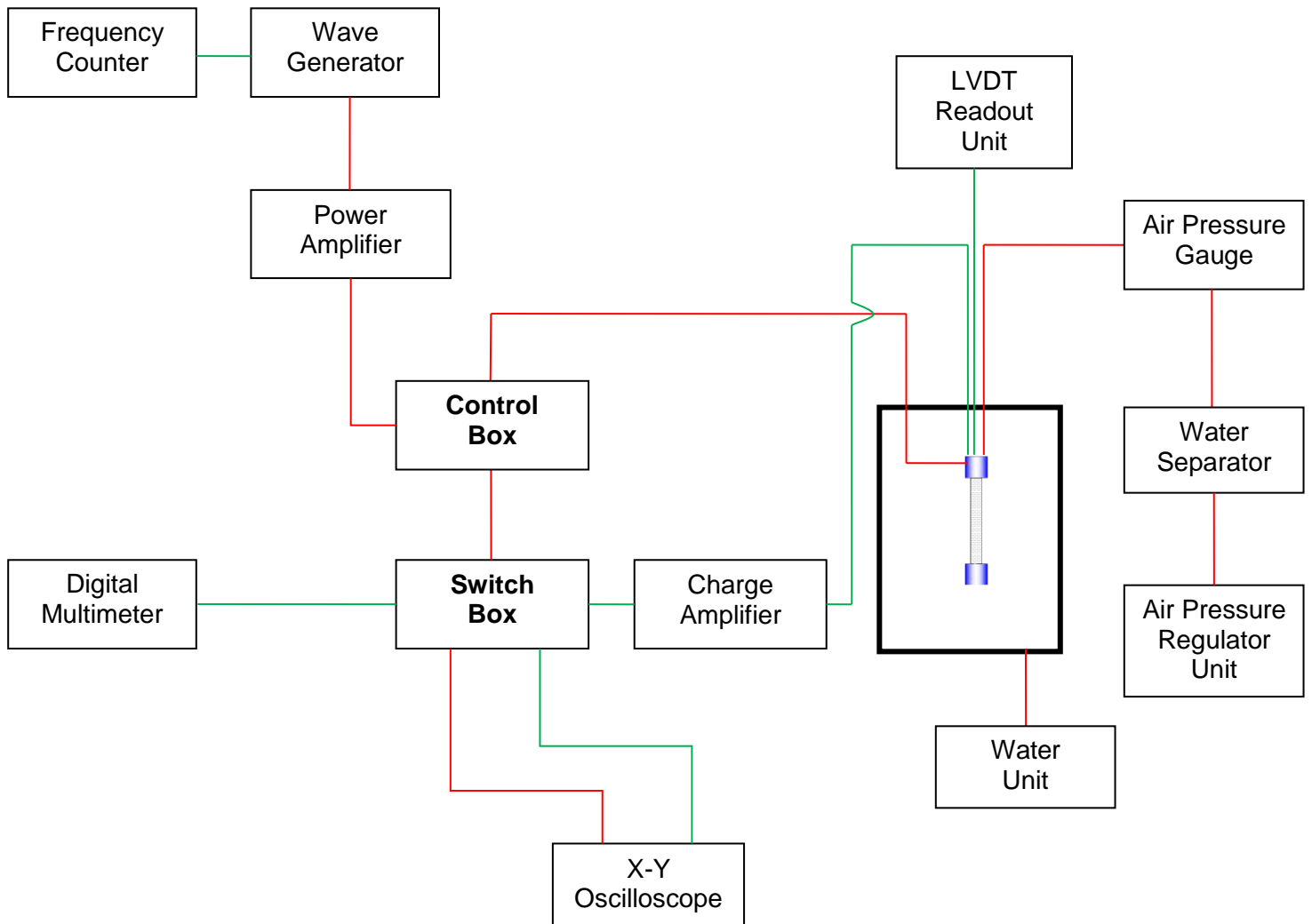
Figure 2-6: Schematic diagram of the resonant column testing system
(Red lines are input lines; Green lines are output lines)

An air pressure regulator unit, Tri-Flex 2, manufactured by ELE International was
used to maintain the pressure at 5 psi during the consolidation period and during the test.
The use of an air pressure regulator unit can prevent the air flow from any fluctuation
during consolidation period and testing. In addition, a water separator was placed in the
air feeding line with the purpose of keeping the water and moisture out of the air. A

digital pressure regulator gauge was also installed in the air feeding line prior to the point where the air is to enter the resonant column chamber to measure the air pressure at the point of air entry. Figure 2-7 shows the digital pressure gauge and water separator.

Figure 2-7: Digital pressure gauge and water separator

2.3   Calibration of the Test Equipment

Calibration is a comparison between measurements read from two test equipment, one of known magnitude and other not known. The device with the known or assigned correctness is called the Standard. The other equipment is the unit under test (test equipment). There are two types of calibration, absolute and relative calibrations. The absolute calibration is performed at the manufacturer's factory; whereas, the relative

calibration can be conducted by operators at soil mechanics laboratories when Standard

equipment is available or the magnitude of the expected measurements are known.

From cost prospective, when a large number of equipment is needed to be

calibrated, it is more economical to send out one unit to be calibrated at the

manufacturer's factory (absolute calibration) and use the newly calibrated unit as the

Standard equipment for calibrating other equipment (relative calibration) at a laboratory.

2.3.1 Resonant Column Apparatus Calibration

To calibrate a resonant column (RC) apparatus, a rod of known torsional stiffness

properties is needed to calibrate the results obtained from the testing. In order to do that

the apparatus shall be operated with a slender aluminum calibrating rod in place of the

specimen. One end of the rod shall be rigidly fixed and the other end shall be rigidly tied

to the magnet platen after taking out the top platen. The system then approximates a

single degree of freedom (SDF) system. Figure 2-8 shows an approximate cross section

of the apparatus showing the placed calibration rod (Drnevich, et al., 1978).
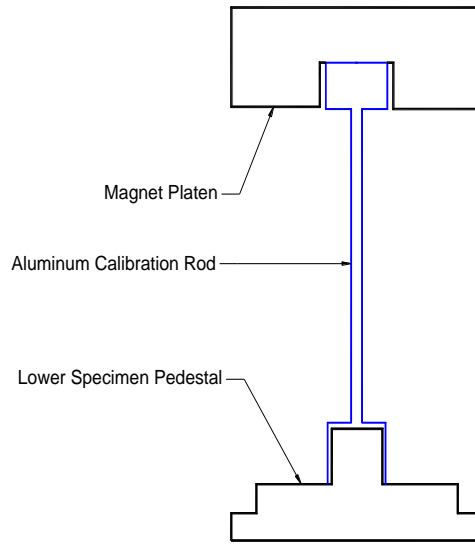
Figure 2-8: Approximate cross section of RC apparatus showing the calibration rod in blue

With the torsional calibration rod in place, a small current should be sent to the torsional coils. The voltage associated with this current should be approximately 0.05 V_{rms}. The loading frequency should be adjusted to obtain resonance. The resonant frequency (f_t) should be recorded and the value of $\frac{\overline{2}}{2}f_t$ and $\overline{2}f_t$ should be calculated. A large current with voltage of approximately 1.0 V_{rms} should be applied while the frequency of oscillation is set to $\frac{\overline{2}}{2}f_t$. The corresponding output of the torsional accelerometer should be recorded. The same large current now should be applied at $\overline{2}f_t$ and the corresponding outputs should be recorded. Then, two coefficients, C_1 and C_2, can be calculated from equations 2.1 and 2.2.

$$C_1 = \frac{\frac{4.43}{f_1^2} \times TO_1}{2CR_1} \tag{2.1}$$

$$C_2 = \frac{\frac{4.43}{f_2^2} \times TO_2}{CR_2} \qquad (2.2)$$

where: C_1 and C_2 are calibration coefficients,

CR_1 and CR_2 are excitation voltages corresponding to $\frac{\overline{2}}{2}f_t$ and $\overline{2}f_t$ frequencies, respectively,

TO_1 and TO_2 are response voltages corresponding to $\frac{\overline{2}}{2}f_t$ and $\overline{2}f_t$ frequencies, respectively.

The values of C_1 and C_2 should agree within 10 percent otherwise the calibration should be repeated (ASTM D4015-07). From C_1 and C_2 the torsional coils Torque Calibration Factor (TCF) can be calculated using equation 2.3.

$$TCF = 0.5 \; C_1 + C_2 \; K_{cr} \qquad (2.3)$$

where, K_{cr} is spring constant of the calibration rod and is equal to 265.4 $\frac{N-m}{radian}$,

TCF is Torsional Calibration Factor in $\frac{N-m}{V_{rms}}$.

The torsional calibration factor was calculated to be 7.05 $\times$ 10^{-2} $\frac{N-m}{V_{rms}}$ for the apparatus using the above mentioned procedure.

2.3.2 Acceleration Transducers and Charge Amplifiers

Prior to starting the test, the acceleration transducer and charge amplifier need to be calibrated. To meet this goal, the standard transducer (a recently calibrated transducer) and the to-be-calibrated acceleration transducer are symmetrically attached together with

wax and are glued on the plate of a shaking table (vibrator), as shown in Figure 2-9. The

transducer to be calibrated and the standard transducer are respectively connected to the

charge amplifier to be calibrated and the standard charge amplifier. The shaker vibrates

sinusoidally from a frequency of 10Hz to 1,000Hz. Although the expected frequencies for

conducting the resonant column testing are less than 100Hz, responses up to 10 times the

highest frequency of interest are compared. It is advised by the manufacturer that

accelerometers should be calibrated in regard to resonant frequencies up to five times the

highest frequency of interest.
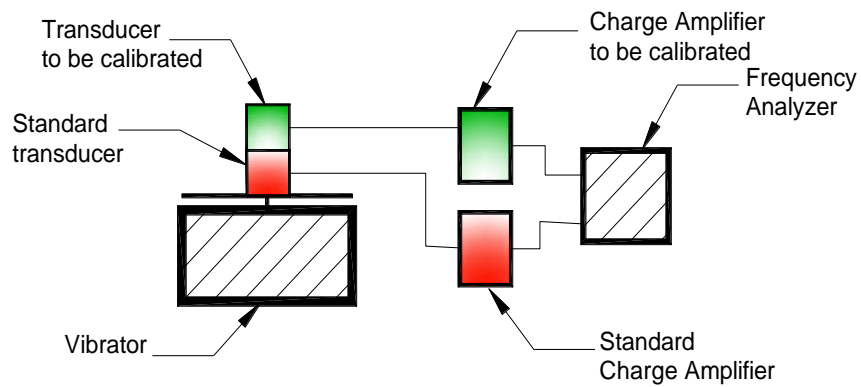
Figure 2-9 Set-up diagram for calibration of transducer and charge amplifier

Relative calibration was performed for the transducer and charge amplifier. The

calibration set up is shown in Figure 2-9. After performing the relative calibration, due to

the importance of accuracy of the measurements from the charge amplifier and transducer

(model 200-1-H serial no. 858), both devices were sent to Columbia Research Labs, Inc.

for absolute calibrations. Charge sensitivity of 36.3 $\frac{pk.pcmb}{pk-g}$ for the frequency ranges

between 2 Hz to 5 kHz was determined for the transducer.

2.3.3 Linear Variable Differential Transformer (LVDT) and LVDT Readout

The absolute calibration was conducted on the LVDT 300HR by the manufacturer. After the calibration, the LVDT was installed on the apparatus and connected to an LVDT Readout, PML 1000. Before the LVDT can be used it must first be calibrated to the LVDT Readout. Please note that the calibration of LVDT, which was performed by the manufacturer, is different from calibrating the LVDT to the LVDT readout. The calibration of the LVDT to the LVDT readout is a procedure conducted so that the numbers obtained from the LVDT can be defined for the LVDT readout. The LVDT was connected to the LVDT Readout at the appropriate input measurement mode and correct excitation voltage. Frequency was selected from the input menu. The Automatic Gain selection option was used from the input menu and was set to ON.

It is significant that the LVDT operates around the midpoint of its stroke as this gives the best results by minimizing any errors due to non-linearity. A feature of the PML 1000 is the ability to locate the midpoint of the LVDTs measurement range (null point). The LVDT was mounted so that the required measurement range is equally divided by the null position. The displayed value started flashing when the LVDT was closer to its null position.

To perform an initial calibration of the LVDT to the PML 1000 the CAL option from the main menu was selected. The display showed the message L-iP (low input). At this time, the position of the LVDT was set to its minimum displacement position (minimum stroke). When the LVDT was set at its low calibration point (displacement of 0 mm), the Enter key was pressed, the display showed WAit while the PML 1000 measured the output from the LVDT. This took a few seconds. After a few seconds, the

display showed H-iP. This indicated that the PML 1000 was ready to calibrate the high

point. At this time, the LVDT was set to its high calibration point (maximum

displacement position of 200 mm) and pressed Enter. The unit displayed the message

WAit while it was measuring the output from the LVDT. At the end of the calibration

sequence, the PML 1000 used the two measured output values from the LVDT to

calculate its own calibration constants that would be utilized in all future measurements.

2.4   Coupling between Soil Specimen and Top Platen

Having complete coupling between stiff soil specimens and the top platen could

be a problem if precautions are not taken. At very low strains, coupling can exist but as

the strain amplitude increases, shear stresses increase and incomplete coupling may

occur. Incomplete coupling results in lower shear modulus and higher damping than what

should be at a given shear-strain amplitude. To ensure a complete coupling, razor blade

vanes are placed in top platen. The protrusion of the blades should be greater than or

equal to 1.5 mm (Drnevich, 1978).

2.5   Resonant Column Data Reduction Calculations

In the resonant column technique, a column of material is excited either

longitudinally or torsionally. The Young's Modulus (E) or Shear Modulus (G) of the soil

can be evaluated employing the wave propagation theory. The wave propagation theory

will depend on the specimen configuration. In this research a "Fixed-Free" configuration

resonant column was used for studying the shear modulus properties of clay and fiber

reinforced clay. In the following section the equations used to calculate shear modulus,

damping, and shear strain from resonant column testing are presented.

2.5.1 Calculation of Shear Modulus

In the resonant column tests where soil specimens are subjected to torsional vibration with fixed-free conditions, the wave propagation is expressed as follows:

$$\frac{\Delta^2 \theta}{\Delta t^2} = V_s^2 \frac{\Delta^2 \theta}{\Delta x^2} \tag{2.4}$$

where: $\Delta\theta$ = angle of twist (rad),

I_s = polar moment of inertia of the soil specimen (m^4),

J_T = polar mass moment of inertia of the top platen (kg-m^2),

V_s = shear wave velocity in soil specimen (m/s).

The wave velocity V_s can be calculated from equation 1.19. The solution to the wave equations for short bars or soil column vibrating in a natural mode can be written in the general form as equations 2.5 and 2.6.

$$U\ x,t\ = U(x)(A_1 sin\omega_n t\ + A_2 cos\omega_n t) \tag{2.5}$$

where ω_n is the undamped natural circular frequency; A_1 and A_2 are constants; and U(x) is the amplitude of displacement along the length of the soil column and is independent of time, and

$$U\ x\ = B_1 sin(\frac{\omega_n}{V_c}x)\ + B_2 cos(\frac{\omega_n}{V_c}x) \tag{2.6}$$

where B_1 and B_2 are constants. These constants may be determined by the end condition to which the rod or soil column may be subjected.

Using the boundary conditions for the fixed-free case, at x = 0 (fixed end), U(x) = 0 and

at X = L (free end), $\frac{dU(x)}{dx} = 0$ and U(x) is:

$$U\ x\ = B_2 \cos(\frac{\omega_n}{V_c}x) \qquad (2.7)$$

The inertia force (F) on the soil column under torsion can be expressed in equation 2.8 in

terms of polar mass moment of inertia (J_T) and the shear strain at x = L.

$$F = -J_T \frac{\Delta^2 \theta}{\Delta t^2} \qquad (2.8)$$

It can also be rephrased in terms of polar moment of inertia as:

$$F = GI_s \frac{\Delta \theta}{\Delta x} \qquad (2.9)$$

The following can be obtained by substituting second derivatives of combined equations

2.5 and 2.7 in equations 2.8 and 2.9.

$$F = J_T \omega_n^2 B_1 \sin(\frac{\omega_s}{V_s}L)(A_1 \sin\omega_n t + A_2 \cos\omega_n t) \qquad (2.10)$$

$$F = GI_s \frac{B_1 \omega_n}{V_s} \cos(\frac{\omega_s}{V_s}L)(A_1 \sin\omega_n t + A_2 \cos\omega_n t) \qquad (2.11)$$

Equating equations 2.10 and 2.11 and expressing G in terms of mass density and shear

wave velocity the following solution can be obtained.

$$\frac{\omega_n L}{V_s} \tan(\frac{\omega_n L}{V_s}) = \frac{J_s}{J_T} \qquad (2.12)$$

and

$$F_T \tan F_T = \frac{1}{T_T} \tag{2.13}$$

where F_T = dimensionless frequency factor, which can be calculated from the following

equation:

$$F_T = \frac{1}{(0.405 + T_T)} \tag{2.14}$$

And $T_T = \frac{J_T}{J_s}$, and J_s = polar mass moment of inertia of soil specimen (kg-m^2) and is equal

to

$$J_s = \frac{M_s d^2}{8} \tag{2.15}$$

where d = diameter of the soil specimen (m),

M_s = mass of the soil specimen.

With the value of F_T, shear modulus (G) of the soil specimen can be determined from:

$$G = \rho\ 2\pi L^{\ 2}\ \frac{f_{nT}}{F_T}^{\ 2} \tag{2.16}$$

where f_{nT} = resonant frequency in torsional vibration (Hz).

2.5.2   Calculation of Damping Ratio

The Resonant Response Method was used to calculate the damping ratio using the

following equation (Drnevich, 1978):

$$D = \frac{1}{(A \times MMF)} \tag{2.17}$$

where $A = 2\ (T_L + 0.405)$ and MMF is calculated from the following equation:

91

$$MMF = \frac{RCF \times RTO}{TCF \times INP} \times J \times \ 2\pi f_{nT} \ ^2 \qquad\qquad (2.18)$$

where, RCF = rotational calibration factor (rad/V),

TCF = torque calibration factor (N-m/V),

INP = input reading of torsional coil (V),

RTO = response or output reading of torsional coil (V),

J = total polar mass moment of inertia including the top platen and soil column (Kg-m^2),

f_{nT} = resonant frequency of the system in the torsional direction.

2.5.3   Calculation of Shear Strain

The moduli and damping ration of soil depend upon the magnitude of the strain. For sinusoidal torsional excitation, the shear strain amplitude can be obtained using Drnevich's approach as follows:

$$\gamma = \ RCF \ \times RTO \times \frac{d}{3L} \qquad\qquad (2.18)$$

where γ = shear strain; RCF = rotational calibration factor (rad/V)$_{rms}$; RTO = rotational transducer output V$_{rms}$; d = diameter of specimen; L = length of the specimen.

CHAPTER 3 DETERMINATION OF OPTIMUM FIBER CONTENT

This chapter deals with the testing undertaken prior to the dynamic testing program. The study discussed in this chapter involves a new compaction procedure developed for finding the optimum fiber content (OFC) of fiber-clay mixtures. The purpose of this procedure is to determine the optimum fiber content that produces the largest maximum dry density ($\gamma_{d\ max}$). Samples for dynamic testing were prepared at their maximum dry density. The results of this study will be useful for fiber selection in terms of fiber type and percentage content and also will establish a procedure that can be followed to obtain the proper fiber-clay composite mix design.

3.1   Current State of the Research

Researchers have added fiber to soil and found that it improves the soil behavior. However, they followed the same approach that is being used in concrete. In concrete, fiber is added to improve its behavior as well. The amount of fiber added is usually an arbitrarily specified percentage to increase the strength properties of the concrete. The percentage usually varies with the intended use of the concrete. Soil behavior is a function of its density, which is not the case with concrete. Thus, the concrete approach will not provide a matrix with improved geotechnical properties. Therefore, it should not be adopted in adding fiber to soils.

The other approach is the metallurgical approach to form desired composite systems, such as Metal Matrix Composites (MMC), Ceramic Matrix Composites (CMC), or Polymer Matrix Composites (PMC). The percentage of mixture constituents is obtained using the traditional rule of mixtures. In this approach, composite properties are

traditionally predicted using a micro-mechanics approach termed the rule of mixtures.

The Rule of mixtures is mathematical expression that describes some properties of the composite in terms of the properties, quantities and arrangements of its constituents. The rule of mixtures is widely used for different composite systems, i.e., MMC, CMC, and PMC. The density of a general composite can be predicted from the following equation:

$$\rho = \frac{M_{clay} + M_{fiber}}{V} = \frac{V_{clay} \times \rho_{clay} + V_{fiber} \times \rho_{fiber}}{V} \tag{3.1}$$

where: ρ is density of a general composite; M_{clay} is mass of clay; M_{fiber} is mass of fiber;

V is the total volume of composite.

The above equation can be rewritten based on volume fractions of clay (V_{fclay}) and fiber (V_{ffiber}) as follows:

$$\rho = (V_{fclay} \times \rho_{clay}) + (V_{ffiber} \times \rho_{ffiber}) \tag{3.2}$$

where: ρ_{clay} is density of clay; ρ_{fiber} is density of fiber.

The above equation can be rewritten based on volume fraction of fiber knowing that V_{fclay} + V_{ffiber} = 1. Thus,

$$\rho = \ 1 - V_{ffiber} \ \times \rho_{clay} \ + \ V_{ffiber} \times \rho_{fiber} \ \rightarrow \tag{3.3}$$

$$\rho = \ \rho_{clay} + [V_{ffiber} \ \times \ \rho_{fiber} - \ \rho_{clay} \ ]$$

The equation shows that the density of the composite is a function of the density of the clay, density of the fiber, and the volume fraction of the fiber. The following schematic

graph, Figure 3-1, shows that the density of matrix can vary based on the fiber volume fraction and the density of the fiber and clay.
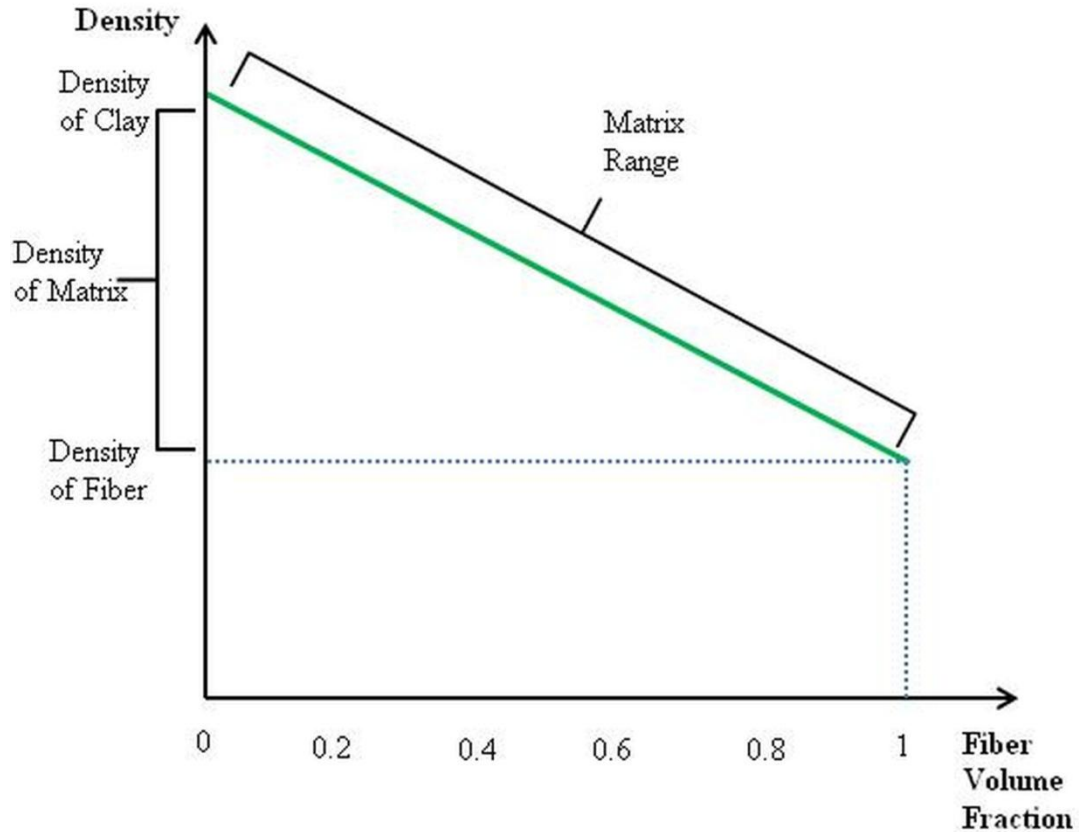
Figure 3-1: Schematic graph of density of matrix versus fiber volume fraction

The schematic sketch in Figure 3-1 shows that the density of the matrix cannot be greater than the density of the material with the larger density, in this case, clay. Other properties of a composite, e.g., stiffness, can also be predicted using this approach.

The following assumptions have been made in the rule of mixtures:

1- Fibers are uniformly distributed throughout the matrix.

2- Perfect bonding between fibers and matrix.

95

3- Matrix is free of voids.

4- Applied loads are either parallel or normal to the fiber direction.

5- Fiber and matrix behave as linearly elastic materials.

All soils including clay are composed of solids and voids as shown in the schematic Figure 3-2. Voids are filled with both air and water. Thus soil is a three-phase material. Using soils in construction or as a foundation material requires mechanical stabilization to rearrange its structure and thus improve its behavior. Compaction of soil applies mechanical energy to rearrange its particles and reduce its air voids and thereby improve its behavior by increasing its density, strength, and reducing its compressibility.
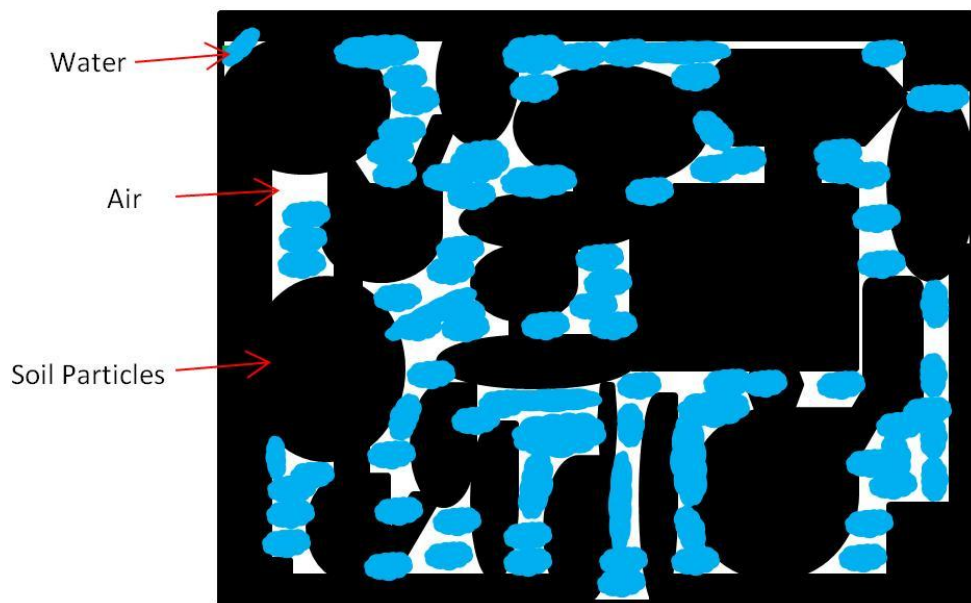
Figure 3-2: Schematic graph of soil composition

In the process of compaction water is added to allow soil particles to slide over each other more easily (a lubricant) up to a certain point; further addition of water beyond this point will occupy space that could be filled with soil and thus the density of the soil will be reduced. Therefore, geotechnical investigators perform compaction tests at

different water content levels and determine the amount of water needed that produces

the maximum density of the soil, which is termed the optimum moisture content.

However, it is impossible to get rid of all the air voids, thus at the end the soil will be still

composed of solids, air and water, but at a higher density and a specified moisture

content.

Using the rule of mixtures is appropriate if the matrix is free of voids. The matrix

is made up of solids and voids filled with water, air, and fiber as shown in Figure 3-3,

which is then compacted. Compaction does not eliminate air voids. Also, different

degrees of compaction will have different amounts of voids remaining. The existence of

voids violates the rule of mixtures assumptions.
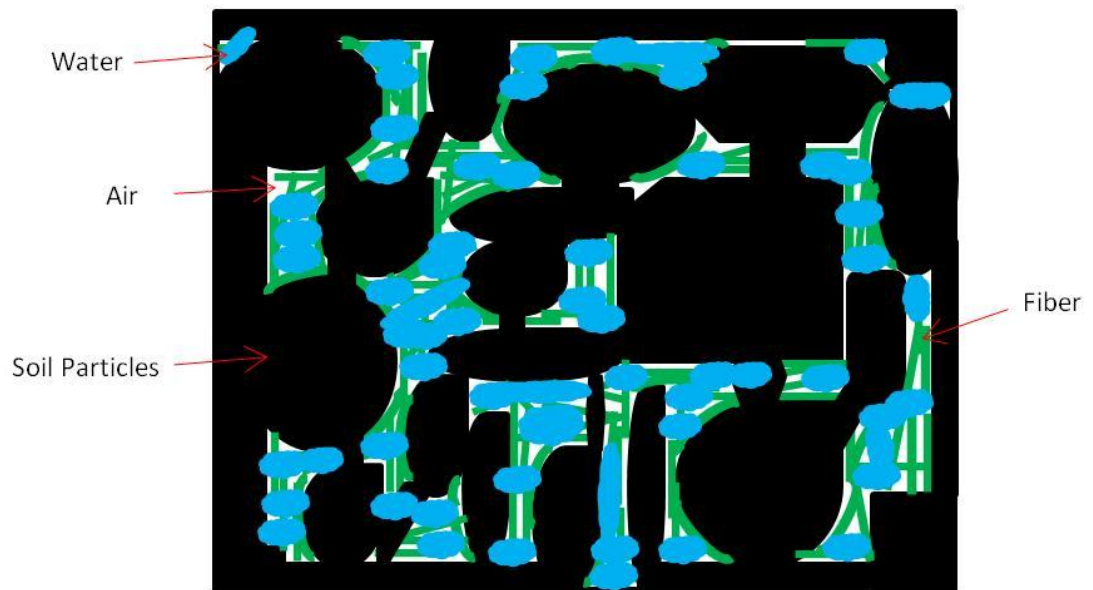
Figure 3-3: Schematic graph of fiber reinforced soil composition

Another assumption made in the rule of mixtures approach is that the matrix and

fiber are assumed to behave as linearly elastic materials. Soils in general tend to behave

as non-linear materials and clays in particular can also behave as plastic materials

97

depending on the clay's plasticity index. So, in dealing with soils, testing is the only way to determine the characteristics and behavior.

3.2 Density and Compaction

For many civil engineering projects, soils are compacted to a denser state to enhance their engineering properties. Soil compaction consists of packing the soil particles together by mechanical means so that it increases the soil dry unit weight. Soils are made of solid particles with voids filled with air and water. Compaction only reduces the air fraction of the voids. In theory, the most effective compaction process should completely remove the air fraction. However, in practice, compaction cannot completely eradicate the air fraction, but only reduces it to a minimum. In the following sections, the compaction behavior of fiber added clayey soil is discussed.

3.2.1 Soil and Fiber Materials

The synthetic soil used in this study was Kaolinite obtained from Feldspar Corporation[23]. The soil was commercially obtained in a dry, powdered form (50 lbs per bag). The chemical components of the soil are listed in Table 3-1. The Kaolinite mineral is the simplest and best understood clay mineral. This clay can be considered as a standard clay, like Ottawa sand is used as a standard sand. Because the Kaolinite was received in a powdered form, the properties of the prepared specimens might vary depending on the uniformity of the batches; therefore, two bags were thoroughly mixed together in a large container and stored in a dry place.

---

[23] Edgar, FL 32149

Table 3-1: Chemical properties of Kaolinite Soil

Component	Percentage	Component	Percentage	Component	Percentage
SiO_2	45.2	Al_2O_3	38.8	Fe_2O_3	0.3
FeO	-	MgO	0.3	CaO	0.05
Na_2O	0.3	K2O	0.05	TiO_2	1.4
CO_2	-	SO_2	-	H_2O	0.7
P_2O_5	-				

The Atterberg limits were determined following ASTM D4318 to be LL = 49, PL = 29, and PI = 20. The liquid limit device used in this research was equipped with a motor to turn the cam at 2 ± 0.1 revolutions per second. This device also has an automatic and adjustable counter for counting the blows. A Casagrande grooving tool was used in the test. The calibration of the apparatus was performed in accordance with steps provided in ASTM D4318.

The most commercially available fiber sizes were used for this study. As shown in Figure 3-4, the polypropylene fibers were 1.9 cm (0.75 in) and 1.27 cm (0.5 in) in length virgin homopolymer monofilament and fibrillated fibers obtained from ABC Polymer Industries, LLC (ABC)[24] for the testing.

---

[24] Helena, AL 35080 USA
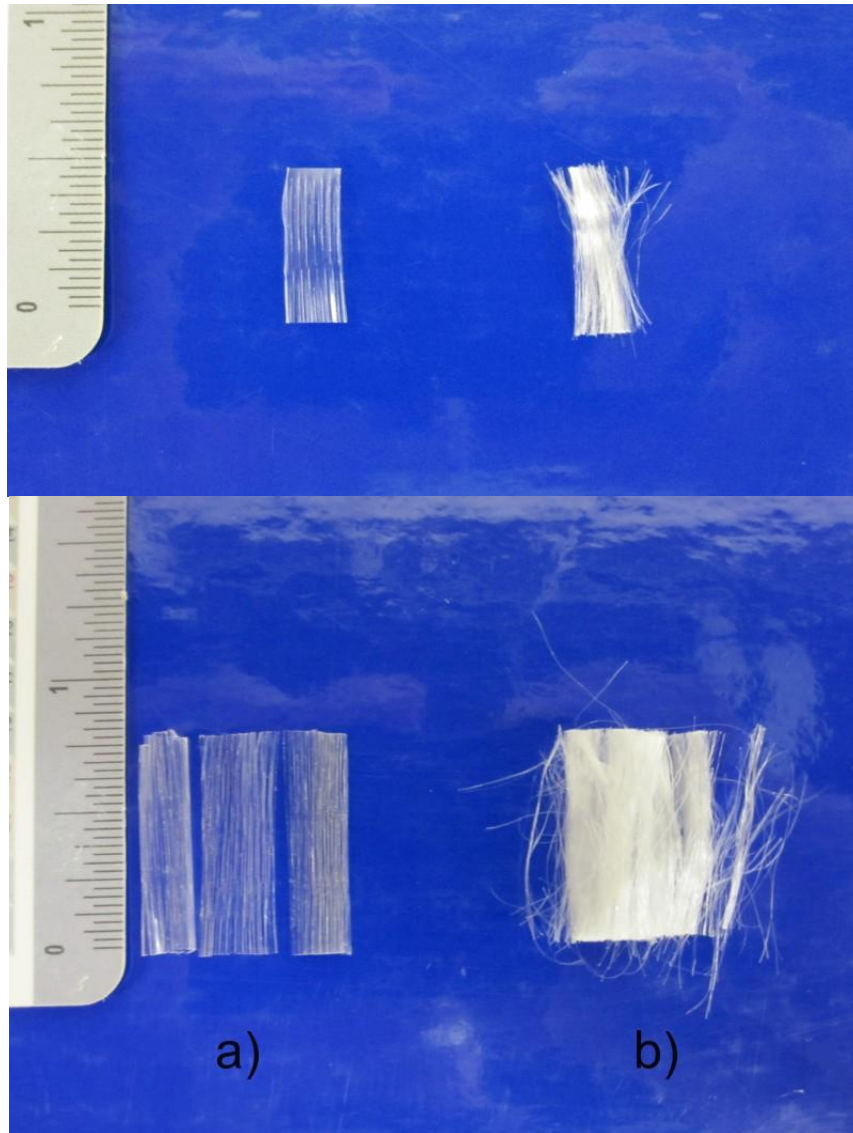
Figure 3-4: Polypropylene fibers used in the experiments. a) Fibrillated fiber b) Monofilament fiber

Summary of the properties of both PP fibers are presented in table 3-1.

Table 3-2: Properties of polypropylene fibers

Properties	Monofilament Fiber	Fibrillated Fiber
Specific Gravity	0.91	0.91
Tensile Strength	552-758 MPa (80-110 ksi)	552-758 MPa (80-110 ksi)
Denier	6	1500
Thickness*	0.030 mm (0.0012 in)	0.48 mm (0.019 in)
Melting Point	Above 160C (320F)	Above 160C (320F)
Flash Point	Above 329C (624F)	Above 329C (624F)
Autoignition Temperatures **	Above 357C (675F)	Above 357C (675F)
Electrical & Thermal Conductivity	Low	Low
Acid & Salt Resistance	High	High
Alkali Resistance	Alkali Proof	Alkali Proof

* The following formula can be used in order to measure thickness of a fiber using the denier and specific gravity of the fiber:

$$Thickness\ (in\ \mu m) = \frac{Denier \times 141.6}{Specific\ Gravity}$$

** The Autoignition Temperatures or Kindling Point of a substance is the lowest temperature at which it will spontaneously ignite in a normal atmosphere without an external source of ignition, such as a flame or spark.

3.2.2 Sample Preparation and Compaction Criteria

The soil-water mixture for compaction was prepared by first mixing a measured amount of dry soil with a predetermined amount of water (about 2 kg for each test) by hand and then by a mechanical mixer as shown in Figure 3-5.

Figure 3-5: Mixing using mechanical mixer

In the case of fiber addition, the weight of specific content of fibers was calculated based on the weight of air dried soil. The required amount of fiber was first mixed with the dry soil and then water was added. Mixing continued until a uniform mix is produced. Figure 3-6 shows a mixture of soil and fibrillated fibers.

Figure 3-6: Mixture of kaolinite soil and fibrillated fibers (FC = 0.6%)

The specimens were prepared by mixing the soil with various percentages of fiber

content (FC), determined by weight. Table 3-3 shows the composition of the mixtures

used in this study.

Table 3-3: Composition of mixtures

Number of Mixtures	By weight (%)
1	Soil + 0.0% Fiber
2	Soil + 0.2% Fiber
3	Soil + 0.4% Fiber
4	Soil + 0.6% Fiber
5	Soil + 0.8% for 0.5" Fiber

A compaction test was performed for each mixture immediately after achieving a uniform

and homogeneous mixture. To obtain four well-placed points on the compaction curves, a

low water content was selected for the first test point and was gradually increased for the

subsequent points. The water content should ideally be about 4 to 5% below the optimum

water content for the first point, and 4 to 5% above the optimum for the fourth and last point. For 2 kg of clayey soil, about 500 g of water was used for the first point, about 100 g of water was added for the second point and 50 g of water was added for the third and fourth points to achieve totals of about 600 g, 650 g, and 700 g of added water for the mixture at the second, third, and fourth points.

The soil-fiber composite was compacted in three layers, each with 25 blows in the 4 inch (101.6 mm) standard proctor mold following ASTM D 698 using standard effort (12,400 ft-lbf/ft^3(600 kN-m/m^3)). Figure 3-7 shows a compacted soil-fiber composite being extruded from the standard mold.

Figure 3-7: Compacted soil-fiber composite being extruded from the standard mold

3.2.3 Compaction Data and Discussion

Compaction tests were performed on a mixture of kaolinite soil with monofilament and also with fibrillated fibers at the following fiber contents: 0%, 0.2%,

0.4%, and 0.6% for 0.5 and 0.75 inch of fiber length, and 0.8% for only 0.5 inch of fiber

length. The results are presented below for monofilament and fibrillated fibers.
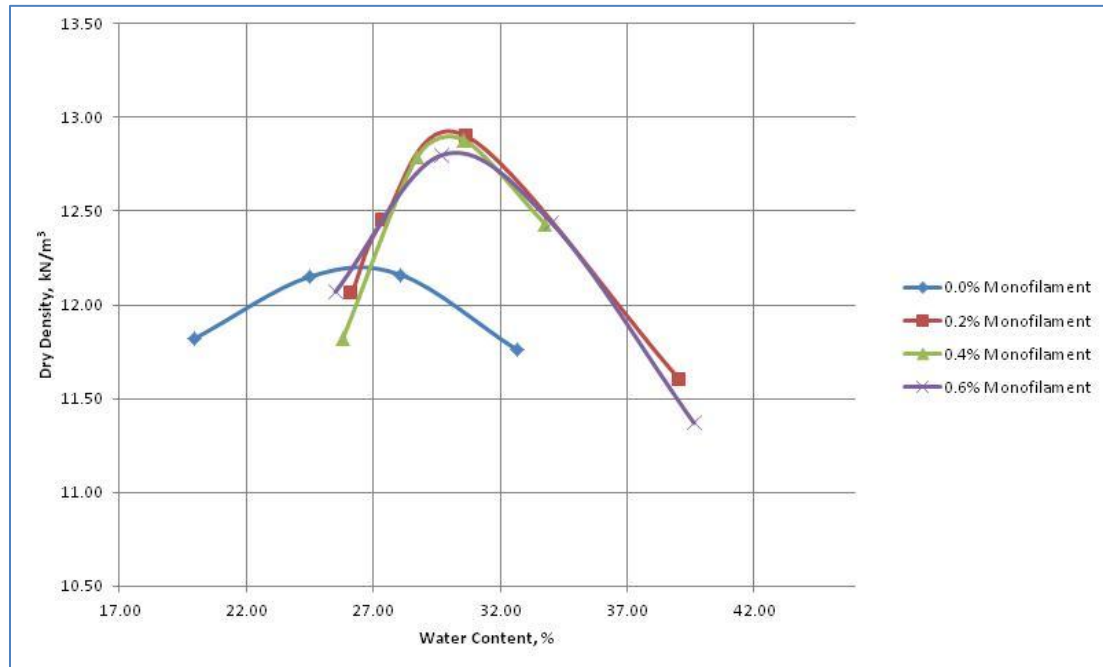
Figure 3-8: Compaction curves for composites of kaolinite soil and monofilament fibers
with various fiber contents (fiber length = 0.75 in)
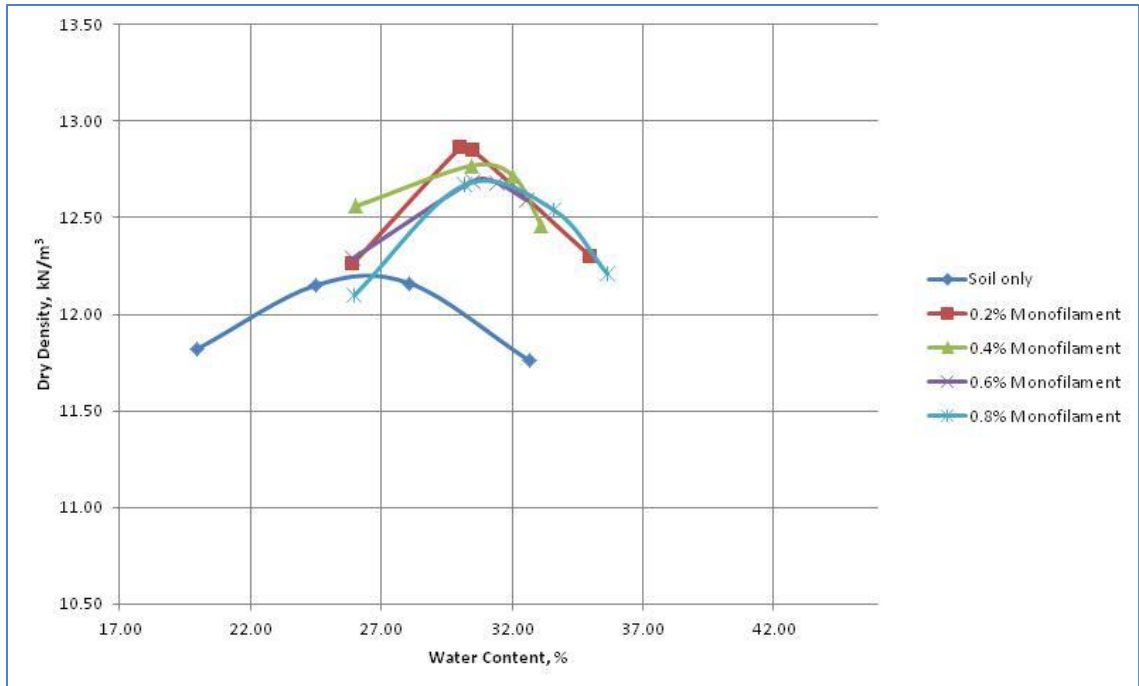
Figure 3-9: Compaction curves for composites of kaolinite soil and monofilament fibers with various fiber contents (fiber length = 0.5 in)
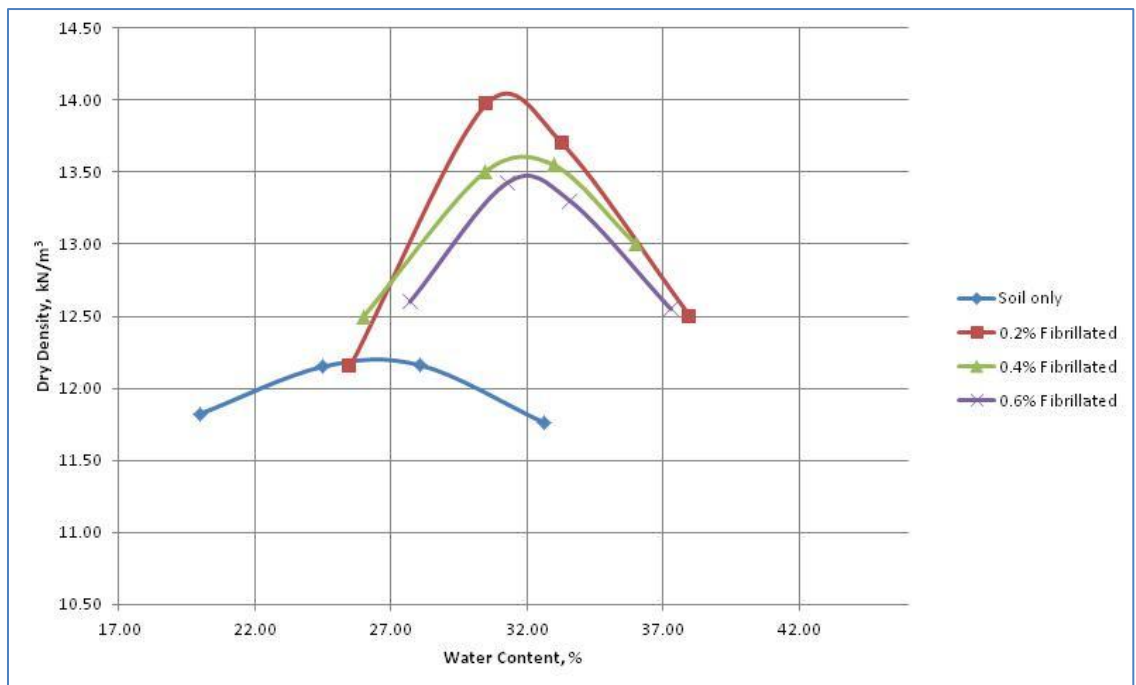
Figure 3-10: Compaction curves for composites of kaolinite soil and fibrillated fibers with various fiber contents (fiber length = 0.75 in)

106
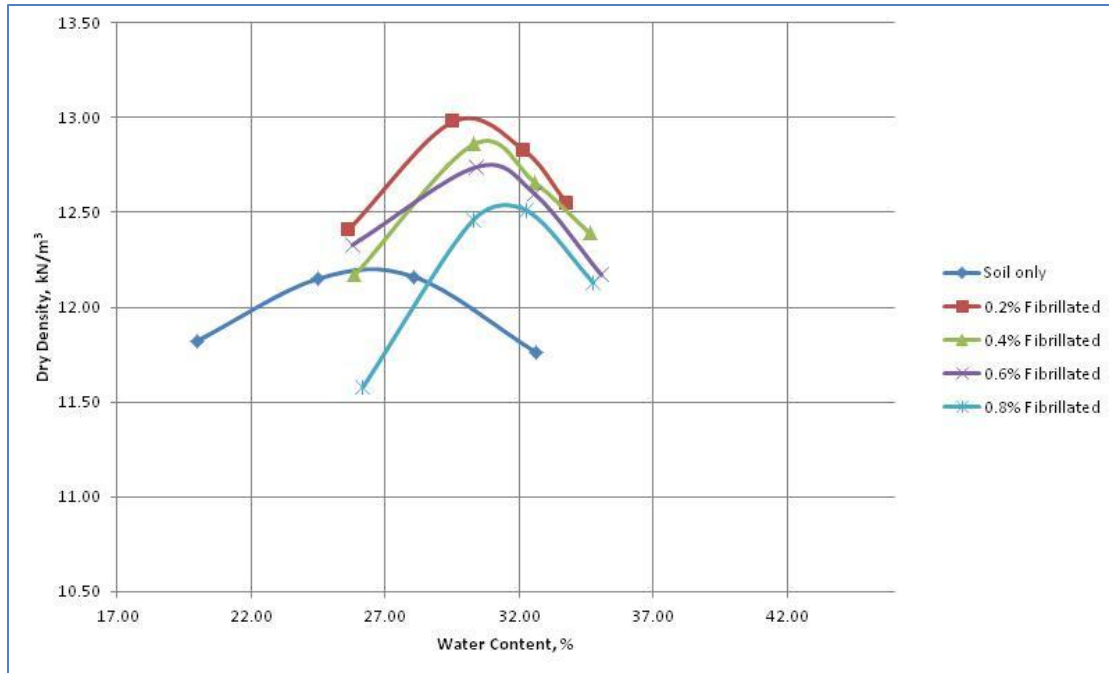
Figure 3-11: Compaction curves for composites of kaolinite soil and fibrillated fibers with various fiber contents (fiber length = 0.5 in)

A Summary of the compaction test results is presented in Table 3-4 and Figures 3-12 through 3-15 in the form of bar charts.

Table 3-4: Compaction test result for various fiber contents

FL (in)	FC (%)	Monofilament Fiber		Fibrillated Fiber	
		MDD[25] (kN/m^3)	OMC[26] (%)	MDD (kN/m^3)	OMC (%)
0.75	0.0	12.18	26.0	12.18	26.0
	0.2	12.95	29.9	14.04	31.0
	0.4	12.82	30.6	13.60	32.0
	0.6	12.89	30.2	13.45	32.3
0.50	0.0	12.18	26.0	12.18	26.0
	0.2	12.87	30.2	13.00	30.0
	0.4	12.78	30.8	12.88	30.7
	0.6	12.71	30.9	12.75	30.9
	0.8	12.69	31.0	12.55	31.2

---

[25] Maximum Dry Density
[26] Optimum Moisture Content
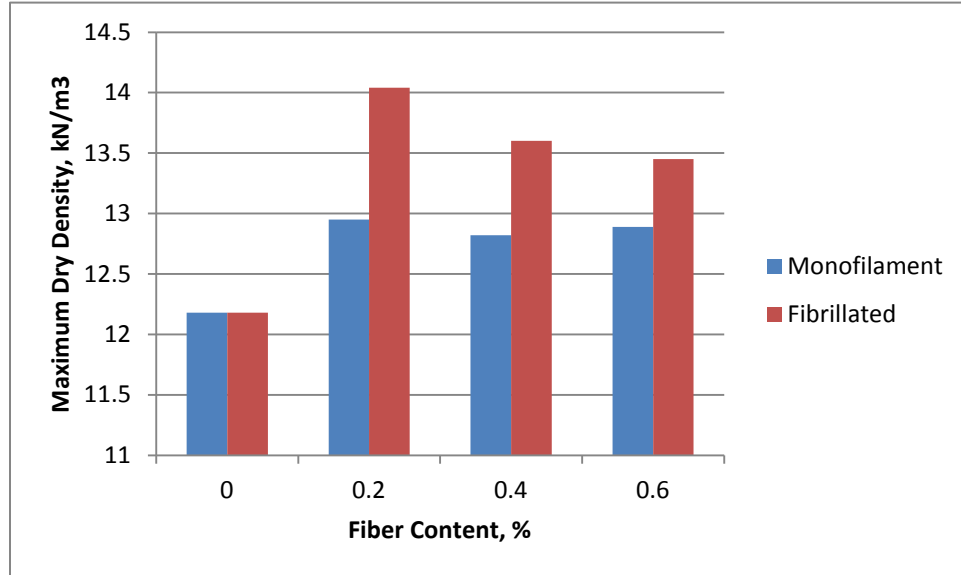
Figure 3-12: Change in $\gamma_{d\,max}$ with various fiber contents (fiber length = 0.75 in)
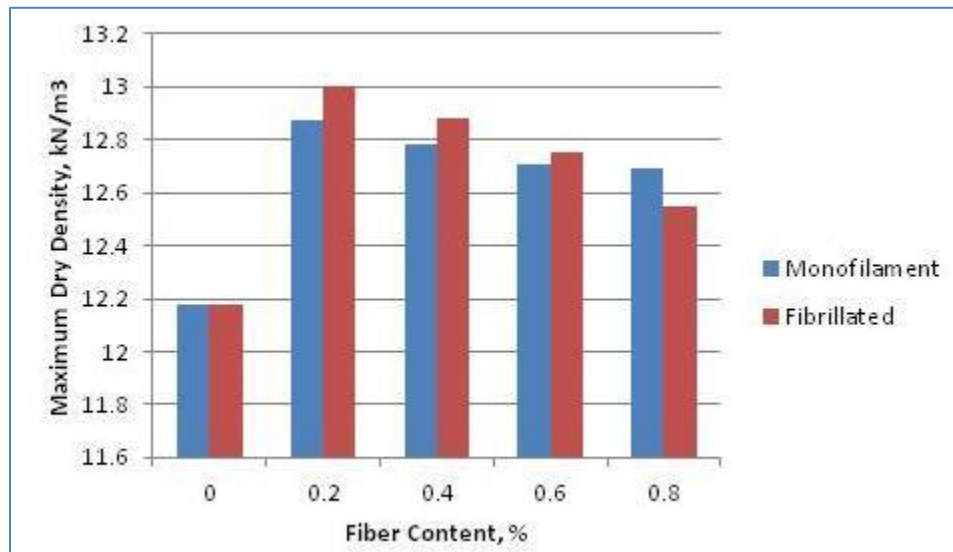
Figure 3-13: Change in $\gamma_{d\,max}$ with various fiber contents (fiber length = 0.5 in)
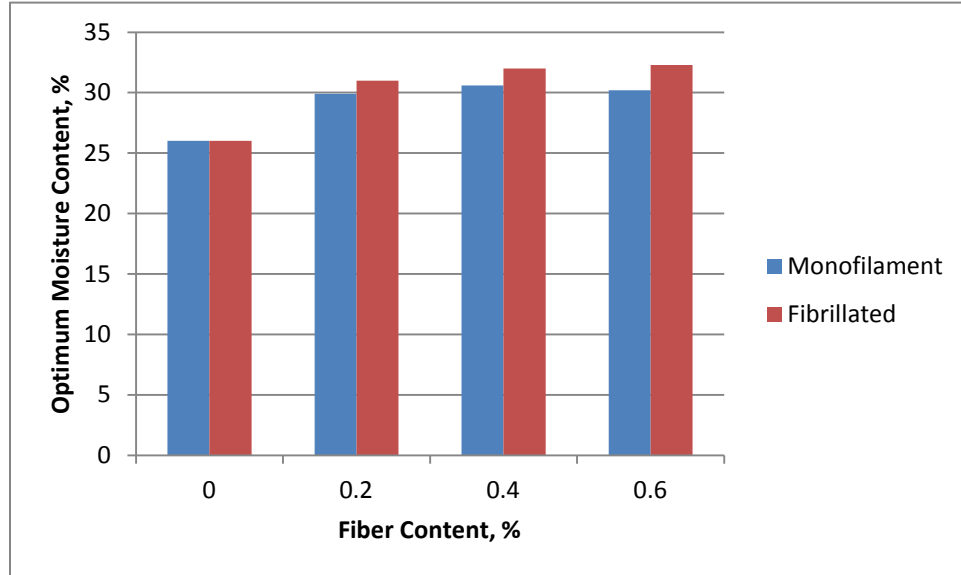
Figure 3-14: Change in OMC with various fiber contents (fiber length = 0.75 in)
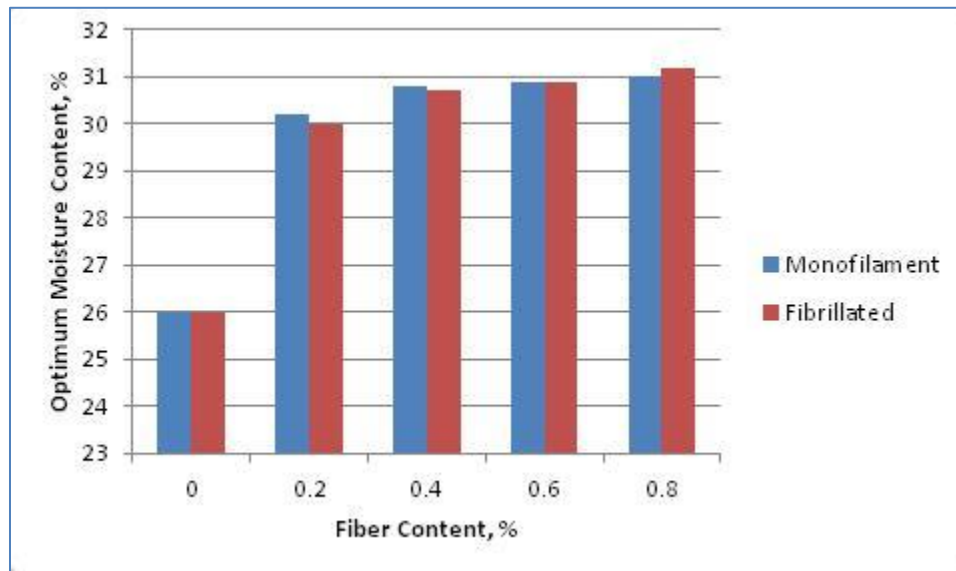
Figure 3-15: Change in OMC with various fiber contents (fiber length = 0.5 in)

Based on the above results, it can be seen that the addition of fibers affected both the $\gamma_{d\ max}$ and OMC. The $\gamma_{d\ max}$ of soil increased with the inclusion of fiber. It shows the fiber inclusion can more effectively eradicate the air fraction of the voids and can increase the dry density of the soil. The maximum value for $\gamma_{d\ max}$ for both type of fibers and lengths were at 0.2% fiber content. The value of $\gamma_{d\ max}$ increased approximately 6% and 15%, respectively, for mixtures with monofilament and fibrillated fibers of 0.75 inch length compared to the soil without fibers. The value of $\gamma_{d\ max}$ also increased approximately 5.5% and 7%, respectively, for mixtures with monofilament and fibrillated fibers of 0.5 inch length compared to soils without fiber. The largest increase in the value of $\gamma_{d\ max}$ was determined for the mixture with fibrillated fiber of 0.75 inch length. The results of maximum dry density for mixtures of 0.2% fiber and clay are shown in Figure 3-16. An increase in the value of OMC was also observed when comparing to soil with no fiber content. The lowest values for OMC of the soil-fiber composites were for the fiber inclusion of 0.2%.
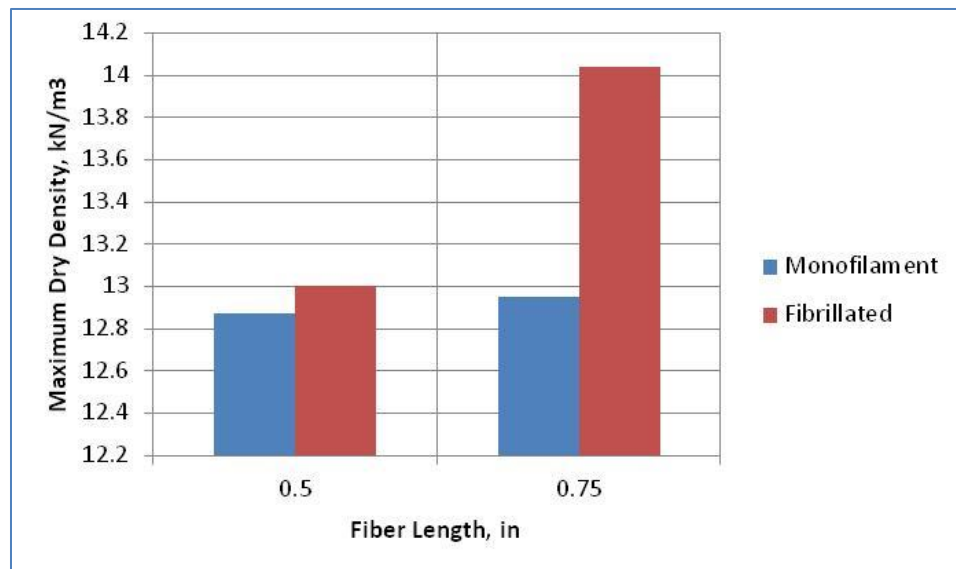
Figure 3-16: Change in MDD with various fiber lengths and types

3.2.4 Conclusion

It can be concluded that the changes in $\gamma_{d\ max}$ are mainly due to the displacement and rearrangement of soil particles caused by the inclusion of fibers. With the inclusion of fiber in general, fibers will fill the voids in the soil and therefore the soil specimen density becomes higher. At the optimum fiber content (OFC = 0.2%), fibers have effectively filled in the pore voids of the soil. As the amount of fiber exceeds the optimum value, the extra fibers will be placed in between soil particles and will not allow the soil particles to come close to each other and thus result in the reduction in the $\gamma_{d\ max}$ value. To obtain the maximum benefit of adding fiber, the optimum fiber could be determined from compaction tests.

Soil behavior is a function of its density. By performing compaction tests on soils with different percentages of fiber it is shown that there is an optimum percentage of fiber that produces the maximum density of soil and determines the optimal water content needed for that percentage of fiber. Such percentages will produce the maximum benefit of the fiber. It is expected that the optimum percentage of fiber will be different for different types of fibers and for different types of soil, as well as for different degrees of compaction. Thus geotechnical engineers need to perform compaction tests if different fibers or soils are used and the percentage of fiber will likely be different for different situations (Amir-Faryar & Aggour, 2012a).

The proper selection of the fiber content for each mixture is also important. It is suggested that fiber contents be selected with small intervals, at least 0.2%. As an example, in our study, the optimum fiber content could have been missed if fiber contents of 0, 0.5%, and 1% had been selected (0.5% intervals). Hence, the fiber contents of 0,

0.5%, and 1% could not provide the trend necessary to determine the optimum fiber content for the used fiber-reinforced composite. Furthermore, fiber content should be increased until a reduction in the value of the maximum dry density is observed for each particular clay type. The reduction will take place when all the soil voids are filled in with fibers and additional fibers are placed in between soil particles rather than in the voids.

CHAPTER 4 DYNAMIC TESTING PROGRAM AND RESULTS

4.1   Introduction

The research presented in this chapter has been performed for five main purposes: (1) to investigate the effect of fiber inclusion on the dynamic properties of clay; (2) to study the effect of the fiber content on the dynamic properties of the composite; (3) to investigate the effect of the type of fibers on the dynamic properties of clay; (4) to determine an analytical relationship between shear modulus and shear strain and also between material damping and shear strain of the composite; (5) to develop a general formula correlating material damping to the shear strain of soil. The developed formula is applied to all soil types, clayey, sandy, and fiber-reinforced soil composites.

Formulas play a central role in predicting variables across various fields of study. Mathematical modeling of empirical data contains a general discussion about the experimental data obtained and its integration with data obtained from various experimental works in the field. A curve fitting model function correlating shear modulus with shear strain for soils is proposed in this chapter. Analytical relationships are then developed for clay and also fibrillated fiber-clay composites at fiber contents of 0.2% and 0.4%.

There are several mathematical models, formulas, and methods available to predict the material damping of soil. The majority of the available models and methods are lengthy and do not describe the damping system accurately. Some of them are limited to training data (the data used to develop that particular formula) or developed using a specific type of soil experiment in a particular condition that does not apply to a different

soil when the conditions are dissimilar. The available formulas are not universal, meaning if developed for sandy soils; it may not be able to be used for clays or vice versa. Therefore, developing a general formula that can correlate damping ratio to shear strain was needed. A general universal mathematical model was developed and evaluated using verification data (data that was not used to set the model's parameter) to determine if the developed mathematical model can describe a soil damping system accurately. The obtained "General Material Damping Formula for Soils" was evaluated against different soil types; i.e., sandy, clayey soils as well as fiber-clay composites.

4.2   Testing Apparatus

The Drnevich resonant column apparatus, a relatively nondestructive testing equipment, was used for this research. The resonant column testing apparatus employs a chamber having a lower and a top active platen confining a column of soil in between and with means to provide water and compressed air into the chamber for subjecting the column of soil to conditions representative of in-situ soil. A magnetic plate supporting torsional and longitudinal accelerometers, in association with fixed coils connected with an electrical circuit, provides for torsional vibration of the soil column. A centrally placed coil on the torsional magnet plate provides for torsional vibration of the soil column and a length measuring transducer (LVDT) in the upper platen serves to give constant readings of the length changes of the soil column.

The excitation system of the resonant column device is an electromagnetic system comprising of a permanent magnet and coil, which can move in the gap between the north and south poles of the permanent magnet. For the torsional mode, the assembly comprises four rectangular coils and horseshoe-shaped magnets. The coils are connected

to the brackets and the magnets are connected to the top active platen. Equal gaps should be maintained between the magnets and the coils to minimize the development of any bending forces. The torsional coils allow movements (1.3 cm) in the vertical direction to accommodate the change in length during the consolidation process of clay. By generating an AC current of controlled frequency through the coils a magnetic field would be generated that in turn develops torsional forces on the top of the soil column.

During each testing routine, the wave oscillator signals are amplified by the power amplifier and then inputted to the drive coils after passing through the power resistor in the control box. The pick-up system comprises of a piezoelectric meter (Columbia Model 200-1-H) placed in the active-end platen. The transducer is mounted at a distance of 0.0316 meters from the axes of rotation. The digital multimeter and oscilloscope are used to record the responses. A digital multimeter gives readings of sample acceleration in terms of rms; which in turn can be converted to define the shear strain. The oscilloscope monitors the frequency response of the sample.

Sinusoidal excitation is used to study the dynamic properties, usually shear modulus and shear damping ratio, of soil in resonant column devices. In the tests, soils specimens vibrate torsionally under a sinusoidal excitation, and the shear modulus and damping ratio are measured from the resonant frequency and response, which are obtained by adjusting the frequency of the sinusoidal signal generator to a situation in which a vertical ellipse is observed.

4.3   Low-Amplitude Moduli of Fiber Reinforced Clay

Low-amplitude moduli, or the maximum moduli of soils, are important to practical engineering, for example, low-amplitude moduli of soils are used in evaluating wave velocities, strength, etc. of soil. Currently, many methods are used to evaluate the low-amplitude moduli of soil in the field and laboratory as stated in chapter 1. In the Resonant Column Test, a confining pressure of 5 psi (34.5 kPa), corresponding to approximately six feet of soil in an in situ condition, was applied to the specimen.

4.4   Sample Preparation

The specimens were prepared by mixing kaolinite with various percentages of fiber content (FC) and percentages of mixtures by weight, per Amir-Faryar and Aggour's established compaction procedure (Amir-Faryar and Aggour, 2012a) as explained in Chapter 3. The soil-water mixture for compaction was prepared by first mixing a measured amount of dry soil (about 2 kg in each test) with a predetermined amount of water by hand and then by a mechanical mixer. In the case of fiber addition, the weight of the specific fiber contents was calculated based on the weight of the air dried soil. The required amount of fiber was first mixed with the dry soil, and then water was gradually added. Mixing continued until a uniform mix was produced. Compaction tests were performed on a mixture of kaolinite soil with fiber immediately after achieving a uniform and homogeneous mixture. Mixtures of monofilament fiber and kaolinite soil and also fibrillated fiber and kaolinite were made at their maximum dry densities and optimum moisture contents. Resonant Column tests were performed on composites with different fiber contents. An undisturbed sample from the fiber-clay composite at fiber contents of

116

0.2%, 0.4%, and 0.6% were carefully obtained using a hollow brass cylinder shown in Figure 4-1.

Figure 4-1: Hollow brass cylinder with clay sample inside

The inside and outside of the hollow cylinder was lubed using 3M Silicone Lubricant.

The hollow cylinder was pushed into the already-compacted-clay in the standard mold, using a Tinius Olson Compressor. Then, the clayey soil was taken out of the standard mold using a standard mold extruder as shown in Figure 4-2.

Figure 4-2: Hollow brass cylinder pushed into the compacted soil

The brass cylinder with soil inside was recovered as shown in Figure 4-1. Then,

the soil specimen was gently taken out of the brass hollow cylinder using a filled cylinder

shown in Figure 4-3, and a Tinius Olson Compressor. The diameter of the filled cylinder

is slightly smaller than the diameter of the brass hollow cylinder.

Figure 4-3: Filled cylinder

Caution should be undertaken when the specimen is taken out of the hollow cylinder in order to obtain a specimen with the least amount of disturbance. Shear wave velocity and maximum shear modulus measurements in the field and laboratory are very sensitive to sample disturbance effects. Therefore, field values may be 20 % to 100 % higher than lab values. Specimens of approximately 35 mm diameter and 82 mm length were prepared.

The dynamic test should not be started until the resonant column apparatus and all its attached devices are assured to be properly working. Hence, each time a soil specimen was made it was kept inside a lidded jar to maintain its moisture content and minimize the loss of moisture. The specimen is shown inside a lidded jar in Figure 4-4.
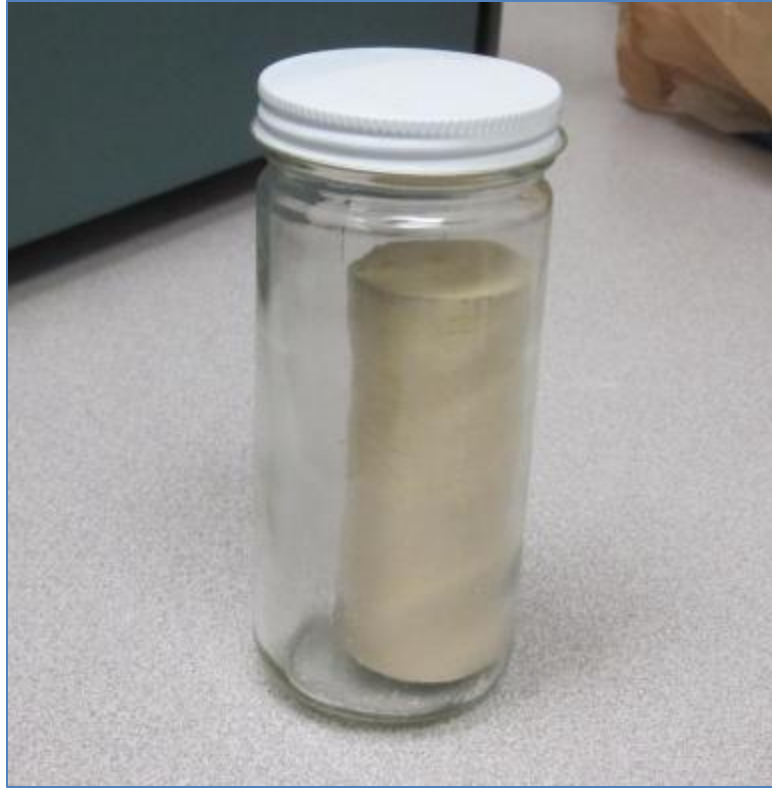
Figure 4-4: Soil specimen held inside a lidded jar

When the testing was about to start, a thin membrane was wrapped around the specimen then placed inside the resonant column apparatus. Two O-rings were used to block water from seeping into the specimen as shown in Figure 4-5.

Figure 4-5: Membrane wrapped around soil specimen. Two o'rings can be seen in the picture

Specimens for all different mixtures were placed under 34.5 kPa (5 psi) pressure for 1020 minutes in order to have the primary consolidation completed prior to starting the dynamic testing. It is indicated that under uniform confining pressure primary consolidation of clay can be completed after approximately 1000 minutes of pressure application (Afifi & Richart, 1973). Some researchers have indicated that the completion of the primary consolidation can take place at approximately 100 to 200 minutes after which secondary consolidation begins (Kokusho, et al., 1982). After placement of the specimen under confining pressure for 1020 minutes (17 hours), no longitudinal strain

was recorded. Therefore, 1020 minutes appeared to be sufficient for our testing. The dynamic testing was also performed under 34.5 kPa confining pressure.

4.5   Dynamic Testing Procedure

After the weight, diameter, and length of the specimen was determined, the specimen was inserted in the rubber membrane and set up on the bottom platen of the resonant column and the top platen attached when the magnet platen was lowered and placed on the top of the specimen. Two rubber O-rings were used close to each end of the specimen to protect the specimen from being soaked by the confining media. Then, the torsional drive coil system and LVDT were assembled. Vacuum grease was used prior to placing the pressure chamber in order to seal the chamber. The pressure chamber was filled with water to the top porous stone to ensure a uniform confining pressure around the specimen. After allowing the water turbulence to settle, the initial reading of the LVDT was recorded. Then, the specimen was placed under the confining pressure as described in Section 4.4. After the confining period, the sample was torsionally excited with sinusoidal waves. The resonance condition of the system at each strain amplitude was established by adjusting the frequency of the excitation until a Lissajous figure was observed as shown in Figure 4-6. A Lissajous figure is a vertical ellipse that corresponds to a 90 degree phase angle between the acceleration response and the excitation.

Figure 4-6: Observed Lissajous figure on oscilloscope

The resonant frequency of the system was measured with a digital frequency counter and

the excitation and response accelerations were measured by a digital multimeter in

millivolt (rms).

The dynamic testing was performed on clay with 0%, 0.2%, 0.4%, and 0.6% fiber

contents with an initial frequency and voltage amplitude of 15 Hz and 50 mV,

respectively. The frequency was gradually increased to reach up to the sample's resonant frequency while the voltage amplitude remained constant. The test was repeated for each sample with 100, 200, and 300 mV voltage amplitudes to obtain data for different shear strains. The test was performed on clay mixtures with fibrillated fibers as well as monofilament.

4.5   Dynamic Testing Results for Fibrillated Fiber Reinforced Clay

The resonant column tests were conducted on clay as well as mixtures of clay and 0.75 inch fibrillated fiber with different fiber contents in order to study the effect of fiber inclusion as well as fiber content on the dynamic properties of clay. As for fiber lengths, a 0.75 inch length was selected over a 0.5 inch length because it was shown in Chapter 3 that the composites made with 0.75 inch fiber provided denser mixtures, as shown in Table 3-3. The results of the dynamic testing are discussed in the following sections.

4.5.1   Effect of Fibrillated Fiber Inclusion and Fiber Content on Shear Modulus of Clay

It was observed that the addition of fibrillated fibers affected the shear modulus of clay. The results indicated that the inclusion of fibrillated fiber increased the maximum shear modulus of the clay. Figure 4-7 shows the maximum shear modulus versus fiber content of the composite.

Figure 4-7: Maximum shear modulus versus fiber content graph (fibrillated fiber)

From Figure 4-7, it can be seen that the inclusion of fiber can increase the value of the maximum shear modulus as much as 17.5%. It can also be seen that the maximum value for the maximum shear modulus (G_{max}) is when the fiber content of the composite is equal to 0.2%. It also corresponds to the optimum fiber content value of the mixture obtained in Chapter 3. The value of the maximum shear modulus was increased when the fiber content increased until it reached up to 0.2%, then, by increasing the fiber content the value of the maximum shear modulus started to decrease.

The rate of degradation of the shear modulus is normally done by dividing the shear modulus by the maximum shear modulus at different shear strains. It is called the Normalized Shear Modulus (G/G_{max}). The curve of normalized shear modulus versus shear strain can provide valuable information about the soil as to how gradually the soil can lose its shear modulus value when the shear strain increases. In general, soils that lose their maximum shear modulus value faster due to larger strains are less stiff than the

125

ones that lose their maximum shear modulus slower. Figure 4-8 shows graphs of normalized shear modulus versus shear strain of clay and fiber reinforced composites with 0.2%, 0.4%, and 0.6% fibrillated fiber.
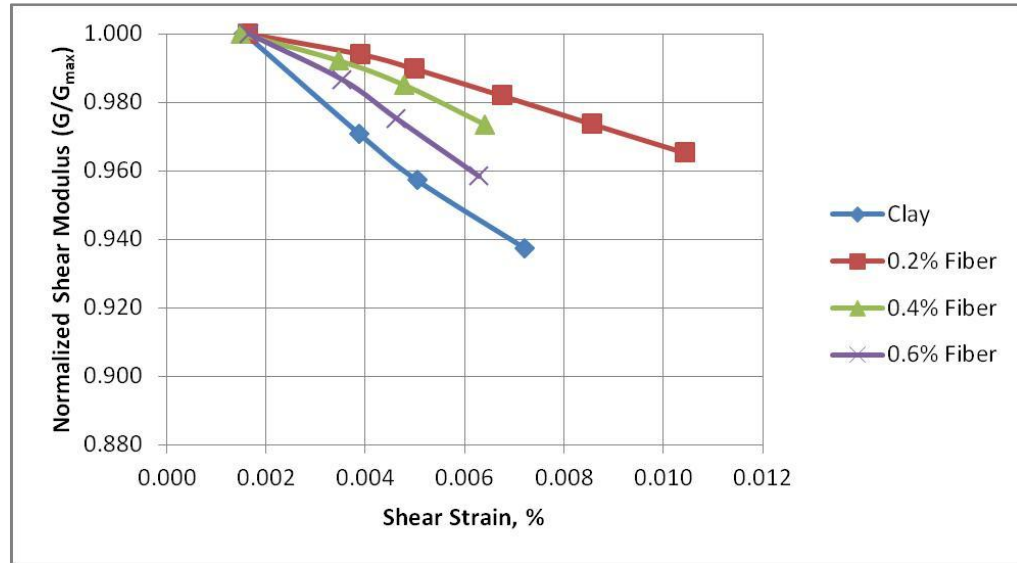
Figure 4-8: Normalized shear modulus versus shear strain graph for different fiber contents (Fibrillated fiber)

The results of Figure 4-8 generally indicated that fibrillated fiber, if used as reinforcement, could improve the shear modulus, which is an indication of torsional stiffness of the clay. Fiber reinforced composites showed that they had larger normalized shear modulus at the same shear strain. It was also shown that the composite with 0.2% fibrillated fiber lost its maximum shear modulus value slower than the other composites and the clay.

4.5.2   Effect of Fibrillated Fiber Inclusion and Fiber Content on Damping Ratio of Clay

It was also seen that the addition of fibers affected the damping ratio of the clay. The results indicated that the inclusion of fibrillated fiber increased the material damping

126

of the clayey soil. Figure 4-9 shows the minimum damping ratio (D_{min}) versus fiber content of the composite.
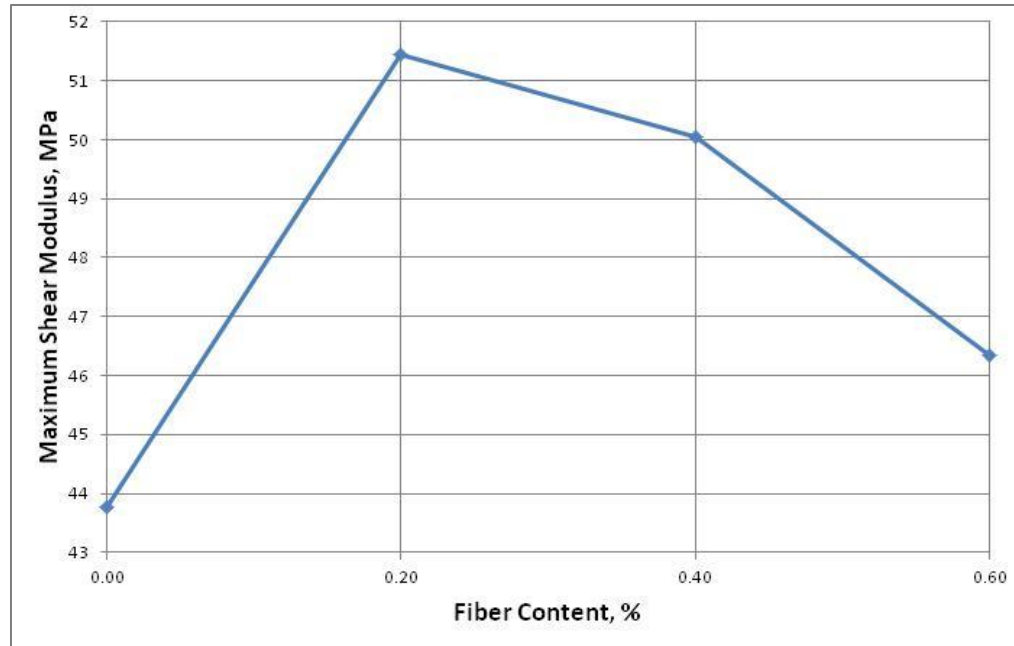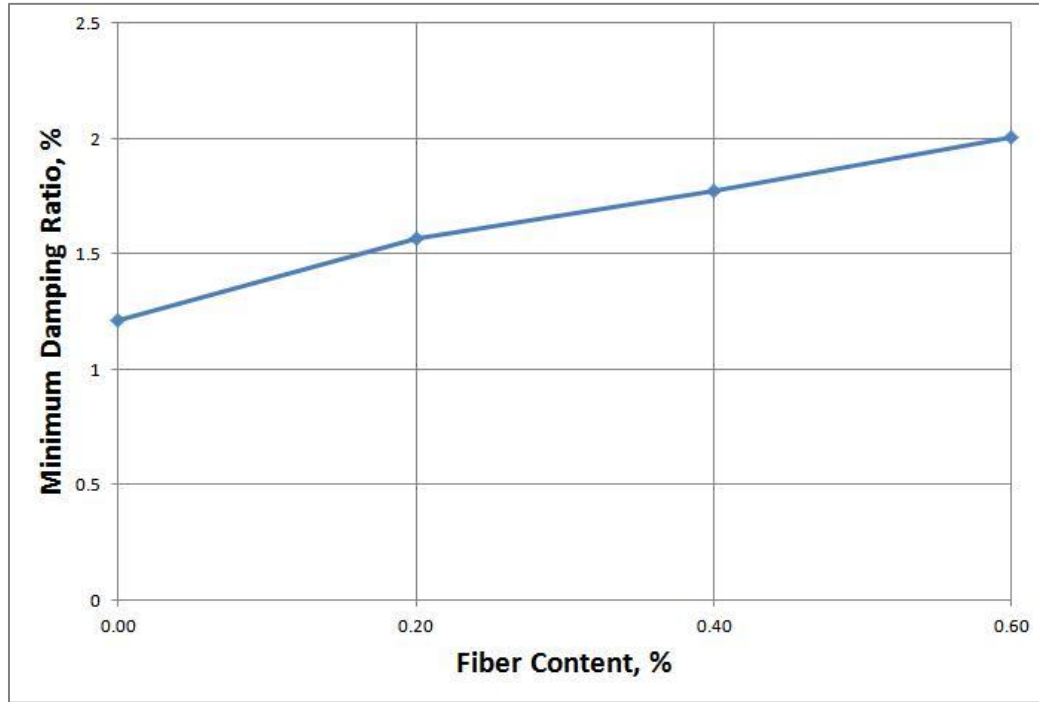

Figure 4-9: Minimum damping ratio versus fiber content graph (fibrillated fiber)

From Figure 4-9, it can be seen that the inclusion of fiber can increase the value of the damping ratio of the clay. It was observed that the increase in the value of material damping of the soil would be greater in composites with larger fiber content values. Figure 4-10 shows the graphs of damping ratio versus shear strain of clay and fiber reinforced composites with 0.2%, 0.4%, and 0.6% fibrillated fiber. It was observed that the value of the damping ratio of the clayey soil as well as fiber reinforced composites increased when the shear strain increased.
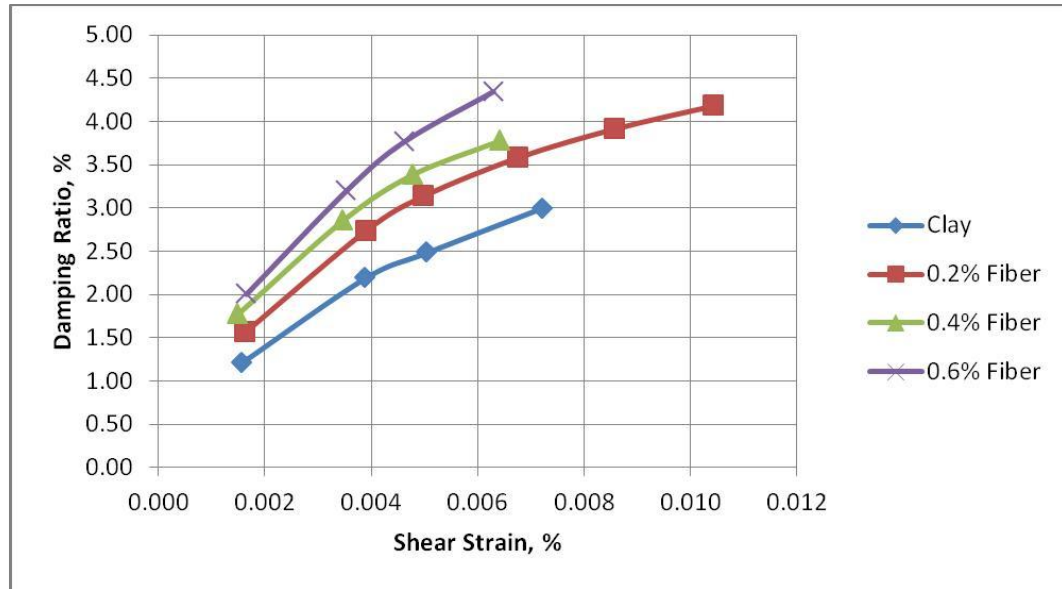
Figure 4-10: Damping versus shear strain graph for different fiber contents (fibrillated fiber)

4.6   Dynamic Testing Results for Monofilament Fiber Reinforced Clay

In order to further study the effect of fiber type, the length of the fiber was kept constant at 0.75 inch and mixtures with assigned fiber compositions, i.e., 0.2%, 0.4%, and 0.6% of monofilament type were made for testing.

4.6.1   Effect of Monofilament Fiber Inclusion and Fiber Content on Shear Modulus of Clay

The addition of monofilament fibers also affected the shear modulus of the clay. The results indicated that the inclusion of monofilament fiber increased the maximum shear modulus of the clay. Figure 4-11 shows the maximum shear modulus versus fiber content of the composite.

128

Figure 4-11: Maximum shear modulus versus fiber content graph (monofilament fiber)

From Figure 4-11, it can be seen that the inclusion of monofilament fiber can increase the value of the maximum shear modulus as much as 14.7%. It can also be seen that the maximum value for the maximum shear modulus (G_{max}) is when the fiber content of the composite is equal to 0.2%. It also corresponds to the optimum fiber content value of the composite. The value of the maximum shear modulus was increased when the fiber content increased until it reached up to 0.2% fiber, then by increasing the fiber content the value of the maximum shear modulus started to decrease.

Figure 4-12 shows the graphs of normalized shear modulus versus shear strain of clay and fiber reinforced composites with 0.2%, 0.4%, and 0.6% monofilament fiber.
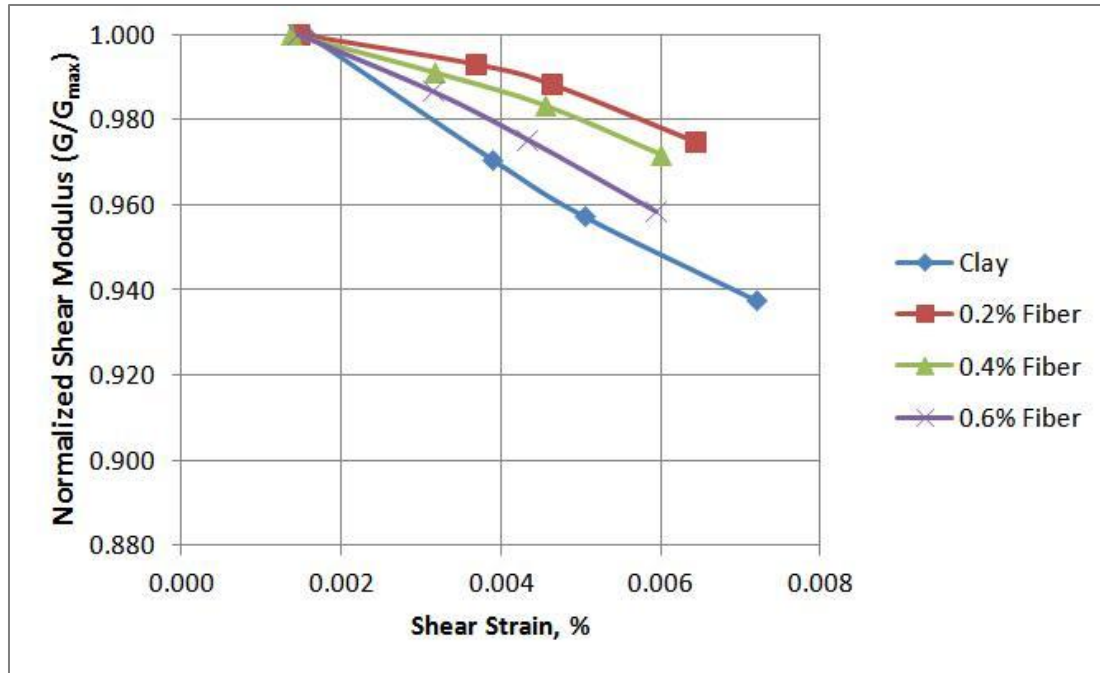
Figure 4-12: Normalized shear modulus versus shear strain graph for different fiber contents (monofilament fiber)

The results of Figure 4-12 generally indicated that monofilament fiber, if used as reinforcement, could improve the torsional stiffness of the clay. Fiber reinforced composites showed that they had a larger normalized shear modulus at the same shear strain. It was also shown that the composite with 0.2% monofilament fiber lost its maximum shear modulus value slower than the other composites and clay (Amir-Faryar & Aggour, 2012b).

4.6.1 Effect of Monofilament Fiber Inclusion and Fiber Content on Damping Ratio of Clay

The addition of monofilament fibers affected the damping ratio of the clay. The results indicated that the inclusion of monofilament fiber increased the material damping of the clayey soil. Figure 4-13 shows the minimum damping ratio (D_{min}) versus fiber content of the composite.
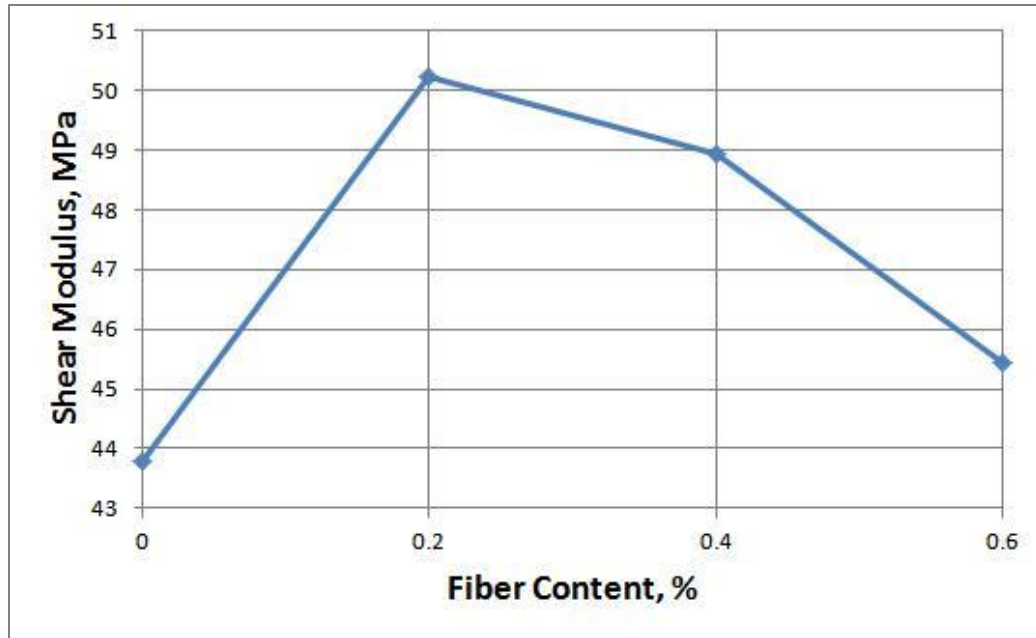
130
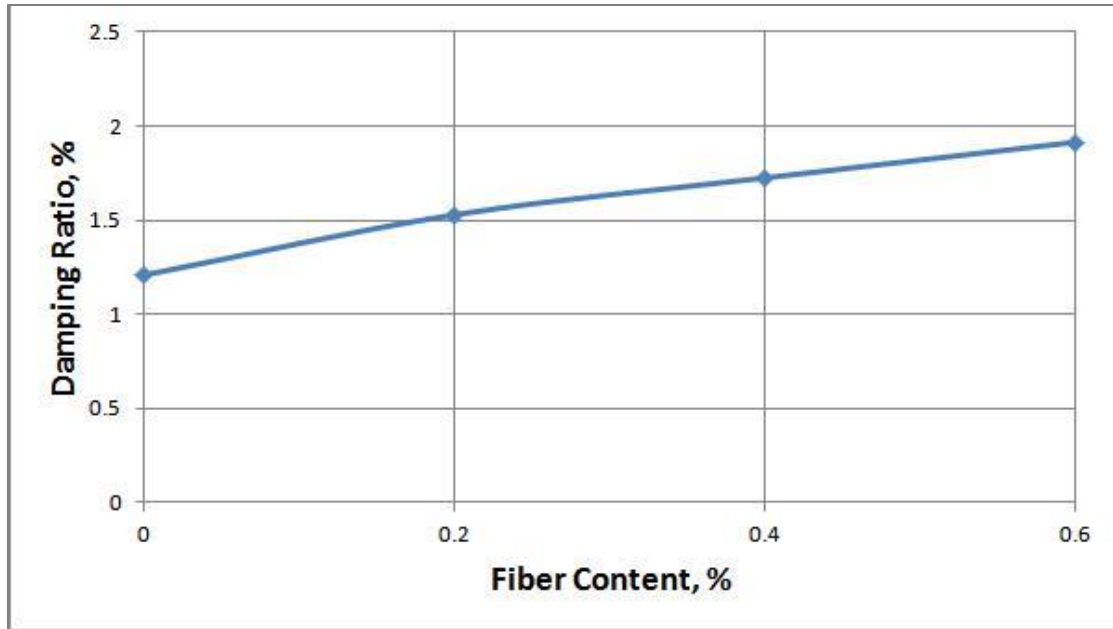
Figure 4-13: Minimum damping ratio versus fiber content graph (monofilament fiber)

From Figure 4-13, it can be seen that the inclusion of fiber can increase the value of the damping ratio of the clay. It was also observed that the increase in the value of material damping of the soil would be greater in composites with larger fiber content values. Figure 4-14 shows the graphs of damping ratio versus shear strain of clay and fiber reinforced composites with 0.2%, 0.4%, and 0.6% fibrillated fiber. It was observed that the value of the damping ratio of the clayey soil as well as fiber reinforced composites increased when the shear strain increased (Amir-Faryar & Aggour, 2012b).

131
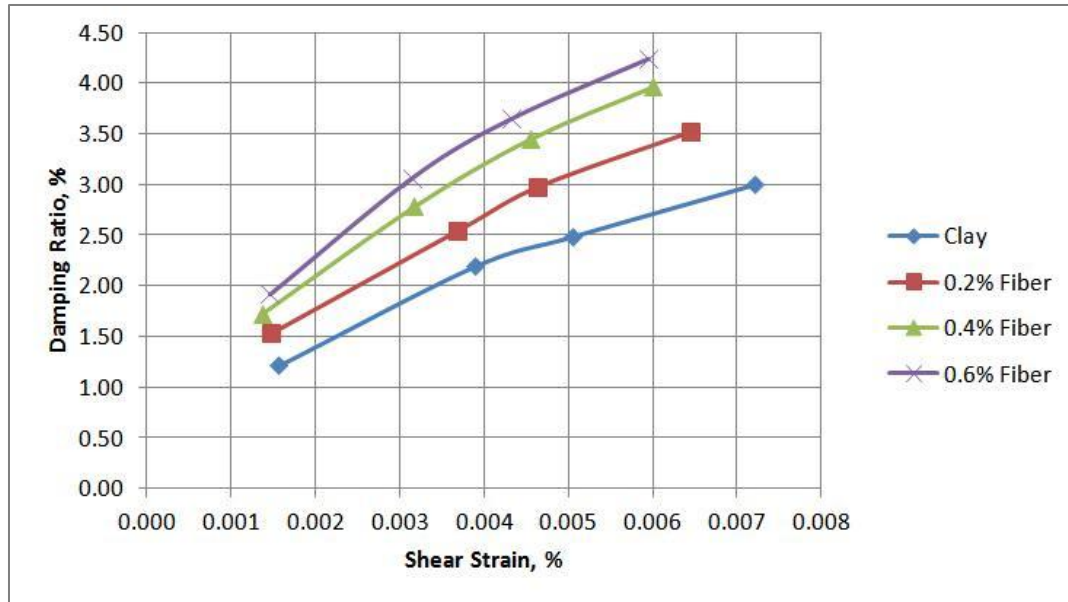
Figure 4-14: Damping versus shear strain graph for different fiber contents
(monofilament fiber)

It should be noted that the shear strain axis plotted is not in a logarithmic scale so as to

emphasize the changes in both the shear modulus and damping ratio in the low shear

strain range tested for the clay and the fiber reinforced clay.

4.7 Effect of Fiber Types on the Dynamic Properties of Clay

The results show that the inclusion of both types of fiber at optimum fiber content

can improve the shear modulus of clay. It was observed that the inclusion of fiber can

increase the maximum shear modulus of clay as much as 17.5% and 14.7% for fibrillated

and monofilament fibers, respectively. The maximum shear modulus of the fiber

reinforced clay is greater in the case of using fibrillated fiber as fiber reinforcement. This

observation could be due to the fact that a mixture made with fibrillated fiber is denser

than that made with monofilament fiber at the same fiber content. A conclusion can also

be drawn by comparing fiber deniers. A fiber's denier is 1500 and 6 in case of fibrillated

and monofilament fibers, respectively. It means that 9000 meters of fibrillated fiber is

250 times heavier than 9000 meters of monofilament fiber, based on the denier definition. That could be a reason for producing a denser composite when mixed with soil.

In addition, the inclusion of fiber increased the material damping ratio of the clay. The increase in the material damping ratio was 29.7% and 26.4% for fibrillated and monofilament fibers, respectively. The experiments showed that the inclusion of fibrillated fiber can improve the dynamic properties of clay slightly more than monofilament fiber. In order to better understand the damping results and why damping results in these two types of fiber were slightly different, we need to understand the fundamentals of damping in composites. The damping in composites is controlled by the matrix (clay) properties, the fiber properties, the interaction between fibers and the matrix. The matrix properties remained constant for composites made up of monofilament and fibrillated fibers when the dynamic testing was conducted. Hence, the effect of matrix properties and its contribution to the total material damping in each composite was the same. Since both fiber types, monofilament and fibrillated fibers, are made up of polypropylene fibers, the effect of fiber material on the total composite damping can also be similar. The fiber length and orientation for both types of composites were also kept constant. Therefore, the fiber properties could be eliminated as a cause in damping result differences between these two types of composites. The fiber-matrix interface or interphase region is an area where energy can be converted into heat is the most probable cause of obtaining slightly different material dampings. Different fiber-matrix adhesion and molecular motion within the interphase can be the reason for the slight difference in the material damping of these two types of composites.

4.8   Comparison of the Dynamic Response of Clay with Published Data

The results obtained from the dynamic testing of clay for this study were compared with the results of Vucetic and Dorby's (1991) general curves for clay at a similar plasticity index. Vucetic and Dorby's general curves for clay are used extensively to predict the dynamic properties of clay at different shear strains. The comparison shows that the normalized shear modulus and damping ratio obtained in this study agree with the Vucetic and Dorby's results. Figures 4-15 and 4-16, respectively, show normalized shear modulus versus shear strain and damping ratio versus shear strain developed from this study data and also Vucetic and Dorby's data.
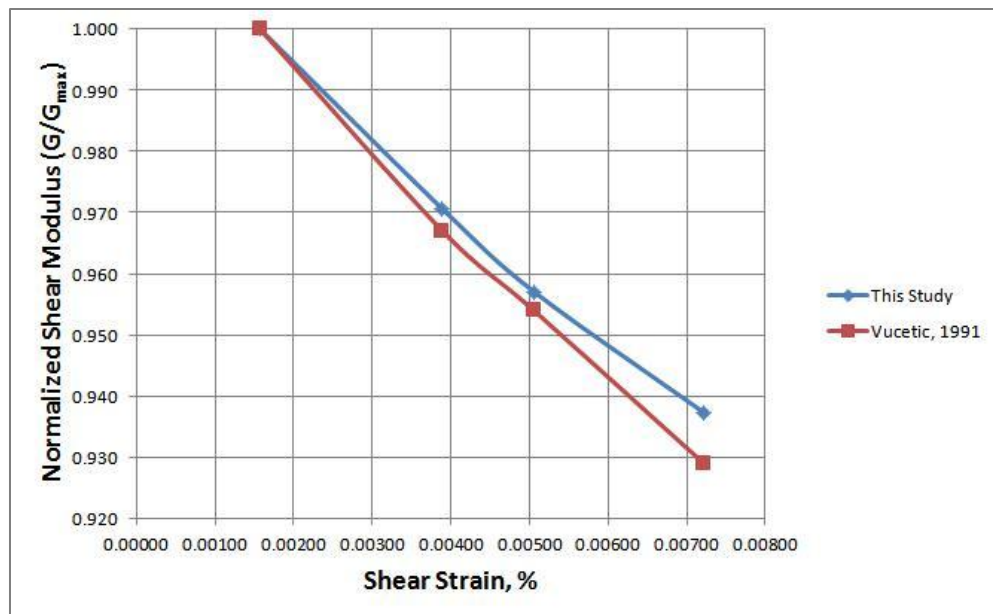
Figure 4-15: Normalized shear modulus versus shear strain comparison graph
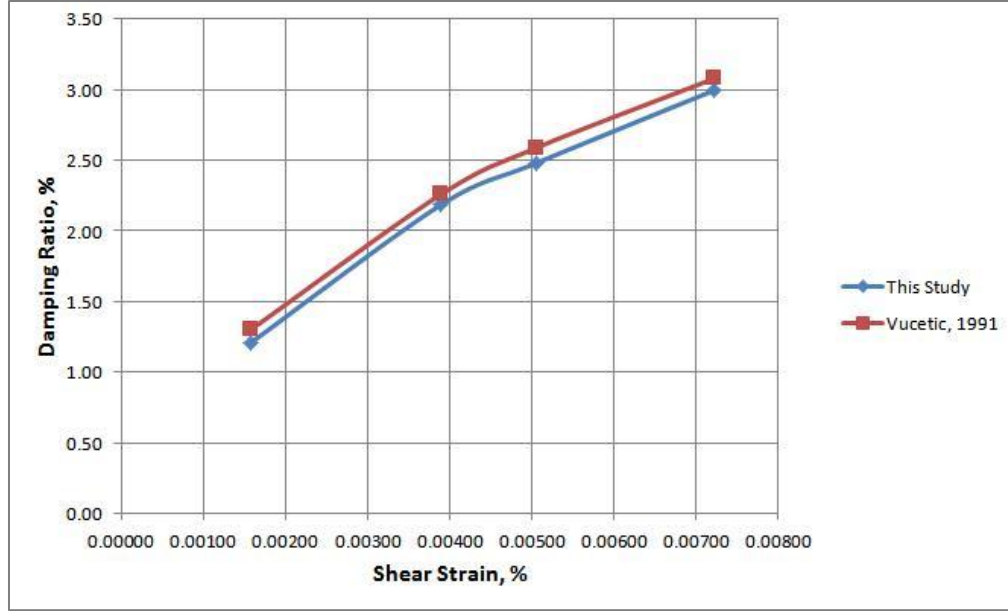
Figure 4-16: Damping versus shear strain comparison graph

4.9   Repeatability

Three samples of kaolinite were mixed and prepared with fibrillated fiber at optimum fiber content. The normalized shear moduli at low shear strains were determined. The mean and standard deviation (SD) of the samples are 0.99275 and 0.001at the shear strain of 0.00388 %, respectively. The mean and standard deviation of the samples for shear modulus are 51.71 MPa and 0.6 at the shear strain of 0.00388 %. All three samples fall within the 95 % mean confidence level (Varde, et al., 1996). The damping ratios at low shear strains were determined. The mean and standard deviation of the samples are 2.74 % and 0.02 at the shear strain of 0.00388 %, respectively. All three samples fall within the 95 % mean and ±4 SD confidence levels. Normalized shear modulus and damping ratio versus shear strain curves of all the three series of samples are shown in Figures 4-17 and 4-18.

135
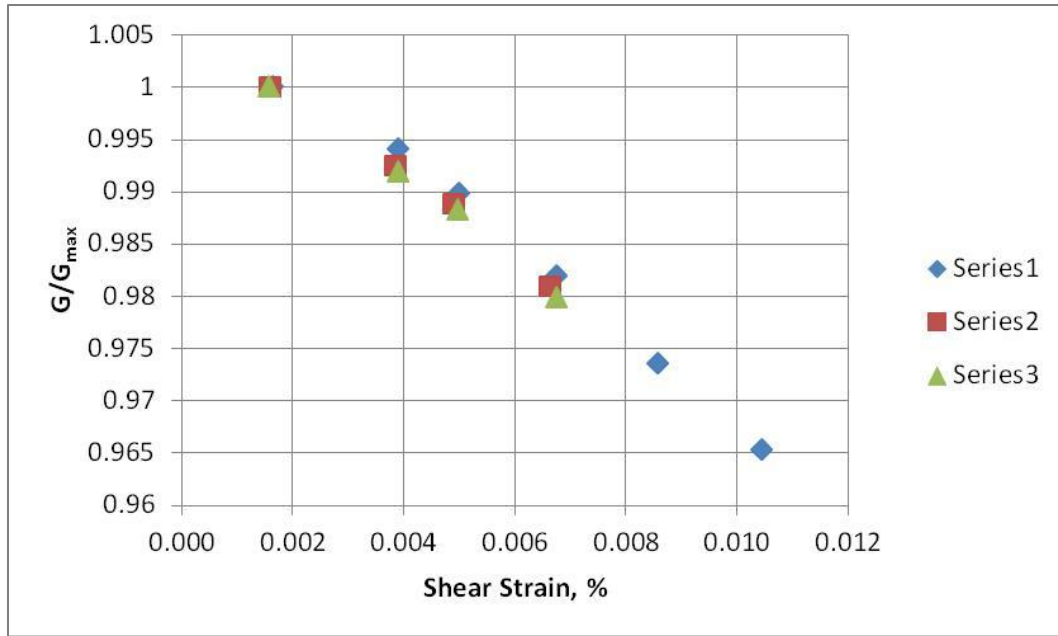
Figure 4-17: Normalized shear modulus versus shear strain series of data
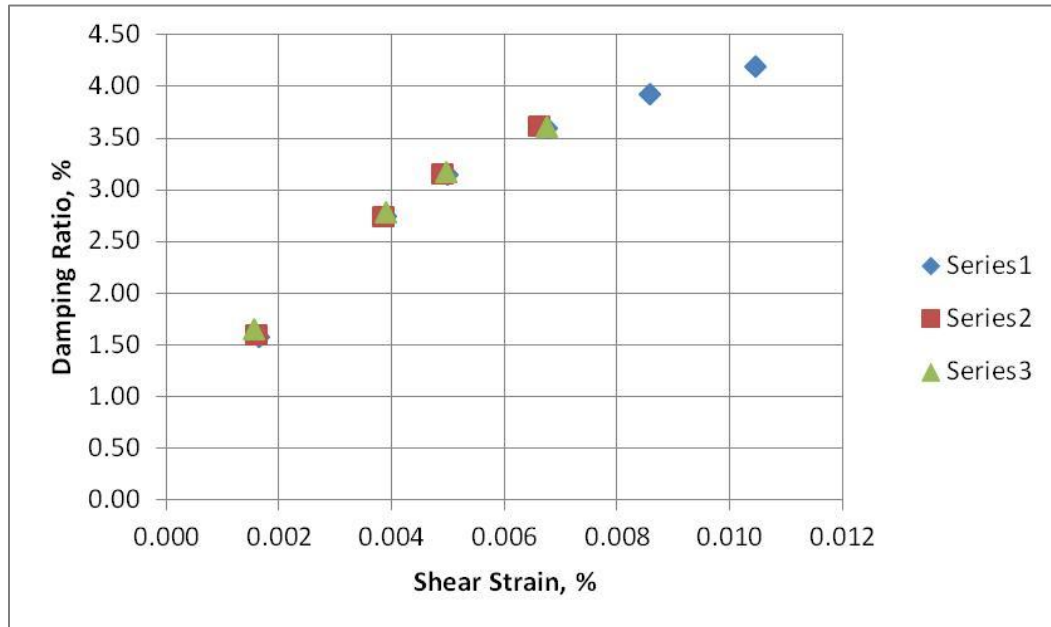
Figure 4-18: Damping ratio versus shear strain series of data

Figure 4-19 shows the damping data and also the confidence levels.
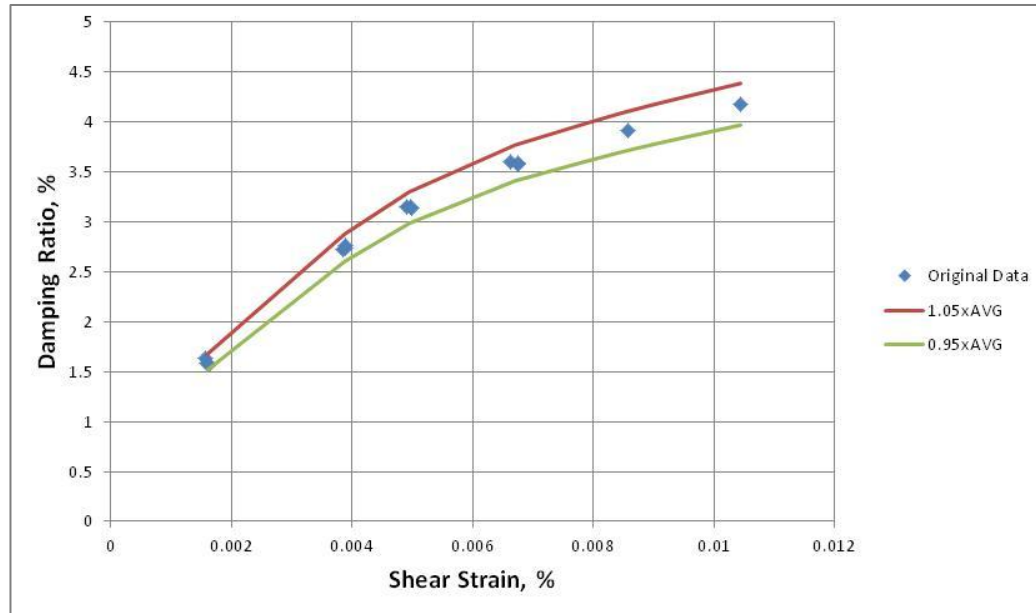
Figure 4-19: Modeling of damping ratio as function of shear strain

The results show that the obtained data are within the acceptable confidence level expected in soil preparation variability.

4.10   Mathematical Modeling of Empirical Data

A formula with four coefficients was proposed to be used as the function for the curve-fitting. Non-linear curve-fitting was performed to determine an analytical relationship between the shear modulus and shear strain of clay and fiber-clay composite using the proposed function. The measured and predicted values provided a good agreement for clay and fiber reinforced clay.

For damping ratio, there have been several equations and methods that they have been developed for a specific type of soil, and thus for other types of soils, do not provide a suitable agreement between experimental data and predicted data. Some of the methods are very lengthy and time-consuming and the ultimate predicted data is not accurate. Therefore, a general formula was developed for the damping ratio that can correlate soil

137

and composite's material damping to shear strain. The obtained formula is universal and can be used for any type of soil; i.e., clay, sand or even a fiber-clay composite. It is of paramount importance to form an effective strategy to determine coefficients of the formula. Hence, non-linear curve fitting using the least square error method following a procedure explained in Section 4.10.1 was utilized.

A function can be either linear or non-linear in the coefficients. The word "linear" in linear curve-fitting (regression) does not mean that the function is a straight line, but that the partial derivatives with respect to each coefficient are not a function of other coefficients. There are many published computer programs and commercial software packages that perform non-linear regression analysis. Out of which, Mathcad, Matlab, and Microsoft Excel Add-in Solver are the most popular applications to use for a non-linear least square method.

4.10.1 Non-linear Least Square Method

Least Square analysis is used to fit a set of 'm' observations with a model that is non-linear in n unknown parameters (m>n). A set of 'm' data points (x_1,y_1), (x_2,y_2), ..., (x_m,y_m) and a model function $y = f(x,b)$ where x is an independent variable and 'b' is unknown parameters, $b = (b_1, b_2, ..., b_n)$, with m>n. The objective is to obtain 'b' parameters such that the model best fits the given data in the least squares sense, that is the sum of residual squares as shown in Equation 4.1. The difference between the actual data point and the point predicted by the model function is called residual (error).

$$S = \sum_{i=1}^{m} r_i^2 \qquad\qquad (4.1)$$

where, r_i = residuals, S = sum of residual squares.

To obtain the best fit the sum of residual squares (S) should be minimized, where the residuals are given by equation 4.2.

$$r_i = y_i - f(x_i, b)$$
$$for\ i = 1, 2, ..., m \qquad\qquad (4.2)$$

The minimum value of S occurs when the gradient is equal to zero. Since the model contains n parameters there will be n gradient equations as equation 4.3.

$$\frac{\partial S}{\partial b_j} = 2 \sum_{i=1}^{m} r_i \frac{\partial r_i}{\partial b_j} = 0 \qquad\qquad (4.3)$$
$$(j = 1, ..., n)$$

In a non-linear system, the derivatives $\frac{\partial r_i}{\partial b_j}$ are functions of both the independent variables and the parameters. Therefore, these gradient equations do not have a closed solution. Instead, initial values must be chosen for the parameters, then, the parameters are refined iteratively to obtain optimized solutions. The optimization process can be done by published software packages. For instance, Mathcad has a function called "genfit" that can be used to find the best-fit coefficients. Matlab software also has a similar function called "fmins", which provides the same results as Mathcad function. There is also an add-in software package to a Microsoft Excel program that provides the same results as commercial software packages such as Mathcad and Matlab. The Solver

139

code is not written by Microsoft, but instead is a product of Frontline Systems, Inc. (www.frontsys.com) (Billo, 2001). The Solver add-in was used as an optimization tool for this research.

The Solver is an optimization package that attains a maximum, minimum, or specified value of a target cell by varying the values in one or several cells. It can achieve these tasks by means of an iterative process, beginning with trial values of the parameters (coefficients). The value of each parameter is changed by a suitable increment, the new value of the function is obtained and the change in the value of the function is used to calculate improved values for each of the parameters. The process is repeated until the desired result is achieved. The Solver uses the above mentioned gradient method to find the optimum set of parameters. Since the Solver operates by a search routine, it will obtain a solution most efficiently if the initial provided estimates are close to the final values. On the contrary, it may not be able to obtain a solution if the initial estimates are far from the final values (Billo, 2001). To ensure that the Solver has obtained a global minimum rather than a local minimum, a different set of initial estimate values was used to obtain a solution.

To obtain an equation covering a wide strain range with data points in a wide strain range using a function model, all district point data were used for the optimization. In addition, to obtain an equation covering a wide strain range with data obtained in a small strain range using a function model, an iterative method was established using the data points for a small range and also one arbitrary data point selected in a larger strain part of the curve, i.e., (a,b), where a is a dependent parameter (normalized shear modulus or damping ratio), b is shear strain in a larger strain part of the curve. The non-linear

140

curve fitting was performed and the coefficient of regression using experimental data points and point (a,b) was obtained. While the value of "b" remained constant, the value of "a" changed to improve the coefficient of regression. This iterative process was continued until no improvement in the coefficient of regression was observed. A schematic sketch showing the curve fitting approach is shown in Figure 4-20. This procedure can provide a suitable result if a correct model is used for the data set. For normalized shear modulus versus shear strain amplitude, a model function, Equation 4.4, was proposed in Section 4.10.2 and used for curve-fitting. For the damping ratio versus shear strain amplitude a general equation developed in Section 4-10.3 of this manuscript was used.
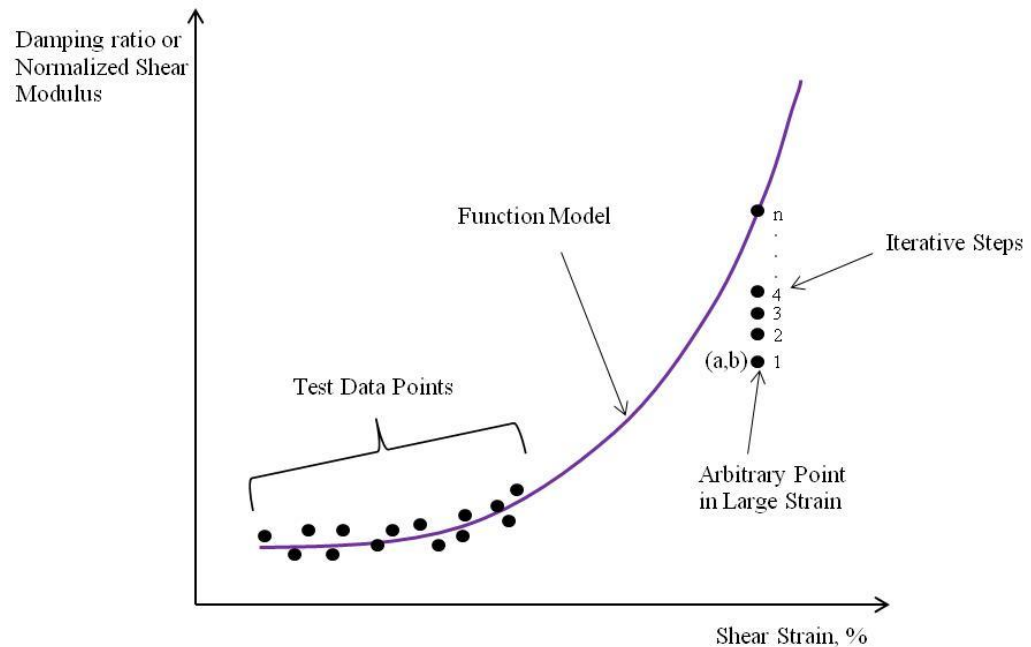

Figure 4-20: Schematic sketch showing the curve fitting approach

After developing the equations, the predicted values from the developed equation and measured values were compared. The values were generally within ± 5%.

4.10.2 Normalized Shear Modulus Equations

A formula with four coefficients was proposed to be used as the function for the curve-fitting. Non-linear curve-fitting was performed to determine an analytical relationship between the shear modulus and shear strain of clay and fibrillated fiber-clay composite using the proposed function. The proposed function is a modification of Borden's equation (Borden, et al., 1996). The measured and predicted values were compared to examine the accuracy of the proposed model for clay and fiber reinforced clay.

A curve fitting model function for soils are proposed in this section. The function correlates the normalized shear modulus G/G_{max} with an increase in shear strain amplitude (γ). The suggested function is presented in Equation 4.4.

$$\frac{G}{Gmax} = \frac{1}{1 + a\,\gamma^{b^{c^{d}}}} \tag{4.4}$$

where, constants a, b, c, and d represent the decay rate of G/G_{max} with an increase in shear strain amplitude (γ). The equations developed for clay and fiber-reinforced clay at optimum fiber content and 0.4% fiber content are presented in Equations 4.5, 4.6, and 4.7, respectively.

Clay
FC = 0.0%
R^2=0.99

$$\frac{G}{Gmax} = \frac{1}{1 + 3.4231\,\gamma^{0.4848^{2.0774^{0.6909}}}} \tag{4.5}$$

142

Fibrillated Fiber- Clay Composite at FC = 0.2% R^2=0.99

$$\frac{G}{Gmax} = \frac{1}{1 + \ 0.1158 \ \gamma^{6.7415^{0.1253^{1.6173}}}} \tag{4.6}$$

Fibrillated Fiber- Clay Composite at FC = 0.4% R^2=0.99

$$\frac{G}{Gmax} = \frac{1}{1 + \ 1.7122 \ \gamma^{2.9166^{0.2948^{1.3531}}}} \tag{4.7}$$

Figure 4-21 shows a graph of shear modulus versus shear strain of clay and fiber-clay composites using Equations 4.5 to 4.7.
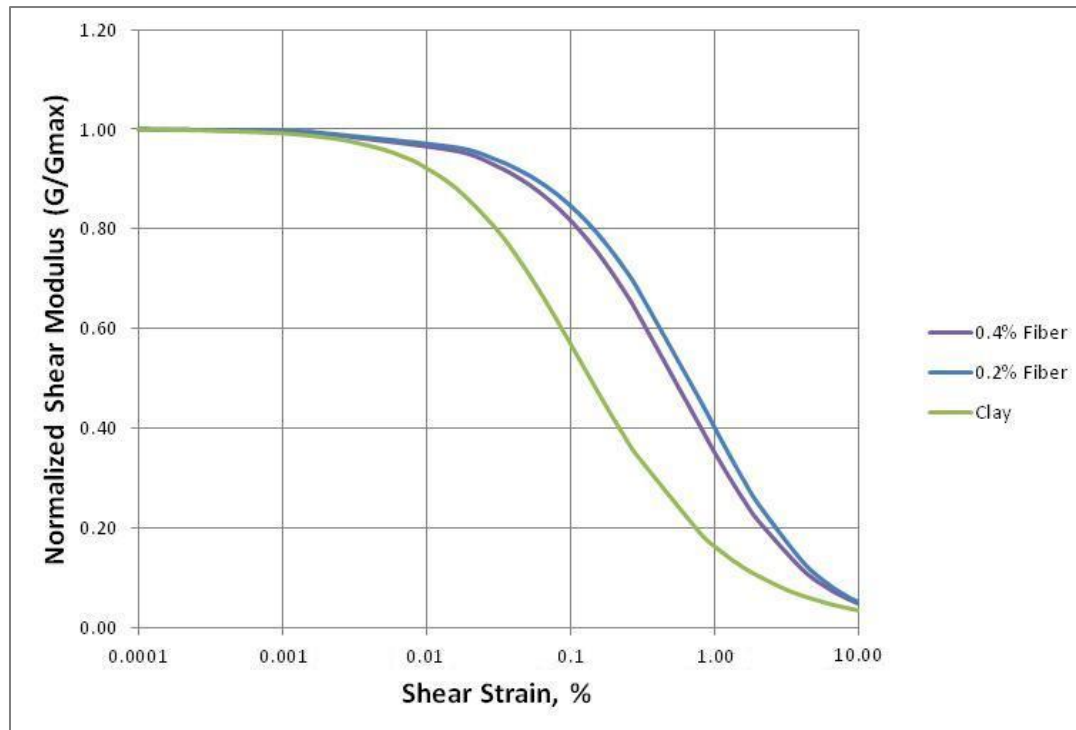
Figure 4-21: Graph of shear modulus versus shear strain for clay and fiber-reinforced clay (FC = 0.2% & 0.4%)

A graph of measured versus predicted was presented in Figures 4-22, 4-23, and 4-24 to show how accurate the obtained values are using the developed Equations 4.5, 4.6 and 4.7.

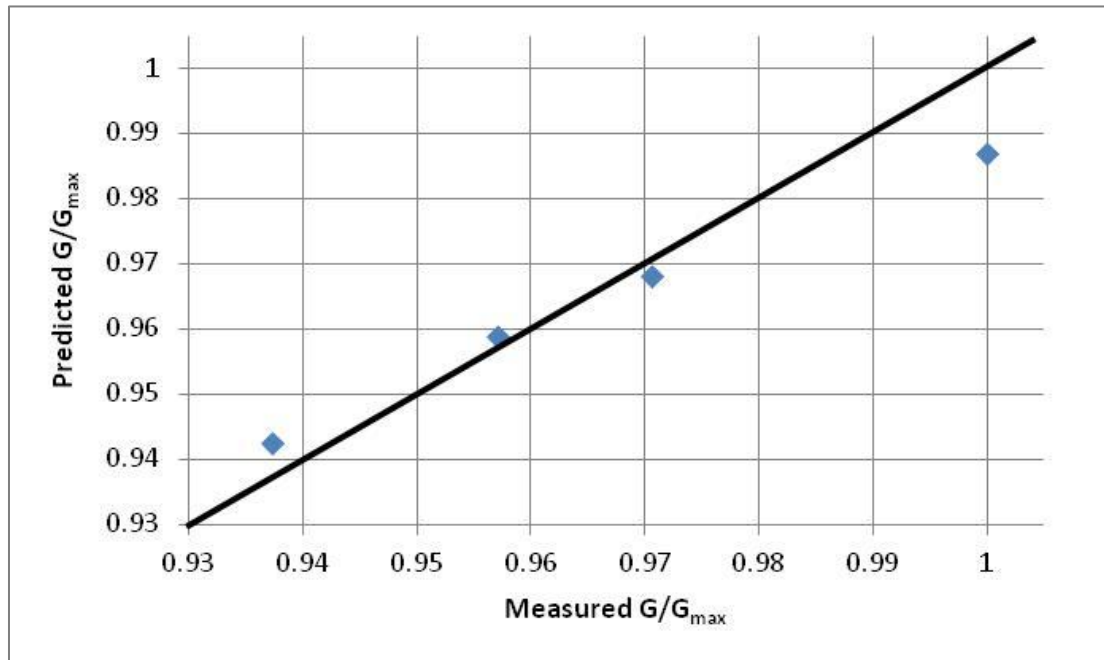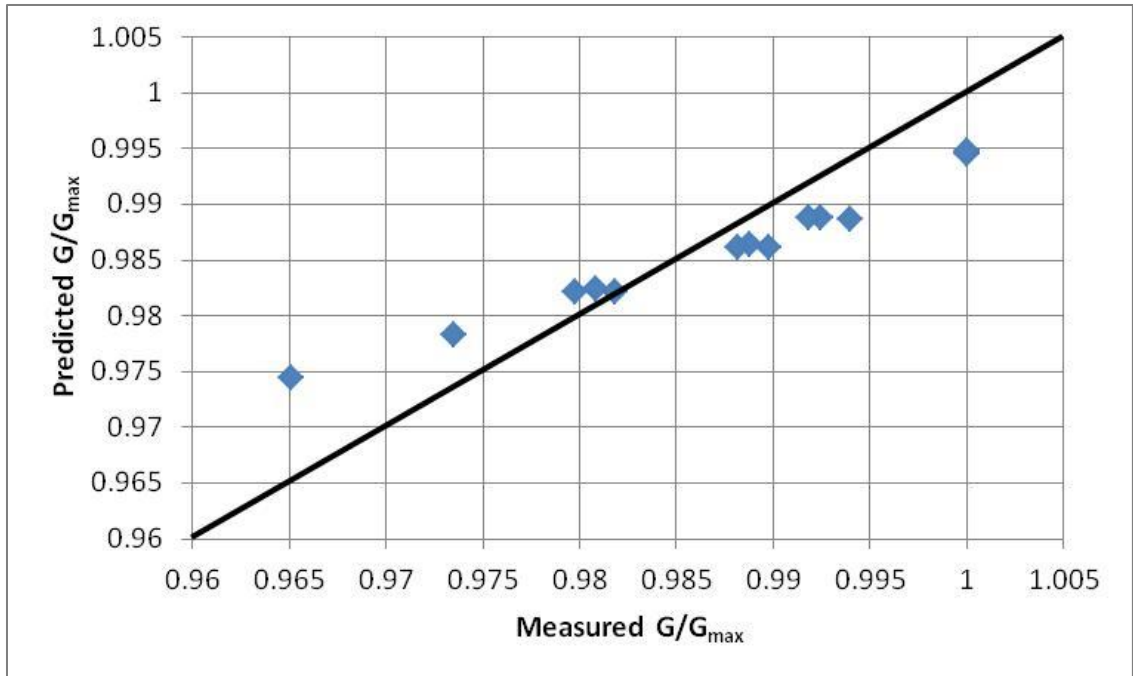Figure 4-22: Graph of measured G/Gmax versus predicted G/Gmax for clay (FC = 0.0%)

Figure 4-23: Graph of measured G/Gmax versus predicted G/Gmax for fiber-reinforced clay (FC = 0.2%)
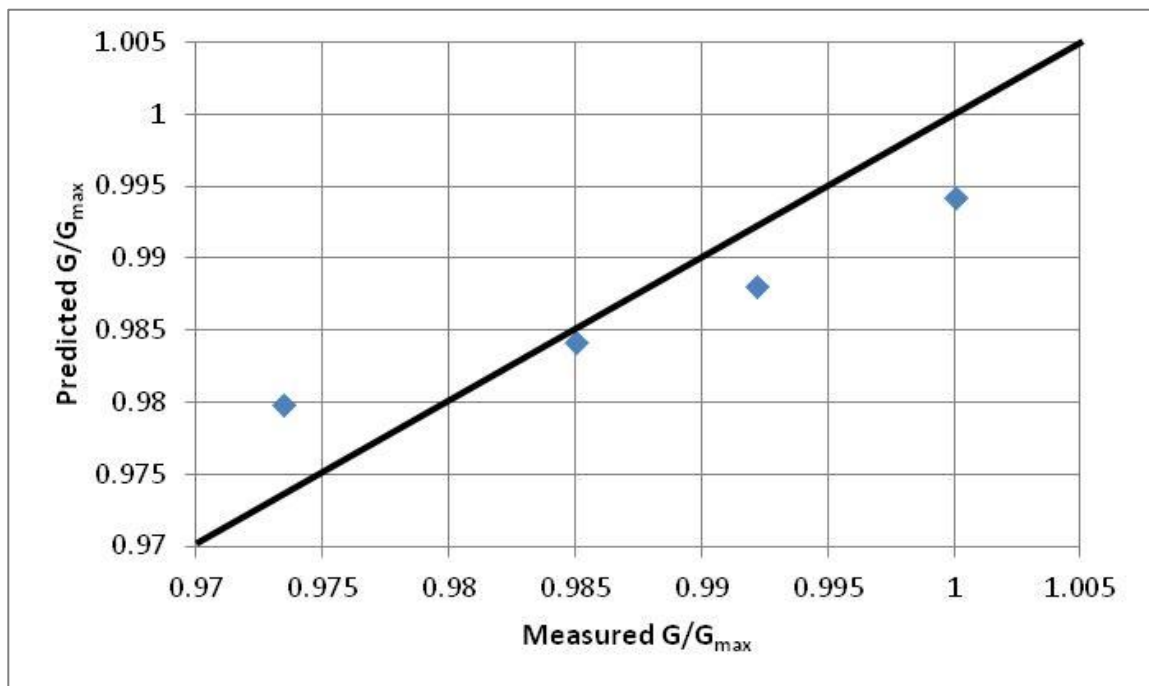

Figure 4-24: Graph of measured G/Gmax versus predicted G/Gmax for fiber-reinforced clay (FC = 0.4%)

Figures 4.22 through 4.24 show that the obtained data are well-fitted into the formula developed to predict shear modulus values for clay and fiber-clay composites.

4.10.3 General Material Damping Formula for Soils

There are several available functions, formulas, and methods to predict the material damping of soil. A majority of the available models and methods cannot describe the damping system accurately. Some of them are limited to training data (the data used to develop that particular formula) or developed using a specific type of soil experiment in a particular condition that does not apply to a different soil or similar soil with dissimilar conditions. Therefore, a general universal mathematical model was proposed and evaluated using our experimental data and verification data (data that was not used to set the model's parameter) to determine if the developed mathematical model can describe a soil damping system accurately. The obtained "Damping General Formula for Soils" was evaluated against different soil types; i.e. sandy, clayey soils as well as fiber-clay composites.

After prudently studying material damping ratio versus shear strain curves for cohesive and cohesionless soils and performing extensive non-linear curve fitting using different mathematical functions, it was realized that curves represent damping versus shear strain are similar to power equations ($y = x^n$) with a more gentle slope inclination at larger shear strains. Therefore, some modification to power equations was made to take the gentle slope inclination into consideration. A curve fitting model function that correlates the damping ratio (D) with an increase in shear strain amplitude (γ) is proposed as below:

146

$$D\ \% \ = \ a\gamma^b \ - \ c\gamma^d \ - e \quad 0.001\ \% < \gamma < 3\ \% \tag{4.8}$$

where, constants a, b, c, d, and e represent the increasing of D with an increase in shear

strain amplitude (γ). The equation is valid when the shear strain is in the range of

$0.001\ \% \ < \gamma < 3\ \%$. The damping ratio in a strain smaller than 0.001% can be assumed

to be constant and similar to a damping ratio corresponding to 0.001% shear strain. The

damping equations developed for clay and fiber-reinforced clay at optimum fiber content

are presented in equations 4.9, and 4.10, respectively.

Clay
FC = 0.0%
R^2=0.99
$$D\ \% \ = \ 22.731\gamma^{0.3034} \ - \ 4.5991\gamma^{0.6747} \ - 1.94$$
$$0.001\ \% \ < \gamma < 3\ \% \tag{4.9}$$

Fibrillated
Fiber- Clay
Composite at
FC = 0.2%
R^2=0.99
$$D\ \% \ = \ 29.4186\gamma^{0.3662} \ - \ 3.2961\gamma^{0.9904} \ - 1.1257$$
$$0.001\ \% \ < \gamma < 3\ \% \tag{4.10}$$

Figure 4-25 shows a graph of shear modulus versus shear strain of clay and fiber-clay

composites using equations 4.9 and 4.10.
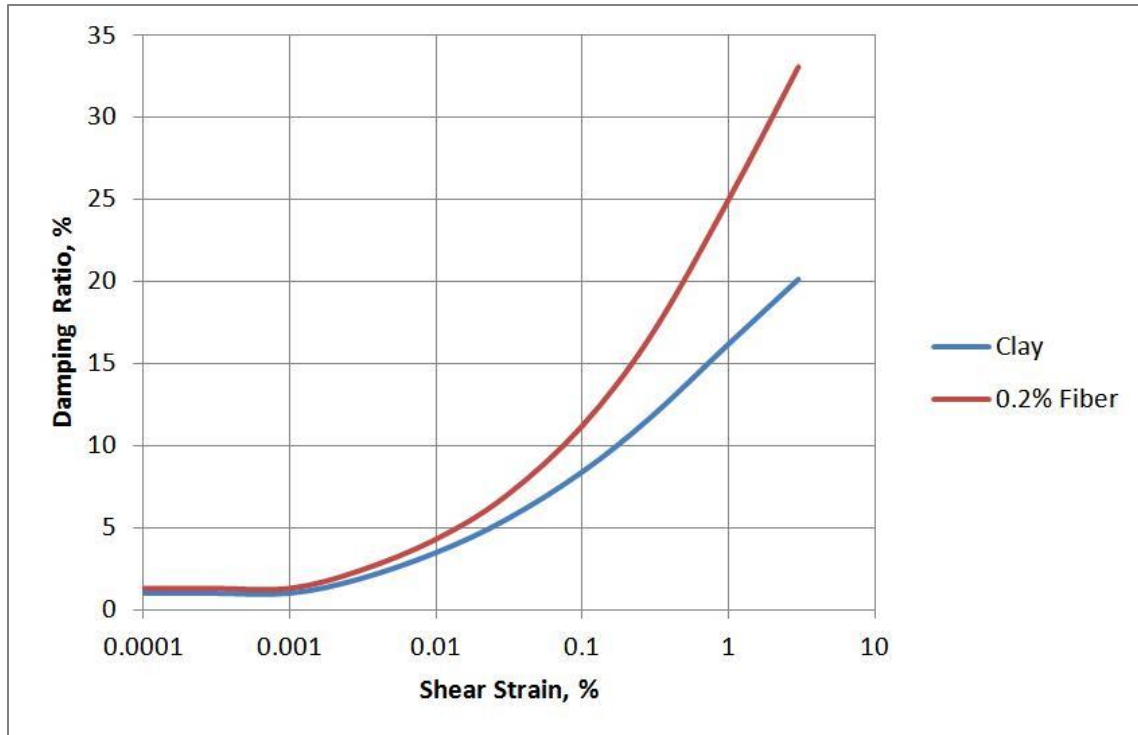
Figure 4-25: Graph of damping ratio versus shear strain for clay and fiber-reinforced clay (FC = 0.2%)

A graph of measured versus predicted is presented in Figures 4-26 and 4-27 to show how accurate the obtained values are using the developed equations 4.9 and 4.10.
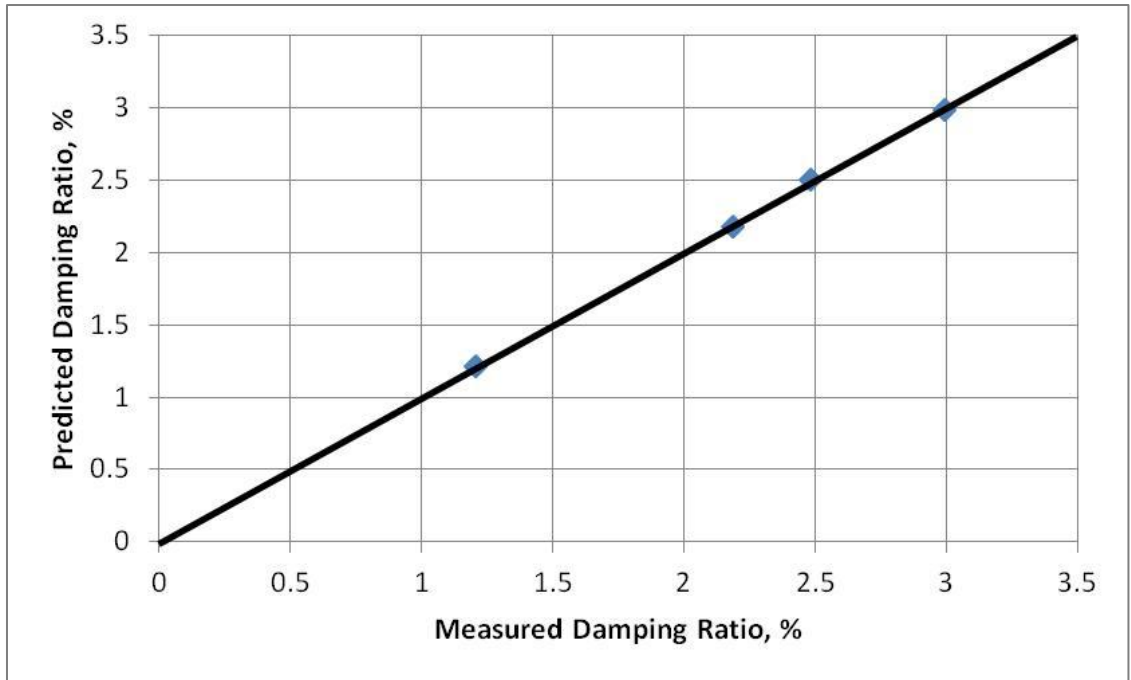
Figure 4-26: Graph of measured damping ratio versus predicted damping ratio for clay (FC = 0.0%)
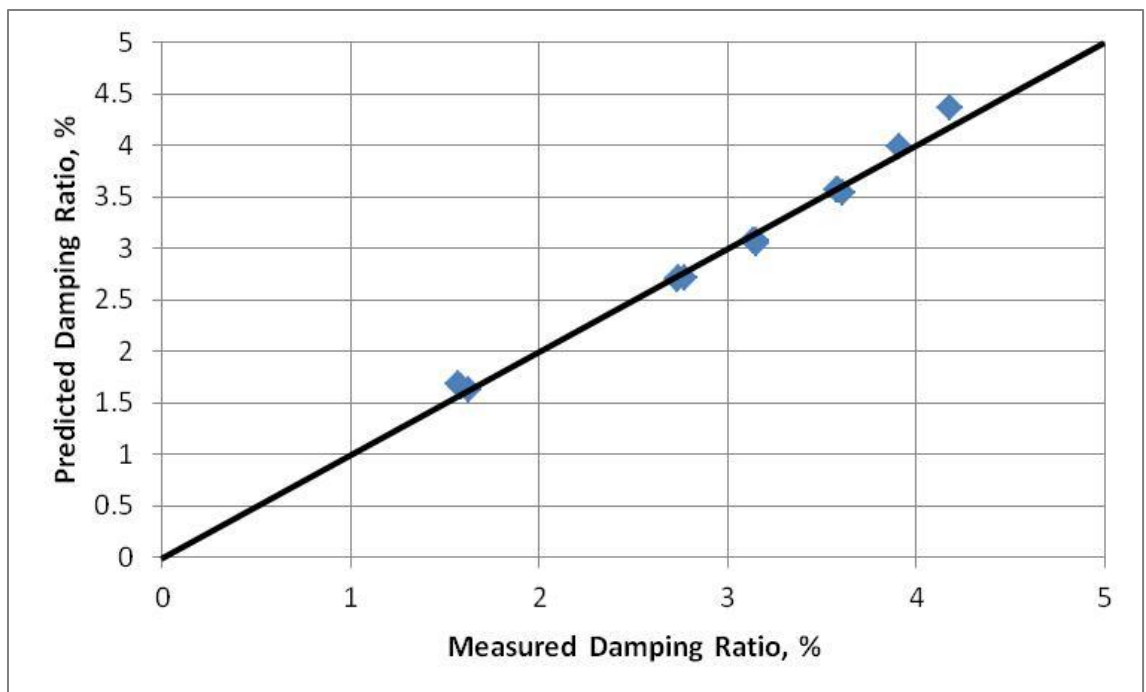
Figure 4-27: Graph of measured damping ratio versus predicted damping ratio for fiber-reinforced clay (FC = 0.2%)

Figures 4.26 and 4.27 show that the obtained data are well-fitted to the formula developed to predict damping ratio values for clay and fibrillated fiber-clay composite.

4.11   Damping Formula Evaluation Using Verification Data

In order to validate the accuracy of the proposed damping formula, Seed and Idriss 1991's data for sand as well as Vucetic and Dorby 1991's data for clay was used as verification data. Non-linear regression was performed on the data and the coefficient of regression was obtained to confirm the accuracy of the fit. Seed and Idriss 1991 has three sets of data called Upper Limit, Mean Limit, and Lower Limit. The data are presented in Table 4.1. Normalized shear modulus and damping versus shear strain curves were drawn in Figures 4.28 and 4.29, respectively.

Table 4-1: Upper, mean, and lower limits data, after Seed and Idriss, 1991

Upper Limit Data		
Strain	G/Gmax	Damping
0.0001	1	0.24
0.0003	1	0.42
0.001	0.99	0.8
0.003	0.96	1.4
0.01	0.85	2.8
0.03	0.64	5.1
0.1	0.37	9.8
0.3	0.18	15.5
1	0.08	21
3	0.05	25
10	0.035	28

Mean Limit Data		
Strain	G/Gmax	Damping
0.0001	1	0.48
0.0003	0.99	0.8
0.001	0.96	1.5
0.003	0.9	3.2
0.01	0.76	5.7
0.03	0.57	9.5
0.1	0.3	15.2
0.3	0.15	20.5
1	0.06	24.6
3	0.04	27
10	0.03	28.5

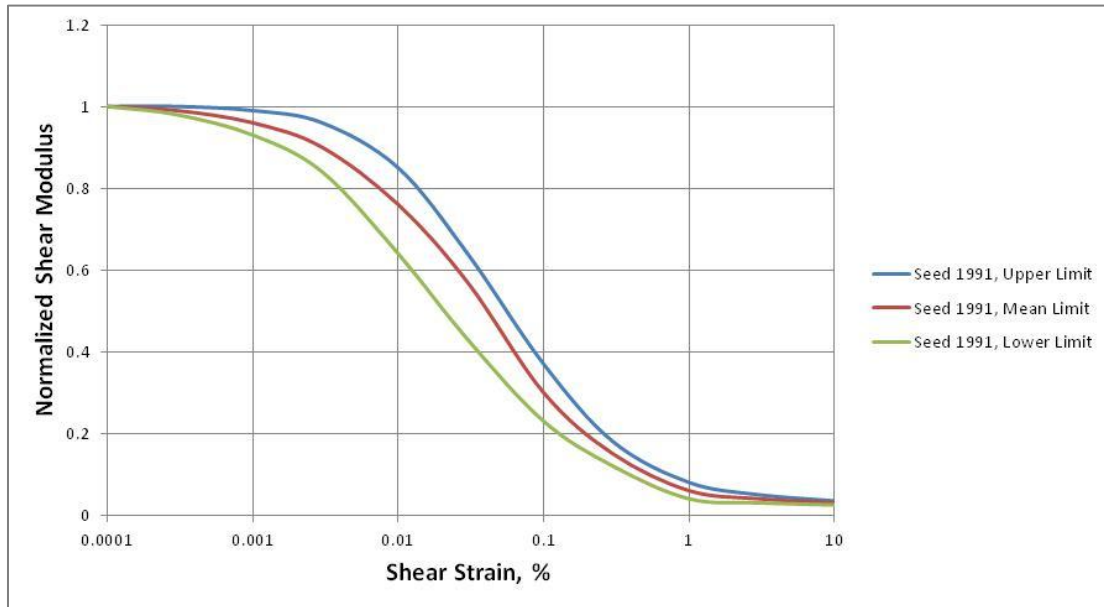| Lower Limit Data		
Strain	G/Gmax	Damping
0.0001	1	0.75
0.0003	0.98	1.1
0.001	0.93	3
0.003	0.84	5.5
0.01	0.64	9.5
0.03	0.43	15
0.1	0.23	21.2
0.3	0.12	25.4
1	0.04	28
3	0.03	28.8
10	0.025	29

Figure 4-28: Graph of normalized shear modulus versus shear strain for sand, after Seed and Idriss 1991
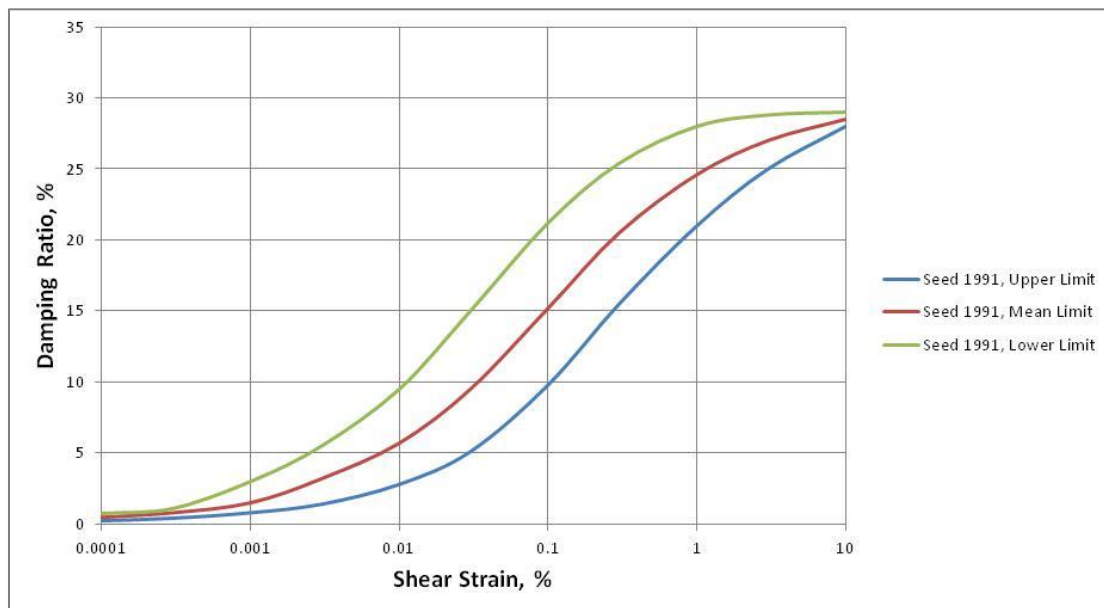

Figure 4-29: Graph of damping ratio versus shear strain for sand, after Seed and Idriss 1991

The damping equations developed for sand are presented in equations 4.11 through 4.13.

152

$$D\ \% \ = \ 129.4077\gamma^{0.2603} \ - \ 92.8645\gamma^{0.3313}$$

Sand –
Lower Limit
$R^2 = 0.9899$

$$- \ 8.1716 \tag{4.11}$$

$$0.001\ \% \ < \gamma < 3\ \%$$

$$D\ \% \ = \ 74.6757\gamma^{0.3349} \ - \ 47.0281\gamma^{0.4423}$$

Sand – Mean
Limit
$R^2 = 0.9940$

$$- \ 3.1362 \tag{4.12}$$

$$0.001\ \% \ < \gamma < 3\ \%$$

Sand –Upper
Limit
$R^2 = 0.9957$

$$D\ \% \ = \ 72.0013\gamma^{0.4565} \ - \ 50.3511\gamma^{0.5462} \ - 1.1458$$

$$\tag{4.13}$$

$$0.001\ \% \ < \gamma < 3\ \%$$

A graph of measured versus predicted is presented in Figures 4-30 through 4-32 to show how well the verification values for sands fit into the general damping equation. Equations 4.11 through 4.13 were used to determine the predicted values for the damping ratio of sand.
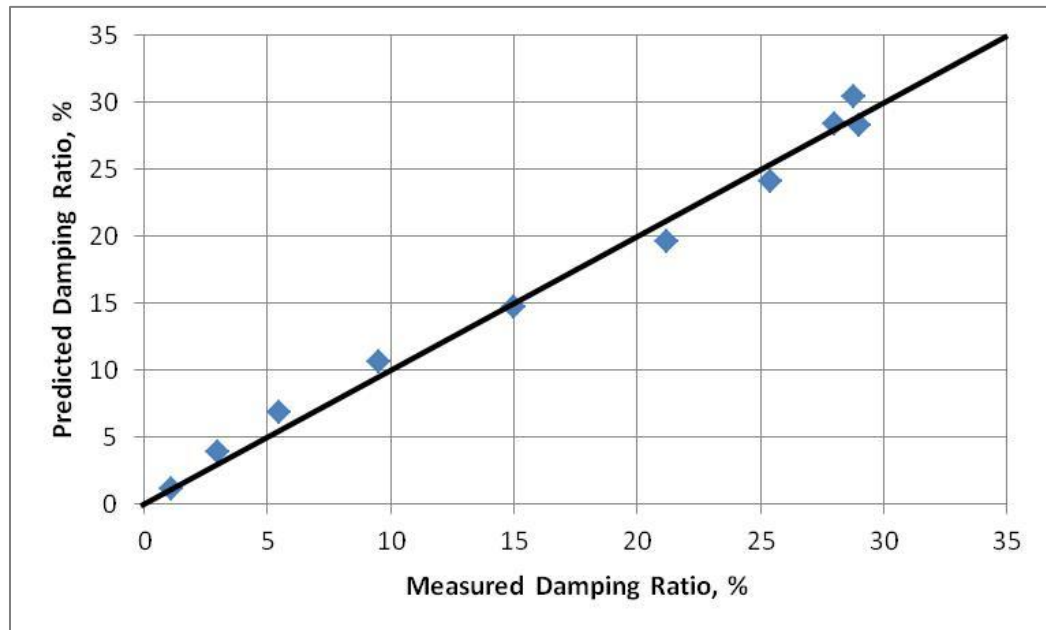

Figure 4-30: Graph of measured damping ratio versus predicted damping ratio for lower limit sand, after Seed and Idriss, 1991
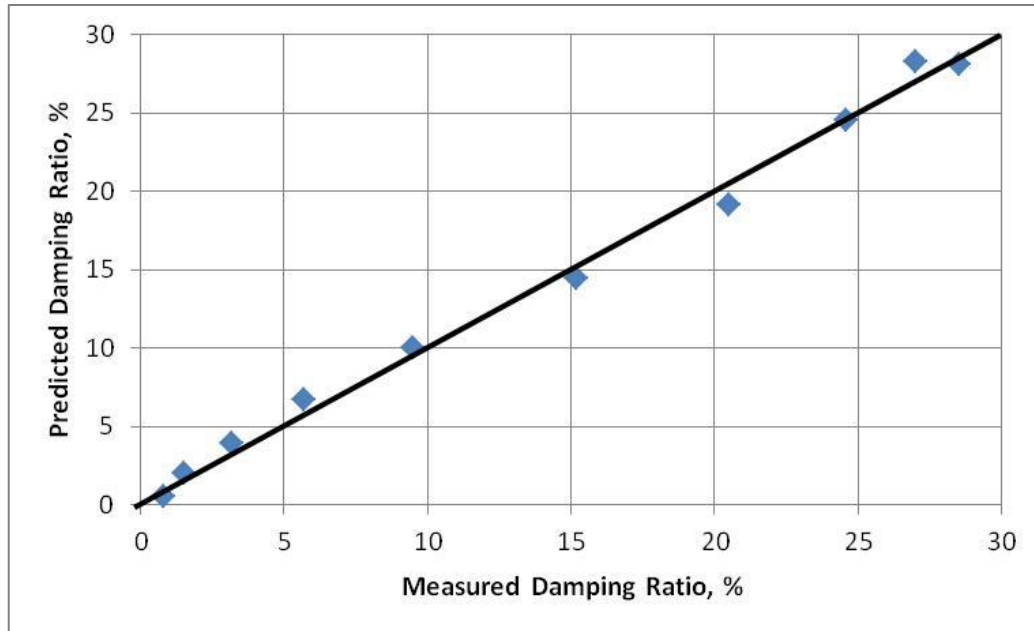
Figure 4-31: Graph of measured damping ratio versus predicted damping ratio for mean limit sand, after Seed and Idriss, 1991
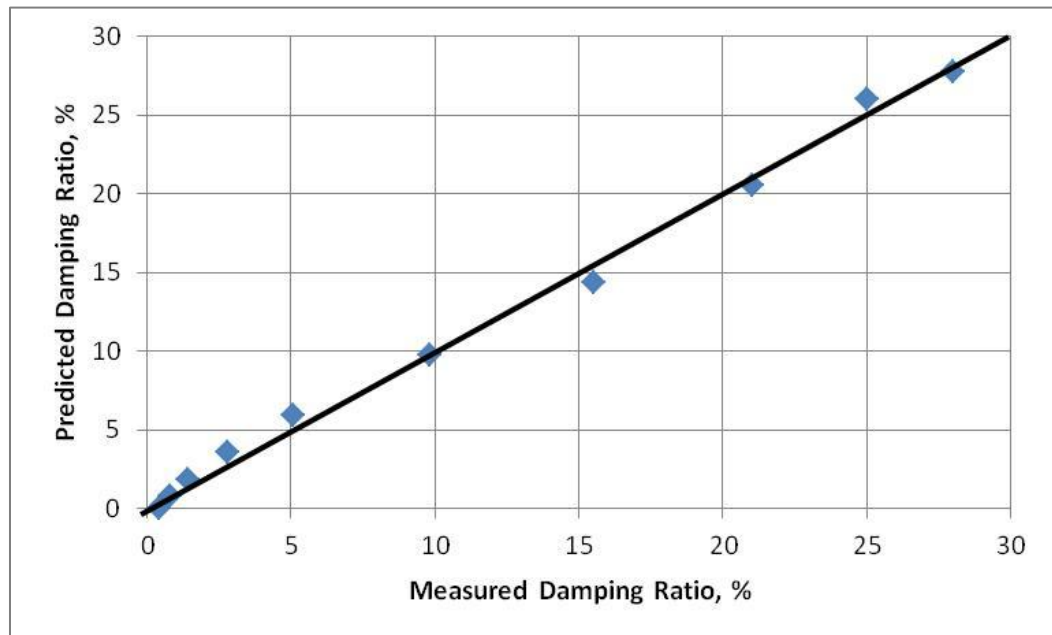
Figure 4-32: Graph of measured damping ratio versus predicted damping ratio for upper limit sand, after Seed and Idriss, 1991

Figures 4.30 through 4.32 plus developed equations that have high coefficients of

regression show that the data for sand are well-fitted to the formulas developed to predict

damping ratio values.

The other verification data that was used to evaluate the accuracy of the general

damping formula is Vucetic and Dorby (1991) data for clay. The damping equations

determined using Vucetic and Dorby 1991's data is presented in Equation 4.14.

Clay
$R^2 = 0.9985$
$$D \ \% \ = \ 21.8682\gamma^{0.3590} \ - \ 5.376\gamma^{0.7123} \ - 0.3074$$
$$0.001 \ \% \ < \gamma < 3 \ \%$$
(4.14)

A graph of measured versus predicted is presented in Figures 4-33.

Figure 4-33: Graph of measured damping ratio versus predicted damping ratio for clay,
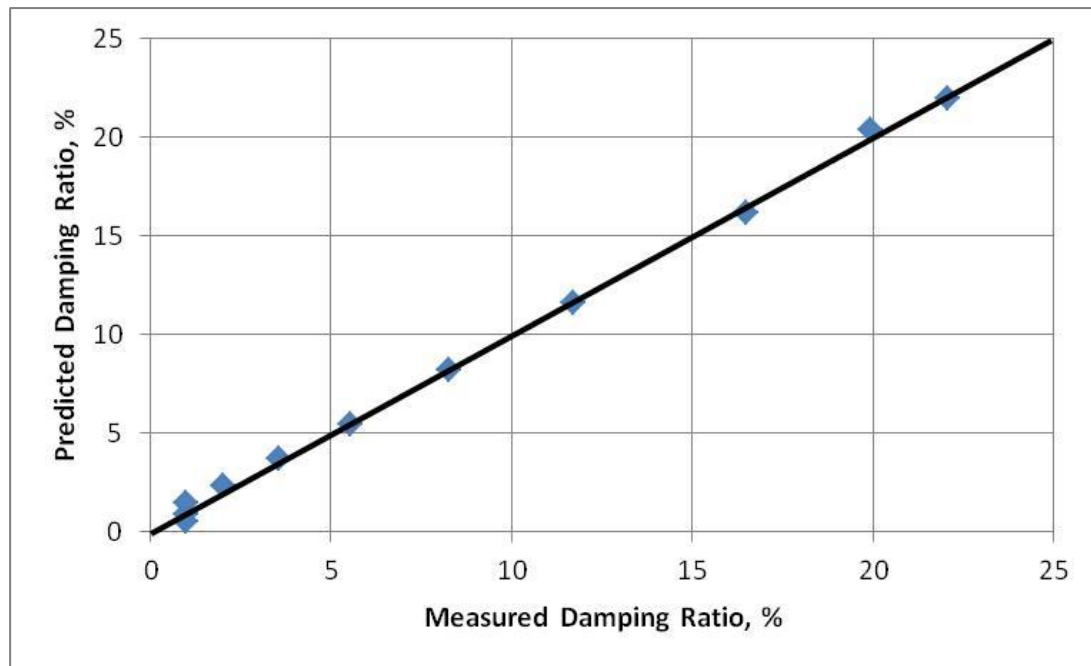after Vucetic and Dorby 1991

4.12   Conclusions

This research shows that the addition of fiber to clay has improves its dynamic

properties. It increases the shear modulus as well as its damping. The main conclusion of

this study is that the inclusion of fiber at optimum fiber content as a ground improvment

technique can improve the dynamic properties of soft and weak clayey soils at low shear

strains. This increase in the value of dynamic properties of clay can be mainly due to the

rearrangement of soil particles caused by the addition of fibers. Since the soil at its

optimum fiber content becomes fiber-saturated, meaning that all soil voids are mostly

filled with fiber, it produced a stiffer composite while benefiting from the material

damping properties of the polypropylene materials. It is important to note that the fact

that both the shear modulus and damping increased provides a double benefit for the

dynamic response of a site by increasing the stiffness of the site and reducing its

amplitude of vibration.

If the foundation of a building is planned to be placed on a soft clayey soil and the

building foundation is planned to be subjected to a limited amount of vibration, the

density of soft clayey soil and its stiffness can be improved using fiber as reinforcement

while increasing the clay's damping ratio. The fiber modification will reduce the

vulnerability of the building foundation to seismic loads.

The other use of the fiber reinforced clay could be when a machine foundation is

to be designed. The inclusion of fiber in clayey soil can limit and attenuate the vibration

and could be a desirable method to limit the amplitude of vibration of the machine

foundation system. It is recommended to first obtain the optimum fiber content for the

composite and select the fiber type based on the extent to which the vibration is desired to be controlled.

A general damping equation as well as a shear modulus equation was developed correlating the dynamic properties of soil material to shear strain. The proposed equations can predict dynamic soil behaviors for all types of soils.

CHAPTER 5 EFFECT OF FIBER REINFORCEMENT OF CLAY ON SEISMIC SITE RESPONSE

In recent years, earthquakes such as the Haiti 2010, Alaska (USA) 2011, Tohoku (Japan) 2011, Talca (Chile) 2012, and the most recent Ahar (Iran) 2012 have caused considerable damage to buildings and infrastructure. One of the causes of heavy damages due to earthquake motions is the role of soft clay in amplifying bedrock ground motions. Modifying the soil conditions of a site in order to mitigate the earthquake damage can be one of the methods of enhancing site conditions and its effects on seismic site response.

In the previous chapter the results of fiber inclusion on dynamic properties of clayey soil, normalized shear modulus and damping ratio, were presented. This chapter presents the results of a study on the clay's seismic site response and the effect of fiber inclusion on the site response. DEEPSOIL software was used to perform one dimensional wave propagation analysis. Equivalent-linear material property characterization was employed in the analysis. Two different material types, clay and fibrillated fiber reinforced clay, were used for different soil columns.

The research presented in this chapter was performed to: (1) investigate the effect of the modification of clay using fibrillated fiber reinforcements on the site response; (2) study the effect of depth to bedrock on the site response of the fiber reinforced site; (3) further investigate the effect of the thickness of soil reinforced layer; (4) study the effect of different earthquake motions on the site response.

5.1   Seismic Response of Horizontally Layered Soil

There are several methods for evaluating the effect of soil conditions on the site's response during an earthquake. Most of these methods assume that the main response of a soil layer is caused by the upward spread and propagation of shear waves (S Waves) from the underlying bedrock formation. Figure 5.1 shows a schematic figure of the upward propagation of a shear wave from bedrock.

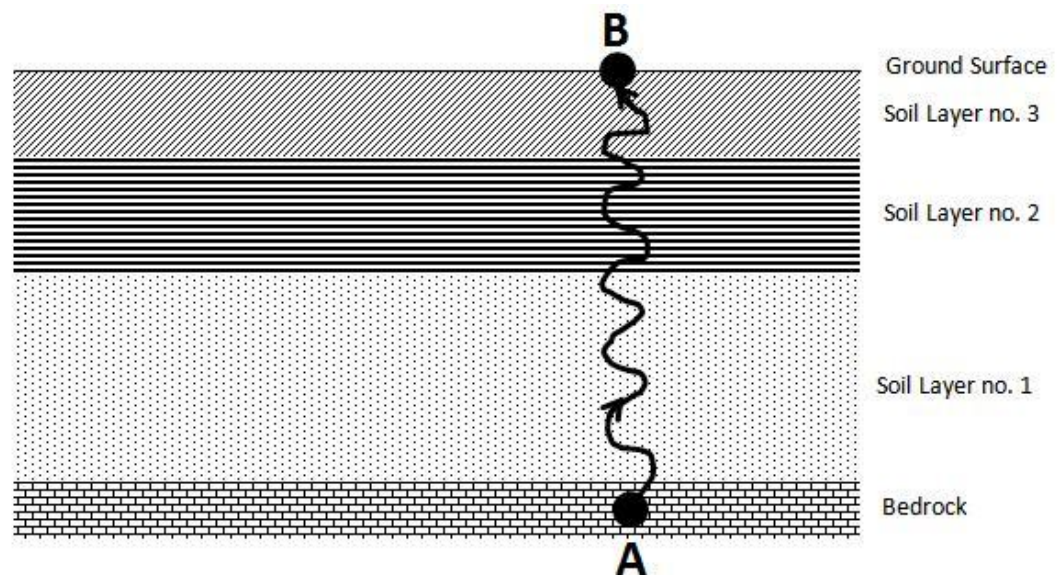Figure 5-1: Schematic figure showing the upward propagation of a shear wave from bedrock

Analytical methods based on this assumption of incorporating a linear estimate of the nonlinear soil behavior, have been shown to provide results in reasonable agreement with field data.

5.1.1   Seismic Site Response Evaluation Procedure

The analytical procedure performed in this chapter involves the following steps:

a) Determine the characteristics of the motions likely to propagate from a bedrock formation underlying the site.

b) Determine the dynamic properties of the soil layers.

c) Compute the response of the soil layers to the bedrock motions at the ground surface.

The maximum acceleration, predominant period, and effective duration are the most essential parameters of an earthquake motion. These parameters should be considered when an earthquake motion is selected as a design motion for the site response analysis. The predominant period (T_p) is a period at which the maximum spectral acceleration takes place in an acceleration response spectrum obtained for 5% viscous damping. The maximum response acceleration is the maximum response of a single degree of freedom (SDOF) system to a particular input motion. It is a function of the natural period and damping ratio of the SDOF system. The dynamic properties of the soil deposits also play an important role in the site response analysis. A dynamic testing procedure can provide accurate input for the analysis. A one-dimensional method of analysis can be used if the soil formations are largely horizontal. Computer programs developed for performing such analysis are usually based on either the solution to the wave equation or a lumped mass simulation. Finite element analysis can be used if more irregular soil layers are dealt with. For our study, one dimensional analysis has been selected because of the fact that it is commonly used in engineering practice and also for the purpose of comparison of the values of unreinforced clay and fiber reinforced clay, it provides acceptable results.

5.1.2　Equivalent Linear Approach

The equivalent linear method was based on the work of Idriss and Seed (Idriss & Seed, 1968); (Seed & Idriss, 1970). Seed and Idriss works are also employed in the extensively used program SHAKE (Schnabel, Lysmer, & Seed, 1972) and its later version SHAKE91 (Idriss & Sun, 1992). The option of equivalent linear in the DEEPSOIL software assumes that the layers are horizontal and are infinite in the horizontal direction. The non-linear dynamic soil moduli and damping as a function of shear strain are entered into the program as discrete points. Then, the actual nonlinear hysteresis stress-strain behavior of cyclically loaded soils is estimated by the equivalent linear soil dynamic properties. The equivalent linear shear modulus (G) is taken as a secant shear modulus, and the equivalent linear damping ratio is taken as the damping ratio that generates the same energy loss in a single cycle in the developed hysteresis loop. These equivalent linear dynamic properties are strain dependent. In the equivalent linear approximation, it is common to determine the strain level in terms of an effective shear strain. The shear strain has been found to be in a range between 50% and 70% of the maximum shear strain (Kramer, 1996). For our analysis, the effective shear strain was taken as 65% of the peak strain. An iterative procedure is required because of the fact that the values of the computed strain level depend on the values of the equivalent linear dynamic properties. The use of an iterative procedure makes certain that the properties used in the analysis are representative properties in all layers. It also ensures that the computed response is not specifically sensitive to the effective shear strain.

5.1.3   Analysis using DEEPSOIL Software Program

DEEPSOIL is a one-dimensional site response program application that can perform the frequency domain analysis method (linear, equivalent linear) as well as the time domain non-linear wave propagation analysis method (Hashash, et al., 2011). DEEPSOIL software was initially developed as a Matlab program in 1998 and later reprogrammed as a C based executable software to improve computational capabilities (Hashash, et al., 2011). The program can calculate the response for a design motion given anywhere in the soil profile. Hence, acceleration obtained from the lower soil layers can be obtained and used to generate new rock motions which, in sequence, can be used as a design motion for upper soil layers. Figure 5-1 shows a schematic sketch of the procedure for computing the ground response at point B from a design motion propagated from bedrock formation (point A).

The version 5 of the software has five graphical interfaces (windows) to input data. The interfaces are designed to obtain data for initialization, analysis type selection, define soil profile and model properties, motion and output control, and output. Figure 5.2 shows the input soil properties interface of the software.
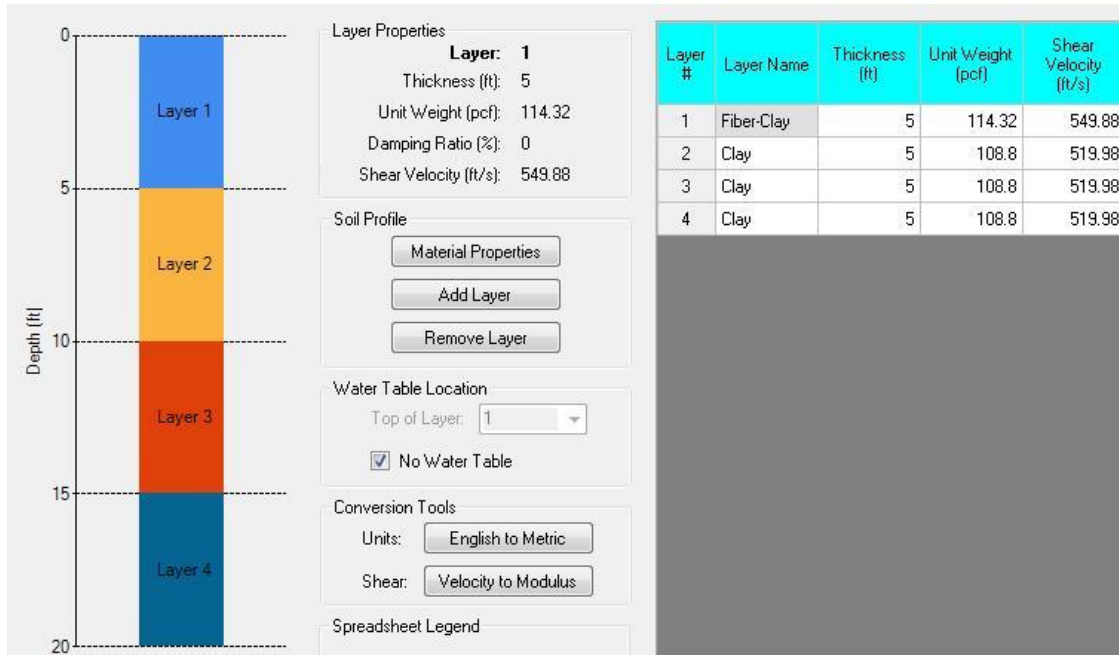
Figure 5-2: Input graphical interface of DEEPSOIL software

After the soil and the model properties are defined in the software, the shear strength is calculated from the normalized shear modulus curves. At each point on the curve, shear stress can be calculated using:

$$\tau = \rho\, V_S^2\, \frac{G}{Gmax}\, \gamma \tag{5.1}$$

where, τ is shear stress at given points; V_S is the shear velocity in a given layer; ρ is the mass density of the soil; G is the shear modulus at given points; $Gmax$ is the maximum shear modulus; and γ is shear strain at given points.

The software provides the strength of the soil profile, shear strength versus depth, normalized shear strength ($\frac{Shear\ Strength}{Effective\ Vertical\ Stress}$), and the friction angle versus depth. By using the maximum value for shear stress, the software can calculate the friction angle using Equation 5.2.

163

$$\emptyset = \tan^{-1} \times \left(\frac{\tau max}{\sigma_v'}\right) \tag{5.2}$$

where, $\emptyset$ is the friction angle; τmax is maximum shear stress; σ_v' is effective vertical stress at the mid-depth of the layer.

In the frequency domain analysis, there are three most commonly used methods to estimate response spectra of single degree of freedom (SDOF) systems, the frequency domain solution, Newmark β method, and Duhamel integral solutions. A brief description is provided for each method. The dynamic equilibrium equation of motion is expressed as (Newmark, 1959); (Chopra, 1995):

$$mu + cu + ku = -mu_g \tag{5.3}$$

where m, c, and k are the mass, viscous damping and stiffness of a SDOF system, respectively. u, u, and u are the nodal relative accelerations, relative velocities and relative displacements, respectively. u_g is the exciting acceleration applied at the base of SDOF.

In the frequency-domain solution method, a modification is performed on the Fourier Amplitude Spectra (FAS) by a transfer function. The transfer function is defined as:

$$H f = \frac{-f_n^2}{f^2 - f_n^2 - 2iDff_n} \tag{5.4}$$

where f_n is the natural frequency of the oscillator obtained from $f_n = \frac{1}{2\pi} \sqrt{\frac{k}{m}}$, and D is the damping ratio obtained from $D = \frac{c}{2\sqrt{km}}$. In order to move between the frequency-domain and the time domain, fast fourier transforms (FFT) are used. The frequency-

domain is used where the oscillator transfer function is applied and the time-domain is

where the peak oscillator response is approximated. The frequency-domain is only exact

in the frequency range of the bedrock motion.

The Duhamel integral solution is another method to compute the response of

linear SDOF systems. It linearly interpolates the excitation function $(-mu_g)$ and solves

the dynamic equilibrium equation of motion meeting the following conditions:

a) Free-vibration due to initial displacement and velocity

b) A response step force $(-mu_g)$ with zero initial conditions

c) Response of the ramp force $-m \; \dfrac{u_{g_{i+1}} - u_{g_i}}{\Delta t}$

The solution in terms of velocities and displacements can be solved by:

$$u_{i+1} = A'u_i + B'u_i + C' \; -mu_{gi} \; + D(-mu_{gi+1}) \tag{5.5}$$

$$u_{i+1} = A'u_i + B'u_i + C' \; -mu_{gi} \; + D(-mu_{gi+1}) \tag{5.6}$$

where:

$$A = \; e^{-D\omega_n \Delta t (-\frac{D}{1-D^2} \sin \; \omega \Delta t \; + \cos(\omega \Delta t))} \tag{5.7}$$

$$B = \; e^{-D\omega_n \Delta t (\frac{1}{\omega} \sin \; \omega \Delta t \;)} \tag{5.8}$$

$$C = \frac{1}{k} \left[\frac{2D}{\omega_n \Delta t} + e^{-D\omega_n \Delta t}((\frac{1-2D^2}{\omega \Delta t} - \frac{D}{1-D^2})\sin \omega \Delta t - (1+\frac{2D}{\omega_n \Delta t})\cos(\omega \Delta t)) \right] \quad (5.9)$$

$$D = \frac{1}{k} \left[1 - \frac{2D}{\omega_n \Delta t} + e^{-D\omega_n \Delta t}(\frac{2D^2-1}{\omega \Delta t}\sin \omega \Delta t + \frac{2D}{\omega_n \Delta t}\cos(\omega \Delta t) \right] \quad (5.10)$$

$$A' = e^{-D\omega_n \Delta t}(-\frac{\omega}{1-D^2}\sin \omega \Delta t) \quad (5.11)$$

$$B' = -e^{-D\omega_n \Delta t}(\cos(\omega \Delta t) - \frac{D}{1-D^2}\sin \omega \Delta t) \quad (5.12)$$

$$C' = \frac{1}{k} \left[-\frac{1}{\Delta t} + e^{-D\omega_n \Delta t}((\frac{\omega_n}{1-D^2} + \frac{D}{\Delta t\ 1-D^2})\sin \omega \Delta t + (\frac{1}{\Delta t})\cos(\omega \Delta t)) \right] \quad (5.13)$$

$$D' = \frac{1}{k\Delta t} \left[1 - e^{-D\omega_n \Delta t}(\frac{D}{1-D^2}\sin \omega \Delta t + \cos(\omega \Delta t) \right] \quad (5.14)$$

The third method in calculating the response spectra is the Newmark β method. In the Newmark β method, the nodal relative velocity u_{i+1} and displacement u_{i+1} can be obtained at any time $i + 1$ by using:

$$u_{i+1} = u_i + (1 - \gamma)\Delta t\ u_i + (\gamma \Delta t)u_{i+1} \quad (5.15)$$

$$u_{i+1} = u_i + (\Delta t)u_i + [0.5 - \beta]\Delta t^2\ u_i + \beta(\Delta t)^2\ u_{i+1} \quad (5.16)$$

where, Δt is the time step, and β and γ are parameters assuming the acceleration variation.

The drawback of using Newmark β method is that the method under-predicts the high frequency responses (Chopra, 1995), (Mugan & Hulbe, 2001). The frequency-domain solution method was used in the analyses.

In order to be consistent when analysis is performed for each layer and to compare the results, the layers were broken down into sublayers of 5 ft thicknesses. For instance, if the total column of soil was 60 feet, the total thickness was divided into 12 sublayers, each with the thickness of 5 feet. Following this procedure, the comparisons will be performed when software analyses are conducted for the same points in the soil profile.

5.2   Design Earthquake Parameters

When performing soil behavior assessments under earthquake motion, it is essential to know the magnitude of the earthquake and to define the ground motion in expressions that can be used for engineering analysis. Design earthquake waves were traditionally described in terms of the peak acceleration, but modern techniques nowadays use the response spectrum or time histories of motion. The most reliable approach for achieving this is to perform the analysis based on data obtained at the site. A second option is to find another site similar in seismic and geologic setting where ground motion was measured during a design level magnitude earthquake. However, the chance of finding such a site that measurements at a design level magnitude had been done is very slim. Therefore, estimates of ground motions based on correlations and geologic and seismologic evidence for the specific site are essential (Department of Defense Handbook, 1997).

5.2.1   Earthquake Motions

Earthquakes are one of the most costly natural hazards posing a significant risk to people living in earthquake zones. Earthquakes are the result of a sudden release of energy in the Earth's crust that forms seismic waves. Two different earthquake motions,

the Parkfield and the Imperial Valley, were used in the analysis. The Imperial Valley

earthquake was a magnitude 6.5 and happened in Imperial Valley on the Mexico-

California border on October 15, 1979 at 4:54 pm local time. The main earthquake

injured 91 people and caused structure damages estimated at 30 million dollars. The

shock destroyed two houses and 11 commercial buildings and damaged 1,565 houses and

440 commercial buildings in the Imperial Valley. Older buildings were severely

damaged. The Imperial Valley earthquake was the result of a rupture along the Imperial

fault, with the epicenter 4 kilometers north of the International Border (Stover &

Coffman, 1993).

Moderate-sized earthquakes of magnitude 6 have occurred on the town of

Parkfield section of the San Andreas Fault at fairly regular intervals – in 1857, 1881,

1901, 1922, 1934, and 1966. The last earthquake in the year 1966 motion has been used

in this study. The most recent earthquake happened in the Parkfield area on September

28, 2004. A summary of the earthquake motions used in the analysis is listed below.

Table 5-1: Earthquake motions data used in the analysis (Hashash, et al., 2011)

Motion Name	Date of Event	Magnitude	Hypocentral Distance to Fault Rupture (km)	Geomatrix USGS Site Class	PGA (g)
Imperial Valley	10/15/1979	6.5	26.5	B	0.169
Parkfield	06/28/1966	6.1	9.9	B	0.357

In the analysis, these two motions are considered to be two extreme conditions.

Parkfield is the one with large peak ground acceleration (PGA) of 0.357 g but the

earthquake duration is very short (less than 30 seconds). On the contrary, Imperial Valley

has not as large a PGA as Parkfield had but its duration is very long (slightly greater than 60 seconds). Acceleration versus time graphs for these two motions are shown in Figure 5.3.
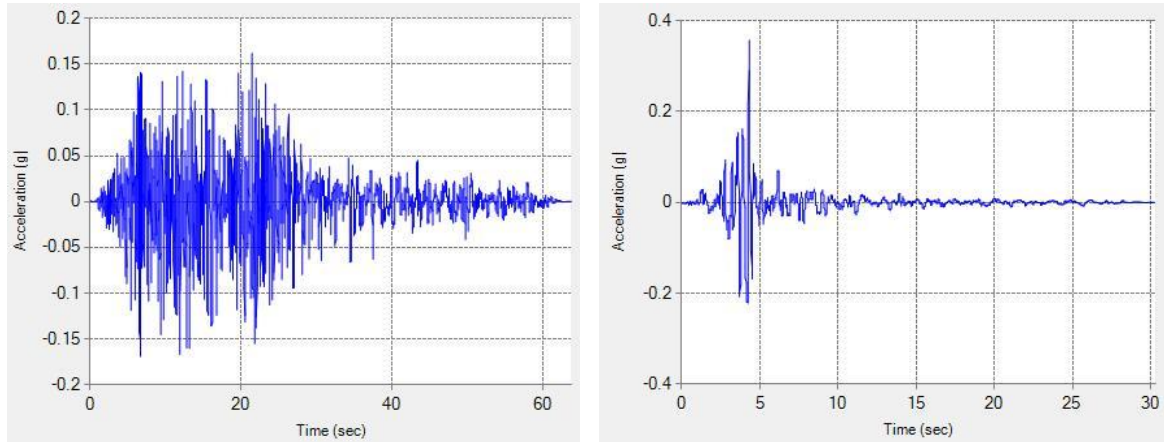

Figure 5-3: Graph of Imperial Valley motion and Parkfield acceleration versus time are shown on the left and right, respectively.

5.3   Factors Affecting Ground Shake

Factors that affect strong ground shake comprise:

a) Wave types – S and P waves that travel through the earth and surface waves.

b) Earthquake magnitude

c) Depth to bedrock (distance from epicenter)

d) Soil deposit conditions (site conditions)

e) Fault type, depth, and recurrence interval

As part of this research, the effect of two different motion types, depth to bedrock, and soil conditions using clay and fiber modified clay was studied.

5.4   Materials Used in the Analysis

To study the effect of fiber inclusion on the site response of a clayey soil column, two different material types, clay and fibrillated fiber modified clay, were used for different soil column analyses. In the previous chapters, fibrillated fiber had shown that it can provide a denser mixture than monofilament fiber if mixed with clay at optimum fiber content. Hence, the experimental data for 0.75 inch fibrillated fiber was used for the analysis. In addition, the experimental data for kaolinite soil tested at optimum moisture content was used in the analysis to allow a comparison with fiber modified clay. In the experimental stage of the research, the mass density and maximum shear modulus (G_{max}) for each soil/composite type were determined. By knowing the mass density and maximum shear modulus of each soil layer, unit weight and shear wave velocity can be calculated, respectively. The values of unit weight and shear wave velocity defined in the software are listed in Table 5.2.

Table 5-2: Properties of materials

Soil/Composite Layer	Unit Weight (lb/ft^3)	Shear Wave Velocity (ft/s)
Clay	108.8	519.98
Fiber-Soil Composite	114.32	549.88

5.5   Dynamic Properties of Clay and Fiber Modified Clay Used in the Analysis

The program models the non-linear dynamic soil modulus and damping as a function of shear strain. The equations developed in Chapter 4 for soil modulus and damping ratio of clay were used to plot soil modulus and damping ratio curves. The Equations 4.5 and 4.6 were used to model shear modulus versus shear strain curve and Equations 4.9 and 4.10 were used to model damping ratio versus shear strain curves.

Then 10 discrete points on each curve were input to the software. The software can

simulate the curves by entering the discrete points. Please note that a better curve can be

plotted if the discrete points cover a large range of shear strain. The curves of shear

modulus and damping ratio as functions of shear strain are shown in Figures 5-4 and 5-5,
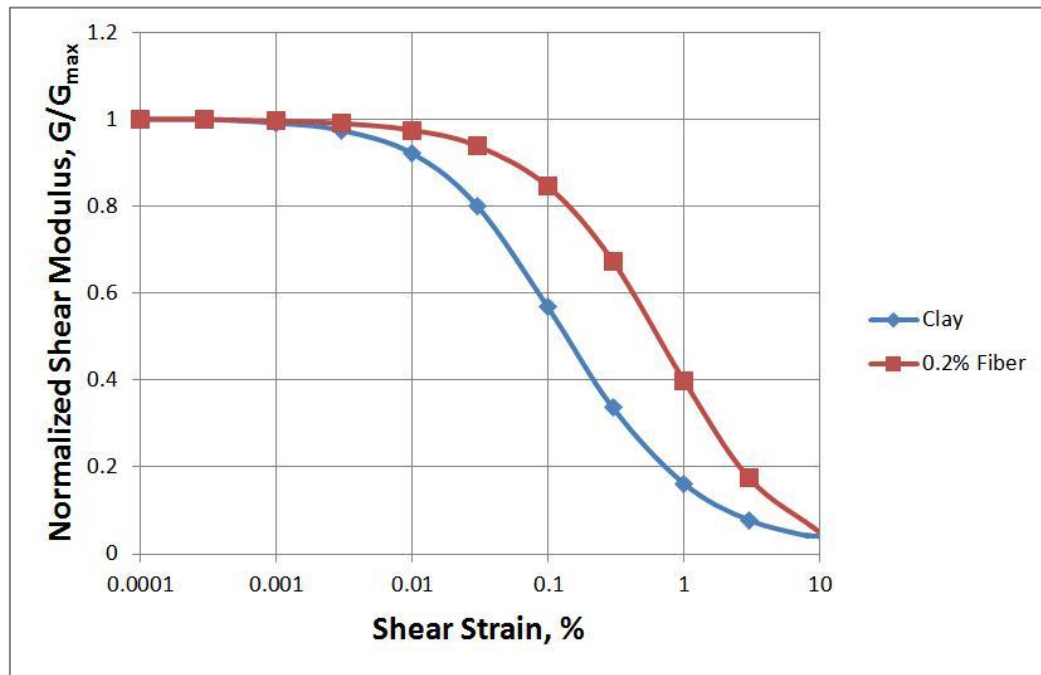
respectively.

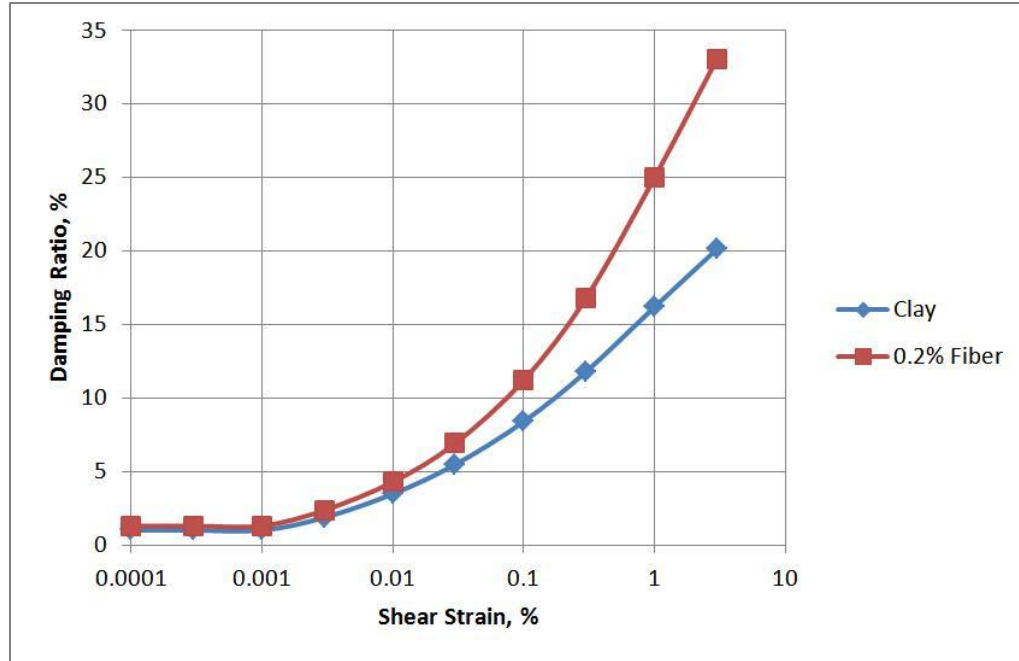Figure 5-4: Normalized shear modulus versus shear strain for clay and fiber-clay composite with FC = 0.2%

Figure 5-5: Damping ratio versus shear strain for clay and fiber-clay composite with FC = 0.2%

5.6 Effect of Fiber Reinforcement on Dynamic Response of a Clayey Site

Clay and fiber reinforced material properties were assigned to a soil column of 60 feet and were separately studied. Firstly, for case 1, one column of soil was studied using clay material. Then for case 2, 10 feet off the top of soil column was replaced with fiber modified clay using properties presented in Section 5.4 of this manuscript, as shown in Figure 5-6.
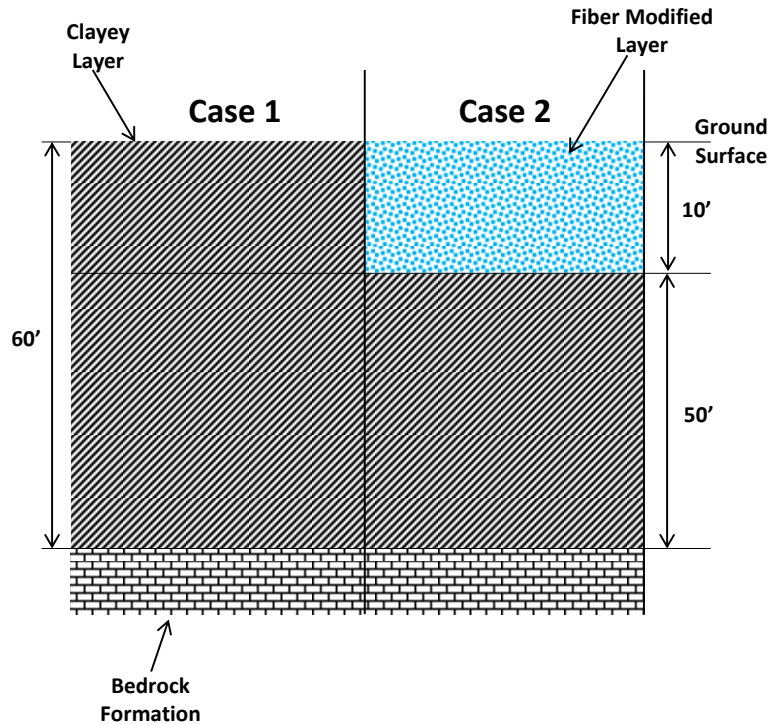
Figure 5-6: Site profile sketch - soil column = 60 ft

5.6.1 Seismic Site Response of 60 feet Column of Soil

After performing equivalent linear analysis applying two different earthquake motions, Imperial Valley and Parkfield, at the bedrock for a 60 foot column of clayey soil in case 1, the graphs of acceleration versus time, amplitude ratio versus frequency, and response spectra versus period were developed for the ground surface for all-clay (case 1) and fiber modified condition (case 2). The graphs are shown in Figure 5-7 to 5-9 for all-clay condition.
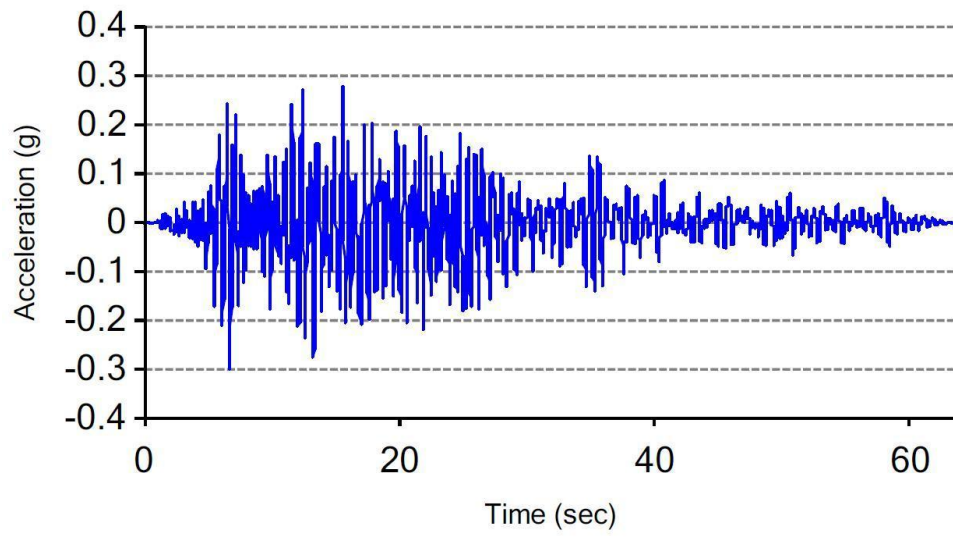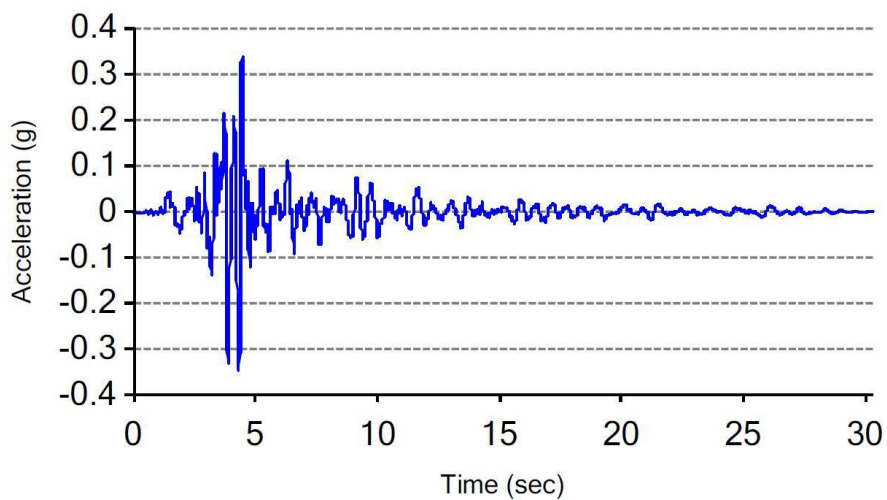
Figure 5-7: Acceleration versus time graph for all-clay condition, 60 ft column of soil, Imperial Valley motion (case 1)
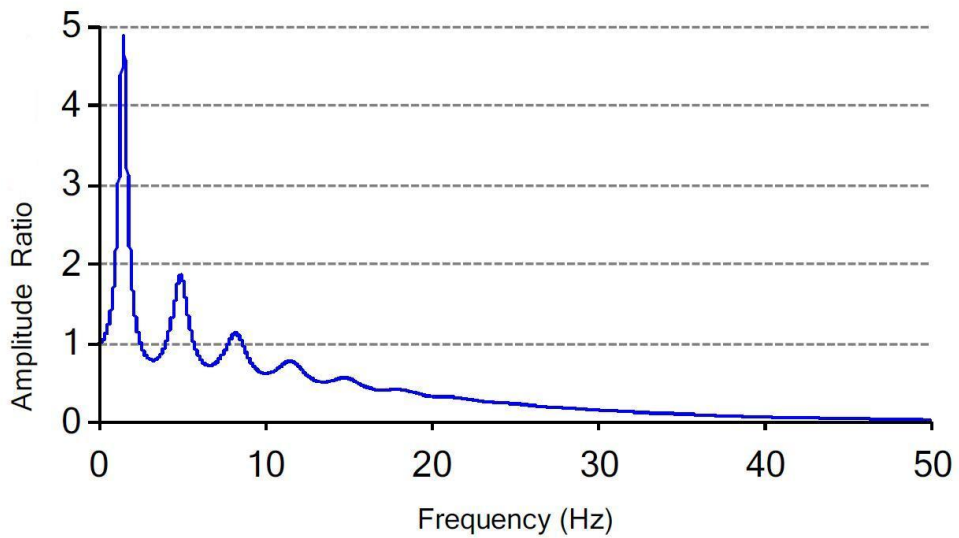
Figure 5-8: Amplitude ratio versus frequency graph for all-clay condition, 60 ft column of soil, Imperial Valley motion (case 1)

174
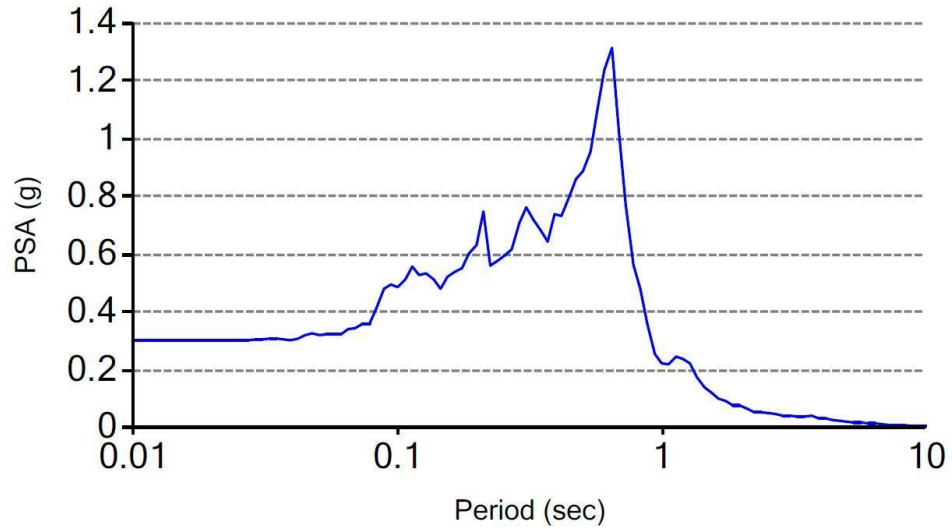
Figure 5-9: Response spectra versus period graph for all-clay condition, 60 ft column of soil, Imperial Valley motion (case 1)

The site response graphs were also determined when Parkfield motion was applied. The graphs are shown in Figures 5-10 to 5-12 in all-clay condition (case 1).

Figure 5-10: Acceleration versus time graph for all-clay condition, 60 ft column of soil, Parkfield motion (case 1)
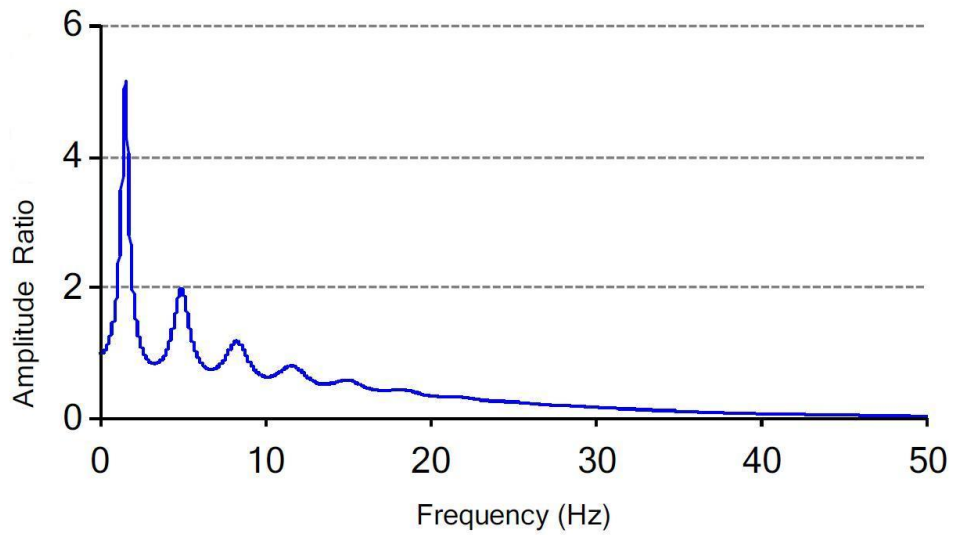
Figure 5-11: Amplitude ratio versus frequency graph for all-clay condition, 60 ft column of soil, Parkfield motion (case 1)
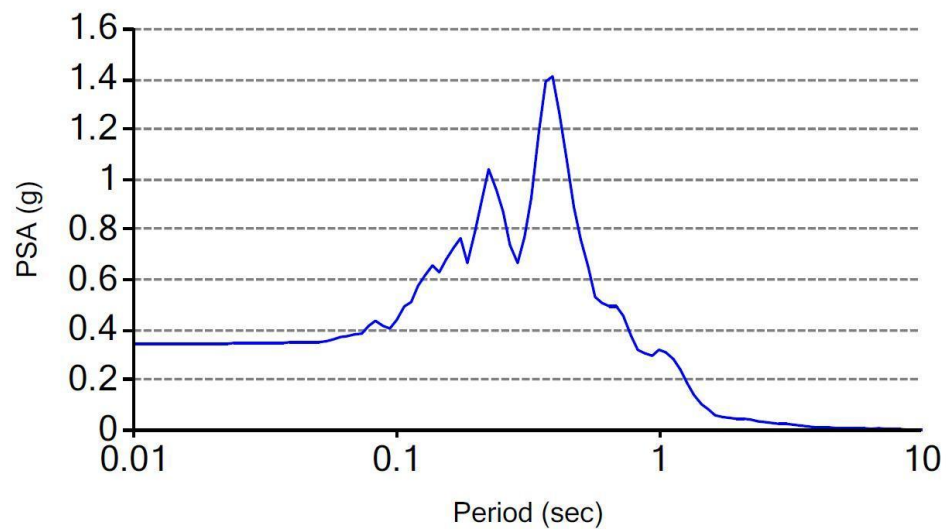

Figure 5-12: Response spectra versus period graph for all-clay condition, 60 ft column of soil, Parkfield motion (case 1)

The analysis was performed on the 60 foot column of clay in the condition where the top

10 feet of the column was fiber modified (case 2). Then, the soil column was analyzed

under the application of the Imperial Valley and Parkfield motions separately at the

bedrock. The ground surface site response graphs are shown in Figures 5-13 to 5-15 for

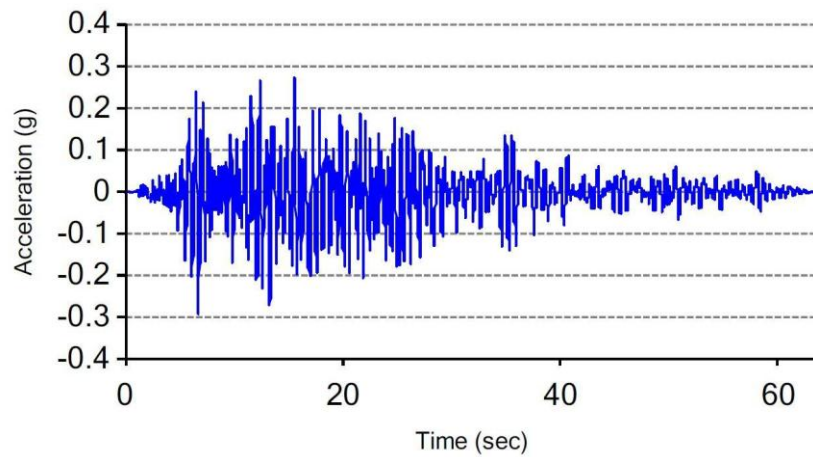Imperial Valley and in Figures 5-16 to 5-18 for Parkfield motions.

Figure 5-13: Acceleration versus time graph, 60 ft column of soil, Imperial Valley
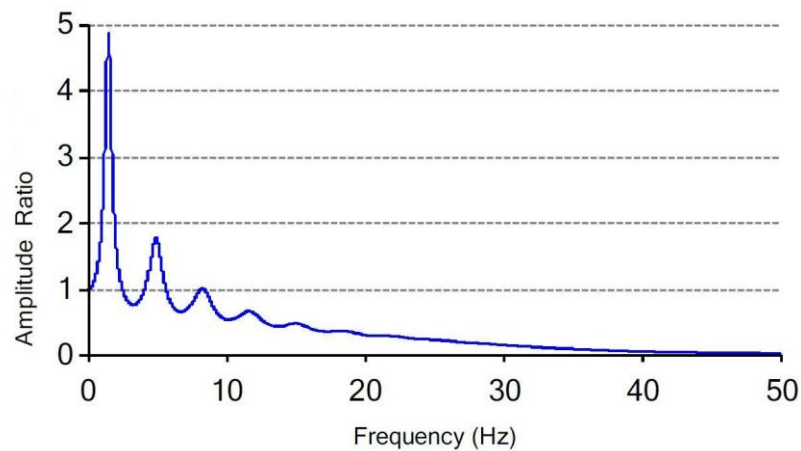motion, thickness of fiber modified layer is 10 ft (case 2)

Figure 5-14: Amplitude ratio versus frequency graph, 60 ft column of soil, Imperial
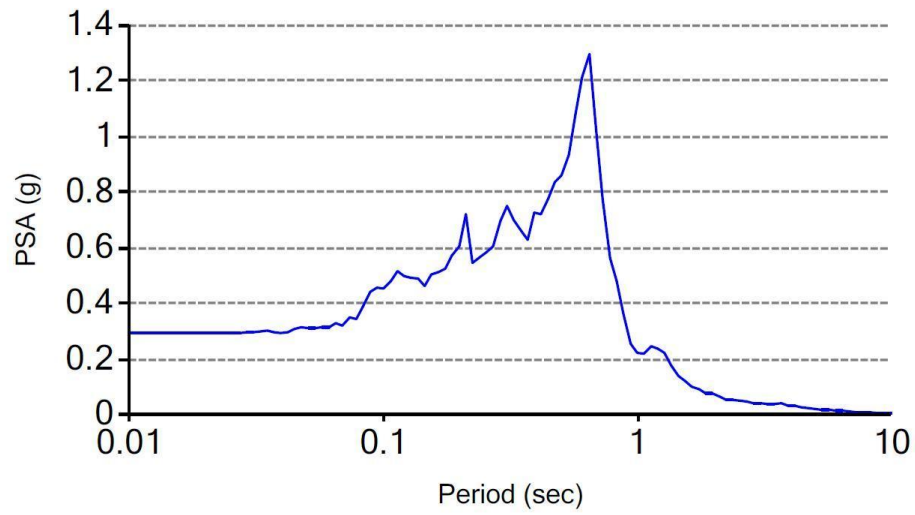Valley motion, thickness of fiber modified layer is 10 ft (case 2)

Figure 5-15: Response spectra versus period graph, 60 ft column of soil, Imperial Valley motion, thickness of fiber modified layer is 10 ft (case 2)
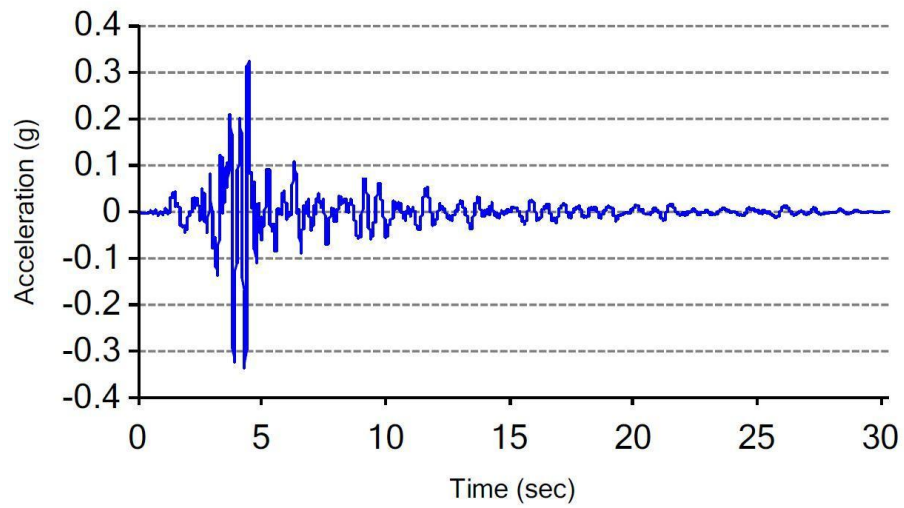

Figure 5-16: Acceleration versus time graph, 60 ft column of soil, Parkfield motion, thickness of fiber modified layer is 10 ft (case 2)
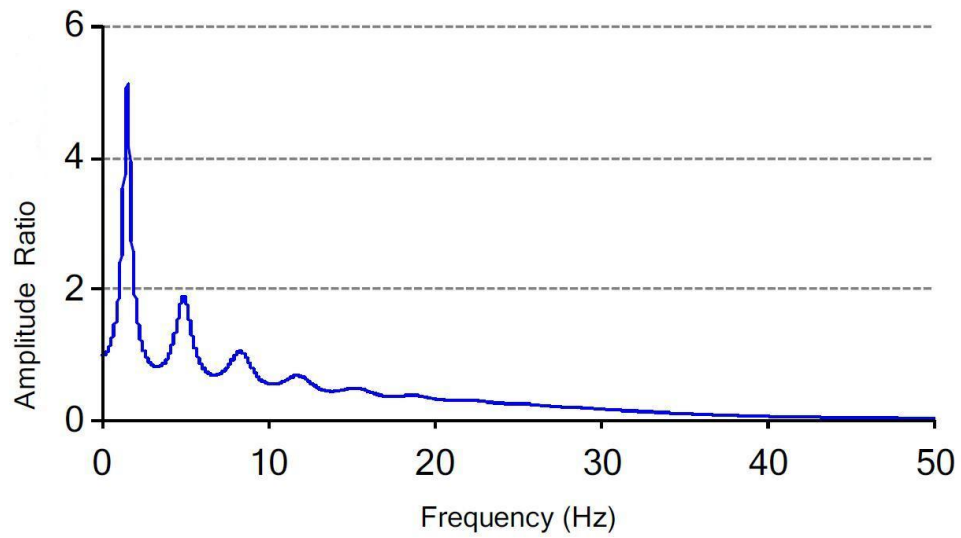
Figure 5-17: Amplitude ratio versus frequency graph, 60 ft column of soil, Parkfield
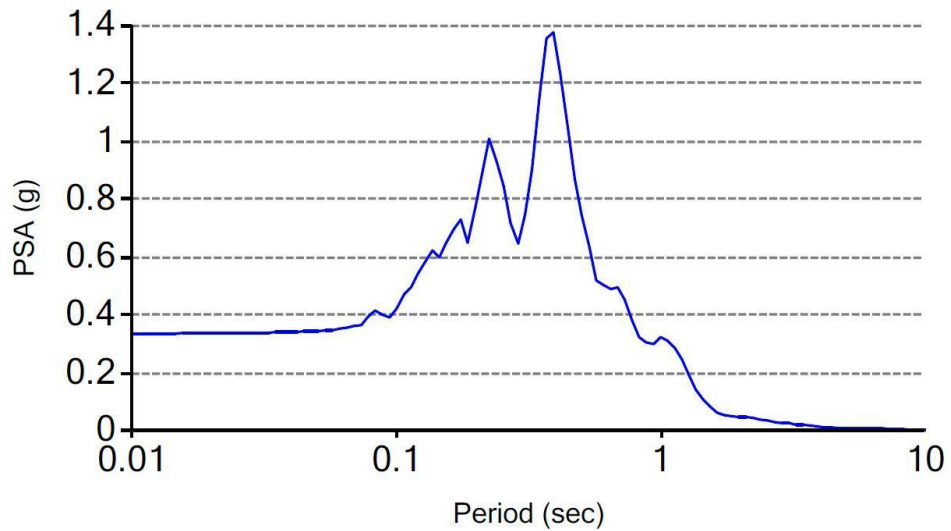motion, thickness of fiber modified layer is 10 ft (case 2)

Figure 5-18: Response spectra versus period graph, 60 ft column of soil, Parkfield
motion, thickness of fiber modified layer is 10 ft (case 2)

5.6.2 Analysis for 60 feet Column of Soil

The comparison of the results between all-clay condition (case 1) and fiber modified clay condition (case 2) indicated that the inclusion of fiber in the top 10 feet of the clayey site improved the dynamic response of the clayey site on the ground surface. Figures 5-19 to 5-21 compare the site response of the all-clay and fiber modified conditions when Imperial Valley motion was applied.
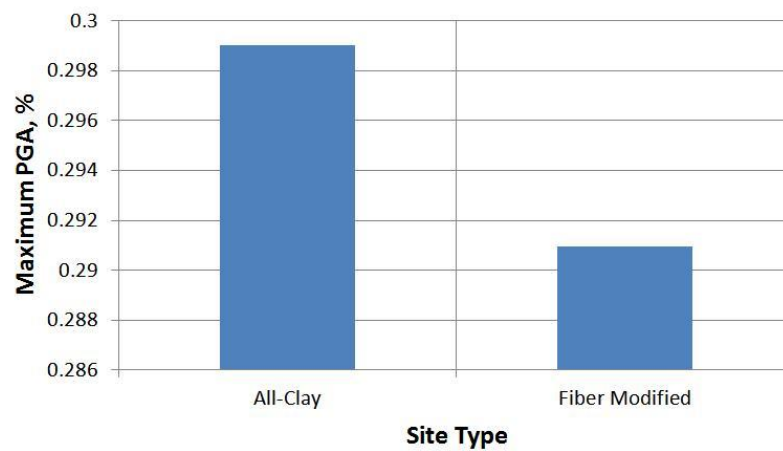

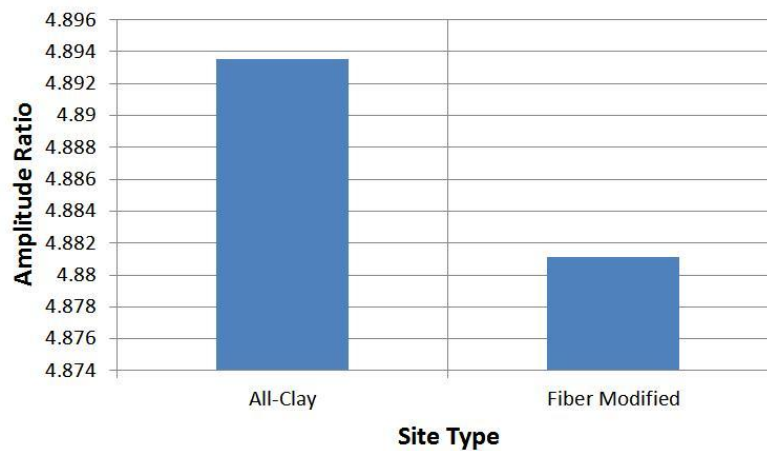Figure 5-19: Maximum PGA comparison graph, 60 ft column of soil, Imperial Valley motion

Figure 5-20: Amplitude ratio comparison graph, 60 ft column of soil, Imperial Valley motion
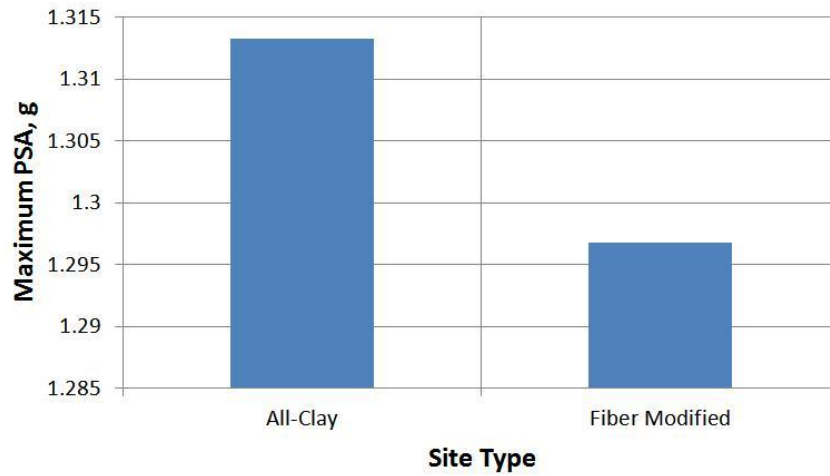
180

Figure 5-21: Maximum PSA comparison graph, 60 ft column of soil, Imperial Valley motion

Figures 5-22 to 5-24 compare the site response of the all-clay and fiber modified conditions when Parkfield motion applied.
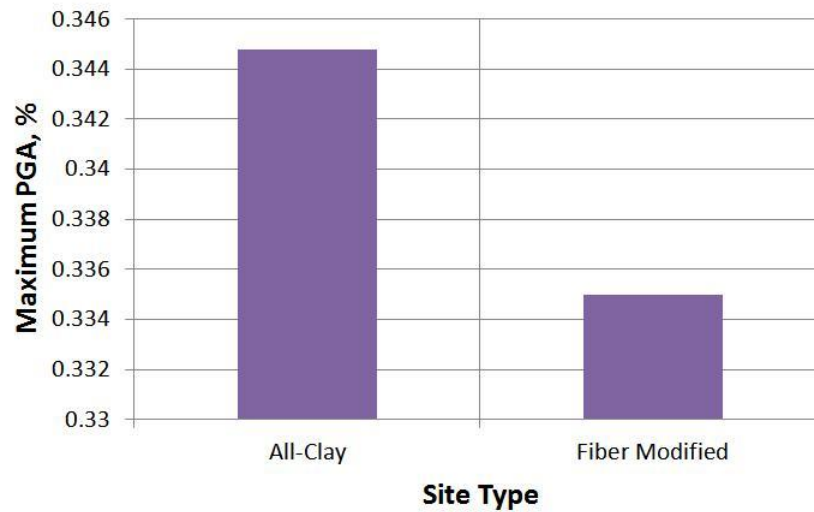

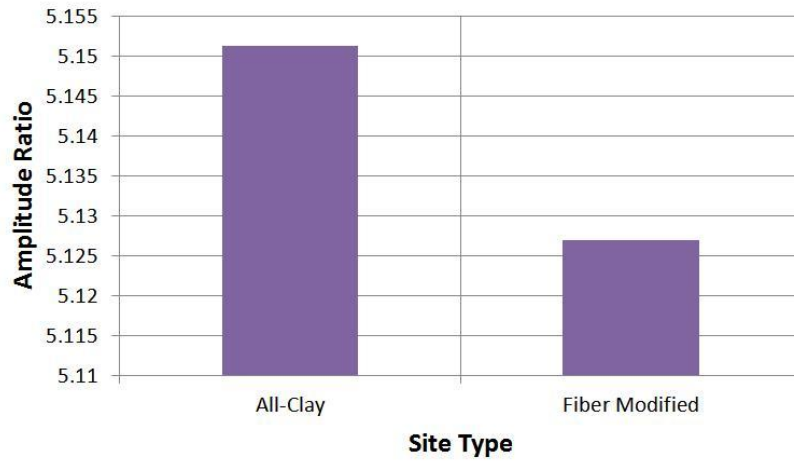Figure 5-22: Maximum PGA comparison graph, 60 ft column of soil, Parkfield motion

Figure 5-23: Amplitude ratio comparison graph, 60 ft column of soil, Parkfield motion
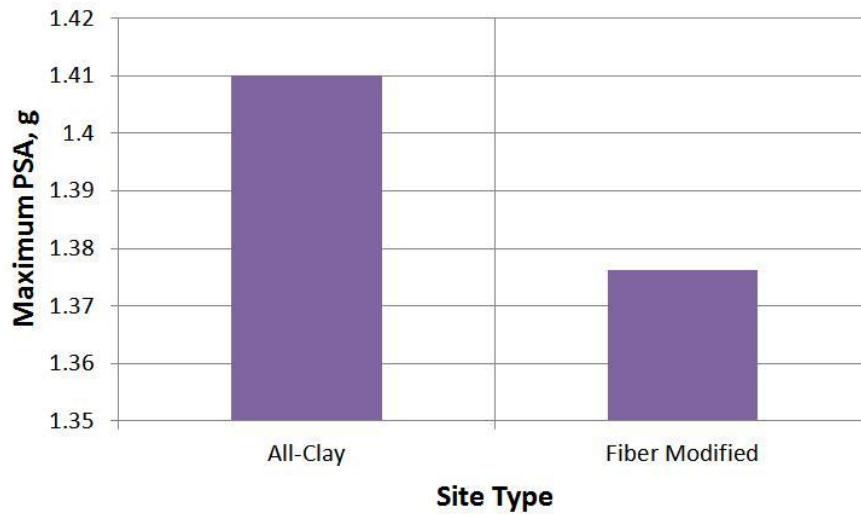

Figure 5-24: Maximum PSA comparison graph, 60 ft column of soil, Parkfield motion

The summary of the analyses and percentage changes between fiber modified and all-clay

conditions are shown in Table 5-3.

Table 5-3: The results of site response analyses for all-clay and fiber modified conditions (60 ft column)

Motion	Site Response Type	All-Clay Condition (Case 1)	Fiber Modified Condition (Case 2)	Percentage Change (%)
Imperial Valley	Peak Ground Acceleration (PGA)	0.2990232	0.2909593	-2.70
	Amplitude Ratio	4.89354389	4.8811289	-0.25
	Maximum PSA	1.3133	1.2968	-1.26
Parkfield	Peak Ground Acceleration (PGA)	0.34479423	0.33499685	-2.84
	Amplitude Ratio	5.15131805	5.12702791	-0.47
	Maximum PSA	1.14008	1.37634	-2.39

The site response analyses show an improvement of the site condition when the top 10 feet of the clayey site is fiber modified and being subjected to two different earthquake motions.

5.7   Effect of Depth to Bedrock on Seismic Response of Clayey Sites

Clay and fiber reinforced material properties were assigned to a soil column of 20 feet and were similarly studied. First for case 1, a column of soil was studied using all clay material properties. Then for case 2, 10 feet off the top of the clay column was replaced with fiber modified clay using properties presented in Section 5.4 of this manuscript as shown in Figure 5-25.

The results were then compared with the 60 foot column to investigate the effect of depth to bedrock in seismic site response of clayey sites.
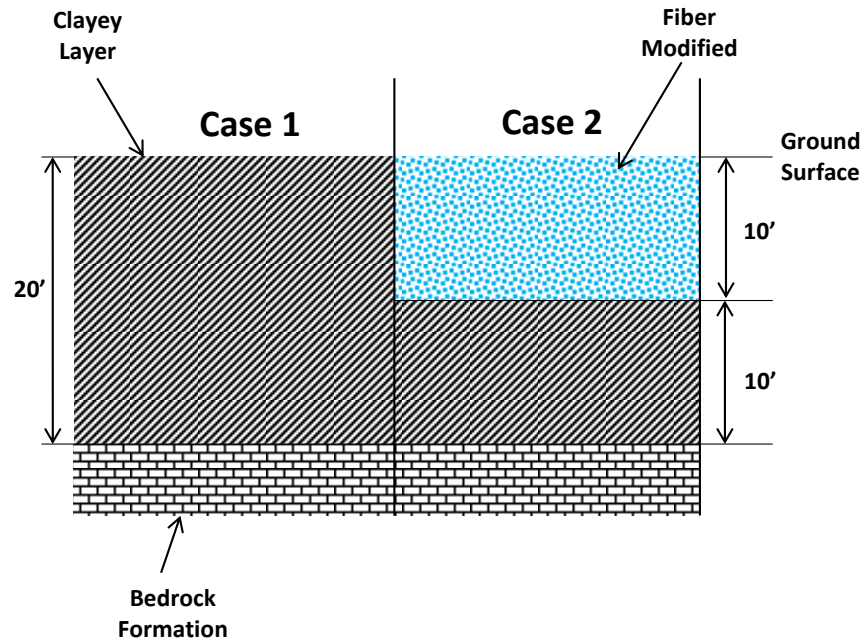
183

Figure 5-25: Site profile sketch- soil column = 20 ft

5.7.1 Seismic Site Response of 20 feet Column of Soil

After performing equivalent linear analysis applying two different earthquake motions, Imperial Valley and Parkfield, at the bedrock for 20 feet column of clayey soil, the graphs of acceleration versus time, amplitude ratio versus frequency, and response spectra versus period were generated for the ground surface for all-clay and fiber modified conditions. The graphs are shown in Figures 5-26 to 5-28 for the all-clay condition for the Imperial Valley motion and Figures 5-29 to 5-31 for the all-clay condition for the Parkfield motion.

Figure 5-26: Acceleration versus time graph for all-clay condition, 20 ft column of soil, Imperial Valley motion

Figure 5-27: Amplitude ratio versus frequency graph for all-clay condition, 20 ft column of soil, Imperial Valley motion

185

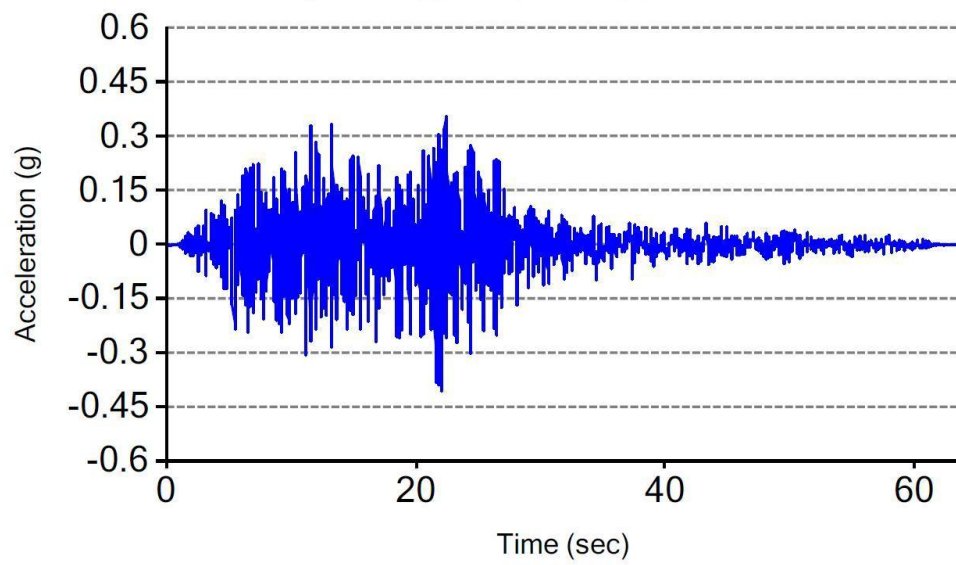Figure 5-28: Response spectra versus period graph for all-clay condition, 20 ft column of soil, Imperial Valley motion

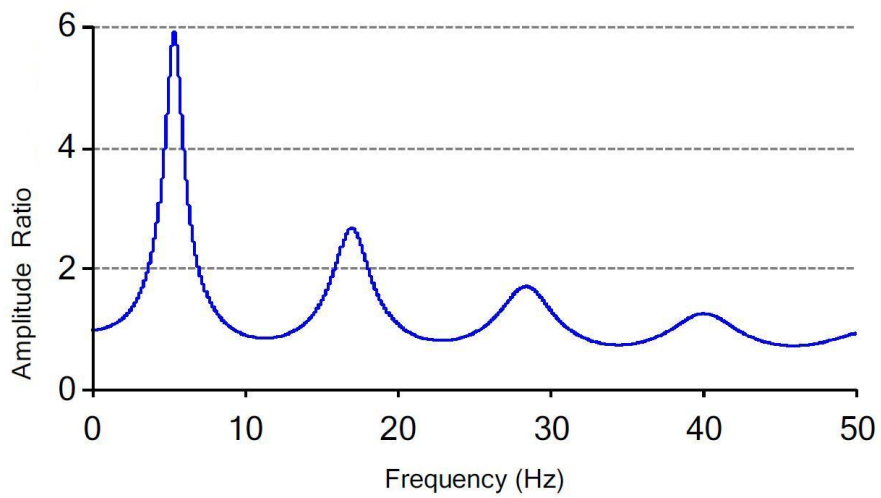Figure 5-29: Acceleration versus time graph for all-clay condition, 20 ft column of soil, Parkfield motion

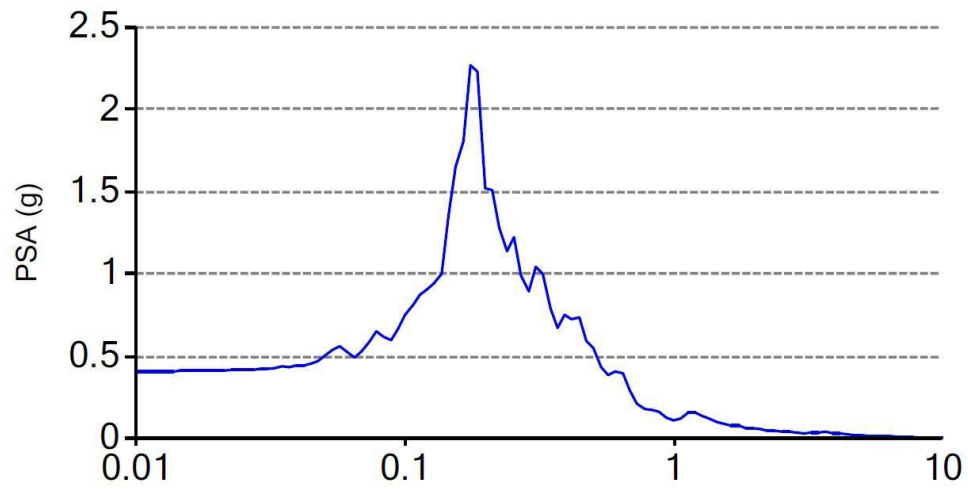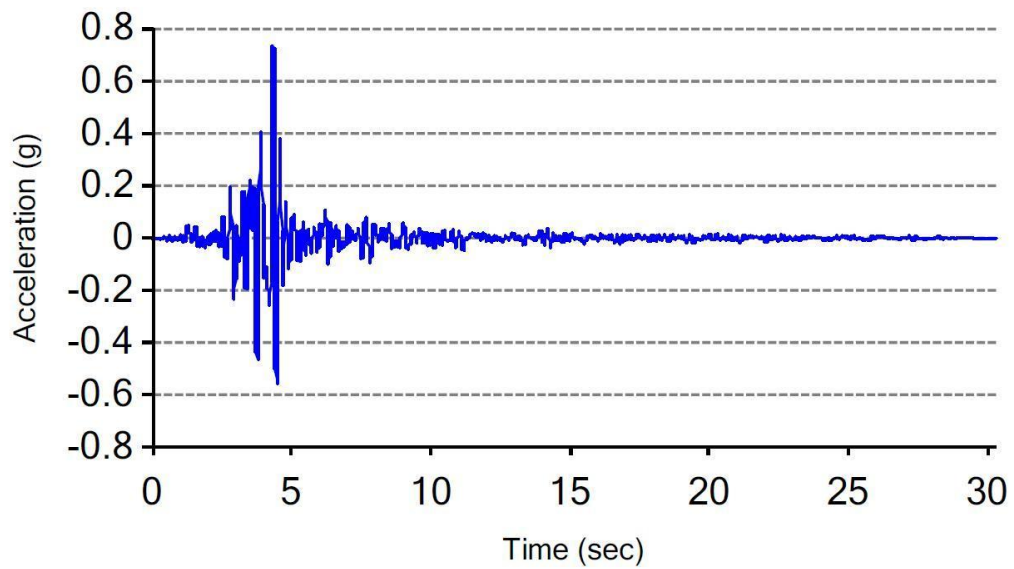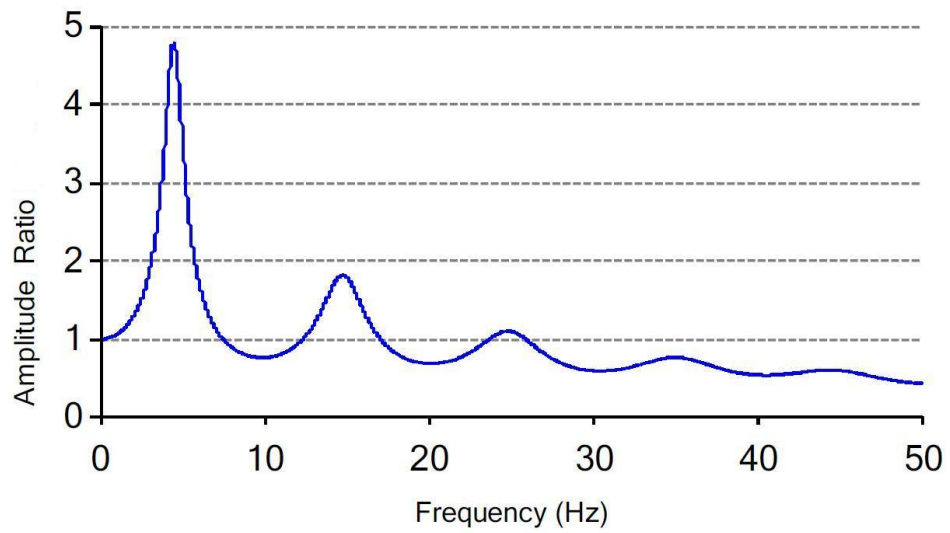Figure 5-30: Amplitude ratio versus frequency graph for all-clay condition, 20 ft column of soil, Parkfield motion
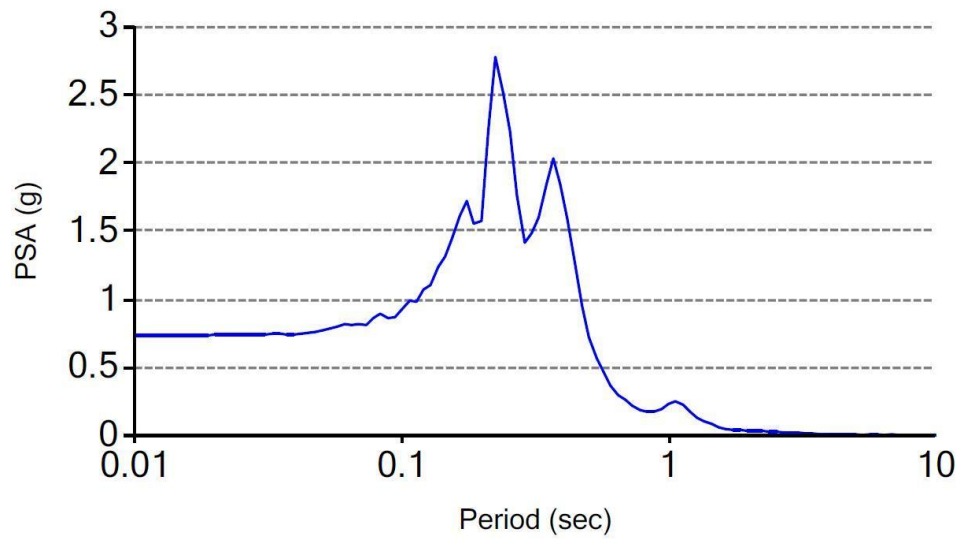
Figure 5-31: Response spectra versus frequency graph for all-clay condition, 20 ft column of soil, Parkfield motion

The analysis was then performed on the 20 foot column of clay where the top 10 feet of the column was fiber modified. The column was analyzed applying Imperial Valley and Parkfield motions separately at the bedrock. The ground surface site response graphs are shown in Figures 5-32 to 5-34 for Imperial Valley and in Figures 5-35 to 5-37 for Parkfield motions.
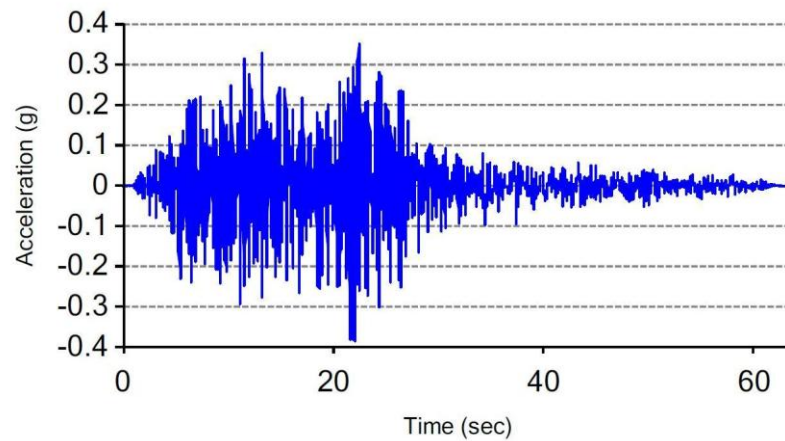
Figure 5-32: Acceleration versus time graph, 20 ft column of soil, Imperial Valley motion, thickness of fiber modified layer is 10 ft
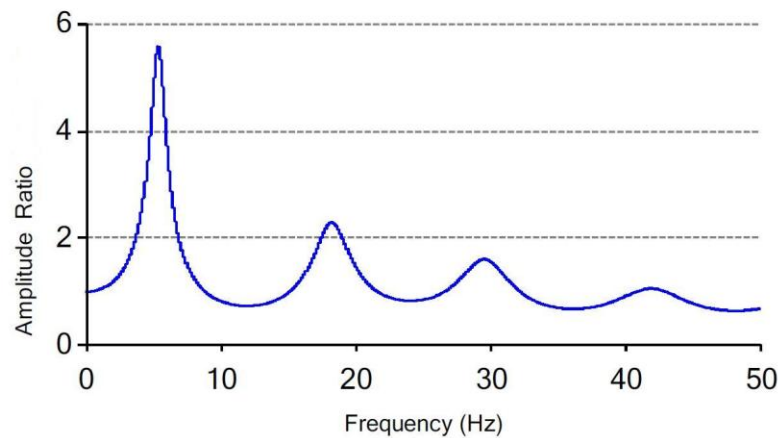
Figure 5-33: Amplitude ratio versus frequency graph, 20 ft column of soil, Imperial Valley motion, thickness of fiber modified layer is 10 ft

188
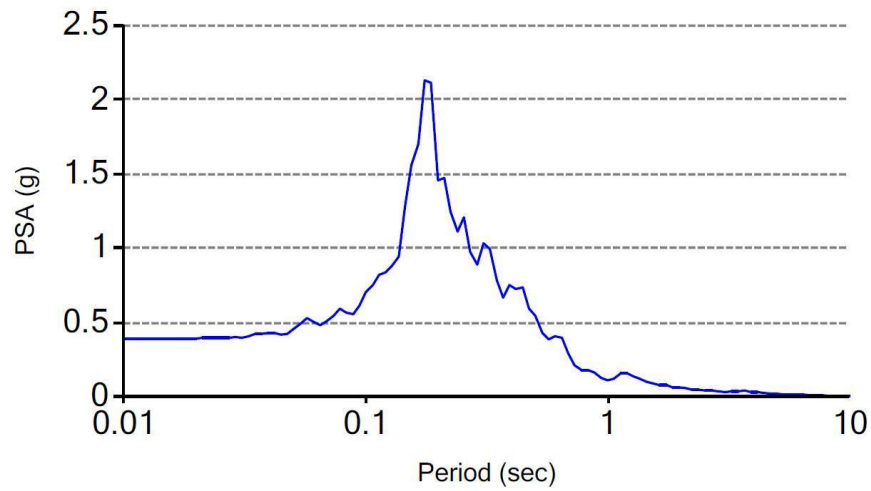
Figure 5-34: Response spectra versus period graph, 20 ft column of soil, Imperial Valley motion, thickness of fiber modified layer is 10 ft
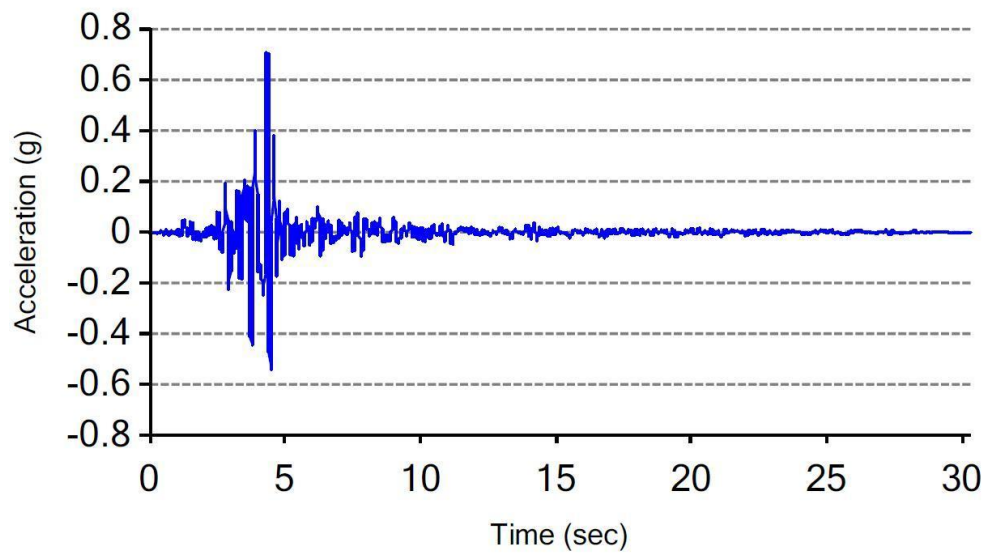
Figure 5-35: Acceleration versus time graph, 20 ft column of soil, Parkfield motion, thickness of fiber modified layer is 10 ft
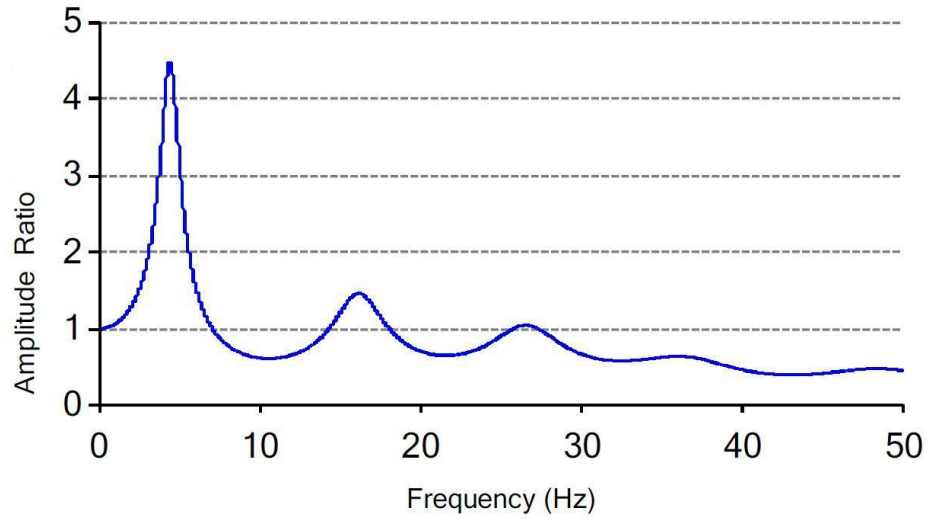
Figure 5-36: Amplitude ratio versus frequency graph, 20 ft column of soil, Parkfield
motion, thickness of fiber modified layer is 10 ft
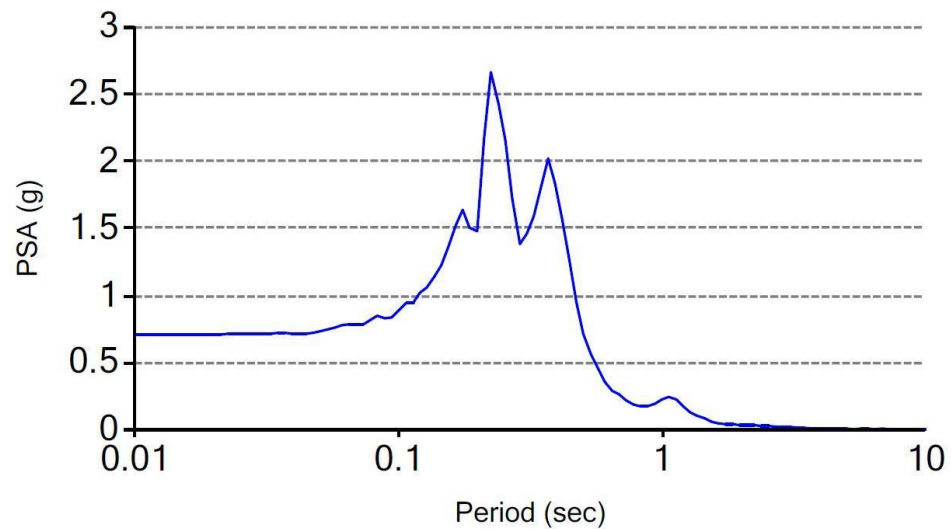
Figure 5-37: Response spectra versus period graph, 20 ft column of soil, Parkfield
motion, thickness of fiber modified layer is 10 ft

5.7.2   Analysis for 20 feet Column of Soil

The comparison of the results between all-clay condition and fiber modified clay

condition indicated that the inclusion of fiber in the top 10 feet of the clayey site

190

improved the dynamic response of the clayey site on the ground surface. Figures 5-38 to 5-40 compares the site response of the all-clay and fiber modified conditions in the case of the Imperial Valley motion.
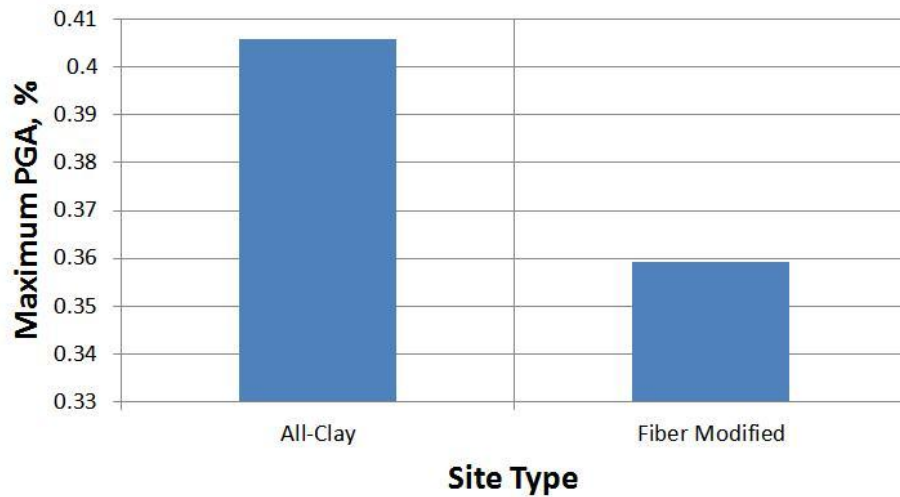
Figure 5-38: Maximum PGA comparison graph, 20 ft column of soil, Imperial Valley motion
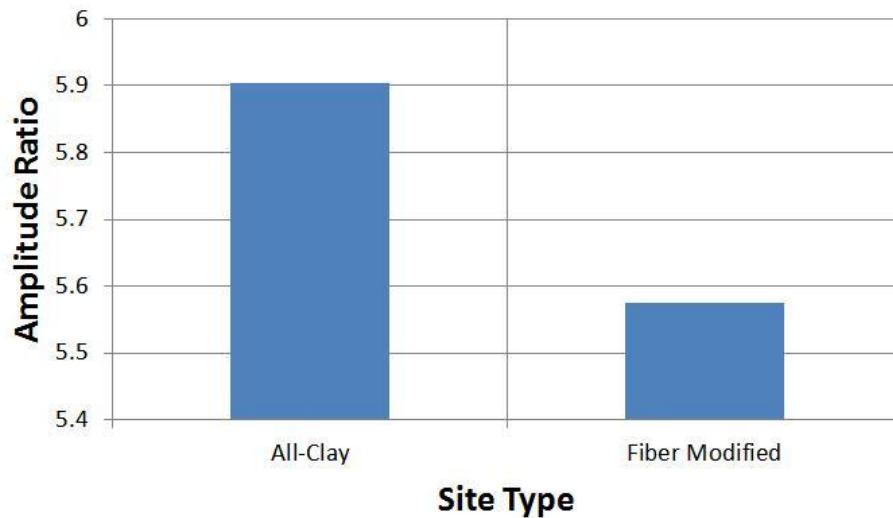
Figure 5-39: Amplitude ratio comparison graph, 20 ft column of soil, Imperial Valley motion
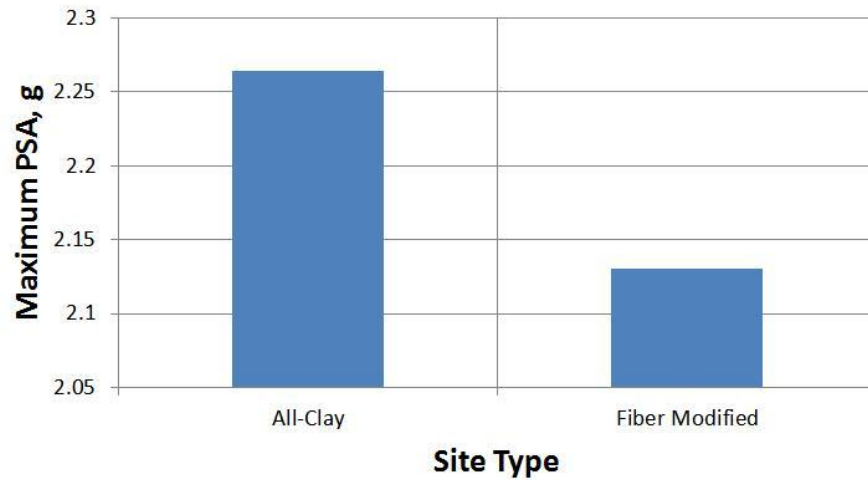
Figure 5-40: Maximum PSA comparison graph, 20 ft column of soil, Imperial Valley motion

Figures 5-41 to 5-43 compares the site response of the all-clay and fiber modified

conditions in the case of the Parkfield motion.
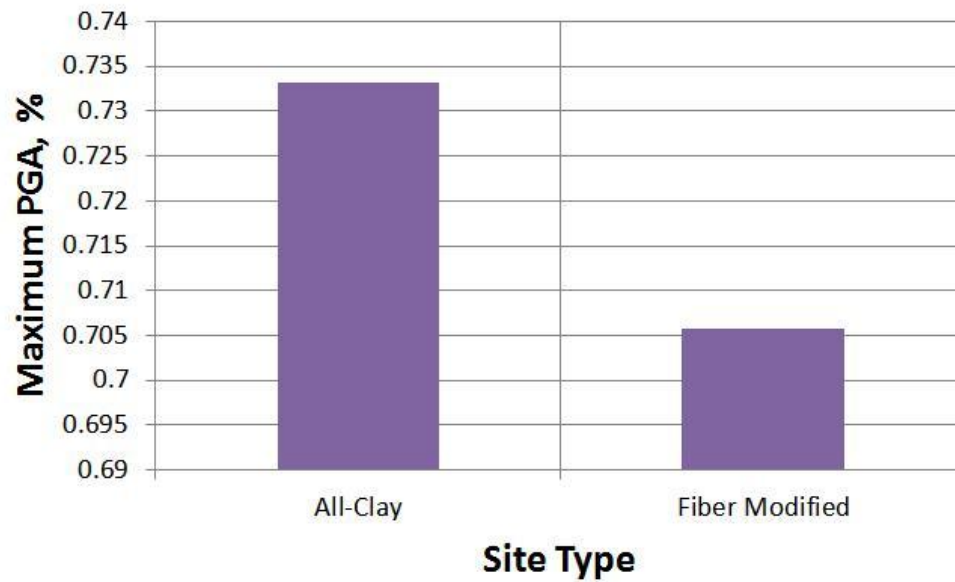
Figure 5-41: Maximum PGA comparison graph, 20 ft column of soil, Parkfield motion
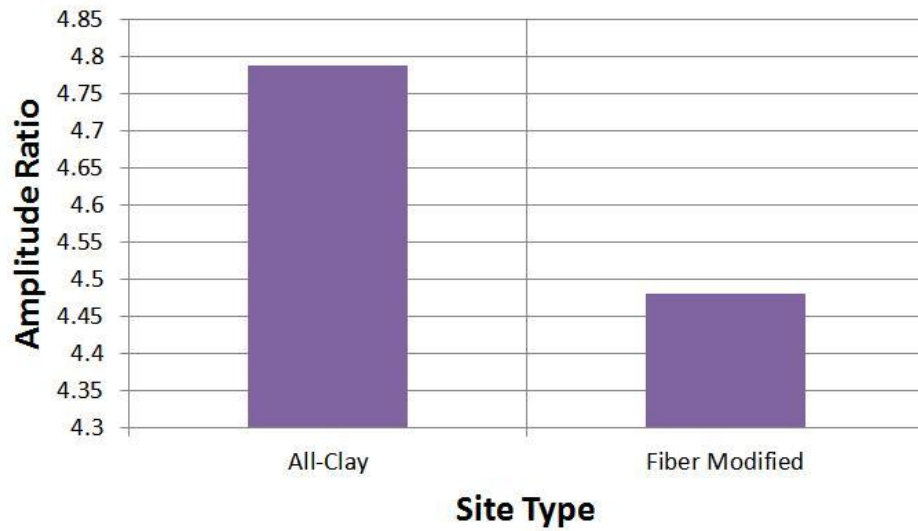
Figure 5-42: Amplitude Ratio comparison graph, 20 ft column of soil, Parkfield motion
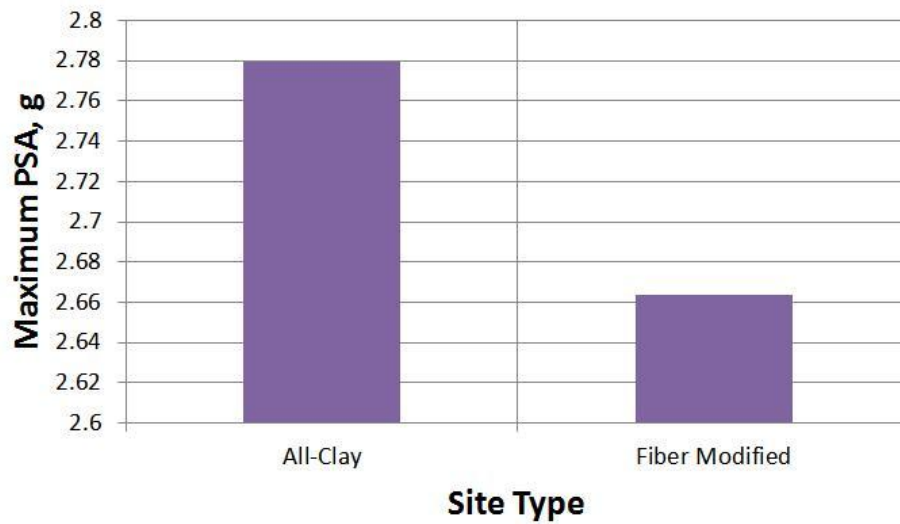
Figure 5-43: Maximum PSA comparison graph, 20 ft column of soil, Parkfield motion

The summary of the analyses and percentage changes between fiber modified and all-clay conditions are shown in Table 5-4.

Table 5-4: The results of site response analyses for 20 ft soil column

| Motion	Site Response Type	All-Clay Condition	Fiber Modified Condition	Percentage Change (%)
Imperial Valley	Peak Ground Acceleration (PGA)	0.4058655	0.359121541	-11.52
	Amplitude Ratio	5.90347087	5.57596176	-5.55
	Maximum PSA	2.26456	2.13058	-5.92
Parkfield	Peak Ground Acceleration (PGA)	0.73319242	0.7058454	-3.73
	Amplitude Ratio	4.78843299	4.47991985	-6.44
	Maximum PSA	2.77943	2.66402	-4.15

The site response analyses of 20 feet clayey soil column show an improvement of the seismic response of the site when the top 10 feet of the clayey site is fiber modified.

The comparison between the percentage changes in 60 and 20 foot soil columns indicates that if the same amount of fiber improvement is performed (10 feet) on clayey sites, the site that has a shallower bedrock formation can experience a larger reduction in seismic site response values.

5.8   Effect of Thickness of Fiber Improvement on Seismic Site Response of Clayey Sites

The 20 feet clayey site was used for site response analysis using two different motions. The fiber improvement increment was chosen as 5 feet and the direction of the improvement was chosen from the ground surface downward. Therefore, five cases of, 0 (all-clay condition), 5, 10, 15, and 20 (all fiber modified condition) feet of soil improvement were analyzed to compare the effect of thickness of fiber improvement on the seismic site response of a clayey site. Figure 5-44 shows the five cases used in the analyses.
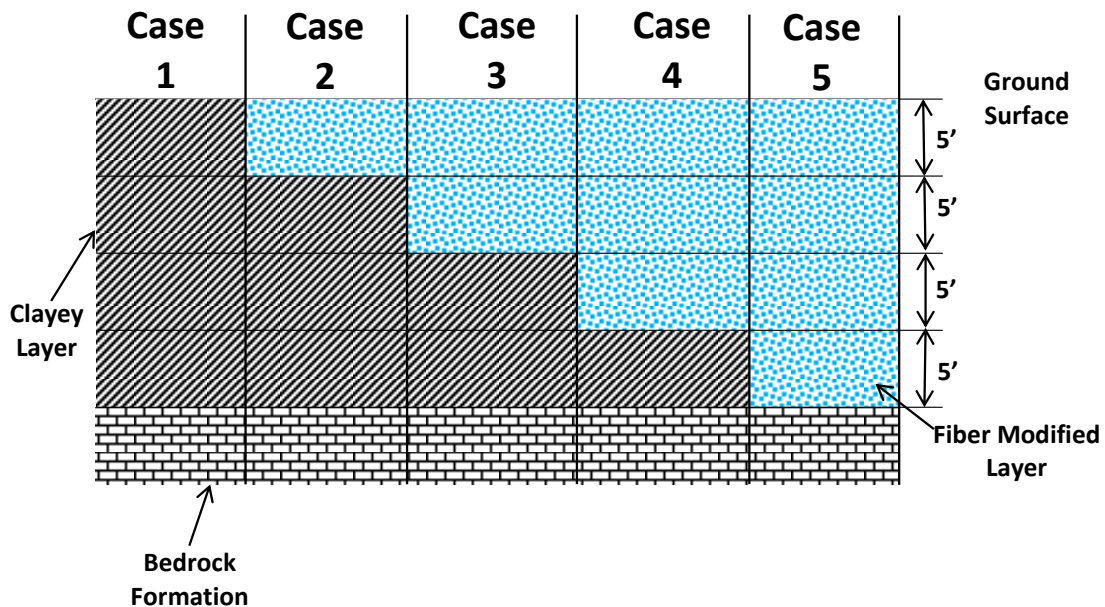
Figure 5-44: Site profile sketch, soil column = 20 ft (fiber improvement increment is 5 feet)

Site response analysis was performed separately using two different earthquake motions, Imperial Valley and Parkfield, at the bedrock for all five cases. The graphs of acceleration versus time, amplitude ratio versus frequency, and response spectra versus period were developed for every case. For the all-clay condition (case 1), the graphs are shown in Section 5.7.1, Figures 5-26 to 5-28 for the Imperial Valley motion and in Figures 5-29 to 5-31 for the Parkfield motion. For the case of 5 feet of fiber improvement (case 2), the graphs are shown in Figures 5-45 to 5-47 for the Imperial Valley motion and in Figures 5-48 to 5-50 for the Parkfield motion. For the case of 10 feet of fiber improvement (case 3), the graphs are shown in Section 5.7.1, Figures 5-32 to 5-34 for the Imperial Valley motion and in Figures 5-35 to 5-37 for the Parkfield motion. For the case of 15 feet of fiber improvement (case 4), the graphs are shown in Figures 5-51 to 5-53 for

the Imperial Valley motion and in Figures 5-54 to 5-56 for the Parkfield motion. For the

case of 20 feet of fiber improvement (case 5, all fiber modified), the graphs are shown

Figures 5-57 to 5-59 for the Imperial valley motion and in Figures 5-60 to 5-62 for the

Parkfield motion.
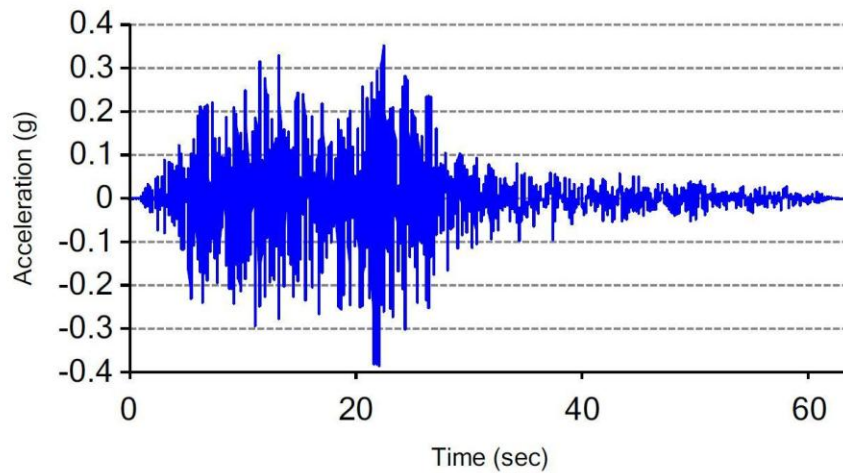
Figure 5-45: Acceleration versus time graph for case 2 (5 feet of fiber improvement), 20 ft column of soil, Imperial Valley motion
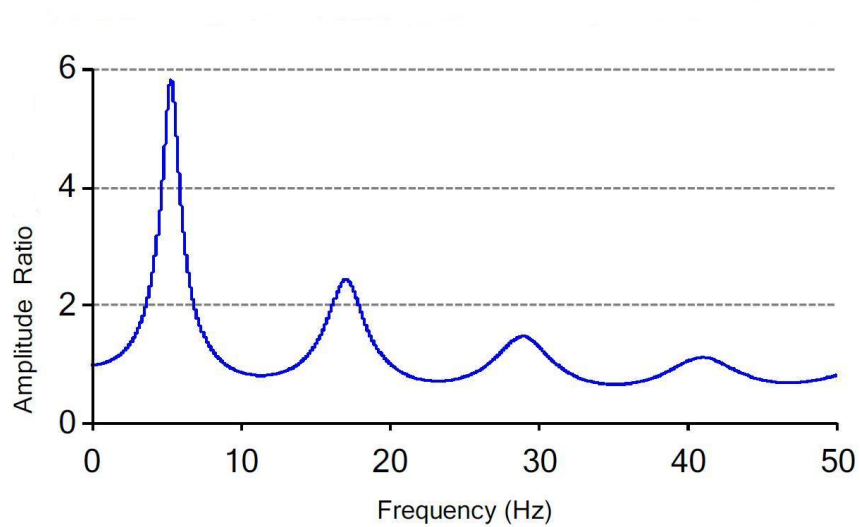
Figure 5-46: Amplitude ratio versus frequency graph for case 2 (5 feet of fiber improvement), 20 ft column of soil, Imperial Valley motion

196
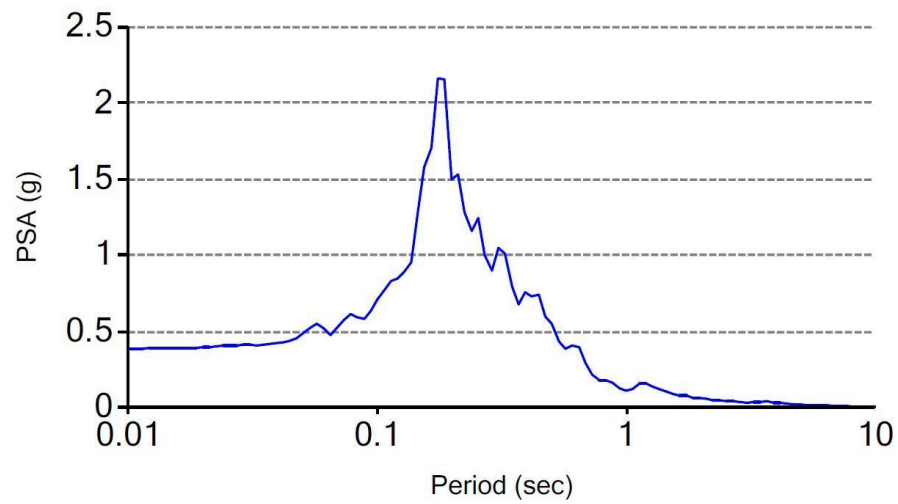
Figure 5-47: Response spectra versus period graph for case 2 (5 feet of fiber improvement), 20 ft column of soil, Imperial Valley motion
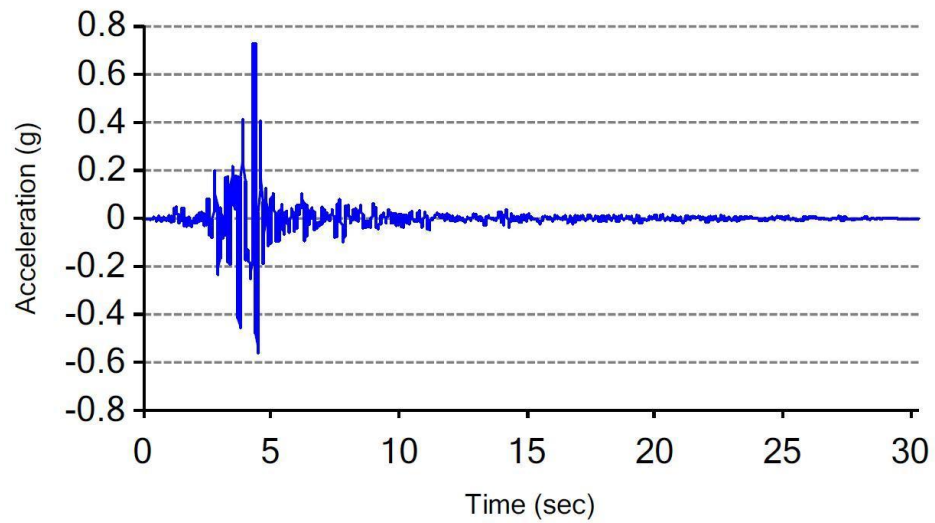
Figure 5-48: Acceleration versus time graph for case 2 (5 feet of fiber improvement), 20 ft column of soil, Parkfield motion

197
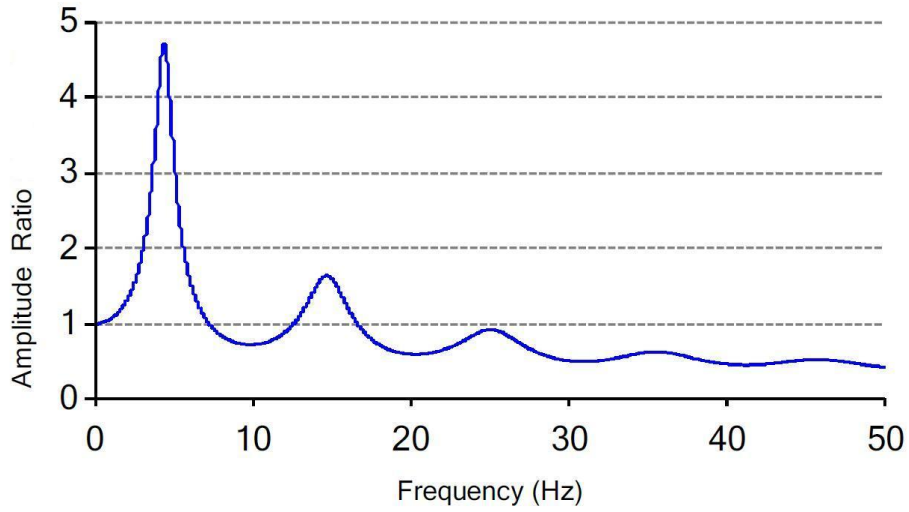
Figure 5-49: Amplitude ratio versus frequency graph for case 2 (5 feet of fiber improvement), 20 ft column of soil, Parkfield motion
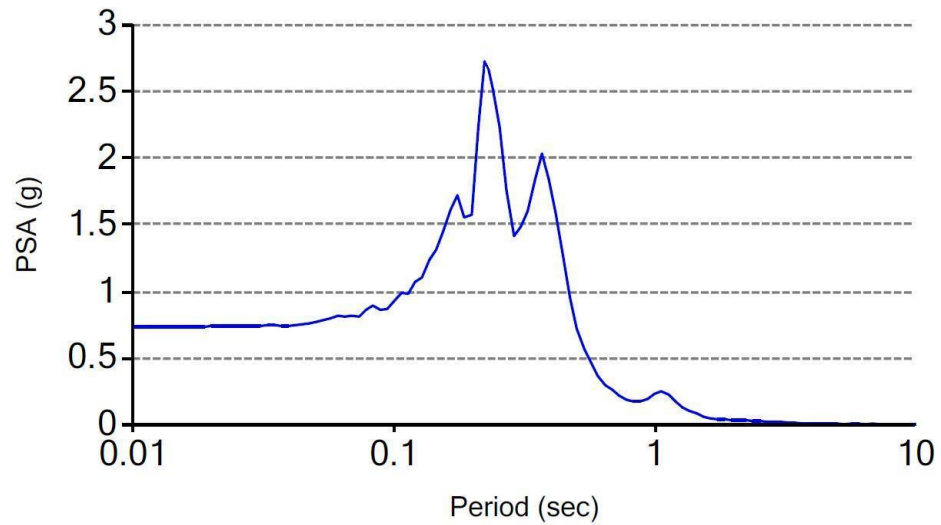
Figure 5-50: Response spectra versus Period graph for case 2 (5 feet of fiber improvement), 20 ft column of soil, Parkfield motion

198
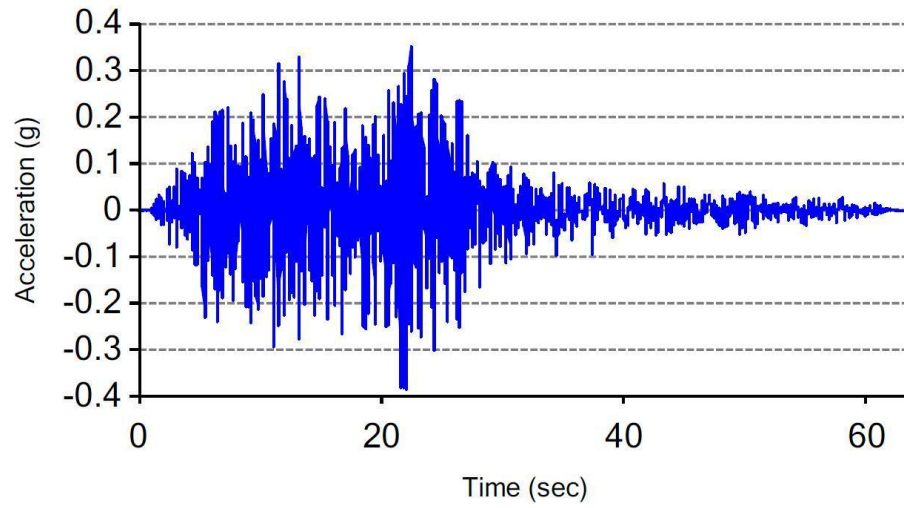
Figure 5-51: Acceleration versus time graph for case 4 (15 feet of fiber improvement), 20 ft column of soil, Imperial Valley motion
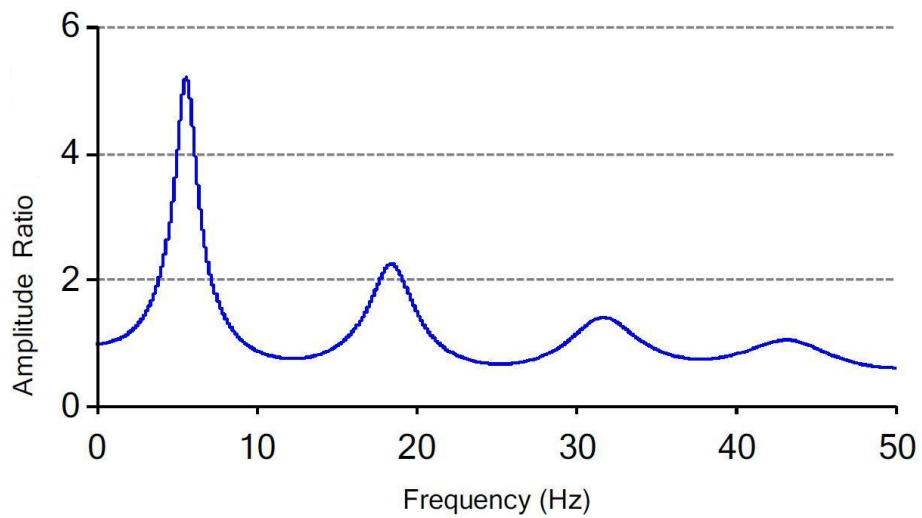
Figure 5-52: Amplitude ratio versus frequency graph for case 4 (15 feet of fiber improvement), 20 ft column of soil, Imperial Valley motion
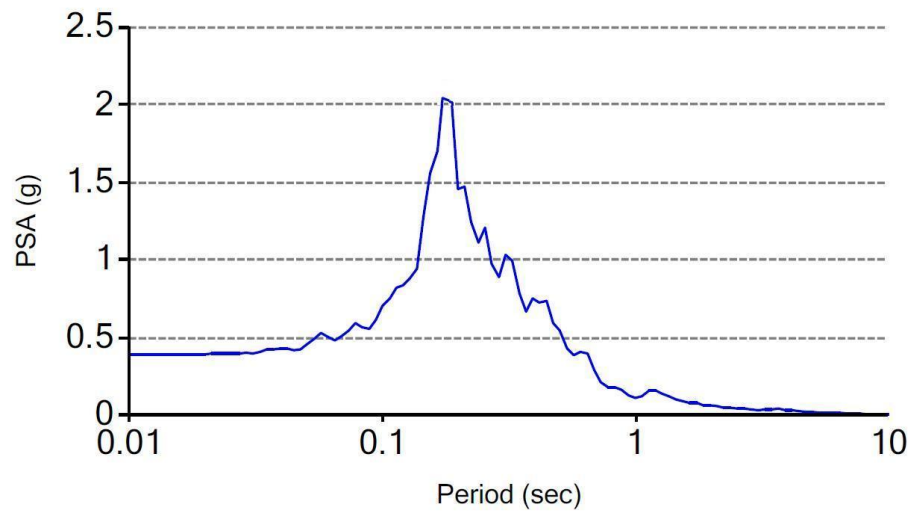
Figure 5-53: Response spectra versus period graph for case 4 (15 feet of fiber improvement), 20 ft column of soil, Imperial Valley motion
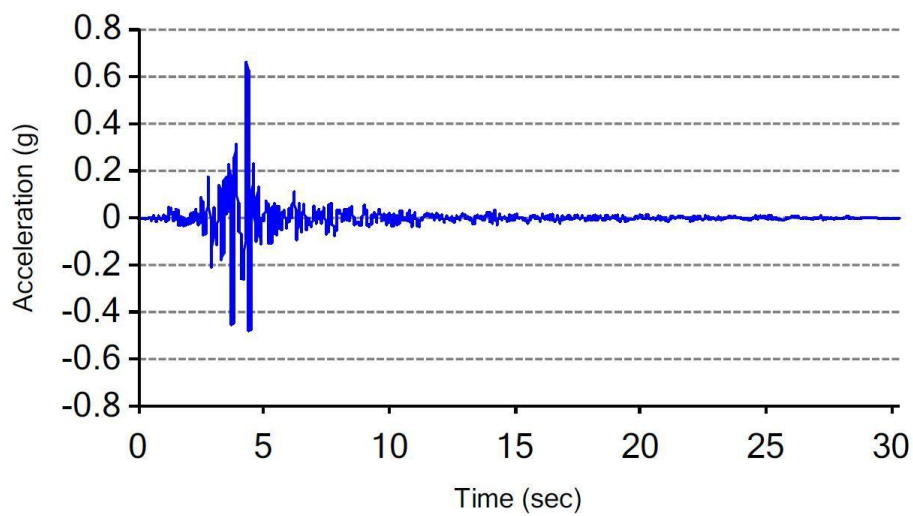
Figure 5-54: Acceleration versus time graph for case 4 (15 feet of fiber improvement), 20 ft column of soil, Parkfield motion
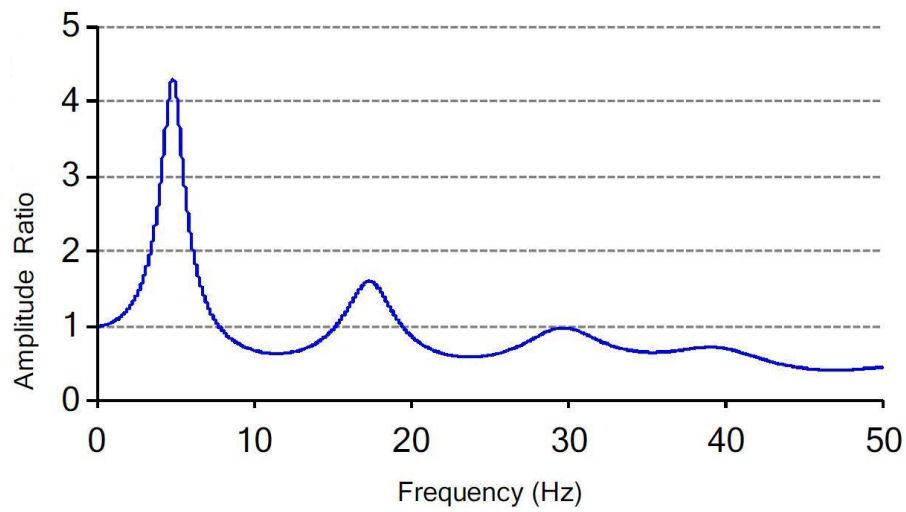
Figure 5-55: Amplitude ratio versus frequency graph for case 4 (15 feet of fiber improvement), 20 ft column of soil, Parkfield motion
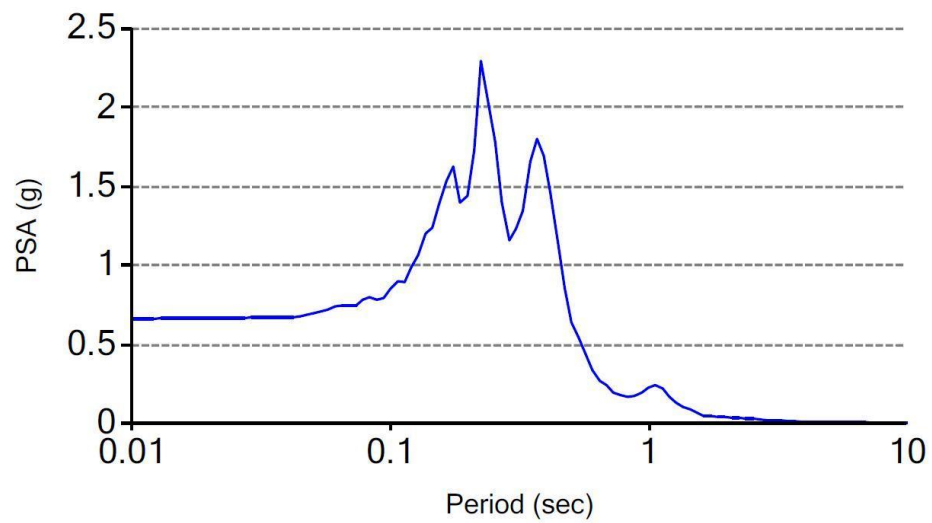
Figure 5-56: Response spectra versus period graph for case 4 (15 feet of fiber improvement), 20 ft column of soil, Parkfield motion
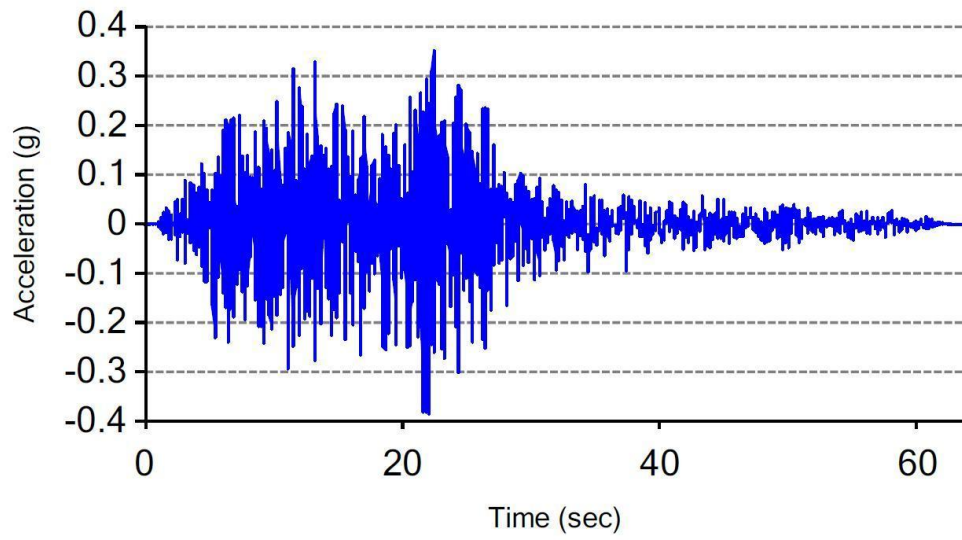
Figure 5-57: Acceleration versus time graph for case 5 (all fiber modified), 20 ft column of soil, Imperial Valley motion
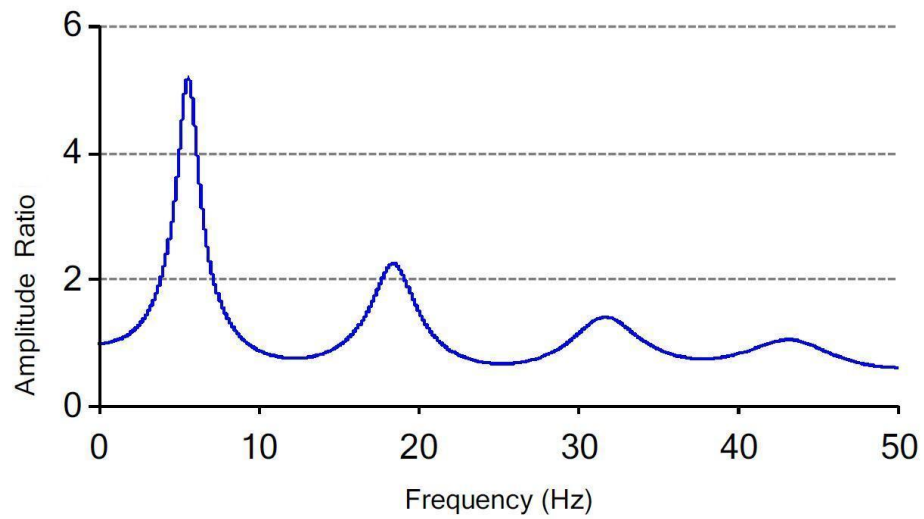
Figure 5-58: Amplitude ratio versus frequency graph for case 5 (all fiber modified), 20 ft column of soil, Imperial Valley motion
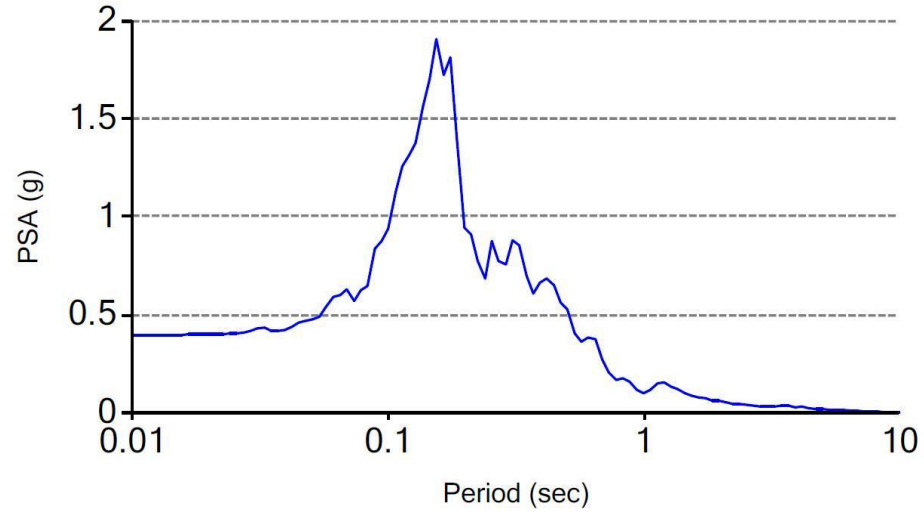
Figure 5-59: Response spectra versus period graph for case 5 (all fiber modified), 20 ft column of soil, Imperial Valley motion
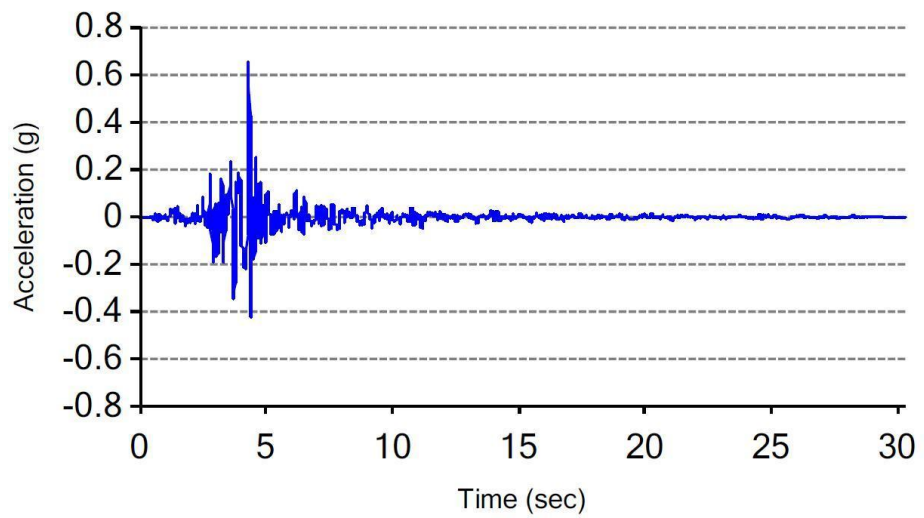
Figure 5-60: Acceleration versus time graph for case 5 (all fiber modified), 20 ft column of soil, Parkfield motion
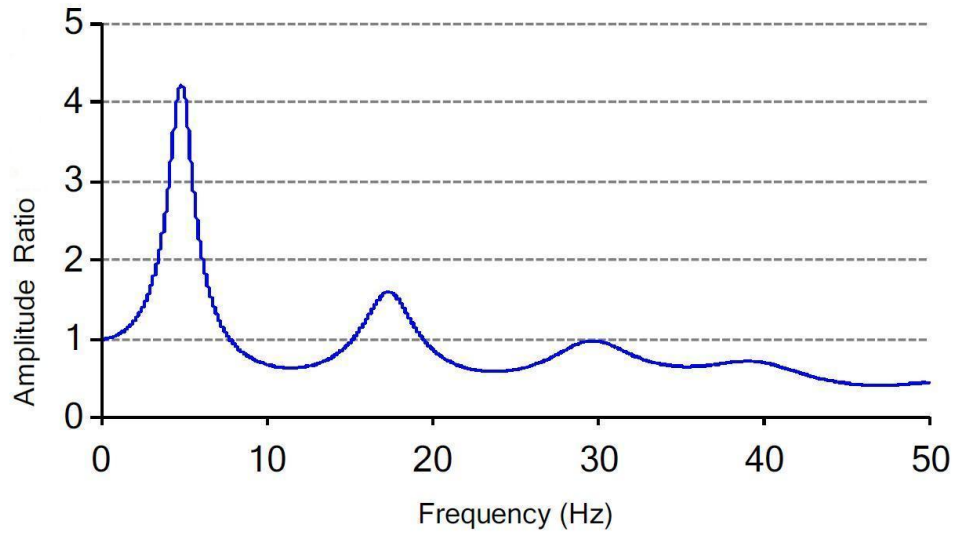
Figure 5-61: Amplitude ratio versus frequency graph for case 5 (all fiber modified), 20 ft column of soil, Parkfield motion
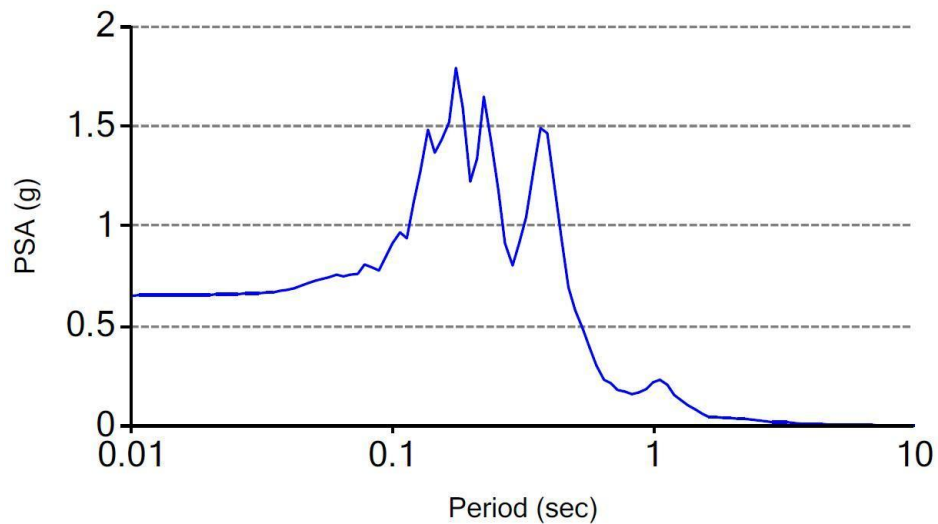
Figure 5-62: Response spectra versus period graph for case 5 (all fiber modified), 20 ft column of soil, Parkfield motion

Figures 5-63 to 5-65 show the seismic site response for all cases at the ground surface

when Imperial Valley motion was used as applied motion to the bedrock formation.
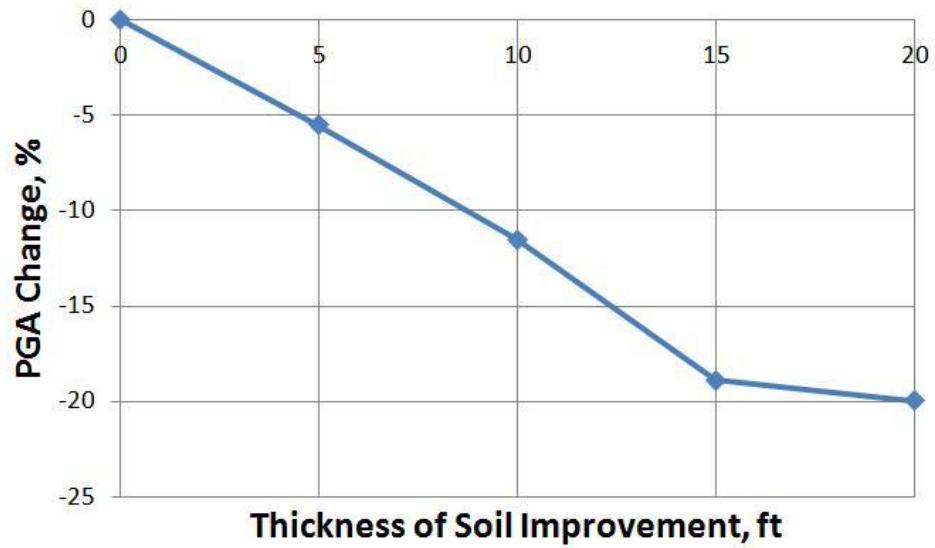
Figure 5-63: Peak ground acceleration change versus thickness of soil improvement
graph for all cases, 20 ft column of soil, Imperial Valley motion
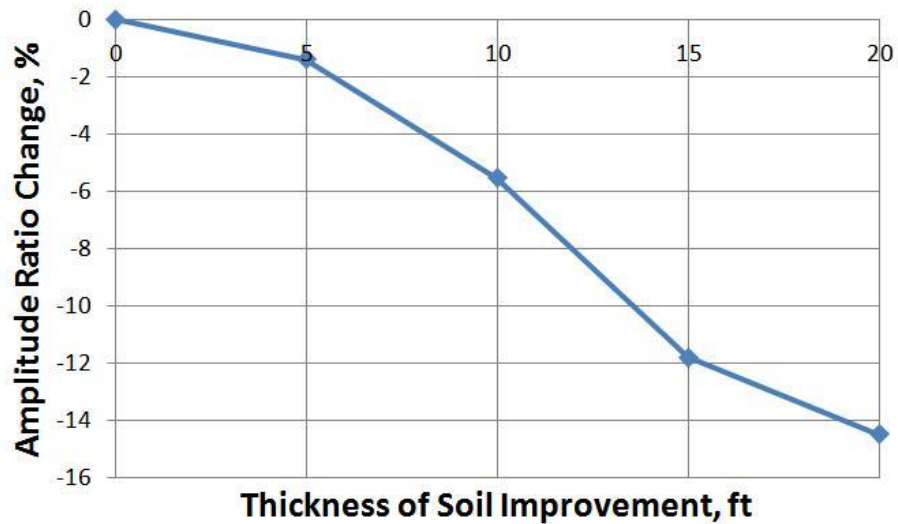
Figure 5-64: Amplitude ratio change versus thickness of soil improvement graph for all
cases, 20 ft column of soil, Imperial Valley motion
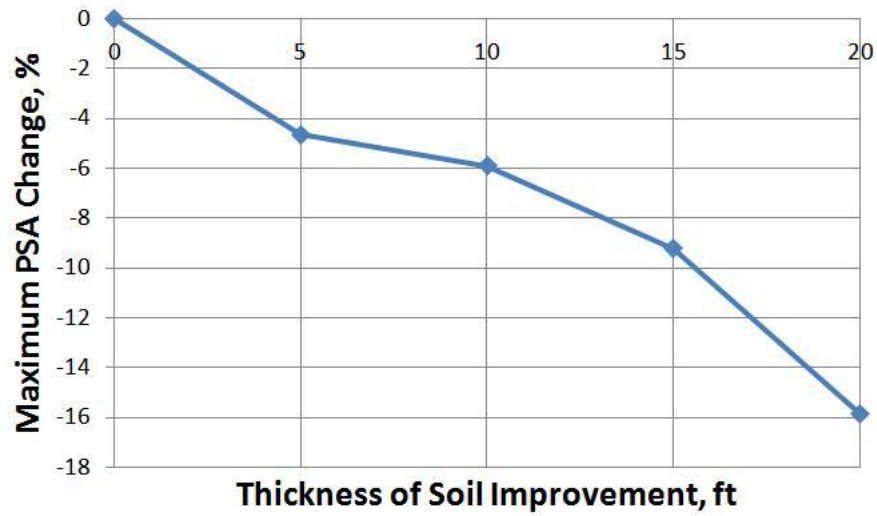
Figure 5-65: Maximum response spectra change versus thickness of soil improvement graph for all cases, 20 ft column of soil, Imperial Valley motion

Figures 5-66 to 5-68 show the seismic site response for all cases at the ground surface when Parkfield motion was used as applied motion to the bedrock formation.
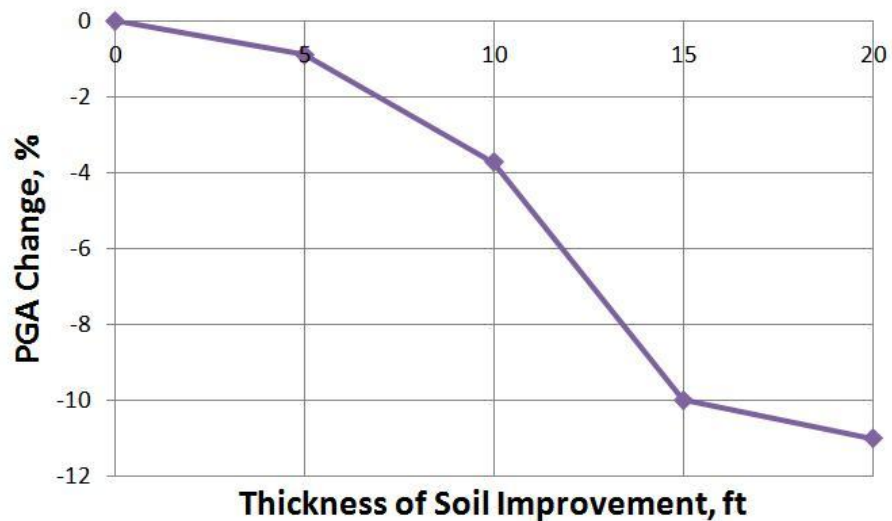
Figure 5-66: Peak ground acceleration change versus thickness of soil improvement graph for all cases, 20 ft column of soil, Parkfield motion
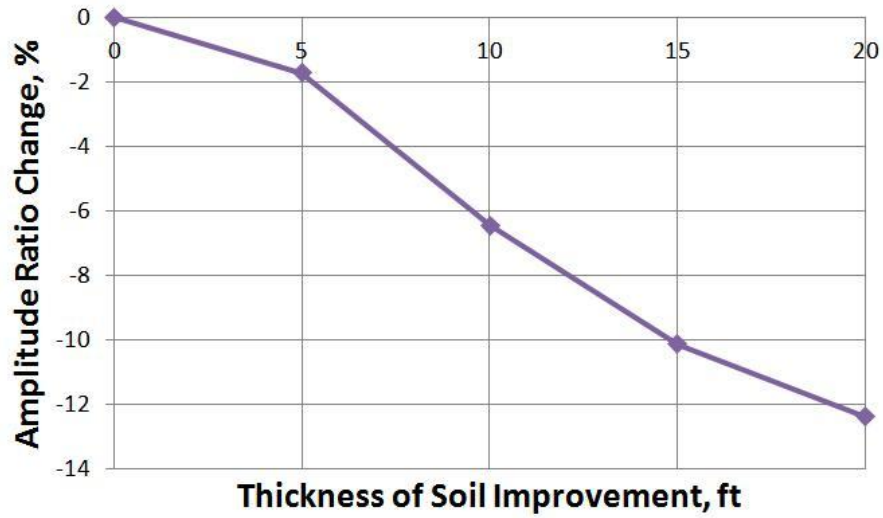
Figure 5-67: Amplitude ratio change versus thickness of soil improvement graph for all cases, 20 ft column of soil, Parkfield motion
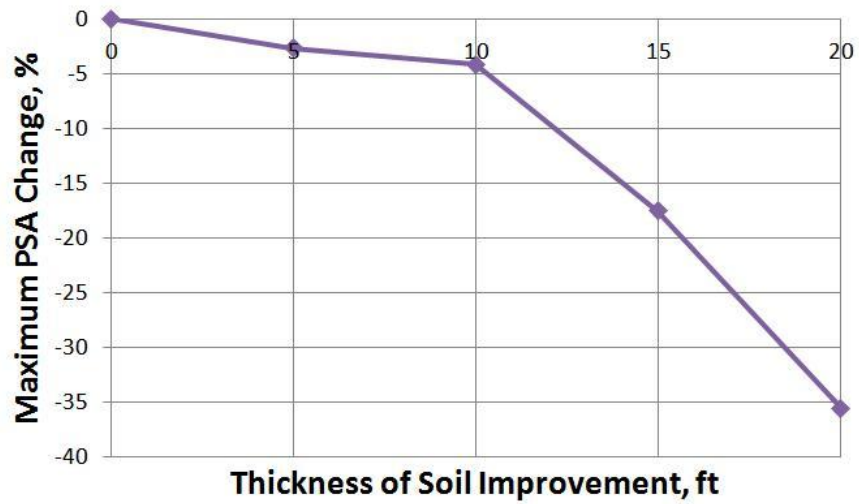
Figure 5-68: Maximum response spectra change versus thickness of soil improvement graph for all cases, 20 ft column of soil, Parkfield motion

The results of the site response analysis for a 20 feet column of soil are shown in Table 5-5.

Table 5-5: The results of site response analyses to investigate the effect of thickness of soil improvement

Motion	Site Response Type	Case Number					Percent Change (%)
		1	2	3	4	5	
		Thickness of Soil Improvement (ft)					
		0	5	10	15	20	
Imperial Valley	Peak Ground Acceleration	0.4058655	0.3834526	0.359121541	0.329149807	0.32483029	-19.97
	Amplitude Ratio	5.90347087	5.82078669	5.57596176	5.20701808	5.047959928	-14.49
	Maximum PSA	2.26456	2.15909	2.13058	2.055746659	1.90566	-15.85
Parkfield	Peak Ground Acceleration	0.73319242	0.72672892	0.7058454	0.65998579	0.65251719	-11.00
	Amplitude Ratio	4.78843299	4.7064245	4.47991985	4.30324353	4.194953124	-12.39
	Maximum PSA	2.77943	2.705904909	2.66402	2.29255	1.79147	-35.54

The results indicated that by increasing the thickness of fiber reinforcement in a clayey site, the seismic site response of the clayey site is improved. The amount of the response reductions is more pronounced when a larger depth of site soil is fiber reinforced.

5.9 Effect of Fiber Improvement on Natural Period of Clayey Site

Determining the natural frequency (f_n) and natural period (T_n) of a site is one of the main steps in predicting the potential effects of earthquakes on a structure erected at the site. The assumption in calculating f_n and T_n is that the main responses in a soil deposit are caused by the upward propagation of a shear wave from the underlying bedrock formation.

The equation of motion describes the behavior of a soil column in terms of its dynamic motion as a function of time.

$$\frac{\partial^2 u}{\partial t^2} = \frac{G}{\rho} \times \frac{\partial^2 u}{\partial z^2} \tag{5.17}$$

where, G is soil shear modulus, ρ is the mass density of soil, u is the displacement, t is the time, and z is the distance.

For calculating f_n and T_n, the solution for an equation of motion for elastic soils,

equation 5.17, was used in the first mode ($\omega = \frac{\pi}{2H} \times \sqrt{\frac{G}{\rho}}$, where ω is the circular

frequency, G is the soil shear modulus, ρ is the mass density of soil, and H is the soil

column thickness). The first mode solution can be rephrased to calculate for f_n and T_n as

$f_n = \frac{V_s}{4H}$ and $T_n = \frac{4H}{V_s}$. Hence, f_n is equal to $\frac{1}{T_n}$. Since structural engineers consider T_n in

their analysis, the data are presented in two forms of T_n and f_n.

When the soil columns contain different soil sublayers with different shear wave

velocities, the weighted average of the shear wave velocity of the sublayers with respect

of each layer thickness should be used for the calculation of f_n and T_n as presented in

Equation 5.18.

$$V_s = \frac{H_i}{\frac{H_i}{v_{si}}} \tag{5.18}$$

where, H_i is the thickness of any sublayer and v_{si} is the shear wave velocity of the

sublayer.

The natural frequency and natural period were calculated for the 20 foot and 60

foot column of soils and the results were compared with the 10 foot fiber modified

condition. The results are shown in Figures 5-69 and 5-70.
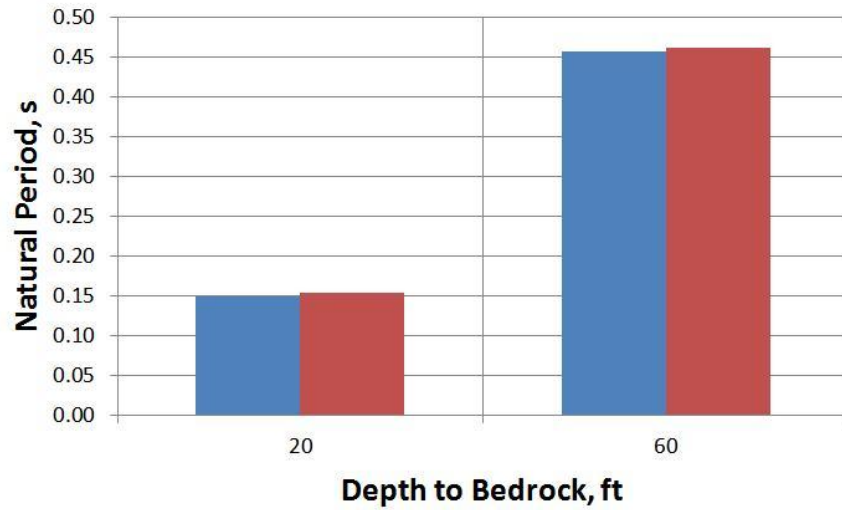
Figure 5-69: Natural period versus depth to bedrock for 20 ft and 60 ft columns of soil. Blue bar: fiber modified condition (thickness of improvement = 10 ft), red bar: all-clay condition
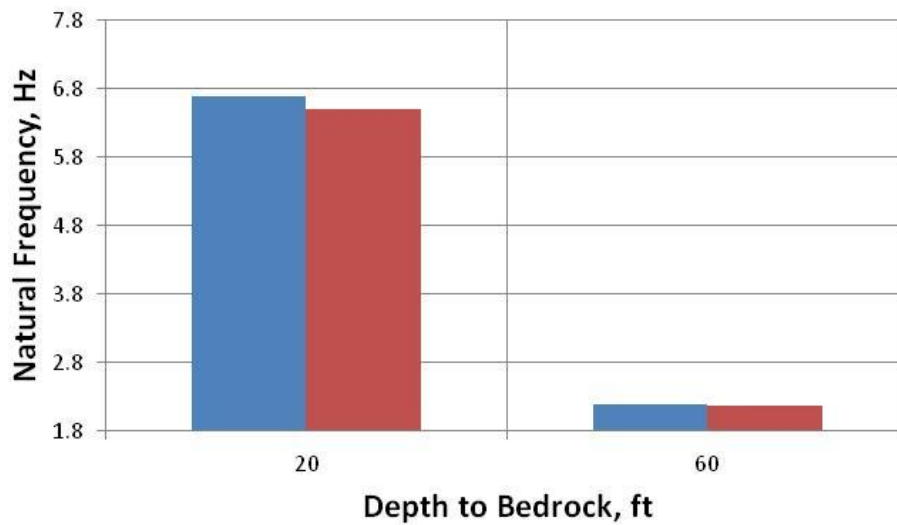
Figure 5-70: Natural frequency versus depth to bedrock for 20 ft and 60 ft columns of soil. Blue bar: fiber modified condition (thickness of improvement = 10 ft), red bar: all-clay condition

The natural period and frequency changes are shown in Figures 5-71 and 5-72.
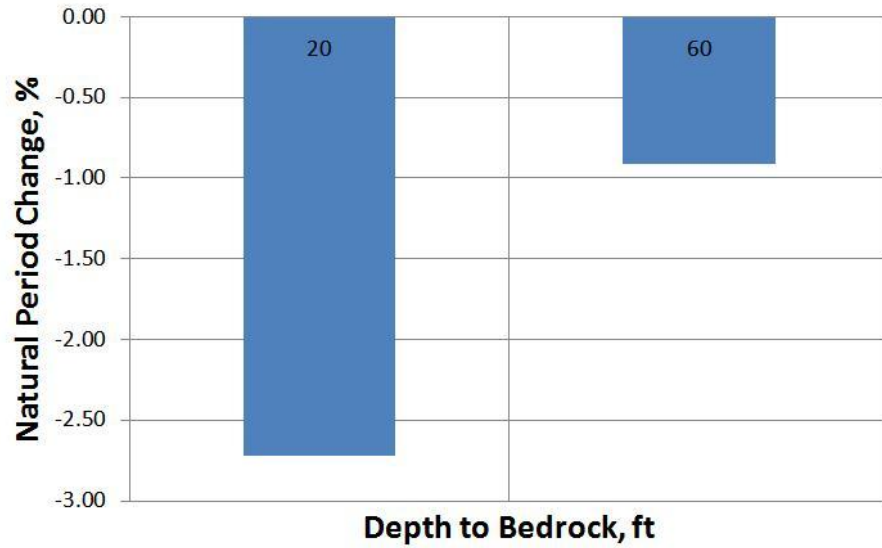
Figure 5-71: Natural period change versus depth to bedrock for 20 ft and 60 ft columns of soil
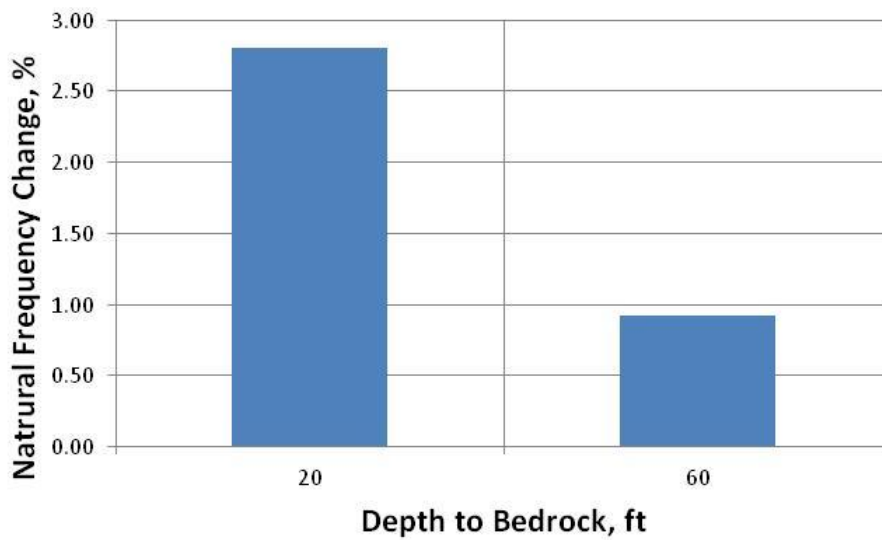
Figure 5-72: Natural frequency change versus depth to bedrock for 20 ft and 60 ft columns of soil

The summary of the results and percentage changes between fiber modified and all-clay conditions is shown in Table 5-6.

Table 5-6: The results of natural frequency and natural period for all-clay and fiber modified conditions

Depth to Bedrock	Thickness of Fiber Modified Layer	Natural Frequency	Natural Period, s	Percentage Change, %
20	0	6.499	0.1539	-
20	10	6.680	0.1497	2.7
60	0	2.166	0.46168	-
60	10	2.186	0.45745	0.9

The presented results show that, in the case of 10 feet of fiber improvement, the natural frequency of the site will increase 2.7 % and 0.9 % for sites with depth to bedrock of 20 and 60 feet, respectively. It can also be resulted in 2.7 % and 0.9 % reductions in the natural period of the site.

In addition, Equation 5-18 was used to determine the natural period and natural frequency of vibration for a 20 foot column of soil with 0, 5, 10, 15, and 20 feet thicknesses of fiber improvement. The results are shown in Figures 5-73 and 5-74.
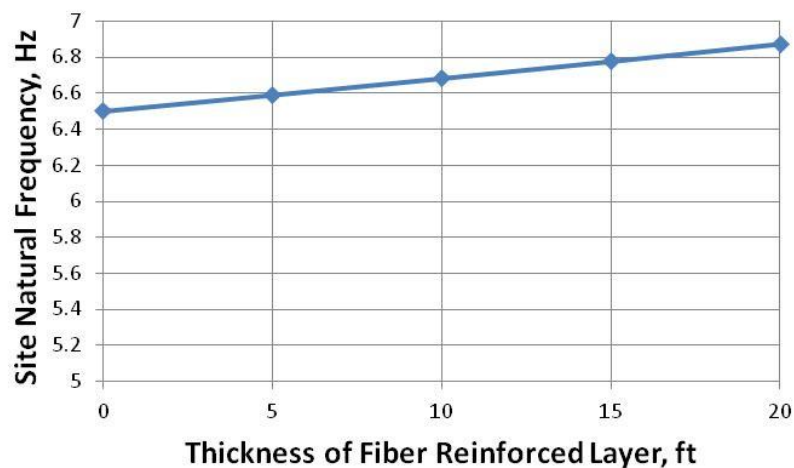
Figure 5-73: Site natural frequency versus thickness of fiber reinforced layer for 20 ft soil column
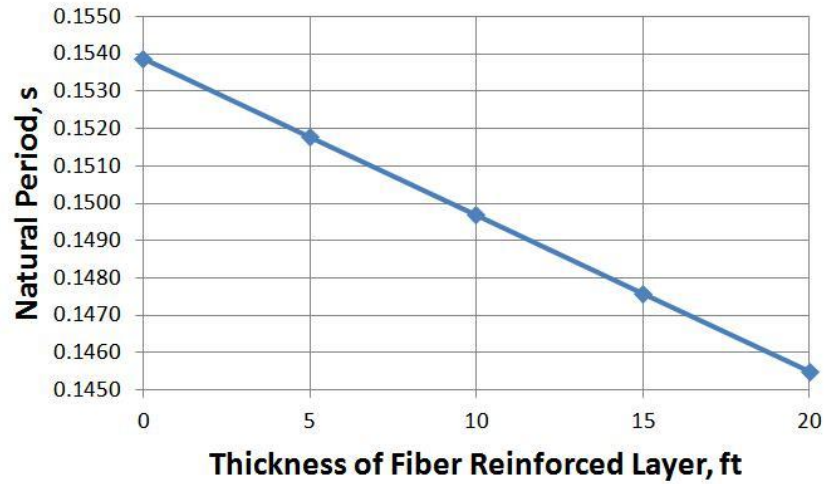
Figure 5-74: Natural period versus thickness of fiber reinforced layer for 20 ft soil column

The results of natural frequency and natural period change due to fiber improvement are

shown in Figures 5-75 and 5-76.
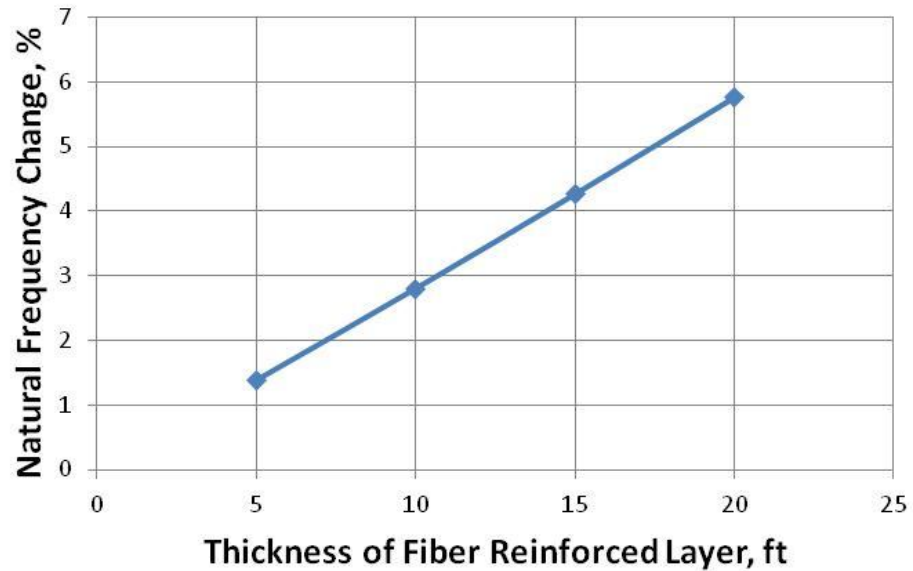
Figure 5-75: Site natural frequency change versus thickness of fiber reinforced layer for 20 ft soil column
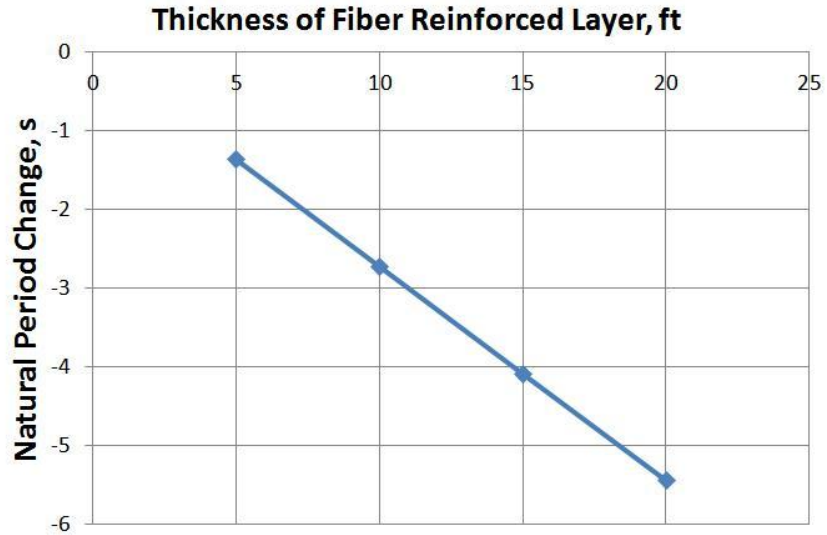
Figure 5-76: Natural period change versus thickness of fiber reinforced layer for 20 ft soil column

Summary of the results are shown in Table 5-7.

Table 5-7: The results of site response analyses for all-clay and fiber modified conditions

Thickness of Fiber Modified Layer	Natural Frequency	Natural Period, s	Percentage Change, %
0	6.499	0.1539	-
5	6.589	0.1518	1.38
10	6.681	0.1497	2.80
15	6.776	0.1476	4.26
20	6.873	0.1455	5.75

The results showed that larger thickness of fiber improvement further increased the natural frequency and further reduced the natural period of the site. The results indicate that the natural frequency of the site increases 1.38 %, 2.80%, 4.26%, and 5.75% in cases where 5, 10, 15, and 20 feet of the site were fiber modified, respectively.

5.10   Conclusions

Seismic site response analyses were performed using DEEPSOIL software for several cases in order to investigate the effect of fiber improvement on seismic ground response. The results showed that the addition of fiber with clay can reduce the ground response when earthquake motions applied. The magnitude of seismic response changes due to fiber modification of the clayey site mainly depends upon the thickness of soil modified layer, depth to bedrock, and also earthquake motion types and properties.

It was also shown that the inclusion of fiber can increase the natural frequency of clayey sites and also reduce the natural period of the clayey sites. Hence, the fiber improvement of clayey sites can benefit the construction considering the natural period of the planned building. Given that fiber reinforcement is able to change the natural frequency of a site, the thickness of fiber improvement can be specifically designed for each building to achieve the required seismic designs.

CHAPTER 6 SUMMARY, CONCLUSIONS, AND RECOMMENDATIONS FOR FURTHER RESEARCH

6.1   Summary

In this study, the effect of fiber modification of clayey soil was investigated. Different commercially available polypropylene fiber types and sizes were used. Since the inclusion of fiber with soil is a relatively new method for the improvement of soft soils, a detailed study was performed to determine the optimum fiber content for both types of fibers, monofilament and fibrillated, as a reinforcement of kaolinite clay. A new procedure, independent of the current state of research that is applied to concrete or using a metallurgical approach, was developed that can be applied to a composite consisting of fiber and soil.

Furthermore, a series of low strain dynamic tests was performed using both types of PP fibers mixed with kaolinite clay to form composites. The effect of fiber inclusion in clay on its dynamic properties was investigated using sinusoidal torsional waves. Plots of normalized shear modulus and damping ratio versus shear strain were generated. In addition, curve fitting model functions correlating shear modulus and material damping ratio with shear strain for soils and fiber-clay composites were proposed. The accuracy of the models was examined using available verification data for sand and clay.

The advantage of using fiber as a modification technique was analytically demonstrated using DEEPSOIL software to show if the fiber inclusion could mitigate earthquake damages by determining the seismic site response of both clayey sites and fiber-modified clayey sites. Two extreme earthquake motions, the Imperial Valley and

216

the Parkfield earthquakes, were used in the analysis. The site responses results were compared between the two sites' conditions. Also, the effect of depth of the soil layer to bedrock on the site response of the fiber reinforced site and the effect of the thickness of soil reinforced layers were also investigated.

6.2   Conclusions

To obtain the maximum benefit of the use of the fiber, the laboratory compaction testing procedure can be adopted to obtain the optimum fiber content. For static or dynamic geotechnical use of any fiber-clay composites, it should be undertaken at the optimum fiber content that produces the proper composite mix design.

Dynamic testing shows that the addition of fiber to clay improves its dynamic properties. It increases the shear modulus as well as its damping. The main conclusion of this study is that the inclusion of fiber at optimum fiber content as a ground improvement technique will improve the dynamic properties of soft and weak clayey soils. This increase in the value of the dynamic properties of clay can be mainly due to the rearrangement of soil particles caused by the addition of fibers. Since the soil at its optimum fiber content becomes fiber-saturated, meaning that all soil voids are mostly filled with fiber, it produces a stiffer composite meanwhile benefiting from the material damping properties of the polypropylene materials. It is important to note that the fact that both the shear modulus and damping increase provide a double benefit for the dynamic response of a site by increasing the stiffness of the site and reducing its amplitude of vibration.

The obtained damping results were slightly different for the composites made up of different PP fiber types, fibrillated and monofilament fibers. Since the fiber-matrix interface (interphase region) is an area where energy can be converted into heat, it is expected to be the main reason for obtaining slightly different material dampings. Different fiber-matrix adhesion and molecular motion within the interphase can be the reason for the slight differences in the material damping of these two types of PP fiber-clay composites.

The developed general model functions for shear modulus and damping ratio at different shear strain levels can be adopted as universal models for sand, clay, and composites. The developed general model functions used the conducted experimental data as well as available data from others to determine the shear modulus and damping ratio as a function of shear strain for the kaolinite clay, and for the fibrillated fiber-clay composites at the optimum fiber content.

Based on the seismic site response analyses performed, it was shown that the addition of fiber to clay can reduce the seismic ground response of the clayey site subjected to earthquake loading. The results showed that modifying the soil conditions of a site using fiber reinforcement in order to mitigate earthquake damage can be one of the methods of improving the site conditions and thus improve the seismic site response. It was shown that by fiber reinforcing the clayey site the natural frequency of the site can be changed. The depth of the fiber improved clayey layer can be specifically designed for each building to achieve the required seismic designs.

6.3   Recommendations

6.3.1   Recommendations for Further Research

The following are recommendations for further research:

1- The effect of plasticity index on optimum fiber content of fiber-clay composites needs to be studied. The study should be performed using cohesive soil with different PI values. Mixtures with different clay fractions can also be examined for their effect on optimum fiber content.

2- The effect of fiber inclusion on large strain dynamic properties of clay needs to be studied using a Cyclic Triaxial test or Cyclic Torsional Shear test.

3- The optimum depth of the fiber improvement can be examined considering seismic properties of different motions, dynamic properties of existing and fiber improved sites, depth to bedrock or earthquake source, etc.

4- The dynamic effect of fiber inclusion can be examined when the matrix of the composite is non-cohesive (sandy). The use of fiber reinforcement with a sandy soil susceptible to liquefaction (loose sand/poorly graded sand) may reduce the possibility of liquefaction while improving the soil dynamic properties.

5- A cost benefit analysis should be undertaken to compare the cost of using fiber as reinforcement for soils with other methods of soil modifications; such as, cement or lime treatments.

6.3.2   Recommendations for Modifying the Equipment

1- When using the Drnevich resonant column apparatus in the torsional mode, the values of resonant frequency of the materials are shown to be highly dependent on

the distance between the coils and magnet. In other words, if the distance between coils and magnet are changed, the value that is obtained can vary. Apparatus calibration is done in a way that coils are set in a certain distance from the magnet using an aluminum rod. The operator has to change this setup when the calibration rod is replaced with the top platen. This action would change all the previous data obtained from the calibration process. It is proposed to modify the coils and magnet placement so that the calibration aluminum rod can be replaced by a top platen without changing the coil-magnet set up.

2- The Drnevich apparatus configuration can be modified by changing the location where the air pipe enters the chamber. In the current apparatus configuration, the compressed air can influence the resonant frequency of the specimen placed for testing. In order to eliminate this influence, the coil and magnet system and air pressured chamber can be placed in different sections/chambers to eliminate the effect of the air pressure on the coil and magnet system.

REFERENCES

Afifi, S. S., & Richart, J. F. (1973, March). Stress-History Effects on Shear Modulus of Soils. *Japanese Society of Soil Mechancis and Foundation Engineering, 13*(1), 77-95.

Aggour, M. S., & Zhang, J. (2006). Degradation of Sands due to Combined Sinusoidal Loading. *ASCE Journal of Geotechnical Geoenvironmental Engineering, 132*(12), 1628–1632.

Aggour, M. S., Taha, M., Tawfiq, K., & Amini, F. (1989). Cohesive Soil Behavior under Random Excitation Conditions. *ASTM Geotechnical Testing Journal, 12*(2), 135-143.

Aggour, M. S., Tawfiq, K., & Amini, F. (1987). Effects of Frequency Content on Dynamic Properties of Cohesive Soils. *Proceedings, Third International Conference on Earthquake Engineering and Soil Dynamics*, *42*, 31-39. Princeton.

Agrawal, Blagwan, D., & Lawrence, J. (1980). *Analysis and Performance of Fiber Composites.* New York: John Wiley and Sons, Inc.

Akbulut, S., Arasan, S., & Kalkan, E. (2007). Modification of Clayey Soils Using Scrap Tire Rubber and Synthetic Fibers. *Applied Clay Science, 38*, 123-32.

Al Wahab, R., & El-Kedrah, M. (1995). Using Fibers to Reduce Tension Cracks and Shrink/Swell in a Compacted Clay. *Proceedings of Geoenvironment 2000, Geotechnical Special Publication* No. 46. 1, 791-805. New York: ASCE.

Allen, H. (1971). The Purpose and Methods of Fiber Reinforcements. *Proceedings of an International Building Exhibition Conference on Prospects for Fiber Reinforced Construction Materails.* London, England: Building Research Establishment.

Al-Sanad, H., & Aggour, M. S. (1984). Dynamic Soil Properties from Sinusoidal and Random Vibrations. *Proceedings, 8th World Conference on Earthquake Engineering, 3,* 15-22. San Francisco, CA.

Al-Sanad, H., Aggour, M., S. & Yang, J. (1983). Dynamic Shear Modulus and Damping Ratio from Random Loading Tests. *ASTM Geotechnical Testing Journal, 6*(3), 120-127.

American Concrete Institute Committee. (1973). State of the Art Report on Fiber Reinforced Concrete. *Proceedings of the American Concrete Institute Journal 70* 729-744, ACI.

Amini, F., Tawfiq, K., & Aggour, M. S. (1988). Cohesionless Soil Behavior under Random Excitation Conditions. *ASCE Journal of Geotechnical Engineering, 114*(8), 896-914.

Amir-Faryar, B., & Aggour, M. S. (2012a). Determination of Optimum Fiber Content in a Fiber Reinforced Clay. *ASTM Journal of Testing and Evaluation, 40*(2), 334-337.

Amir-Faryar, B., & Aggour, M. S. (2012b). Dynamic Properties of Fiber Reinforced Clay. *Proceedings of 15th World Conference in Earthquake Engineering,* Lisbon, Portugal, September 2012, 7pp.

Anderson, D. (1974). *"Dynamic Modulus of Cohesive Soils",* Dissertation Presented to the University of Michigan in Partial Fulfillment of the Requirements for the Degree of Doctor of Philosophy. Ann Arbor, MI: UMICH.

Anderson, D., & Richart, J. (1976). Effects of Straining on Shear Modulus of Clays. *Journal of the Geotechnical Engineering Division, ASCE, 102*(GT9), 975-987.

Argawal, T., & Ishibashi, I. (1991). Multi-Directional Wave Velocity by Piezoelectric Crystals, Proceedings., 102–117. Orlando, FL.

Arulnathan, R., Boulanger, R., Kutter, B., & Sluis, W. (2000). New Tool for Shear Wave Velocity Measurements in Model Tests. *ASTM*.

ASTM D4015-07. (2007). Standard Test Methods for Modulus and Damping of Soils by Resonant-Column Method. West Conshohocken, PA.

Bates, C. (1989). Dynamic Soil Property Measurements During Triaxial Testing. *Geotechnique, 39*(4), 721-726.

Bell, F. (1996). Lime Stabilization of Clay Minerals and Soils. *Engineering Geology*, *42*(4), 223-237.

Biglari, M. (2012). Small-strain Stiffness of Zenoz Kaolin in Unsaturated Conditions. *Canadian Geotechnical Journal, 49*(3), 311-322.

Billo, E. J. (2001). *Excel for Chemists: A Comprehensive Guide.* New York: John Wiley & Sons, Inc.

Blewett, J., Blewett, I., & Woodward, P. (2000). Phase and Amplitude Responses Associated with the Measurements of Shear Wave Velocity in Sand by Bender Elements. *Canadian Geotechnical Journal, 37*, 1348–1357.

Borden, R., Shao, L., & Gupta, A. (1996). Dynamic Properties of Piedmont Residual Soils. *Journal of Geotechnical Engineering, 122*(10), 813-821.

Bottero, J. (1992). *Mesopotamia: Writing, Reasoning, and the Gods.* (Z. Bahrani, & M. Van de Mieroop, Trans.) Chicago, IL: University of Chicago Press.

Bowles, J. (1979). *Physical and Geotechnical Properties of Soils.* New York: McGraw-Hill Book Co.

Boynton, R. S., & Blacklock, J. R. (1986). Lime Slurry Pressure Injection Bulletin. *National Lime Association, 33*, 43 pp.

Brandl, H. (1981). Alteration of Soil Parameters by Stabilization with Lime. *Procedings. 10th ICSMFE*, (pp. 587-594). Stockholm, Sweden.

Brignoli, E., Gotti, M., & Stokoe, K. (1996). Measurement of Shear Waves in Laboratory Specimens by Means of Piezoelectric Transducers. *Geotechnical Testing Journal, 19*(4), 384–397.

Cai, Y., Shi, B., Ng, C., & Tang, C. (2006). Effect of Polypropylene Fibre and Lime Admixture on Engineering Properties of Clayey Soil. *Engineering Geology, 87*(3-4), 230-240.

Carmeuse Technical Training (2002). *Lime in Road Construction.* Carmeuse North America.

Cetin, H., Fener, M., & Gunaydin, O. (2006). Geotechnical Properties of Tire-Cohesive Clayey Soil Mixtures as a Fill Material. *Engineering Geology*, 110-120.

Chen, F. (1988). *Foundations on Expansive Soils.* Elsevier Science, 2nd Edition. 464 pp.

Chepkoit, K. (1999). *"Shear Modulus Determination of Untreated and Treated Cohesive Soils",* Dissertation Presented to the University of Maryland in Partial Fulfillment of the Requirements for the Degree of Doctor of Philosophy. College Park. MD: University of Maryland.

Chopra, A. K. (1995). *Dynamic of Structures, Theory and Applications to Earthquake Engineering.* New Jersey: Prentice Hall.

Darendeli, M. (1997). *Dynamic Properties of Soils Subjected to 1994 Northridge Earthquake (*M.S. Thesis*).* Austin, TX: Unviersity of Texas at Austin.

Darendeli, M. (2001). *Development of a New Family of Normalized Modulus Reduction and Material Damping Curves.* Austin, TX: Ph.D. Dissertation, University of Texas at Austin.

Das, B. (1983). *Advance Soil Mechanics.* New York: McGraw-Hill Book Co.

Das, B. (1984). *Principles of Foundation Engineering.* Boston, MA: PWS Engineering.

De Alba, P., & Pyke, R. (1987). Behavior of Embankments on Soft Soils under Earthquake Loading. *International Symposium on Geotechnical Engineering on Soft Soils. 2*, pp. 125-141. Mexico City, Mexico: Proceedings.

Department of Defense Handbook. (1997). *Soil Dynamics and Special Design Aspects.* Department of Defense (DOD).

Dobry, R., & Vucetic, M. (1987). State of the Art Report: Dynamic Properties and Seismic Response of Soft Clay Deposits. *Proceedings International Symposium on Geotechnical Engineering of Soft Soils, 2*, 51-87.

Donaldson, G. (1969). The Occurence of Problems of Heave and the Factors Affecting its Nature. *Proceedings, The Second Inernational Research and Engineering Conference on Expansive Clay Soils*.

Drnevich, V. (1975). *Resonant Column Testing Apparatus Patent.* United States Patent Office (USPTO).

Drnevich, V. (1978). Resonant Column Testing Problems and Solutions. *ASTM Dynamic Geotechnical Testing, STP 654*, 384-398.

Drnevich, V., Hardin, B., & Shippy, D. (1978). Modulus and Damping of Soils by the Resonant Column Method. *Dynamic Geotechnical Testing*, 91-117.

Dyvik, R., & Madshus, C. (1985). Laboratory Measurements of Gmax using Bender Elements. *Advances in the Arts of Testing Soils Under Cyclic Conditions, ASCE*, 186-196.

Eades, J., & Grim, R. (1960). Reaction of Hydrated Lime with Pure Clay Minerals in Soil Stabilization. *Highway Research Board, Bulletin No. 262, National Research Council*, 51-63.

Eades, J., & Grim, R. (1966). A Quick Test to Determine Lime Requirements for Lime Stabilization. *Highway Research Record*, 139.

Fahoum, K. (1994). *Dynamic Properties of Lime Stablized Cohesive Soils.* College Park, MD: Dissertation presented to the University of Maryland in partial fulfillment of the requirements for the degree of Doctor of Philosophy. College Park, MD: University of Maryland.

Fang, H., & Meleta, H. (1979). Utilization of Sulfur-treated Bamboo for low volume road construction. *Unpublished paper, presented at the 2nd International Conference on Low Volume Roads, TRB.* Ames, IA: Iowa State University.

Freitag, D. (1986). Soil Randomly Reinforced with Fibers. *ASCE Journal of Geotechnical Engineering, 112*(8).

Gaudette, H., Eades, J., & Grim, R. (1964). The Nature OF Illite. *Proceedings, 13th National Conference on Clays and Clay Minerals.*

Gold, V. (1995). *Compendium of Chemical Terminology.* A. McNaught, & A. Wilkinson, Eds. International Union of Pure and Applied Chemistry (IUPAC).

Gray, D., & Ohashi, H. (1983). Mechanics of Fiber Reinforcement in Sand. *Journal of the Geotechnical Engineering Division, 109*(3), 335-353.

Greening, P., & Nash, D. (2004). Frequency Domain Determination of G0 Using Bender Elements. *ASTM Geotechnical Testing Journal*. 27(3), 288-294.

Gromoko, G. (1974). Review of Expansive Soils. *Proceedings, JGED. 100*, 667-687. ASCE.

Halpin, J., & Tsai, S. (1969). *Effects of Environmental Factors on Composite Materials.* Ohio: Airforce Materials Laboratory, Wright-Patterson AFB.

Hannant, D. (1978). *Fiber Cements and Fiber Concretes.* Chichester, England: John Wiley and Sons, Inc.

Hardcastle, J., & Sharma, S. (1998). Shear Modulus and Damping of Unsaturated Loess. *Geotechnical Special Publication, ASCE,* NY, 178-188.

Hardin, B., & Drnevich, V. (1972a). Shear Modulus and Damping in Soils: Measurements and Paramenter Effect. *ASCE Journal of the Soil Mechanics and Foundation, 98*(SM6), 603-624.

Hardin, B., & Drnevich, V. (1972b). Shear Modulus and Damping in Soils: Design Equations and Curves. *ASCE Journal of the Soil Mechanics and Foundations, 98*(SM7), 667-692.

Hardin, K., Drnevich, V., Wang, J., & Sams, C. (1994). Resonant Column Testing and Pressure Up to 305 Mpa (500 psi). *Dynamic Geotechnical Testing II ASTM*, 222-233.

Harianto, T., Du, Y., Hayashi, S., Suetsugu, D., & Nanri, Y. (2008). Geotechnical Properties of Soil-Fiber Mixture as a Landfill Cover Barrier Material. *Journal of Southeast Asian Geotechnical Society*, 137-143.

Hashash, Y., Groholski, D., Phillips, C., Park, D., & Musgrove, M. (2011). DEEPSOIL 5.0 User Manual and Tutorial. 107.

He, J., Zhang, J., & Yang, J. (2006). Experimental Study on Dynamic Properties of Lime Treated Soil. *Ground Modification and Seismic Mitigation*, 81-88.

Hettler, A., & Gudehus, G. (1985). A Pressure-Dependent Correction for Displacement Results from 1G Model Tests with Sand. *Geotechnique, 35*(4), 497-510.

Hoadley, P. (1985). *Analysis and Design of Foundations for Vibrations "Measurements of Dynamic Soil Properties".* (P. Moore, Ed.) Boston, MA: A.A. Balkema.

Hoff, G. (1979). *Chemical, Polymer and Fiber Additives for Low Maintenance Highways* . Pork Ridge, NJ: Noyes Data Corporation.

Holler, F., & Skoog, D. (2006). *Principles of Instrumental Analysis* (6th ed.). Brooks/ Cole, 1056 pp.

Hoover, J. (1982). *Performance of Randomly Oriented, Fiber Reinforced Roadway Soils: a Laboratory and Field Investigation.* Ames: Department of Civil Engineering, Iowa State University.

Hoover, J., Pitt, J., Handfelt, L., & Stanley, R. (1981). Performance of Soil-Aggregate Fabric Systems in Frost Susceptible Roads. *TRB 827, National Academy of Science*, 6-14.

Hoyos, L., Puppala, A., & Chainuwat, P. (2004). Dynamic Properties of Chemically Stabilized Sulfate Rich Clay. *Journal of Geotechnical and Geoenvironmental Engineering, ASCE, 120*(2).

Hoyos, L., Takkabutr, P., Puppala, A., & Hossain, M. (2008). Dynamic Response of Unsaturated Soils Using Resonant Column and Bender Element Testing Techniques. *Geotechnical Earthquake Engineering and Soil Dynamics IV, ASCE*.

Hsay-Yang, F. (1990). *Foundation Engineering Handbook.* New York: Van Nostrand Reinhold.

Hwang, S. (1997). *Dynamic Properties of Natural Soils* - Ph.D. presented to the University of Texas at Austin. Austin, TX: University of Texas at Austin.

Iai, S. (1989). Similitude for Shaking Table Tests on Soil-Structure-Fluid Model in 1G Gravitational Field. *Soils and Foundations, 29*(1), 105-118.

IBC. (2006). *IBC, International Building Code,* ICC.

Idriss, I., & Seed, H. (1968). *ASCE Journal of the Soil Mechanics and Foundations Division,, 94*(SM4), 1003-1031.

Idriss, I., & Sun, J. (1992). *User's Manual for SHAKE91, A computer Program for Conducting Equivalent Linear Seismic Response Analyses of Horizontally Layered Soil Deposits.*

Inci, G., Yesiller, N., & Kagawa, T. (2003). Experimental Investigation of Dynamic Response of Compacted Clayey Soils. *Geotechnical Testing Journal, 26*(2).

International Conference on the Use of Fabrics in Geotechnics (1977). Paris, France: Ecole Nationale des Ponte et Chaussees & Laboratoire Central des Ponts et Chaussees.

Ishibashi, I., & Zhang, X. (1993). Unified Dynamic Shear Moduli and Damping Ratios of
    Sand and Clay. *Soils and Foundations, 33*(1), 182-191.

Ishihara, K. (1996). *Soil Behavior in Earthquake Geotechnics.* Walton Street, Oxford,
    UK: Oxford University Press.

Jeffrey, J. (1997). *An Introduction to Hydrogen Bonding (Topics in Physical Chemistry).*
    Oxford University Press, USA.

Jones, D., & Holtz, W. (1973). Expansive Soils - The Hidden Disaster. *Civil Engineering,
    43*(8), 49 pp.

Kadolph, S., & Langford, A. (2002). *Textile* (9th ed.). Upper Saddle River, NJ: Prentice
    Hall.

Kagawa, T. (1992). Moduli and Damping Factors of Soft Marine Clays. *ASCE Journal of
    Geotechnical Engineering, 118*(9), 1360-1375.

Kalinski, M., & Thummaluru, M. (2005). A New Free-Free Resonant Column Device for
    Measurement of Gmax and Dmin at Higher Confining Stresses. *Geotechnical
    Testing Journal*.

Kallioglou, P., Tika, T., & Pitilakis, K. (2008). Shear Modulus and Damping Ratio of
    Cohesive Soils. *Journal of Earthquake Engineering, 12*, 879-913.

Karl, L., Haegeman, W., Degrande, G., & Dooms, D. (2008). Determination of the
    Material Damping Ratio with the Bender Element Test. *ASCE*.

231

Kawaguchi, T., Mitachi, T., & Shibuya, S. (2001). Evaluation of Shear Wave Travel Time in Laboratory Bender Element Test, *Proceedings. Fifteenth International Conference on Soil Mechanics and Geotechnical Engineering*, 155–158.

Kim, D., & Stokoe, I. K. (1992). *Characterization of Resilient Modulus of Compacted Subgrade Soils Using Resonant Column and Torsional Shear Tests.* TRB.

Klein, C., & Hurlbut Jr., C. (1985). *Manual of Mineralogy* (20th ed.). John Wiley & Sons.

Kokusho, T., Yoshida, Y., & Esashi, Y. (1982). Dynamic Properties of Clay for Wide Strain Range. *Soils and Foundations, 22*(4), 1-18.

Kovacs, W., & Leo, E. (1981). Cyclic Simple Shear of Large-Scale Sand Samples: Effects of Diameter to Height Ratio. *Proceedings, International Conference on Recent Advances in Geotechnical Earthquake Engineering and Soil Dynamics*, *3*, 897-907. St. Louis, MS.

Kovacs, W., Seed, H., & Idriss, I. (1971). Studies of Seismic Response of Clay Banks, *Proceedings. ASCE, JSMFD*, *97*, 441-455.

Kramer, S. (1996). *Geotechnical Earthquake Engineering.* Upper Saddle River, NJ: Prentice Hall.

Krenchel, H. (1973). Fiber Reinforced Brittle Matric Materials. *An international symposium on fiber reinforced concrete.* Ottawa, ON, Canada, Detroit, MI: American Concrete Institute.

Lanzo, G., Vucetic, M., & Doroudian, M. (1997). Reduction of Shear Modulus at Small
Strains in Simple Shear. *ASCE Journal of Geotechnical and Geoenvironmental
Engineering, 123*(11), 1035-1042.

Lawrence, F. (1963). *Propagation Velocity of Ultrasonic Waves Through Sand.*
Cambridge, MA: MIT Research Report R63-8, Massachusetts Institute of
Technology.

Leong, E., Yeo, S., & Rahardjo, H. (2005). Measuring Shear Wave Velocity Using
Bender Elements. *ASTM Geotechnical Testing Journal.28*(5), 11 pp.

Little, D. (1987). *Fundamentals of the Stabilization of Soil with Lime.* Fairfax, VA:
National LimeAssociation.

Little, D., Thomspon, M., Terrel, R., Epps, J., & Barenberg, E. (1987). *Soil Stabilization
for Roads and Airfields.* Tyndall AFB: USAF Technical Report, SFESC.

Maher, M., & Ho, Y. (1994). Mechanical Properties of Kaolinite/Fiber Soil Composite.
Journal of Geotechnical Engineering, 120(8), 1382-1393.

Maier, C., & Calafut, T. (1998). *Polypropylene: the Definitive User's Guide and
Databook.* Norwich, NY,: William Andrew, Inc.

Majundar, A. (1975). Prospects of Fiber Reinforcements in Civil Engineering Materials.
Conference at Shirley Institute on Fibers in Civil Engineering. Manchester,
England: Shirley Institute.

Mangat, P. (1976). Tensile Strength of Steel Fiber Reinforced Concrete. *Cement and
Concrete Research, 6*(2), 245-252.

Masing, G. (1926). Eigenspannungen und Verfestgung Beim Masing. *Proceedings, Second International Congress of Applied Mechanics*, 332-335.

McDowell, C. (1959). Stabilization of Soils with Lime, Lime-Flyash, and Other Lime Reactive Materials. *Highway Research Board*, 60-66.

McMurry, J. (2000). *Organic Chemistry 5th edition.* Brooks/Cole: Thomson Learning.

Meng, J. (2007). Earthquake Ground Motion Simulation with Frequency-Dependent Soil Properties. *Journal of Soil Dynamics and Earthquake Engineering, 27*(3), 234–241.

Mugan, A., & Hulbe, G. M. (2001). Frequency Domain Analysis of Time Integration Methods for Semidiscrete Finite Element Equations - Part II: Hyperbolic and Parabolic-Hyperbolic Problems. *International Journal for Numericcal Methods in Engineering, 51*(3), 351-376.

Naccy, V., & Taylor, K. (1967). Influence of Clay Structure on Elastic Wave Velocities. *Proceedings, International Symposium on Wave Propagation and Dynamic Properties of Earth Materials*, 491-502. Albuquerque, NM.

Nataraj, M., & McManis, K. (1997). Strength and Deformation Properties of Soil Reinforced with Fibrillated Fibers. *Geosynthetic International Journal, 4*(1), 65-79.

Neubauer, D., & Thompson, M. (1972). "Stability Properties of Uncured Lime-Treated Fine Grained Soils" *Highway Research Record 381. HRB, National Research Council*, 20-26.

Newmark, N. M. (1959). A Method of Computation for Structural Dynamics. *Journal of the Engineering Mechanics Division, EM 3*, 67-94.

Nie, Y. (2008). Study on Dynamic Properties of Saturated and Undisturbed Silty Clay. *Geotechnical Engineering for Disaster Mitigation and Rehabilitation; Proceedings of the 2nd International Conference GEDMAR08*, 406-411. Nanjing, China: Springer.

Parrat, N. (1972). *Fiber Reinforced Materials Technology.* Van Nostrand Reinhold Company.

Pennington, D., Nash, D., & Lings, M. (2001). Horizontally Mounted Bender Elements for Measuring Anistropic Shear Moduli in Triaxial Clay Specimens. *Geotechnical Testing Journal, 24*(2), 133–144.

Ple, O., & Le, T. (2012). Effect of Polypropylene Fiber-Reinforcement on the Mechanical Behavior of Silty Clay. *Geotextiles and Geomembranes, 32*, 111-116.

Punthutaecha, K., Puppala, R., Vanapalli, S., & Inyang, H. (2006). Volume Change Bahaviours of Expansive Soils Stabilized with Recycled Ashes and Fibers. *Journal of Geotechnical and Geoenvironmental Engineering, ASCE, 18*(2), 295-306.

Puppala, A., & Musenda, C. (2000). Effects of Fiber Reinforcement on Strength and Volume Change in Expansive Soils. *Transportation Research Record 1736*, 134-140.

Puppala, A., Hoyos, L., Viyanant, C., & Musenda, C. (2001). Fiber and Fly Ash Stabilization Methods to Treat Soft Expansive Soils. *Proceedings, Soft Ground Technology Conference*, 136-145. Noordwijkerhout, The Netherland: ASCE Geotechnical Special Publication No. 112.

Rao, S., & Shivananda, P. (2005). Role of Curing Temperature in Progress of Lime-Soil Reactions. *Geotechnical and Geological Engineering*, 79–85.

Richart, F. (1960). Foundation Vibrations. *Proceedings JSMFD. 86*, 1-34. ASCE.

Rix, G. J., & Meng, J. (2005). A Non-Resonance Method for Measuring Dynamic Soil Properties. *ASTM Geotechnical Testing Journal, 28*(1), 1-8.

Sabry, M., Abdel-Ghani, K., & El Nahas, A. (1996). Strength Characteristics of Soil-Lime Columns Sections. *Proceedings of International Conference on Ground Improvement Geosystems. 1*, 447-452. Tokyo, Japan: Balkema.

Sakr, M., Shahin, M., & Metwally, Y. (2009). Utilization of Lime for Stablizing Soft Clay Soil of High Organic Content. *Geotech Geol Eng*, 105-113.

Schnabel, P., Lysmer, J., & Seed, H. (1972). *SHAKE: A Computer Program for Earthquake Response Analysis of Horizontally Layered Sites, Report No. EERC 72-12*. Berkeley, CA: Earthquake Engineering Research Center, University of California.

Seed, H., & Idriss, I. (1970). *Soil Moduli and Damping Factors for Dynamic Response Analyses, Report No. EERC 70-10*. Berkeley, CA: Earthquake Engineering Research Center, University of California.

Seed, H., Mori, K., & Chan, C. (1977). Influence of Seismic History on Liquefaction of Sands. *Proceeding ASCE, JGED*, *103*, 257-270.

Seed, H., Woodward, R., & Lundgren, R. (1962). Prediction of Swelling Potential for Compacted Clays. *Prceedings, JSMFD. 88*, 53-87. ASCE.

Shannon, & Wilson. (1972). *Soil Behavior Under Earthquake Loadings Conditions, "Evaluation of Soil Characteristics for Seismic Response Analysis".* U.S. Atomic Energy Commission, IIDD-26444.

Shirley, D., & Anderson, A. (1975). *Acoustic and Engineering Properties of Sediments.* Austin, TX: Applied Research Laboratory, University of Texas.

Sowers, G. (1979). *Introductory Soil Mechanics and Foundations: Geotechnical Engineering* (4th ed.). New York: Macmillan Publishing Co., Inc.

Stephenson, R. (1978). Ultrasonic Testing for Determining Dynamic Soil Moduli. *Dynamic Geotechnical Testing*, 179-195. ASTM STP 654.

Stokoe, K. H., Darendeli, M. B., Gilbert, R., Menq, F. Y., & Choi, W. K. (2004). Development of a New Family of Normalized Modulus Reduction and Material Damping Curves. *Proceedings, NSF/PEER Int. Workshop on Uncertanitites in Nonlinear Soil Properties and Their Impact on Modeling Dynamic Soil Response.* Berkeley, CA: University of California at Berkeley.

Stokoe, K. H., Hwang, S. K., Roesset, J. M., & and Sun, C. (1994). Laboratory Measurement of Small-Strain Material Damping of Soil Using a Free-Free

Resonant Column. *Earthquake Resistant Construction and Design, S. A. Savidis, Ed., Balkema, Rotterdam*, 195–202.

Stover, C., & Coffman, J. (1993). *Seismicity of the United States, 1568-1989 (Revised).* Washington: United States Government Printing Office. U.S. Geological Survey Professional Paper.

Sun, J., Goesorkhi, R., & Seed, B. (1988). *Dynamic Moduli and Damping Factors for Cohesive Soils.* Berkeley, CA: University of California.

Tang, C., Shi, B., Gao, W., Chen, F., & Cai, Y. (2007). Strength and Mechanical Behavior of Short Polypropylene Fiber Reinforced and Cement Stabilized Clayey Soil. *Geotextiles and Geomembranes, 25*, 194-202.

Tawfiq, K. (1986). *Effect of Time and Anisotropy on Dynamic Properties of Cohesive Soils,* Dissertation presented to the University of Maryland in Partial Fulfillment of the Requirements for the Degree of Doctor of Philosophy. College Park, MD: University of Maryland.

Tawfiq, K., Aggour, M., & Al-Sanad, H. (1988). Dynamic Properties of Cohesive Soils from Impulse Testing. *Proceedings, 9th World Conference on Earthquake Engineering*, *3*, 11-16. Tokyo, Japan.

Terzaghi, K. (1928). The Physical Properties of Clay. *The Tech. Engineering News, 9*(1), 10-11.

Thompson, M. (1969). Engineering Properties of Lime-Soil Mixture. *Journal of Materials, ASTM, 4*.

Towhata, I. (2008). *Geotechnical Earthquake Engineering.* Berlin, Germany: Springer
series in Geomechanics and Geoengineering.

TRB. (1987). *Lime Stabilization, State of the Art Report 5.* Washington, DC:
Transportation Research Board, National Research Council .

Varde, A., Sandford, T., & Dagher, H. (1996). Model Uncertainty in Anchorage Design
for Anchored Bulkheads. *Proceedings, Uncertainty in the Geologic Environment:
From Theory to Practic, Geotechnical Special Publication No 58*, 727-745.
Madison, WI: ASCE Geotechnical Engineering Division, Vol. 2.

Viana da Fonseca, A., Ferreira, C., & Fahey, M. (2008). A Framework Interpreting
Bender Element Tests, Combining Time-Domain and Frequency-Domain
Methods. *ASTM Geotechnical Testing Journal, 32(*2).

Vidal, H. (1978). The Development and Future of Reinforced Earth. *Proc. ASCE Symp.
on Earth Reinforcement* (1-62). ASCE.

Viswanadham, B., Phanikumar, B., & Mukherejee, R. (2008). Swelling Behaviour of a
Geofiber-Reinforced Expansive Soil. *Geotextiles and Geomembranes*.

Vucetic, M., & Dorby, R. (1991). Effect of Soil Plasticity on Cyclic Response. *Journal of
Geotechnical Engineering, ASCE, 117*(1), 89-107.

Vucetic, M., Lanzo, G., & Doroudian, M. (1998). Damping at Small Strains in Cyclic
Simple Shear Test. *Journal of Geotechnical and Geoenvironmental Engineering,
124*(7), 585-594.

Warner, J., & Brown, D. (1974). Planning and Performing Compaction Grouting. *Proceedings, JGED. 100*, 653-666. ASCE.

Wilson, S. &., & Associates, A.-J. (1972). *"Soil Behavior Under Earthquake Loading Conditions" Evaluation of Soil Characteristics for Seismic Response Analysis.* US Atomic Energy Commission, IID-26444.

Wilson, S., Brown, F., & Schwartz, S. (1978). In Situ Determination of Dynamic Soil Properties. *Proceedings Symposium on Dynamic Geotechnical Testing, ASTM*, 295-317.

Winterkorn, H., & Pamukcu, S. (1991). *Soil Stabilization and Grouting in "Foundation Engineering Handbook"* (2nd ed.). E. H. Fang, Ed., New York: Van Nostrand Reinhold.

Woods, R. (1978). Measurements of Dynamic Soil Properties. *Proc. Earthquake Engineering and Soil Dynamics. 1*, 91-178. Pasadena, CA: ASCE Specialty Conference.

Wray, W., & Meyer, K. (2004). Expansive Clay Soil... A Widespread and Costly Geohazard. *Geostrata, 5*(4), 24-25, 27-28.

Yesiller, N., Hanson, J., & Usmen, M. (2001). Ultrasonic Testing for Evaluation of Stabilized Mixtures. *Transportaion Research Record*, 32-39.

Zhang, J., Andrus, R. D., & Juang, H. (2005). Normalized Shear Modulus and Material Damping Ratio Relationships. *ASCE Journal of Geotechnical and Geoenvironmental Engineering, 131*(4), 453-464.

Zhang, Z., Farrag, K., & Morvant, M. (2000). *Evaluation of the Effect of Synthetic Fibers and Nonwoven Geotextile Reinforcement on the Stability of Heavy Clay Embankments.* Baton Rouge, LA: Louisiana Transportation Research Center.

Ziegler, S., Leshchinsky, D., Ling, H., & Perry, E. (1998). Effect of Short Polymeric Fibers on Crack Development in Clays. *Soils and Foundations, 38*(1), 247-253.